GENOME-WIDE TRANSCRIPTOME ANALYSIS OF LAMINAR TISSUE DURING THE EARLY STAGES OF EXPERIMENTALLY INDUCED EQUINE LAMINITIS

A Dissertation

by

JIXIN WANG

Submitted to the Office of Graduate Studies of
Texas A&M University
in partial fulfillment of the requirements for the degree of

DOCTOR OF PHILOSOPHY

December 2010

Major Subject: Biomedical Sciences

GENOME-WIDE TRANSCRIPTOME ANALYSIS OF LAMINAR TISSUE DURING THE EARLY STAGES OF EXPERIMENTALLY INDUCED EQUINE LAMINITIS

A Dissertation

by

JIXIN WANG

Submitted to the Office of Graduate Studies of
Texas A&M University
in partial fulfillment of the requirements for the degree of

DOCTOR OF PHILOSOPHY

Approved by:

Chair of Committee,	Bhanu P. Chowdhary
Committee Members,	Terje Raudsepp
	Paul B. Samollow
	Loren C. Skow
	Penny K. Riggs
Head of Department,	Evelyn Tiffany-Castiglioni

December 2010

Major Subject: Biomedical Sciences

ABSTRACT

Genome-wide Transcriptome Analysis of Laminar Tissue During the Early Stages of Experimentally Induced Equine Laminitis. (December 2010)

Jixin Wang, B.S., Tarim University of Agricultural Reclamation;

M.S., South China Agricultural University; M.S., Texas A&M University

Chair of Advisory Committee: Dr. Bhanu P. Chowdhary

Equine laminitis is a debilitating disease that causes extreme sufferring in afflicted horses and often results in a lifetime of chronic pain. The exact sequence of pathophysiological events culminating in laminitis has not yet been characterized, and this is reflected in the lack of any consistently effective therapeutic strategy. For these reasons, we used a newly developed 21,000 element equine-specific whole-genome oligoarray to perform transcriptomic analysis on laminar tissue from horses with experimentally induced models of laminitis: carbohydrate overload (CHO), hyperinsulinaemia (HI), and oligofructose (OF). Samples were collected during the developmental (DEV) and Obel grade 1 (OG1) stages of laminitis for the CHO model. For the HI model, samples were collected at the Obel grade 2 (OG2) stage. For the OF model, samples were collected at the 12 h and 24 h time points. Appropriate control samples were obtained for all models.

This is the first genome-wide transcriptome analysis of laminar tissue using an equine 21,000 70-mer long oligoarray approach in CHO, HI and OF induced laminitis.

Overall, we identified the differential expression of genes encoding S100 calcium binding proteins, extracellular matrix proteins, glycoproteins, transporters, olfactory receptors, genes involved in signal transduction, body's homeostasis, apoptosis, and immune response. Between CHO and OF models of laminitis, there were more shared genes. We discovered several common differentially expressed genes (i.e., ADAMTS1, CYCS and CXCL14) among all three models that are likely important to the pathogenesis of equine laminitis. We also discovered what appear to be central roles of apoptosis, inflammatory response, and intracellular ion homeostasis molecular processes in CHO and OF models of laminitis. Pathway analysis detected the NOD-like receptor signaling pathway, which is involved in recognition of intracellular bacteria in both the CHO and OF models of laminitis. Genetic network analysis indicated convergent pathway core molecules present in equine acute laminitis: p38 MAPK and NF-κB. Most importantly, our results of overexpression of anti-microbial genes (i.e., DEFB4, PI3, and CXCL14) suggest the central involvement of these genes in the progression of early equine laminitis and will allow refinement of current hypotheses of disease pathogenesis.

DEDICATION

This work is dedicated to my parents who have supported me so many years for my education.

ACKNOWLEDGEMENTS

I would like to thank my advisor, Dr. Bhanu Chowdhary, for his great supervision, guidance, patience, and support throughout my graduate studies. He not only cares about his students' professional development but also their personal growth. He also told us to learn things well, to do our best and keep the hunger for learning. These teachings have made a great impact on my academic life. Also, I would like to thank my committee members, Dr. Terje Raudsepp, Dr. Loren Skow, Dr. Paul Samollow, and Dr. Penny Riggs for their insightful suggestions and guidance throughout my graduate project.

I gratefully acknowledge Dr. Hannah L. Galantino-Homer and Dr. Rebecca Carter at the Laminitis Institute at the University of Pennsylvania, Dr. Christopher C. Pollitt, Dr. Andrew Van Eps and Ms. Melody De Laat at the Australian Equine Laminitis Research Unit, University of Queensland and Dr. James Belknap and Ms. Mauria Watts at the Department of Veterinary Clinical Sciences at Ohio State University for kindly providing the laminar tissue samples for the study. I also want to extend my gratitude to Dr. Ashley Seabury, Dr. Samantha Steelman, Dr. Xianyao Li, Dr. Huaijun Zhou, Dr. Ivan Ivanov, Dr. Pranab Jyoti Das, Dr. Nandina Paria, Dr. Dhruva Kumar Mishra, Dr. Monika Vishnoi, Dr. Jan Janecka, and fellow graduate students Priyanka Kachroo, Jana Caldwell and Felipe Avila for their help. Finally, thanks to my parents for their love.

NOMENCLATURE

AAEP	American Association of Equine Practitioners
ACTB	Beta Actin
ADAM	A Disintegrin and Metalloproteinase
ADAMDEC1	ADAM-like, decysin 1
ADAMTS	A Disintegrin and Metalloproteinase with Thrombospondin
AGTPBP1	ATP/GTP Binding Protein 1
ANOVA	Analysis of Variance
AP-1	Activator Protein 1
BAX	BCL2-associated X Protein
BCP	Bromochloropropane
BEX2	Brain Expressed X-linked 2
B2M	Beta-2-Microglobulin
BM	Basement Membrane
BP	Biological Process
BPV-1	Bovine Papillomavirus-1
BWE	Black Walnut Extract
CACYBP	Calcyclin Binding Protein
CADS	A Common Array Dye-swap
CC	Cellular Component
CCL	Chemokine (C-C motif) Ligand

CCR	Chemokine (C-C motif) Receptor
CD14	Cluster of Differentiation 14
CD69	Cluster of Differentiation 69
CEBPB	CCAAT/enhancer Binding Protein (C/EBP), beta
CFB	Complement Factor B
CHO	Carbohydrate Overload
CIB1	Calcium and Integrin Binding 1
CILP2	Cartilage Intermediate Layer Protein 2
CITED1	Cbp/p300-interacting Transactivator
CNRQ	Calibrated Normalized Relative Quantity
COX	Cyclooxygenase
CPA6	Carboxypeptidase A6
CPXM	Carboxypeptidase X (M14 Family), Member 2
CRTAC1	Cartilage Acidic Protein 1
CRYAB	Crystallin, Alpha B
CSH	Cross-species Hybridization
CXCL	Chemokine (C-X-C motif) Ligand
Cp	Crossing Point
DAMP	Damage-associated Molecular Pattern
DAPP1	Dual Adaptor of Phosphotyrosine and 3-phosphoinositides
DAVID	Database for Annotation, Visualization and Integrated Discovery
DDB2	Damage-specific DNA Binding Protein 2

DDF	Deep Digital Flexor
DE	Differentially Expressed
DEFB4	Defensin, Beta 4
DMSO	Dimethylsufoxide
ECD	Equine Cushing's Disease
ECEL1	Endothelin Converting Enzyme-like 1
ECM	Extracellular Matrix
EEF1A1	Eukaryotic Translation Elongation Factor 1 Alpha 1
EHC	Euglycemic-hyperinsulinemic Clamp
EHSS	Equine Hindgut Streptococcal Species
EMS	Equine Metabolic Syndrome
ERK	Extracellular Signal-regulated Kinase
ET-1	Endothelin-1
FAP	Fibroblast Activation Protein, Alpha
FGR	Gardner-Rasheed Feline Sarcoma Viral Oncogene Homolog
FIBIN	Fin Bud Initiation Factor
FOSL1	FOS-like Antigen 1
FWER	Family Wise Error Rate
GAPDH	Glyceraldhyde-3-phosphate Dehydrogenase
GI	Gastrointestinal
GLMN	Glomulin
GLUT	Glucose Transporter

GNB2L1	Guanine Nucleotide Binding Protein, Beta Polypeptide 2-like 1
GO	Gene Ontology
GPCR	G-protein Coupled Receptor
GRB7	Growth Factor Receptor-bound Protein 7
GSN	Gelsolin
GWAS	Genome Wide Association Study
HMGB2	High-mobility Group Box 2
HPRT1	Hypoxanthine Phosphoribosyltransferase 1
HD	Hemidesmosome
HI	Hyperinsulinaemia
HR	Heart Rate
ICAM-1	Intercellular Adhesion Molecule 1
IGFBP	Insulin-like Growth Factor Binding Protein
IL	Interleukin
IL10RB	Interleukin 10 Receptor, beta
ING5	Inhibitor of Growth Family, Member 5
IR	Insulin Resistance
KRT17	Keratin 17
LFS	Lavender Foal Syndrome
LIMMA	Linear Models for Microarray Data
LOC554251	Hypothetical Protein LOC554251
LOXL1	Lysyl Oxidase-like 1

LOWESS	Locally Weighted Scatter Plot Smoothing Regression
LPS	Lipopolysacccharide
LTB4R	Leukotriene B4 Receptor
MAF	V-maf Musculoaponeurotic Fibrosarcoma Oncogene Homolog
MAIL	Molecule Possessing Ankyrin-repeats Induced by LPS
MAPK	Mitogen Activated Protein Kinase
MAQC	Microarray Quality Control
MATN2	Matrilin 2
MCP	Monocyte Chemotactic Protein
MF	Molecular Function
MIF	Macrophage Migration Inhibitory Factor
MMP	Matrix Metalloproteinase
MMPI	Matrix Metalloproteinase Inhibitor
MNAT1	Menage A Trois Homolog 1
MSS	Musculoskeletal Syndrome
MYBPC2	Myosin Binding Protein C, Fast Type
MYOD	Maturity Onset Diabetes of Young
NDEL1	NudE Nuclear Distribution Gene E Homolog-like 1
NDUFB3	NADH Dehydrogenase (ubiquinone) 1 Beta Subcomplex, 3
NF	Normalization Factor
NF-κB	Nuclear Factor κB
NFAT	Nuclear Factor of Activated T Cells

NRQ	Normalized Relative Quantity
NSAID	Nonsteroidal Anti-inflammatory Drug
OA	Osteoarthritis
OF	Oligofructose
OR7A10	Olfactory Receptor, Family 7, Subfamily A, Member 10
PAMP	Pathogen Associated Molecule Pattern
P4HA3	Proline 4-hydroxylase, alpha polypeptide III
PI3	Peptidase Inhibitor 3
PI3K	Phosphoinositide 3-kinase
PCA	Principle Component Analysis
PDL	Primary Dermal Laminae
PEL	Primary Epidermal Laminae
PMT	Photomultiplier Tube
PPA1	Pyrophosphatase 1
PPIA	Peptidylprolyl Isomerase A
PROM2	Prominin 2
qRT-PCR	Quantitative Reverse Transcriptase PCR
QSOX1	Quiescin Q6 Sulfhydryl Oxidase 1
RA	Rheumatoid Arthritis
RAD23B	RAD23 Homolog B
RAO	Recurrent Airway Obstruction
REEP3	Receptor Accessory Protein 3

RNF144B	Ring Finger 144B
ROS	Reactive Oxygen Species
RPLP0	Large Ribosomal Protein P0
RPL32	Ribosomal Protein L32
RR	Respiration Rate
RSPH3	Radial Spoke Head 3 Homolog
RXR	Retinoid Receptor
SAA1	Serum Amyloid A1
SAM	Significance Analysis of Microarray
SDL	Secondary Dermal Laminae
SEL	Secondary Epidermal Laminae
SELENBP1	Selenium Binding Protein 1
SEPP1	Selenoprotein P, Plasma, 1
SFRS17A	Splicing Factor, Arginine/serine-rich 17A
SIGLEC10	Sialic Acid Binding Ig-like Lectin 10
SLC24A2	Solute Carrier Family 24, Member 2
SNF8	SNF8, ESCRT-II Complex Subunit, Homolog
SNP	Single Nucleotide Polymorphism
SNRPN	Small Nuclear Ribonucleoprotein Polypeptide N
SOD2	Superoxide Dismutase 2
SOM	Self Organizing Map
S100	S100 Calcium Binding Protein

STC1	Stanniocalcin 1
SUGT1	SGT1, Suppressor of G2 Allele of SKP1
SUPT16H	Suppressor of Ty 16 Homolog
TEM	Transmission Electron Microscopy
TICAM2	Toll-like Receptor Adaptor Molecule 2
TIMP	Tissue Inhibitor of Matrix Metalloproteinase
TK1	Thymidine Kinase 1
TLR4	Toll-like Receptor 4
TMEM49	Transmembrane Protein 49
TNFRSF11B	Tumor Necrosis Factor Receptor Superfamily, Member 11b
T2DM	Type 2 Diabetes Mellitus
TPPP3	Tubulin Polymerization-promoting Protein Family Member 3
TRPM3	Transient Receptor Potential Channel, Subfamily M, Member 3
TUBA1	Tubulin, Alpha 1
VAP-1	Vascular Adhension Protein 1
VDR	Vitamin D Receptor
UBB	Ubiquitin B
USDA	United States Department of Agriculture

TABLE OF CONTENTS

CHAPTER Page

Page

LIST OF FIGURES

FIGURE Page

FIGURE Page

LIST OF TABLES

TABLE Page

CHAPTER I

INTRODUCTION

BACKGROUND

Laminitis is a devastating disease of the equine digits. The disease affects the laminae, which attaches the coffin bone to the inner hoof wall and supports most of the horse's weight (Pollitt, 2004b). Inflammation and subsequent failure of the laminae to remain adhered to the phalanx cause pain and lameness, and with progression of the condition this may lead to death. Several factors may trigger laminitis; these range from mechanical injury caused by exercise, accident or even the walking/training surface to gastrointestinal disturbances, systemic disorders and gut infections. It is due to the latter that laminitis is considered to be a systemic disease which affects the horse's whole body but manifests in a specific region/tissue in the feet (Hood, 1999a). Laminitis occurs primarily in adult horses and has been reported in ponies (Harris et al., 2006). While it is widely accepted that laminitis does not have a hereditary component and is not restricted to a specific breed, it has been reported that some breeds of ponies, particularly the Shetland ponies, show higher incidences relative to other equids (McGowan, 2010). However, it is noteworthy that the incidences are associated with systemic disorders including obesity.

This dissertation follows the style of Veterinary Immunology and Immunopathology.

Approximately 15% of horses are afflicted with laminitis during their lifetime and 75% of the affected horses develop a chronic condition due to which they must be euthanized (Moore et al., 2010). This leads to significant economic losses to the equine industry from loss of animals and recurring veterinary care bills. According to the American Association of Equine Practitioners (AAEP), laminitis is the second most frequent disease affecting horses after colic, and is currently ranked as the most important equine disease requiring research (Harris et al., 2006). The United States Department of Agriculture (USDA) has also listed laminitis as a priority area for equine research funding (www.csrees.usda.gov/funding/afri/pdfs/program_announcement.pdf).

In fact, according to the Louisiana State University Equine Health Studies Program, it is estimated that greater than $13 million was lost annually in the United States as a result of diagnosis, treatment, as well as death of horses affected by the disease (Eades et al., 2002; Moore et al., 2010). While several reports have been published outlining potential causes, methods of prevention and treatment for the disease, an understanding of the molecular progression of the disease is sparse. Furthermore, the presently available therapeutic approaches for laminitis are limited, and their effectiveness is inadequate for complete and/or permanent relief to affected horses. The development of effective therapies requires an improved understanding of disease progression and underlying molecular mechanisms that lead to laminitis (Silver, 2008).

PHASES OF EQUINE LAMINITIS

Laminitis has been divided into three phases: the *developmental phase* (also called the prodromal phase indicating the start of laminitis before the clinical sign of foot pain occurs), the *acute phase* and the *chronic phase* (Pollitt, 2004b). In the *developmental phase*, "laminar separation is triggered" (Pollitt, 2004b). During this phase, horses usually have disturbances in body systems such as gastrointestinal, cardiovascular, respiratory, musculoskeletal, endocrine or immune system (Engiles, 2010). The *developmental phase* may last 8-12 hours when horses have consumed black walnut shavings, or 24 to 32 hours when horses have had excess grain intake. Any changes that occur to the laminae during this phase indicate the initiation of laminitis. Thus, a close scrutiny of pathogenesis during this stage will be particularly important to understand the causes of the progression of this disease and determine triggering factors that cause laminitis.

The *developmental phase* transitions into the *acute phase* when the first clinical sign of laminitis (i.e., foot pain) appears. This phase can last from 34 to 72 hours. Factors like obesity, various metabolic syndromes, endotoxemia and endocrinopathic problems have been shown to be risk factors for the development of *acute* laminitis (Geor and Harris, 2009; Kronfeld et al., 2006; Parsons et al., 2007; Treiber et al., 2006b). If the horse can survive the acute phase, it will recover. However, if progression occurs, laminar separation between the coffin bone (distal phalanx) and the hoof wall will develop (Fig. 1.1). The *chronic phase* is relatively slow. It reflects sustained progression

of the disease that can cause discomfort to the horse for a long time with clinical signs such as continued lameness and hoof wall deformation.

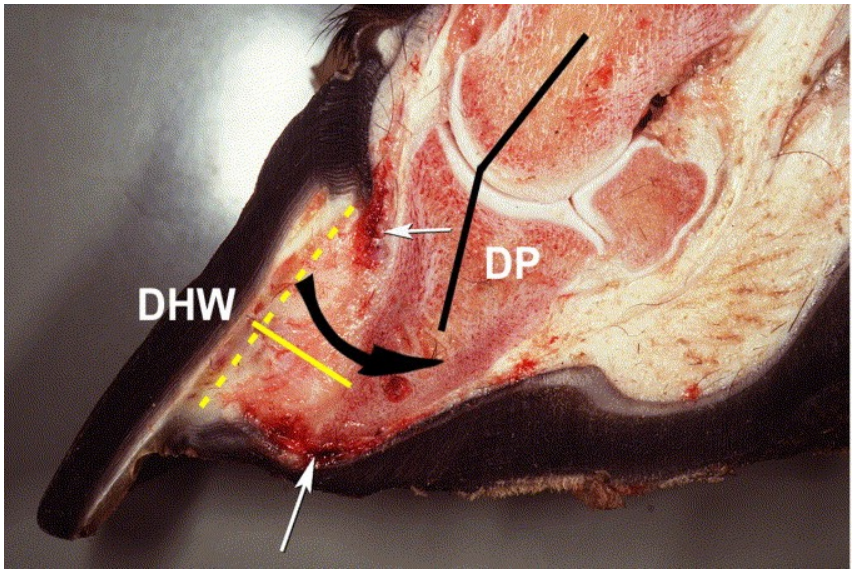

Fig. 1.1. Sagittal section of a foot with chronic laminitis. "The attachment between the distal phalanx (DP) and the dorsal hoof wall (DHW) has failed and hoof and bone are now widely separated. The dashed yellow line shows the original position of the distal phalanx. The solid black line shows that the distal phalanx has rotated (in the direction of the curved black arrow) off the normally straight axis of the proximal and middle phalanges. The material now between the inner hoof wall and the bone is abnormal and consists of epidermal tissue proliferating to form a weak, disorganized mass called the lamellar wedge (yellow line). The descent of the unattached distal phalanx into the hoof capsule has distorted the growth of the proximal hoof wall tubules and has caused the sole to become convex instead of concave (dropped sole). Two dark hemorrhagic zones (white arrows) show the sites of greatest pressure and trauma" (Pollitt, 2004b, ©Elsevier Inc. Reproduced by permission).

CLINICAL SIGNS OF EQUINE LAMINITIS

Laminitis may develop in both front feet, all four feet or in the foot (front and back) opposite to the one with a severe injury or joint infection. It is believed that

because horses bear more than 60% of their weight on their front feet, laminitis is more likely to occur in the front feet (Papakonstantis et al., 2007), which suggests involvement of weight-bearing and other biomechanical forces in the initiation and progression of the disease.

The degree of lameness reflects the severity of laminitis (Obel, 1948). To better define the severity of clinical signs exhibited by horses suffering from laminitis, a grading system of rating the degree of lameness denoted by Obel grades 1-4 (Obel, 1948) was established. Horses with *Obel grade 1* alternately lift the feet but there is no evident lameness at the walk. With *Obel grade 2* laminitis, horses walk with a stilted gait. Horses with *Obel grade 3* resist lifting the foot, and are reluctant to walk. This grade of lameness is the clinical measure for the induction of laminitis (Garner et al., 1975). The most severe grade is *Obel grade 4* where affected horses walk only if forced. Other clinical signs characteristic of laminitis are warm feet with a temperature of up to 40°C, bounding digital pulses, and swelling of the coronary band. More severe signs of laminitis are the detachment of the distal phalanx from the inner hoof wall and the formation of the horizontal rings (Hood, 1999b).

THE ANATOMY OF NORMAL HOOF LAMINAE AND HISTOLOGICAL CHANGES IN LAMINITIS

In the healthy horse, the distal phalanx is attached to the hoof wall by the epidermal and dermal laminae tissue (Black, 2009). The epidermal laminae (primary epidermal laminae or PEL) are associated with the hoof wall and dermal laminae (primary dermal laminae or PDL) are connected with the distal phalanx. Both of the PEL and PDL have

secondary laminae structures to increase the surface area for attachment between the distal phalanx and the hoof wall (Pollitt, 2004a). The basement membrane (BM) is the interface of the secondary dermal laminae (SDL) and secondary epidermal laminae (SEL) (Pollitt and Daradka, 2004). It is composed of the basal cells of the epidermal layer of the laminae (Pollitt, 1996). Laminin protein is distributed within BM and is essential for the differentiation and attachment of epidermal basal cells (Pollitt, 1994). The laminar basal cells are attached to the BM by junctional complexes referred to as hemidesmosomes (HDs) (Borradori and Sonnenberg, 1999). HDs are of fundamental importance in maintaining the contact between epidermal basal cells and the dermis.

Common histological changes that occur during laminitis are degradation of the BM and detachment of epidermal basal cells of the epidermal laminae from BM (Pollitt and Daradka, 1998, 2004). Three laminitis grades based on the histological changes have been established (Pollitt, 2004b; Pollitt and Visser, 2010) (Fig. 1.2). In horses with *grade 1* histological laminitis, laminar basal cells change their normal shape and become longer. As a result, the BM of the SEL detaches away from the basal cells (Fig. 1.2b). The laminar BM disappears between adjacent SELs at *grade 2* histological laminitis (Fig. 1.2c). *Grade 3* histological laminitis is the most severe grade where the SEL laminar tips move away from the BM (Fig. 1.2d).

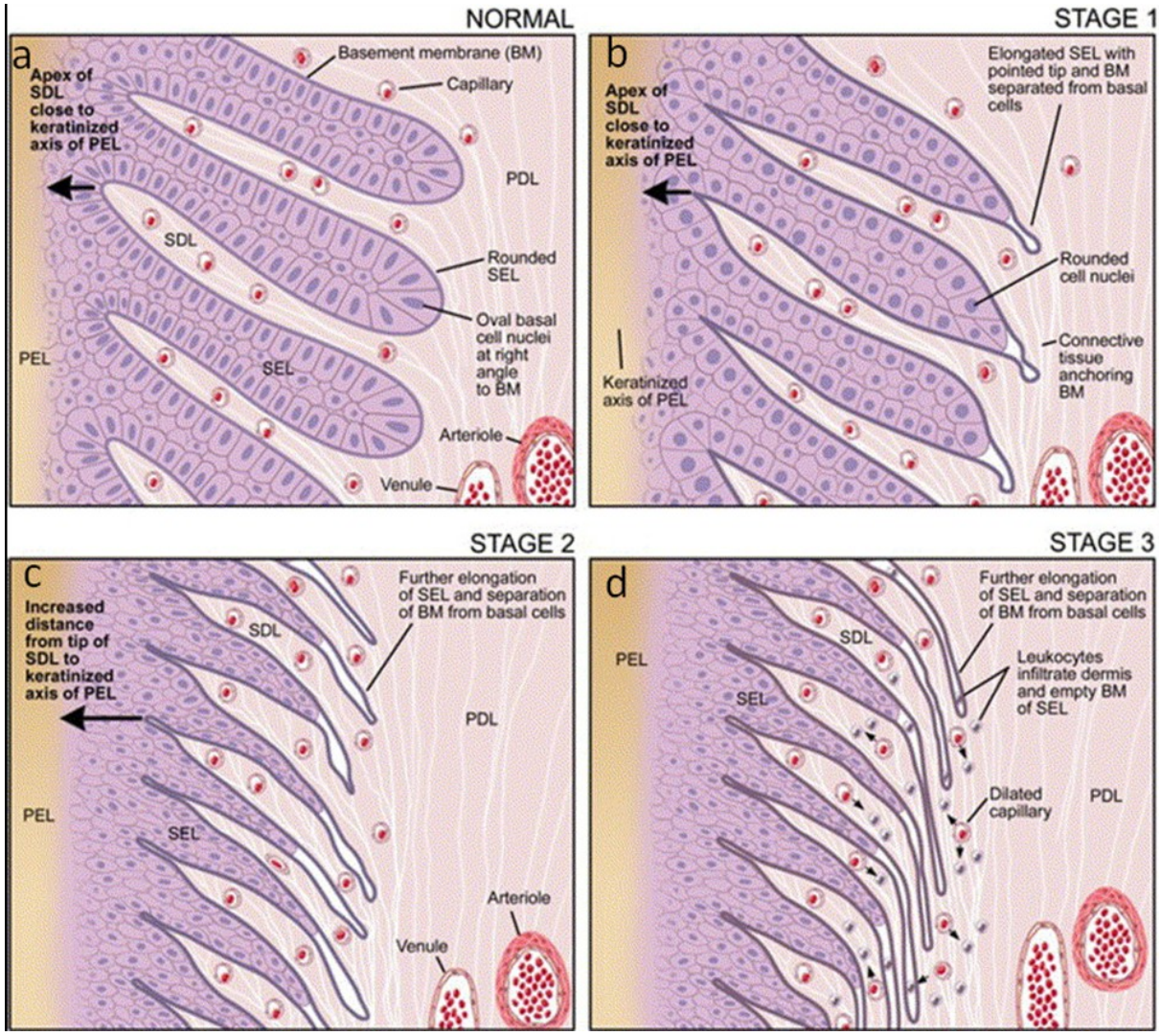

Fig. 1.2. Normal laminar histology and three grades of laminitis histopathology in order of increasing severity (Pollitt, 2004b, ©Elsevier Inc. Reproduced by permission).

EXPERIMENTAL INDUCTION MODELS OF ACUTE LAMINITIS

In order to study the initiation and progression of equine laminitis, four experimentally induced models have been established: carbohydrate overload (CHO) (Garner et al., 1975), black walnut extract (BWE) (Minnick et al., 1987), oligofructose

(OF) (van Eps and Pollitt, 2006) and hyperinsulinaemia (HI) (Asplin et al., 2007; de Laat et al., 2010).

Carbohydrate overload (CHO) model

CHO has become the standard model for induced laminitis studies partially due to its similarity in terms of symptoms caused by grain overload, a common cause of naturally-occurring acute laminitis. These horses experience pathophysiological alterations similar to horses developing naturally-acquired laminitis, such as increased heart rate, arterial pressure, packed cell volume, leukocyte count, and hyperproteinemia (Fagliari et al., 1998; Garner et al., 1975; Harkema et al., 1978; Moore et al., 1981). It is shown that the time between the administration of carbohydrate gruel and the onset of lameness varies from 32 to 48 hours (Garner et al., 1975). This largely corroborates the observations of Pollitt and coworkers who observed that laminar blood flow increases within 12 to 40 h after carbohydrate overload/administration (Pollitt and Davies, 1998). Furthermore, a high vascular resistance in the isolated digit has been noted during the developmental stage of the CHO model of laminitis (Allen et al., 1990). Usually, after an overload of carbohydrate, the BM disintegration is initiated and the attachment between BM and the basal cells of the epidermis start to fail/separate (Pollitt, 1996). Furthermore, the high content of fructan carbohydrate in diet can also contribute to increased production of amine – a bacterial fermentation product - in the large intestine in normal ponies, which may enter the circulation and lead to the downstream laminar failure (Crawford et al., 2007).

Black walnut extract (BWE) model

The BWE model is regarded as an improved model of laminitis compared to the CHO model because of i) reduced time to develop the clinical signs of acute laminitis (Eaton et al., 1995), and ii) high induction rate compared to the CHO model (Minnick et al., 1987). After BWE administration, clinical evidences such as leukopenia and neutropenia develop in horses (Galey et al., 1991). Endotoxins, part of the outer membrane of Gram-negative bacteria, have been regarded as potential laminitis trigger factor for equine laminitis, as is evidenced by clinical signs of endotoxemia in horses that develop laminitis (Bailey et al., 2004). However, lipopolysaccharide (LPS), a biologically active component of endotoxins, was not detected in the plasma of horses post BWE administration (Eaton et al., 1995). It is evident that oxidant stress, as measured by the marker of oxidant stress 4-Hydroxy-2-nonenal (4-HNE) and caused by the production of free radicals, such as reactive oxygen species (ROS), is present in the laminae but not in lung, liver, and intestinal tract of BWE model of laminitis, which indicated that oxidant stress is a possible contributor to laminitis (Yin et al., 2009). In addition to oxidant stress, the pattern of inflammatory events in the lung and liver of BWE model of laminitis is similar to that in human sepsis (Stewart et al., 2009). However, Stewart and coworkers did observe a low inflammatory response in the horse lung and liver compared to that of laminae *post* BWE administration (Belknap et al., 2007; Stewart et al., 2009).

Oligofructose (OF) model

Fructan is a form of oligofructose (OF) and is a component of CHO. The successful induction of laminitis by OF could link increased fructan consumption at pastures to the development of laminitis (van Eps and Pollitt, 2006). Compared to the findings that eight of 10 horses with BWE induction (Minnick et al., 1987) and 11 of 12 horses with CHO induction developed laminitis (Garner et al., 1975), all six horses dosed with OF develop laminitis (van Eps and Pollitt, 2006). Therefore, the OF model is considered an improvement over CHO and BWE models as far as laminitis induction is concerned. The laminar histopathological changes created in the OF model are identical to those observed after CHO (van Eps and Pollitt, 2006). Furthermore, the onset time of laminitis in the OF model is similar to that induced with starch intake (20-44 h post intake; Morgan et al., 2003). A recent study showed that clinical signs of systemic inflammations are typically observed in this induction model of laminitis and a change in glucose dynamics is observed within 24 to 48 hours of OF administration (Kalck et al., 2009). An ultrastructural study of laminar tissue following higher OF dosage discovered that it leads to greater loss of HDs (French and Pollitt, 2004b).

Hyperinsulinaemia (HI) model

Laminitis can also be induced by maintaining prolonged hyperinsulinaemia (HI) with euglycaemia (Asplin et al., 2007; de Laat et al., 2010). Consequently, the laminitis thus caused is also considered as a model of endocrinopathic laminitis where the symptoms are caused due to hormonal influences (Johnson et al., 2004b). Naturally occurring HI is a condition of high levels of insulin in the bloodstream and is proposed

to be caused by insulin resistance (IR) (Frank, 2009; Johnson et al., 2004b). It is noteworthy that IR is the core component of equine metabolic syndrome (EMS) and equine Cushing's disease (ECD) (Frank, 2009; Johnson et al., 2004a), and is defined as failure of tissues to take up glucose via insulin-dependent glucose signaling. Due to IR, glucose remains in the blood and the pancreas continues to secret insulin, which causes HI (Kronfeld, 2005; Shanik et al., 2008). It has long been recognized that IR predisposes horses (e.g., Morgans, Arabians, Norwegian Fjords and Paso Finos) (Frank et al., 2006; Johnson, 2002) and ponies (Welsh and Dartmoor) (Geor, 2008; Treiber et al., 2006b) to laminitis.

Euglycaemia is defined as a normal blood glucose level which in the horse body is 5 mmol/L (Asplin et al., 2007). All ponies (Asplin et al., 2007) and horses (de Laat et al., 2010) in the HI treatment group developed laminitis. Histological results showed BM was disintegrated in laminar tissue in the insulin treated ponies developing clinical laminitis (Asplin et al., 2007). Furthermore, laminar lesions in the hoof of ponies studied in HI induced laminitis using light and transmission electron microscopy (TEM) showed ultrastructural morphology of the laminar tissue affected by HI (Nourian et al., 2009). The changes were not similar to the laminar pathology after CHO and OF administration (Nourian et al., 2007; Pollitt, 1996). Unlike the CHO and OF laminitis pathology, there was no large-scale BM separation in the treated ponies following HI (Nourian et al., 2009).

THEORIES OF PATHOGENESIS

There are many theories regarding the mechanisms of the development of laminitis: *vascular* (Hood et al., 1993), *enzymatic* (Pollitt, 1999), *traumatic/mechanical* (Hood, 1999b), *inflammatory* (Belknap et al., 2007; Loftus et al., 2007), *altered glucose metabolism* (Pass et al., 1998) and *cascade failure* (Orsini et al., 2009) theory.

The *vascular* theory proposes vascular alterations as the initiating factor that contributes to structural failure of the laminae (Hood et al., 1993). The presence of a warm hoof and bounding digital pulses during acute laminitis suggests a vascular component (Moore et al., 2004). Chronic laminitis has many pathological changes similar to those caused by ischemia/reperfusion of the digits (Bailey et al., 2004). The vascular mechanism that contributes in such cases to laminitis is characterized by venoconstriction, which causes decreased laminar perfusion and laminar tissue ischemia. Consequently, the epidermal cells in the laminar tissue are damaged that eventually leads to laminitis (Hood, 1999b). This corroborates with very early observations that decreased central venous pressure (which may be due to venoconstriction) is a feature during the developmental stage of CHO model laminitis (Garner et al., 1975).

The *enzymatic* theory is based on matrix metalloproteinase (MMP) activation in laminar tissue affected by laminitis. MMP enzymes can degrade the BM component of extracellular matrix (ECM) (Pollitt, 1996). Laminin, type IV and type VII collagens are essential components of the laminar BM. MMP-2 and MMP-9 are thought to degrade these proteins and facilitate the detachment between the hoof wall and coffin bone (Pollitt and Daradka, 1998). In addition to ECM degradation, MMPs can also interact

with cytokines and growth factors (Parks et al., 2004) and their activities are tightly regulated by tissue inhibitors of metalloproteinases (TIMPs) (Denhardt et al., 1993). However, factors that trigger MMP activation in laminitis are still not known (Moore et al., 2004).

The *traumatic/mechanical* theory states that laminitis can result from direct trauma as well as mechanical overload of the foot instead of systemic diseases. Road founder laminitis and laminitis secondary to unilateral weight bearing are examples of trauma-linked laminitis (Hood, 1999b). Several hypotheses have been purposed as the causes of laminar structural failure. One is that direct trauma may initiate inflammatory response, which leads to tissue damage (Hood, 1999b). The other hypothesis is that excessive mechanical/pressure forces may result in the tearing of laminar interface, which is followed by "compartment injury" (Hood, 1999b).

Although laminar tissue *inflammation* has long been recognized as a key component of laminitis, it is hypothesized that inflammation is a result of primary pathological changes such as trauma, rather than being the initial event (Hood, 1999b). Nonetheless, recent results suggest that inflammation is indeed likely to be the initiating pathological mechanism with MMP accumulation most likely a downstream event (Belknap et al., 2007; Loftus et al., 2007). In all stages of laminitis that have been investigated after BWE administration, genes encoding proteins associated with inflammation (i.e., IL-1β, IL-6, IL-8, ICAM-1 and COX-2) were induced and inflammation was considered as central to the development of laminar pathogenesis (Loftus et al., 2007).

Another hypothesis of laminar failure states that *alterations in glucose metabolism* lead to destruction of laminar tissue. Glucose is important for maintaining the adhesion between the basal epidermal cell and the BM (Pass et al., 1998). It has been shown that laminar separation occurs when glucose deprivation occurs *in vitro* (French and Pollitt, 2004a). However, the inhibition of glucose metabolism leading to hoof laminar separation *in vivo* has yet to be verified.

Cascade failure theory is an extension of the systems theory for developing an improved understanding of laminitis (Orsini et al., 2009). It is used to unify disparate theories of laminitis pathogenesis for precise identification of the potential cause(s) to eventually find more effective therapeutic strategies. The cascade failure theory states that the failure of a preceding part (e.g., excessive ingestion of grain) can cause the failure of subsequent parts (e.g., MMP activation and BM degradation) and the ultimate failure in laminitis is the laminar separation. The endpoint failure can be reached by mechanisms such as vascular, enzymatic, inflammation or any combination thereof (Orsini et al., 2009).

Among these various theories of laminitis pathogenesis, the inflammation mechanism is regarded as a common denominator (Budak et al., 2009; Orsini et al., 2009) and has recently received more attention by researchers.

INFLAMMATION AND MMPs

Inflammation and the role of MMPs are among the important focus areas in equine laminitis research (Eades, 2010). It has been indicated that inflammatory processes initiated in the beginning due to any stimuli play a key role in the development of

laminitis, and may lead to laminar failure (Belknap et al., 2007; Orsini, 2008). Typically during any inflammatory process, a number of genes are activated, including TNF-α, IL-1β, and IFN-γ, which in turn leads to endothelial activation and leukocyte (predominantly neutrophils) recruitment. Neutrophils generate reactive oxygen species (ROS) and release proteases extracellularly to degrade extracellular matrix resulting in tissue damage (Pham, 2008). Examples of important cytokine levels that are increased in laminar tissue of horses with laminitis are interleukin-1beta (IL-1β) (Fontaine et al., 2001), interleukin-6 (IL-6) (Waguespack et al., 2004a), interleukin-8 (IL-8) (Loftus et al., 2007), cyclooxygenase 2 (COX-2), intercellular adhesion molecule 1 (ICAM-1) and a cytokine-associated molecule possessing ankyrin-repeats induced by lipopolysaccharide (MAIL) (Waguespack et al., 2004b). The induction of cytokines recruits and activates leukocytes into the laminar tissue, which contributes to the inflammation (Kobayashi et al., 2003).

In horses, soft tissue damage had been found to be associated with laminitis (Johnson et al., 2000) and some of the recent studies suggest that it is caused or mediated by MMPs. MMPs are a large family of proteinases that promote degradation of the extra cellular matrix or ECM (Ivan Stamenkovic, 2003). Varying activity as compared to normal has been detected for three members of the MMP family, MMP-2, MMP-9 and MMP-14, in naturally occurring cases (Johnson et al., 1998), the CHO model (Mungall and Pollitt, 1999) and the OF model of laminitis (Kyaw-Tanner et al., 2008). The transcriptional activity of MMP-2 increases during the developmental stage (Kyaw-Tanner and Pollitt, 2004) and the level of tissue inhibitor of metalloproteinase 2 (TIMP-

2) activity decreases in affected laminar tissue at the onset of laminitis (Kyaw-Tanner et al., 2008). Another form of laminar metalloproteinase, a disintegrin and metalloproteinase with thrombospondin motifs (ADAMTS) 4, is found to be activated in BWE and CHO induced laminitis (Coyne et al., 2008). This protein plays an important role in the ECM protein aggrecan cleavage (Kashiwagi et al., 2004). The activation of ADAMTS4 in laminitic horses is possibly necessary for the destruction of the laminar tissue through ECM aggrecan degradation, as BM (a thin layer of ECM) degradation is an early event during acute laminitis pathogenesis (Pollitt and Daradka, 1998).

CURRENT TREATMENTS OF EQUINE LAMINITIS

As inflammation is a key factor or manifestation in laminitis, the drugs of choice to treat this disease have traditionally been anti-inflammatory. Nonsteroidal anti-inflammatory drugs (NSAIDs) are most often used for this purpose primarily to decrease the inflammation and pain within the foot (Baxter and Morrison, 2008; Harman and Ward, 2001). Primarily these drugs are COX-2 inhibitors (Waguespack et al., 2004a). Flunixin meglumine is another commonly used NSAID in horses for treating inflammation although it is not a specific COX-2 inhibitor (Divers, 2003). Phenylbutazone and dimethylsufoxide (DMSO) are also some of the other NSAIDs used for the treatment of acute form of equine laminitis (Parks, 2003).

Other medications used to treat laminitis are targeted towards improving laminar blood flow. These drugs include acepromazine, isoxsuprine, pentoxifylline, nitroglycerin, and ketoprofen (Belknap, 2010; Parks and O'Grady, 2003). Intramuscular administration of acepromazine can increase digital blood flow in healthy horses (Leise

et al., 2007) and is the widely used vasodilator in the treatment of laminitis; however, this drug is not selective in terms of the receptors it antagonizes (Bailey et al., 2004). It not only inhibits α-adrenergic receptors, but also inhibits 5-hydroxytryptamine (HT) receptors (Bailey et al., 2004). Another vasodilator drug isoxsuprine has been shown to reduce lameness with intravenous administration but the reported data are conflicting regarding its effect on laminar blood flow (Erkert and Macallister, 2002; Lizarraga et al., 2004; Rose et al., 1983). Some reported that oral isoxsuprine improved peripheral blood flow (Rose et al., 1983) but others demonstrated that it did not increase laminar blood flow (Ingle-Fehr and Baxter, 1999). Furthermore, application of nitroglycerin for the treatment of laminitis has been shown to improve digital blood flow in CHO-induced cases (Eades et al., 2006) but not in healthy horses (Eades et al., 2006; Gilhooly et al., 2005). Heparin, aspirin, mineral oil and cryotherapy are some of the other therapeutic agents (Baxter and Morrison, 2008) used to treat laminitis. Of these, heparin has been proven to have anti-inflammatory role in equine laminitis (de la Rebiere et al., 2008). Next, aspirin can decrease platelet aggregation in the natural forms of laminitis but the benefits of aspirin therapy have not yet been tested in an experimental model of laminitis (Parks and O'Grady, 2003; Parks, 2003). It has been shown that platelet activation and aggregation occur in the digital blood during the development of acute laminitis (Eades et al., 2007; Weiss et al., 1997). Therefore aspirin therapy is assumed to inhibit platelet aggregation for laminitis relief. Therapeutic shoeing, mechanical support, and deep digital flexor (DDF) tenotomy are the current treatment methods of choice to reduce the structural damage for chronic laminitis cases (Moore, 2008; Wylie et al., 2009) because

they provide considerable relief to the horse from pain and detachment of the BM. Recently it was reported that laminitic horses with different degrees of lameness can improve 1 to 2 Obel grades with botulinum toxin type A treatment (Carter and Ben Renfroe, 2009). The authors hypothesized that the pull of deep digital flexor tendon (DDFT) on the coffin bone contributes to the displacement of distal phalanx from the hoof wall (Carter and Ben Renfroe, 2009). Botulinum toxin injection can relax the DDFT and reduce the rotation of the distal phalanx.

Due to the role of MMPs in ECM component degradation in the pathophysiology of both human and animal diseases, MMPs have become targets for therapeutic treatments/preventatives through the development and use of matrix metalloproteinase inhibitors (MMPIs). Synthetic MMPIs, such as batimastat (Tocris Bioscience) and marimastat (British Biotech) have been developed as potential treatments for diseases such as cancer, osteoarthritis, and rheumatoid arthritis (Lombard et al., 1998). However, it is shown that these compounds are either ineffective or have side effects for humans (Fingleton, 2008; Ramnath and Creaven, 2004). The main side effect was a musculoskeletal syndrome (MSS) that causes joint pain and reduced mobility (Fingleton, 2008). Presently, doxycycline is the only medication approved for use as an MMPI in people with periodontal disease (Fingleton, 2008). Among the synthetic MMPIs, batimastat (BB-94) has been tested on horses with laminitis and is shown to prevent laminar separation in the explants of laminar hoof *in vitro* (Pollitt et al., 1998). However, there is no MMPI therapeutic agent currently under trial for the treatment of equine laminitis.

Many horses are euthanized every year due to the pain and debilitation suffered after developing laminitis. The lack of effective treatments for acute laminitis requires further investigations to improve our understanding about the underlying molecular/genetic mechanisms associated with the causation and progression of the disease, which is a prerequisite for the development of novel and effective therapeutic approaches.

Many novel approaches have been applied in human medicine to study mechanisms of disease progression and to identify the interplay of genes that regulate pathogenic processes associated with the severity of the disease and the lesions/symptoms this may cause. During the past decade, these approaches have included the use of functional approaches and whole genome tools for transcriptome analysis that could provide clues regarding the potential causes of the diseases and insights into how various diseases including complex diseases like cancer progress. Functional genomics is the science of how genes function and how they are regulated on a genome-wide scale. The functions of most genes are mainly regulated by altering their transcription levels (Staudt and Brown, 2000) and these changes in transcription levels have an impact on the normal physiology/biology, leading to disease. Therefore, gene expression profiling based on transcriptional levels is a very useful approach to study the states and changes of cellular activity in normal and diseased condition. One of the most widely used functional genomics tools is a whole genome DNA microarray (Steinmetz and Davis, 2004).

MICROARRAY TECHNOLOGY OVERVIEW

Types

DNA microarray is a high-throughput technology that enables researchers to study gene expression levels of thousands of genes simultaneously at the transcriptional level (Brown and Botstein, 1999). In this technology, thousands of expressed gene sequences are spotted with high-speed robots to a small surface, such as glass microscope slides (Schena et al., 1995). The ability to analyze the transcription profiles on a genome-wide scale through these arrays can greatly enhance our understanding of genes and pathways involved in disease pathogenesis. The objectives of some microarray experiments are "class comparison, class prediction and class discovery" (Simon and Dobbin, 2003). Class is defined as the same tissue under different experimental conditions (e.g., disease and normal), or different category of disease in terms of stage or time point. Class comparison focuses on the identification of differential expression among the classes. Class prediction emphasizes the development of a statistical model to predict the results of an unknown class based on the expression profile. The objective of class-based discovery is to identify undefined classes based on the expression profile. The common goal of many microarray experiments is the identification of differentially expressed (DE) genes between a diseased and control state as these genes are valuable in studying mechanisms of disease progression and eventual pharmaco-genomics based drug discovery. Usually a fold change cut-off (>2) and significant p value (e.g., 0.01 or 0.05) are used to identify the genes that show statistically significant differential expression between conditions (e.g., treatment versus control). The steps of a microarray

experiment include experimental design, hybridization, data preprocessing and normalization, data analysis to identify DE genes, functional annotation of the latter and further analysis to draw biological conclusion (Fig. 1.3).

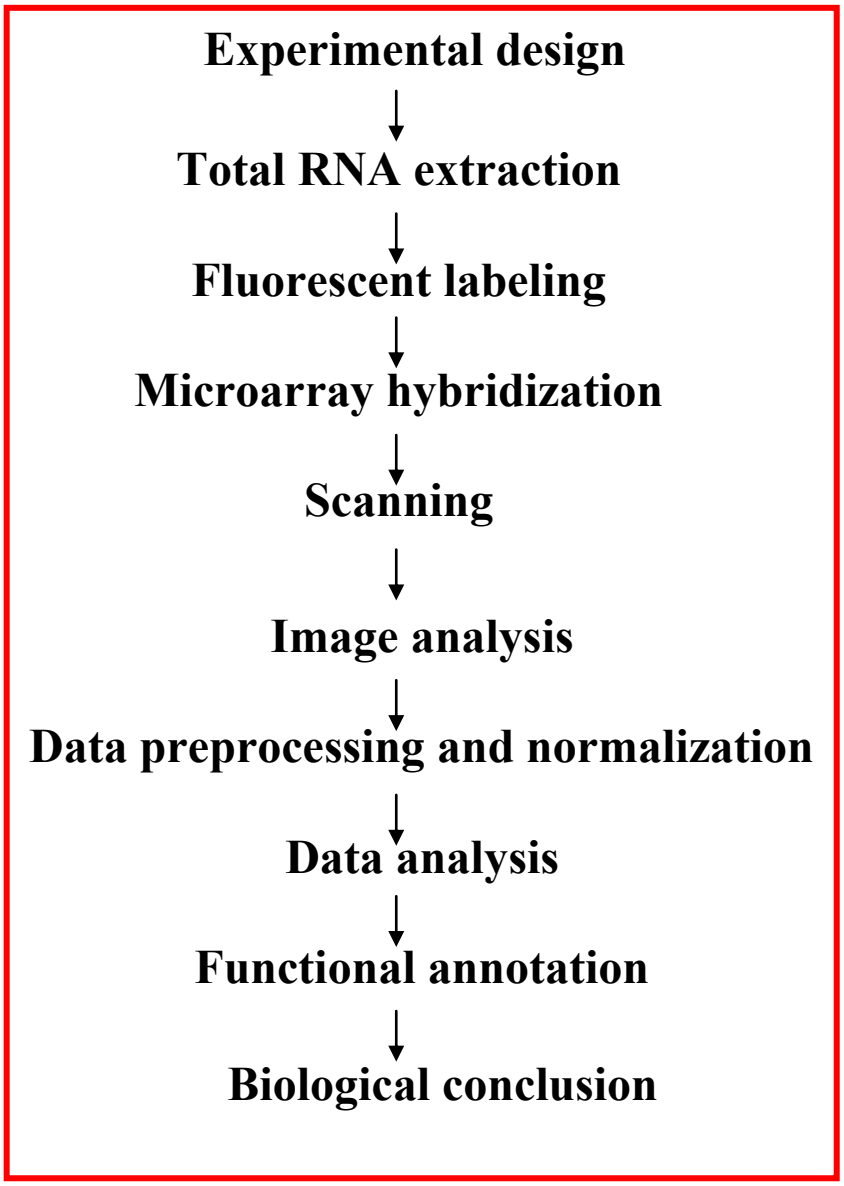

Fig. 1.3. The workflow of a microarray experiment.

During the past decade, three major types of microarray platforms have been developed: spotted cDNA, short oligonucleotide, and long oligonucleotide arrays (Petersen et al., 2005), of which the cDNA arrays were first. The cDNA arrays are prepared by spotting DNA obtained from PCR based amplification of individual cDNA generated via tissue specific cloned libraries of expressed genes (Barrett and Kawasaki, 2003). The oligonucleotide arrays, however, are prepared either by means of ink jet technologies or photolithography directly on the slide or also by large scale production of small or large oligos and then spotting them robotically on the slides (Hughes et al., 2001). The cDNA array technique has two important limitations: tedious lab work of cDNA preparation and low specificity due to cross-hybridization (Li et al., 2002). In cDNA array experiments, certain cDNAs spotted on the slide can hybridize to other undesired DNA that share sequence homology and can result in cross-hybridization (Chuaqui et al., 2002) leading to background and/or non-specific hybridizations that may skew the results. In comparison, oligoarrays are more specific, sensitive and reliable than cDNA arrays (Hardiman, 2004; Hughes et al., 2001; Woo et al., 2004). Among the oligo based arrays, use of short oligos (on average 25 mers) as hybridization spots are less sensitive compared to long oligos because it has less available area for hybridization (Hardiman, 2004). Due to this they may not detect low level gene expression. Therefore, long oligoarrays (on average 60-70 mers) have become arrays of choice for exploring transcriptomes.

Two approaches have traditionally been used for microarray hybridization experiments: single color and dual color. With the single color approach (i.e.,

Affymetrix Gene Chips), the cDNA of sample is labeled with one fluorophore (such as green fluorescent dye cyanine 3 (Cy3) or red fluorescent dye cyanine 5 (Cy5), and hybridized to the individual array. Such hybridization experiments will generate absolute expression levels because the spot fluorescence intensity reflects the absolute mRNA abundance in the single sample. For dual color procedure, however, two cDNA samples are each labeled with a different dye (such as Cy3 and Cy5 dyes) and hybridized on a single slide to obtain relative expression levels. The Microarray Quality Control (MAQC) Consortium tests have indicated that the data obtained from single and dual arrays are comparable (Patterson et al., 2006).

Experimental design

Efficient experimental design is important for a microarray experiment, as it directly affects the downstream data analysis. There are mainly three types of experimental design: reference design, balanced block design and loop design (Simon and Dobbin, 2003; White and Salamonsen, 2005) (Fig. 1.4).

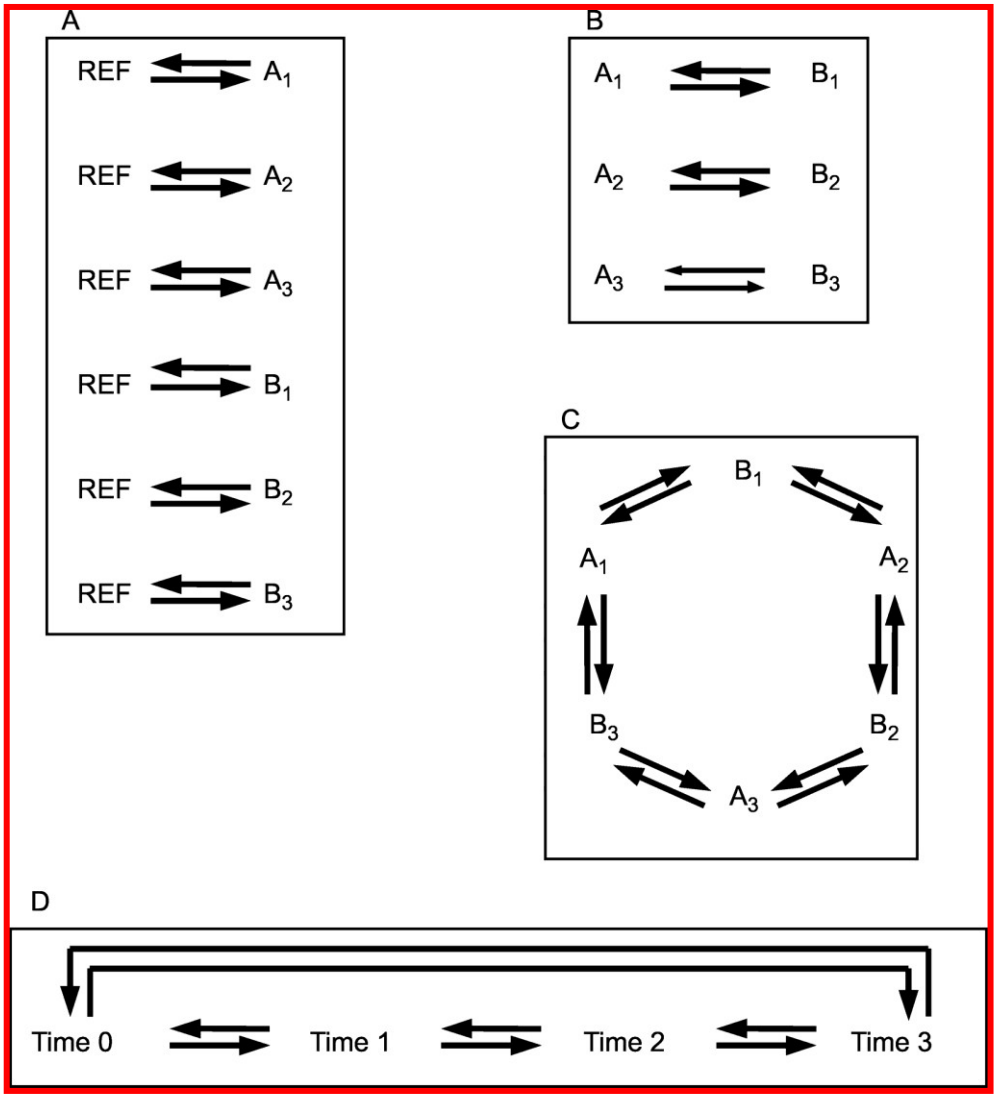

Fig. 1.4. Microarray experimental designs. Letters refer to different treatments and subscripts indicate biological replicates. Each arrow represents one microarray, with the arrow pointing away from the Cy3 labeled sample and towards the Cy5 labeled sample. Double arrows indicate dye-swap pairs. A: Indirect comparison with a common reference B: Direct comparison C: Saturated design and D: Time course experiment loop design (White and Salamonsen, 2005, Reproduction, 130, 4, ©Society for Reproduction and Fertility. Reproduced by permission).

In reference design, a common reference sample is prepared (Fig. 1.4A). This reference sample is used as an internal comparison standard and is prepared by

combining equal amounts (in terms of concentration) of total RNA from different tissues to obtain the widest possible representation of the entire transcriptome; alternative, it is a pool of RNA from the different samples under study (Kim et al., 2002; Novoradovskaya et al., 2004). Genomic DNA has also been used as a universal reference sample in a reference design with two color DNA hybridization microarrays (Gadgil et al., 2005). It is noteworthy that while most studies use reference samples for comparison with the experimental samples, some reports stress that reference sample and reference design is inefficient (Churchill, 2002; Kerr and Churchill, 2001b). In reference design, half of the hybridization experiments are performed on the reference sample, which is probably of no interest.

Although reference design has some advantages, a balanced block design (direct comparison) is preferable because of the gain in efficiency (Dobbin and Simon, 2002). For n samples, n hybridizations can be achieved with direct comparisons but reference design will require 2n hybridizations. Balanced block design does not need reference RNA because it allows direct comparison of case samples on the same microarray with balanced dyes. If there are more than two treatments in the experiment, saturated design may be applied (White and Salamonsen, 2005). Block design have been embedded in the scheme of saturated design (Fig. 1.4C).

In comparison, loop design is usually used in time course experiments and connects the samples in a loop pattern (Fig. 1.4D). It has been proven that loop design is preferable for comparisons between sequential time points (Yang and Speed, 2002). Compared to reference design, loop design is not effective for cluster analysis because

the comparison of two samples far away in the loop involves other samples in between as well (Kerr and Churchill, 2001a). Furthermore, loop design is less efficient than block design for class comparisons because it requires more sophisticated method of analysis (Churchill, 2002).

Sometimes pooling of RNA samples from several subjects is used in microarray experiments when sufficient RNA from individual sample for hybridization can not be obtained. Additionally, it is recommended that pooling biological samples is only appropriate when less than three arrays are used in each condition (Kendziorski et al., 2005). Although a pooling strategy can decrease unwanted biological variability while reducing the number of microarrays used, it should be avoided when the samples can't be synchronized (Sasik et al., 2004).

Replicates

The use of replicates can help distinguish the truly DE genes from those affected by chance alone. This enables researchers to estimate accurately biological variation and minimize the systemic variation through average among replicates.

There are generally two types of replicates in microarray experiments: biological and technical (Churchill, 2002). Biological replicates are replicates that taken RNA samples under the same condition but from different individuals and they are used to address the biological variability (e.g., animal-animal variation). We need to include enough biological replicates in order to make inferences about the population. Technical replicates are replicates that use the same RNA samples multiple times to reduce technical variability between experiments such as RNA isolation, labeling, and

hybridization. Two levels of technical replicates have become standard in microarray experiments: dye swapping and replication of spotting genes on the array. Biological replicates are more important than technical replicates because biological variation is greater than technical variation (Sasik et al., 2004). The number of replicates required for a microarray experiment depends on the type of experiment. In theory, at least five biological replicates are needed for sufficient statistical power, though the best results in statistical analysis are obtained using eight to 15 replicates (Pavlidis et al., 2003). In practice, a minimum of three biological and at least two technical replicates are needed for microarray experimental design (Foster and Huber, 2002; Lee et al., 2000).

Dye bias

In dual color microarray experiments, for certain genes, the Cy3/green channel is always brighter than Cy5/red channel though the expression is the same. This is called dye bias (Dobbin et al., 2005). Furthermore, Cy5 dye is affected by ozone (Branham et al., 2007; Fare et al., 2003). There are four different types of dye bias: "(1) dye bias that is the same for all genes; (2) dye bias that relies on the spot intensity; (3) gene specific dye bias; (4) dye bias that depends on both the sample and the gene" (Dobbin et al., 2005). Type 1 and 2 dye biases can be eliminated by normalization procedures. Type 3 dye bias can't be suppressed by a locally weighted scatterplot smoothing regression (LOWESS) normalization technique (Yang et al., 2002) but can be avoided by statistical analysis. It is difficult to eliminate type 4 dye bias but it was shown to have little effect on the gene expression difference estimation (Dobbin et al., 2005).

For certain genes, the bias is influenced by the dye orientation. This is gene specific dye bias (Kerr, 2003; Tseng et al., 2001). In order to minimize labeling error caused by the gene specific dye effects, the complete dye swap by reversing the dye orientation is an effective way accounting for gene specific dye bias. Dye swap involves changing the dyes used for labeling and prevents the sample being labeled by a single dye. It is recommended to use dye swap in dual color experiments if possible for gene specific dye effect (Martin-Magniette et al., 2005; Yang and Speed, 2002).

Normalization

Normalization is an important preprocessing step in microarray data analysis to adjust individual hybridization intensities to enable meaningful biological comparisons. The statistical tests for differential expression analysis are highly dependent on the choice of normalization methods. The assumption underlying microarray analysis is that the fluorescence signal intensities represent relative mRNA expression levels. However, there are many sources of variation throughout the experiments, such as RNA quality, target labeling, dye incorporation, hybridization, image analysis, and scanner photomultiplier tube (PMT) settings. These systematic variations can be categorized into three: biological, technical and residual variations (Chen et al., 2004).

Normalization is needed to eliminate systematic variation from microarray data and the assumption of normalization is that "the majority of genes on the microarray are not differentially expressed" (Benes and Muckenthaler, 2003; Quackenbush, 2002; Yang, 2008). Generally there are three normalization techniques: total intensity normalization, normalization using regression techniques and normalization using ratio

statistics (Quackenbush, 2001). Normalization consists of two steps: within array normalization and between array normalization.

Yang and coworkers suggest using a non-linear LOWESS regression normalization algorithm for two channel microarrays as they found that this method accounts for intensity and spatial dependent dye bias (Yang et al., 2002). LOWESS normalization is a within array normalization method. Loess, a variant of LOWESS, can also be used for intensity dependent bias elimination. However loess uses a quadratic polynomial and LOWESS uses a linear polynomial (Do and Choi, 2006). Global loess normalization is a form of loess normalization and is usually used to address intensity dependent bias (Bolstad et al., 2003). This normalization assumes the intensity-based bias is global and normalization is applied to the entire data set. Additionally, print-tip LOWESS and print-tip loess are used for normalization considering local effects (i.e., print-tip spatial effect) (Leung and Cavalieri, 2003). LOWESS and Loess can fit in an MA plot where M is the log intensity ratio of the two channels, i.e., $M= \log_2 (Cy5/Cy3)$ and A is the average log intensity values across the two channels, i.e., $A= [\log_2 (Cy5)+\log_2 (Cy3)]/2$. MA plot has been widely used as a diagnostic tool for normalization. A common array dye-swap (CADS) normalization method has been suggested for two channel microarrays and it can remove both dye bias and array effects under general assumptions (Dabney and Storey, 2007).

Alternatively, mixed analysis of variance (ANOVA) models can be applied to normalize microarray data and this method can correct for extraneous effects such as dye and array effects (Cui and Churchill, 2003; Kerr et al., 2000). Scale normalization is

further applied between arrays so that each array has equal median value (Smyth and Speed, 2003). For single channel arrays, the quantile method is proposed to use for normalization (Bolstad et al., 2003). This method is based on quantiles and creates identical distributions of probe intensities for all arrays. Comparative study of the effects of different normalizations (i.e., global normalization, LOWESS normalization and variance stabilization normalization) on the list of DE genes has shown that there are differences among the normalization performances (Chiogna et al., 2009). This study also demonstrated that the data preprocessing, such as negative spot value handling in the case of high background, has a large effect on the list of DE genes, and the combination of two normalizations is effective on the identification of true DE genes (Chiogna et al., 2009). Many freely available software tools for microarray normalization have been developed, such as the Bioconductor project (http://www.bioconductor.org/) in the R statistical computing environment (Gentleman et al., 2004). There is, however, no widely accepted method of microarray data normalization and the combination of different normalizations works well with regard to the identification of DE genes (Chiogna et al., 2009).

MICROARRAY APPLICATION IN THE HORSE - AN OVERVIEW

One of the first microarray experiments in horses used a human cDNA microarray in order to understand the gene regulation during the initiation of spermatogenesis (Ing et al., 2004). Ninety-three genes were identified as differentially expressed between light and dark testicular tissues. In addition, among these DE genes, DYS, DOC1, and GLG1 were highly expressed in dark testis tissue and ODF2 and PDE3B were more expressed

in light testis tissue (Ing et al., 2004). Recently, a human extracellular matrix and adhesion molecule cDNA GEarray (SuperArray Biosciences Co., Fredrick, MD) was used to show that the MMP13 expression level was up-regulated in the granulation tissue of equine digital flexor tendonitis compared to normal tendon in the horse (Nomura et al., 2007). The localization and preferential expression of MMP13 in the granulation tissue of tendonitis indicated that MMP13 may play essential role in tendonitis (Nomura et al., 2007). Another study used a 22,000 Human Genome U133 Plus 2.0 Gene Chip (Affymetrix) to study gene expression profiles during recurrent airway obstruction (RAO) and identified 46 DE genes between RAO-affected horses and the controls (Ramery et al., 2008). STAT3, MARCKS, PTX3, CYBB, PTPRC and BTG1 have potentially functional relevance to RAO among these DE genes (Ramery et al., 2008). It was concluded that since the findings were based on a human expression microarray, studies using equine specific array are needed to fully verify and understand the expression profiles of genes involved in RAO. For example, the human array failed to detect some genes known to be implicated in RAO, such as IL-1β and IL-8 (Ramery et al., 2008).

Some equine studies have used mouse microarrays. Mucher and co-workers (Mucher et al., 2006) utilized a mouse 15,000 cDNA microarray to investigate the gene expression profiles in equine muscle tissues. The results detected 71 DE genes between *gluteus medius* and *longissimus lumborum* muscle and demonstrated the feasibility of using mouse cDNA array to study gene expression profiling of genes involved in equine muscles after exercise (Mucher et al., 2006). Another study used the same mouse cDNA

microarray to investigate gene expression patterns in blood cells of horses who successfully complete competition (S) and those who were disqualified (D) due to metabolic disorders. The comparison showed 130 genes were up-regulated and 288 genes were down-regulated between the successful and disqualified horses, and gene ontology analysis showed that more genes were up-regulated in S than in the D group of animals (Barrey et al., 2006), indicating long exercise affects significant gene expression changes in leukocytes.

The first horse specific expression microarray (Affymetrix Equine Gene Chip) was created using 25-mer oligo probes corresponding to 3,098 equine specific genes (Gu and Bertone, 2004). The utility of this array was evaluated by addition of LPS into equine synoviocytes and 102 genes had changed their expression and many of them encoding inflammatory mediators were up-regulated (Gu and Bertone, 2004). The first study using this array investigated the correlation between the histologic and morphologic signatures through changes in the gene expression patterns in horses with osteoarthritis. Articular cartilage from horses with osteoarthritis in the palmar and dorsal region had different gene expression profiles, compared with control cartilage from normal joints. The authors concluded that the transcriptomic changes were in accordance with the structural features (Ramery et al., 2009; Smith et al., 2006a). Another study using this array investigated transcriptional changes of equine fibroblasts transformed by bovine papillomavirus-1 (BPV-1). A total of 81 genes in the transformed cell line had differential expression compared to the control cell line (Yuan et al., 2008). The results suggested that genes involved in cell adhesion and motility increased their expression

and some genes involved in the immune response decreased their expression during sarcoid development.

Recently, three equine tissue specific cDNA microarrays have been described. One is a 9,367 element equine articular cartilage cDNA microarray (Mienaltowski et al., 2008) that was used to identify genes with a cartilage-restricted pattern of expression (Mienaltowski et al., 2009). The results indicated that different transcriptional profiles present in normal articular cartilage and repair tissue and further study of the factors which lead to this transcriptional difference may help understand repair process. Another tissue specific cDNA microarray was developed and has been applied to study gene expression profiles in leukocytes stimulated *in vitro* with LPS, peptidoglycan or lipoteichoic acid (Vandenplas et al., 2005). An equine specific cDNA microarray, constructed mostly from equine leukocyte cDNA library, has been used to study transcriptional changes during the early stages of equine laminitis (Noschka et al., 2008). In 2008, the first species-specific whole-genome expression oligoarrays were created for the horse. One of these is a 12,000 element equine 25-mer whole transcript oligonucleotide microarray (Affymetrix) that combines equine ESTs, annotated mRNAs, and selected human sequence information (Glaser et al., 2009). This array has been validated in cartilage tissue with good performance and will be useful to study equine diseases. The other is a 21,000 element 70-mer oligo-based-array that uses the available equine EST sequences and the recent horse whole genome sequence data (Bright et al., 2009). The latter is currently the most comprehensive expression microarray available for the horse (Chowdhary and Raudsepp, 2008). The array has been

used in this study and is described in detail (materials and methods section of Chapter III, pages 74 to 75). In summary, human cDNA/oligoarray (22,000), mouse cDNA (15,000), bovine oligoarray (15,000), equine cDNA array (3,076 and 9,367) and oligoarray (3,098) have been used for gene expression study in equine tissues.

THE USE OF EXPRESSION MICROARRAYS TO STUDY LAMINITIS

The equine-specific 3,076 gene cDNA microarray has been used to study gene expression changes in laminar tissue at different time points after BWE administration (Noschka et al., 2008). The results showed that genes associated with inflammation and leukocyte activation, including monocyte chemotactic protein 3 (MCP-3), monocyte chemoattractant protein 1 (MCP-1), chemokine (C-X-C motif) ligand 10 (CXCL10) and ICAM-1 were up-regulated as early as 1.5 h following BWE administration. The results suggested that inflammatory response occurs at early developmental stage of BWE model of laminitis. While these initial attempts using an expression array are worth notating, the array has only 3,076 probes, and thus does not contain many genes that could potentially be involved in modulating changes observed during early stages of the disease.

More recently a 15,000 element bovine microarray chip was used to assess gene expression patterns in the developmental stage of the OF model of laminitis (Budak et al., 2009). The authors found 155 up-regulated genes and none down-regulated in the laminitis group compared to the controls. Further, the up-regulated genes were predominantly involved in inflammatory response and protein turnover (Budak et al., 2009). The results concluded that inflammation occurs at the early developmental stage

of the OF model of laminitis. The authors recognized several limitations of their use of bovine microarray to study equine laminitis. Cross-species hybridization may generate false negative results. Furthermore, 15,000 bovine microarray may fail to identify all the genes with differential expression in the laminar tissue. While cross-species hybridization in microarrays have been used to study equine gene expression, some equine genes with low level of sequence homology with bovine, mouse or human homologues cannot be detected (Ing et al., 2004; Ramery et al., 2008).

Thus, it is evident that the two expression arrays used previously have inherent limitations that limit our ability to draw meaningful conclusions regarding the potential genetic pathways and gene networks associated with the pathogenesis and progression of equine laminitis on a genome-wide scale. Although microarray technology is a comprehensive and powerful functional genomics tool, it has some limitations in disease characterization such as background noise. However, microarray–based genome-wide expression study and recently developed next generation sequencing–based technology for transcriptome profiling are complementary approaches for gene expression studies (Coppée, 2008). Also, microarray is much less costly than RNA sequencing (RNA-Seq) which uses deep sequencing technology. Therefore DNA microarray is still a valuable platform for studying complex diseases. A comprehensive equine whole-genome microarray is needed in order to investigate global gene expression changes in equine disease studies.

We recently developed a comprehensive equine-specific ~21,000 element expression microarray at Texas A&M University for functional analysis of the equine

genome (Bright et al., 2009). This TAMU oligoarray was constructed using a 2.4 Gb whole genome sequence of the horse genome (EquCab2; http://www.broad.mit.edu/mammals/horse/), to which the following available information was added: RefSeq release 26, UniGene build#3, SwissProt release 12 and ~43,000 unpublished ESTs, to identify genes and develop oligos specific for genes. The array thus developed is thus by far the most representative expression microarray tool for examining the equine transcriptome. In this study we utilized the TAMU whole-genome oligoarray to investigate global laminar tissue gene expression changes during the early stages of three different experimentally induced models of equine laminitis. Because the initial stages of laminitis are critical in understanding the progression of the disease, we embarked on identifying the genes and their likely interactions that lead to observed pathological changes during these stages. Knowing the gene expression changes within the laminar tissues during development and progression of laminitis will lead to new ways to predict the outcome of disease and design therapies for treatment/prevention.

THE HYPOTHESES AND OBJECTIVES OF THE DISSERTATION

Various causes of laminitis lead to altered gene function and regulation in the laminar tissue during the developmental and subsequent/advanced stages of the disease. These changes reflect the gross and histological changes that are characteristic of various stages of the disease. Hence our hypothesis is that: *registering gene expression patterns in the laminar tissue at various time-points during the progression of the disease and comparing them in relation to expression in normal laminar tissue will provide insight into the molecular mechanisms associated with the progression of the disease*. In this

dissertation, our focus is on three different models of laminitis and we target the initial stages of the development of the disease, viz., developmental (DEV) and/or the Obel grade 1. The three models chosen for this work are CHO, HI and OF. While our **long-term goals** are to decipher the molecular mechanisms associated with the initiation and progression of laminitis for developing novel and effective approaches to treat the disease, **our goal in this dissertation research** is to understand the molecular processes modulating the initial phase of the disease in three different experimental models of laminitis that fairly closely mimic the acute form of naturally occurring laminitis (the CHO model), endocrinopathic laminitis (the HI model) and pasture associated laminitis (the OF model). Broadly, the specific objectives associated with the goal are to:

(1) identify genes differentially expressed during the early stages (i.e., developmental, Obel grade 1, etc.) of experimentally induced equine laminitis in relation to normal laminar tissue.

(2) perform gene ontology enrichment analysis to obtain information about the predominant functions of DE genes.

(3) identify pathways and associated genetic networks of the DE genes to understand their role during the pathogenesis of equine laminitis.

(4) validate the expression of DE genes that play a key role in above described pathways and networks by quantitative real time PCR.

We expect to find differences, as well as common features of the earliest changes in the laminar tissue among different models of laminitis during disease progression regardless of the triggering factors. The immediate goal and the objectives outlined

above are accomplished through three set of experiments each focusing on individual experimental model of laminitis, and are presented in this dissertation as Chapters III, IV and V as listed below:

1. Genome-wide transcriptome analysis of laminar tissue during the developmental stage and the onset of carbohydrate overload induced equine laminitis
2. Gene expression profiling in induced laminitic horses by prolonged hyperinsulinaemia using an equine whole genome oligoarray
3. Transcriptome profiling of laminar tissue during the early stages of oligofructose induced laminitis in the horse

RATIONALE AND SIGNIFICANCE OF THE PRESENT STUDIES

Equine laminitis is a debilitating disease that causes extreme sufferring in afflicted horses and often results in a lifetime of chronic pain. The economic impact of this disease on the horse industry is also significant as a result of veterinary expenses, cost of long-term care, and loss of use of the animal. The exact sequence of pathophysiological events culminating in laminitis has not yet been characterized, and this is reflected in the lack of any consistently effective therapeutic strategy. The development of more effective therapeutic & preventive strategies requires a better understanding of disease initiation and progression.

Two expression arrays have been used for equine laminitis study. One is equine-specific 3,076 gene cDNA microarray to study gene expression at 1.5, 3 and 12 h of BWE model of laminitis. Another study is that bovine 15,000 bovine microarray was used to investigate gene expression patterns in the developmental stage (24-32 h) of OF

model of laminitis. These two expression arrays used have limitations. For these reasons, an equine specific whole-genome microarray is necessary in order to get broad picture about the gene expression changes during early stages of equine laminitis.

Furthermore, CHO, HI and OF models of laminitis represent most common natural causes of laminitis. Transcriptomic analysis of early stages of different models of laminitis will provide information about gene expression changes resulting from different causes. The common differentially expressed genes identified in this study will be excellent candidates for future functional study and will be potentially therapeutic targets for laminitis treatment.

The rationale of this project is that if we obtain detailed knowledge about the transcriptome expression profiles of laminar tissue of horses at risk for laminitis (i.e., the developmental stage) and at onset when horses first exhibit clinical sign of laminitis (i.e., Obel grade 1 laminitis stage), a clearer picture of the gene expression changes, metabolic pathways, and genetic networks that accompany the development and progression of laminitis will be obtained. This will, in turn, lead to new ways to help develop potential preventions and therapeutic strategies. This could include the design of antagonist or agonist compounds that target the key gene receptor, inhibitor or activator of the target enzyme(s), or anti-inflammatory drugs for equine laminitis that could particularly be affective during early stages of the disease.

The proposed research is innovative because no high-density equine oligonucleotide microarray has been applied in the study of equine laminitis before. In addition, the CHO model of laminitis is more similar to naturally occurring laminitis and

thus superior to the BWE model of laminitis used by the studies of Noschka and co-workers (Noschka et al., 2008). Further, the time points used for OF model of laminitis in our study (i.e., 12 h and 24 h time points) is earlier than that of previous study (24-30 h; Budak et. al., 2009); we may find the very early expression changes in laminar tissue. The knowledge obtained from this study will help us to formulate new effective strategies to prevent and treat this disease.

CHAPTER II

MATERIALS AND METHODS

LAMINAR SAMPLES ACQUISITION

CHO samples

Fifteen clinically normal Quarter horses (10 mares and 5 geldings) between 3 to 12 years old were used in this study. The Animal Care and Use Committee at the Ohio State University approved the experimental protocol. The control samples were obtained 24 h following saline injection (CON, n=5). The experimental samples were obtained at two stages after CHO (starch) administration at a concentration of 17.6 g/kg of body weight via a nasogastric tube according to the method of Garner and coworkers (Garner et al., 1975): a developmental (DEV) group at the onset of fever (12-22 h, DEV, n=5) and Obel grade 1 (OG1) laminitis group at the onset of lameness (20-48 h, OG1, n=5). Physical examination including the measurement of rectal temperature and evaluation of lameness was performed every two hours. Onset of fever means rectal temperature increased two degrees above the starting temperature of individual horse following CHO administration. Samples were collected following euthanasia with pentobarbital sodium and phenytoin sodium and as described earlier (Belknap et al., 2007; Pollitt, 1996). Briefly, the forelimbs were removed by disarticulation of the metacarpophalangeal joint from each horse and sagittal sections of the digit were cut with a band saw. Blocks of laminar tissue were obtained from the mid-point between the level of the coronary band and the ground-bearing surface on the dorsal aspect of the foot by sharp dissection. The

samples were immediately frozen in liquid nitrogen and stored at -80°C following collection. Frozen laminar tissue samples (kindly provided by Dr. James Belknap, Department of Veterinary Clinical Sciences, Ohio State University) were shipped on dry ice for use in our laboratory.

HI samples

Eight clinically normal Standardbred horses ranging from 3-7 years in age were used for this study (7 geldings, 1 filly). The horses were assigned into 4 pairs. Within each pair, one was assigned randomly to control (n=4) or experimental groups (n=4). The Animal Ethics Committee of the University of Queensland approved the experimental protocol. Samples were obtained from horses developed Obel grade 2 laminitis within 48 h (44-48 h, n=4) after hyperinsulinaemia was induced by constant infusion of insulin and from control horses received saline infusion for the same period as their paired horse (de Laat et al., 2010). Physical examination including body temperature, heart rate and respiration rate was recorded. Samples were collected following euthanasia with pentobarbital sodium and as described earlier (de Laat et al., 2010; Pollitt, 1996). Briefly, all hooves of each horse were disarticulated at the metacarpophalangeal joint. The foot was sectioned with a band saw and middle portions of the dorsal hoof wall laminae were obtained and snap frozen in liquid nitrogen and stored at -80°C. The time between disarticulation and snap freezing was less than 5 min. Frozen laminar tissue samples (kindly provided by Dr. Christopher Pollitt, Australian Equine Laminitis Research Unit, the University of Queensland and Dr. Hannah

Galantino-Homer, Laminitis Institute, University of Pennsylvania) were shipped on dry ice for use in our laboratory.

OF samples

Eighteen clinically normal Standardbred horses (3 mares, 15 geldings) from 2 to 12 years of age were used in this study. The Animal Ethics Committee of the University of Queensland approved the experimental protocol. The animals were divided into three groups: control (CON; n=6) animals given water, experimental animals fed oligofructose for 12 h (12 h; n=6) and 24 h (24 h; n=6) at a concentration of 10g/kg of body weight via a nasogastric tube according to the method described by van Eps and Pollitt (van Eps and Pollitt, 2006). Physical examination including the measurement of rectal temperature and evaluation of lameness was performed every two hours. Twelve and 24 hours post OF administration the horses were anaesthetized with xylazine and ketamine and a rubber tourniquet was applied to the fetlock of one fore foot which was then disarticulated through the distal metacarpophalangeal joint. The foot was sectioned with a band saw and middle portions of the dorsal hoof wall laminae were obtained and snap frozen in liquid nitrogen and stored at -80°C. The time between disarticulation and snap freezing was always less than 5 min. After this procedure was repeated on the opposite fore foot the horse was euthanized by overdosing with pentobarbital sodium. Frozen laminar tissue samples (kindly provided by Dr. Christopher Pollitt, Australian Equine Laminitis Research Unit, the University of Queensland and Dr. Hannah Galantino-Homer, Laminitis Institute, University of Pennsylvania) were shipped on dry ice for use in our laboratory.

MICROARRAY EXPERIMENTAL DESIGN

CHO experiment

A two color, balanced design was used for microarray hybridizations. Three different comparisons were performed (DEV vs. CON, OG1 vs. CON, and DEV vs. OG1) as shown in Figs 2.1-2.3. Five biological replicates were included in each comparison. Dye swap was embedded in biological replicates to eliminate dye bias. The dyes and samples were balanced throughout 15 hybridizations (five laminar samples from controls labeled with Cy5 and five laminar samples from controls labeled with Cy3, five laminar samples from horses at the developmental stage labeled with Cy5 and five laminar samples from horses at the developmental stage labeled with Cy3, and five laminar samples from horses at the Obel grade 1 stage labeled with Cy5 and five laminar samples from horses at the Obel grade 1 stage labeled with Cy3). A total of 15 slides (5 slides per comparison) were used.

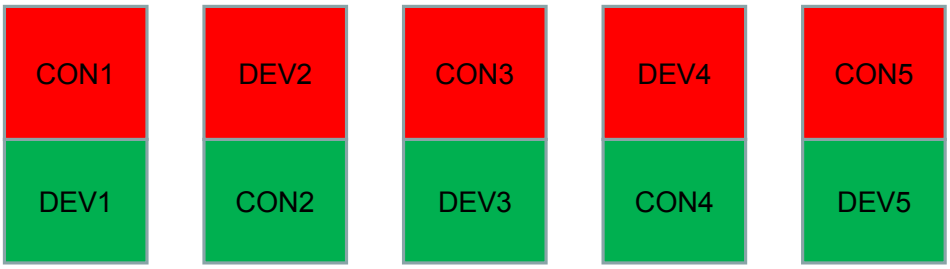

Fig. 2.1. Experimental design of the comparison of developmental (DEV) vs. control (CON). The green color represents Cy3 and the red color represents Cy5. The laminar samples labeled with CON1, CON2, CON3, CON4, and CON5 were from control horses. The laminar samples labeled with DEV1, DEV2, DEV3, DEV4, and DEV5 were from horses at the developmental stage.

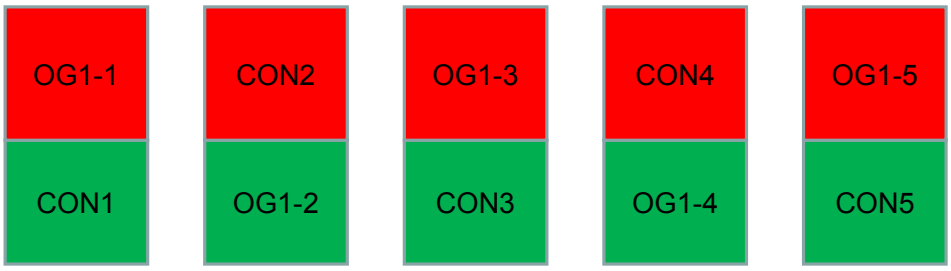

Fig. 2.2. Experimental design of the comparison of Obel grade 1 (OG1) vs. control (CON). The green color represents Cy3 and the red color represents Cy5. The laminar samples labeled with CON1, CON2, CON3, CON4, and CON5 were from control horses. The laminar samples labeled with OG1-1, OG1-2, OG1-3, OG1-4, and OG1-5 were from horses at the Obel grade 1 laminitis stage.

Fig. 2.3. Experimental design of the comparison of developmental (DEV) vs. Obel grade 1 (OG1). The green color represents Cy3 and the red color represents Cy5. The laminar samples labeled with DEV1, DEV2, DEV3, DEV4, and DEV5 were from horses at the developmental stage. The laminar samples labeled with OG1-1, OG1-2, OG1-3, OG1-4, and OG1-5 were from horses at the Obel grade 1 laminitis stage.

HI experiment

A two color, balanced block design was used for microarray hybridizations. The hybridizations were carried out based on their matched pairs during HI induction as shown in Fig 2.4. Four biological replicates were included in the comparison. Dye swaps

were incorporated into the hybridization scheme of the experiment. A total of four microarray slides were used.

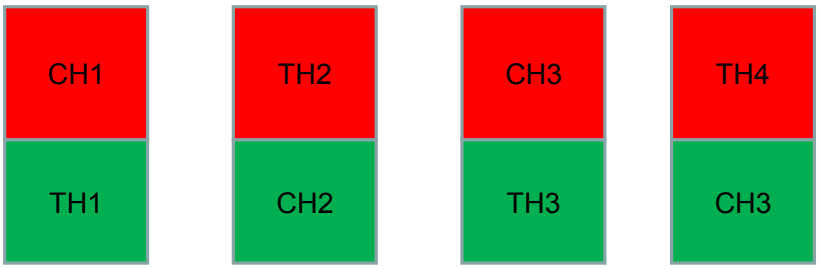

Fig. 2.4. Experimental design of the comparison of 48 h time point vs. control. The green color represents Cy3 and the red color represents Cy5. The laminar samples labeled with CH1, CH2, CH3, and CH4 were from control horses. The laminar samples labeled with TH1, TH2, TH3, and TH4 were from HI 48 h induced horses.

OF experiment

A two color, balanced design was used for microarray hybridizations. Three different comparisons were performed (12 h vs. CON, 24 h vs. CON, and 12 h vs. 24 h) as shown in Figs 2.5-2.7. Six biological replicates were included in each comparison. Dye swap was embedded in biological replicates to eliminate dye bias. Samples were paired to maximize similarity in age, sex and weight. The dyes and samples were balanced throughout 18 hybridizations (six laminar samples from controls labeled with Cy5 and six laminar samples from controls labeled with Cy3, six laminar samples from horses at the 12 h time point with OF induction labeled with Cy5 and six laminar samples from horses at the 12 h time point with OF induction labeled with Cy3, and six laminar samples from horses at the 24 h time point with OF induction labeled with Cy5

and six laminar samples from horses at the 24 h time point with OF induction labeled with Cy3). A total of 18 slides (6 slides per comparison) were used.

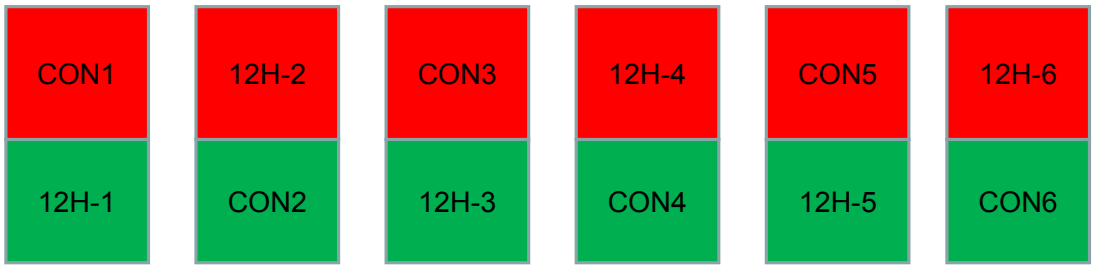

Fig. 2.5. Experimental design of the comparison of 12 h time point (12H) vs. control (CON). The green color represents Cy3 and the red color represents Cy5. The laminar samples labeled with CON1, CON2, CON3, CON4, CON5, and CON6 were from control horses. The laminar samples labeled with 12H-1, 12H-2, 12H-3, 12H-4, 12H-5, and 12H-6 were from horses at the 12 h time point.

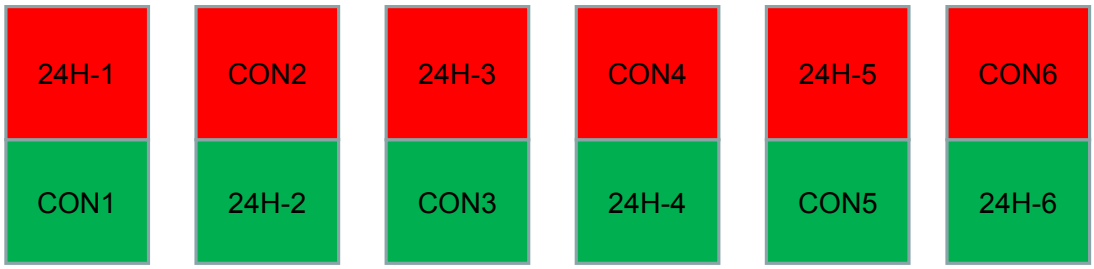

Fig. 2.6. Experimental design of the comparison of 24 h (24H) time point vs. control (CON). The green color represents Cy3 and the red color represents Cy5. The laminar samples labeled with CON1, CON2, CON3, CON4, CON5, and CON6 were from control horses. The laminar samples labeled with 24H-1, 24H-2, 24H-3, 24H-4, 24H-5, and 24H-6 were from horses at the 24 h time point.

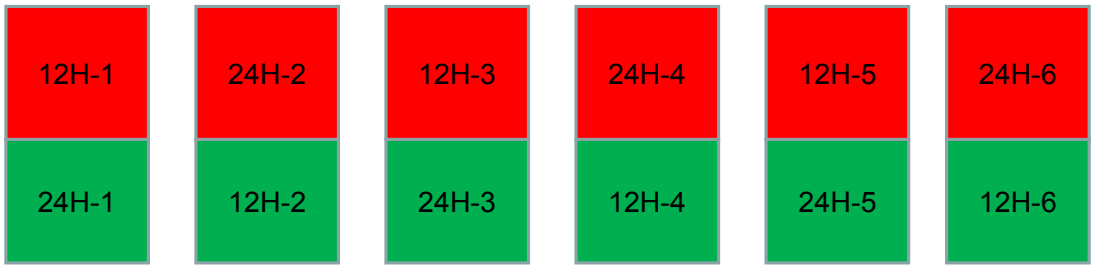

Fig. 2.7. Experimental design of the comparison of 12 h (12H) time point vs. 24 h time point (24H). The green color represents Cy3 and the red color represents Cy5. The laminar samples labeled with 12H-1, 12H-2, 12H-3, 12H-4, 12H-5, and 12H-6 were from horses at the 12 h time point. The laminar samples labeled with 24H-1, 24H-2, 24H-3, 24H-4, 24H-5, and 24H-6 were from horses at the 24 h time point.

RNA ISOLATION

Total RNA was isolated from frozen laminar samples using Tri reagent (MRC, Cincinnati, OH) following RNA cleanup with RNase-free DNase treatment (Qiagen, Valencia, CA) according to the manufacturer's protocol. Briefly, 80-100 mg of frozen laminar tissue sample was disrupted using a mortar and pestle in liquid nitrogen followed by homogenization using a needle (18 gauge 1 1/2, PrecisionGlide®) and syringe (10 ml NORM-JECT®) (Fisher Scientific, Pittsburgh, PA) in Tri reagent. Then RNA was purified by bromochloropropane (BCP) and precipitated with isopropanol. After centrifugation, the RNA pellet was washed with 70% ethanol and then with 100% ethanol and dissolved in 100 µl RNase-free water. The RNA was cleaned up following the Qiagen RNeasy cleanup protocol (RNeasy Mini Kit, Qiagen, Valencia, CA). RNA was eluted with 35 µl RNase-free water. RNA concentration was quantified using a

spectrophotometer (NanoDrop Technologies, Wilmington, DE) and the quality was evaluated using an Agilent 2100 Bioanalyzer and RNA Lab Chip – RNA 6000 Nano Assay (Agilent Technologies, Palo Alto, CA).

MICROARRAY HYBRIDIZATION

Pre-hybridization treatment of microarray slide

The microarray slide rehydration and crosslinking step was done to make sure that the probe was spread evenly in the spot and immobilized on the slide. A water bath was set at 50°C and a heat block was set at 65°C. The slides were rehydrated by holding the slide label side down (spots down) over the steam from the 50°C water bath for 10 sec and making sure spots don't over hydrate and merge. Then the slides were snap dried for 5 sec on the heat block with label side up. At the end the slides were brought to room temperature (20°C) for 1 min. The process was repeated up to four times. After rehydration, the slides were subjected to "crosslinking". The crosslinking steps were as follows: a UV crosslinker was turned on and the energy level was set at 750 MJ/CM^2. A piece of clean Kim Wipe was put inside the UV crosslinker and the START button was pressed. The slides were exposed to UV for 2 minutes. The slides were ready for hybridization after the exposure was finished.

CHO experiment

(1) cDNA synthesis and labeling

Labeled cDNAs were synthesized from total RNA with the **3DNA Array 350 Expression Array Detection Kit** (Genisphere, Hatfield, PA). This kit was developed based on 3DNA dendrimer technology and dendrimer-based detection system has shown

ideal signal detection for DNA microarrays (Stears et al., 2000). Three micrograms of total RNA was combined with 1 µl of 1pmol/µl oligo-d(T) primer in a final volume of 11 µl. The mixture was incubated at 80°C for 10 min and cooled on ice for 2 min. Four microliters of 5x SuperScript II first strand buffer, 1 µl of dNTP mix, 2 µl of 0.1M dithiothreitol and 1 µl of Superase-In RNase inhibitor were added to the RNA sample along with 1 µl of SuperScript II reverse transcriptase (200 U/µl) (Invitrogen, Carlsbad, CA). The reaction was incubated at 42°C for 2 hours. After that, 3.5 µl of 0.5M NaOH/50mM EDTA was added to degrade RNA with a 15 min incubation at 65°C. The reaction was neutralized with 5 µl of 1 M Tris-HCl (pH 7.5).

(2) Microarray cDNA hybridization and wash

A 580 µl reaction was used for the cDNA hybridization mix. Hybridization buffer (2x enhanced) was thawed and resuspended by heating at 70°C for 10 min. Then the buffer was vortexed and centrifuged at 4000 rpm for 1 min. The hybridization mix was constituted as follows: 28.5 µl of Cy3 cDNA and 28.5 µl of Cy5 cDNA were mixed with 2 µl of LNA dT blocker, 201 µl of nuclease-free water, 30 µl of 1x TE buffer and 290 µl of hybridization buffer (2x enhanced). The hybridization mix (580 µl) was gently vortexed, microfuged, and incubated at 75°C for 10 min. The mixture was again vortexed, microfuged and applied to the gasket slide of an Agilent microarray hybridization chamber. Considerable care was taken to prevent the mixture from splashing under the edges of the gasket slide. The microarray slide (array side down) was laid on top of the gasket slide and the hybridization chamber was subsequently assembled tightly. The hybridization chamber was rotated to make sure the gasket slide

was wet and the bubbles moved to the side and were removed. The slides were then incubated at 55°C while gently rotating at a speed of 5 rpm in a hybridization oven (Agilent Technologies, Santa Clara, CA) for 16 hours. After overnight incubation, the hybridization chamber was taken out of the incubator and disassembled. The "microarray-gasket slide sandwich" was soaked in a Wheaton jar with pre-warmed (42°C) 2x SSC-0.2% SDS wash buffer for 3 min while gently agitating up and down by hand. The array slide always remained in the solution. Then a tweezer was used to separate the microarray slide from the gasket slide until the gasket slide fell off. The slides were transferred to another Wheaton jar with pre-warmed (42°C) 2x SSC-0.2% SDS wash buffer and the holder with slides was agitated up and down 10 times and then incubated at 42°C for 15 min. Following this, the slides were transferred to a new Wheaton jar with 2x SSC wash buffer and the holder with slides was agitated up and down for 10 times and incubated at room temperature for 15 min. Following this, the slides were transferred to a new Wheaton jar with 0.2x SSC wash buffer and incubated and gently rinsed at room temperature for 15 min. The slides (label side up) were dried in a 50 ml conical tube with cap off and centrifuged at 1000 rpm for 4 min. Finally, the slides were put in a clean slide box and were stored prior to the second hybridization.

(3) 3DNA hybridization and wash

3DNA Array 350 capture reagents were thawed in the dark for 20 min at room temperature. The capture reagents were then vortexed, microfuged and incubated at 50°C for 10 min. At the same time, 2x SDS-based hybridization buffer was thawed and resuspended by heating at 70°C for 10 min. 3DNA hybridization master mix was

prepared by combining 2.5 µl of 3DNA Array 350 capture reagent 1 (Cy3, red cap tube), 2.5 µl of 3DNA Array 350 capture reagent 2 (Cy5, blue cap tube), 20 µl of nuclease-free water, 25 µl of 2x SDS-based hybridization buffer and 0.25 µl of anti-fade reagent. The 3DNA hybridization mix was incubated at 75-80°C for 10 min, applied to the array (label side) and covered with a coverslip in the dark. Care was taken to avoid any bubbles under the coverslip. The slide was placed in a 50 ml conical tube with 400 µl of nuclease-free water and incubated horizontally at 55°C in a hybridization oven (Agilent Technologies, Santa Clara, CA) for 4 hours in the dark. The cap of the tube was closed to maintain humidity.

All washing steps following 3DNA hybridization step were conducted in the dark. The 50 ml conical tube with the slide was taken out of the incubator and immersed in a Wheaton jar with pre-warmed (42°C) 2x SSC-0.2% SDS wash buffer. The cover slip was removed from the array slide by gently agitating the slide up and down without touching the bottom of the jar. The array slides were transferred to another Wheaton jar with pre-warmed (42°C) 2x SSC-0.2% SDS wash buffer and the holder with slides was agitated up and down for 10 times and incubated at 42°C for 15 min. The slides were then transferred to a new Wheaton jar with 2x SSC wash buffer and the holder with slides was agitated up and down for 10 times and incubated at room temperature for 15 min. Following this, the slides were transferred to a new Wheaton jar with 0.2x SSC wash buffer and incubated and gently rinsed at room temperature for 15 min. The slides (label side up) were dried in a 50 ml conical tube with the cap off and centrifuged at

1000 rpm for 4 min. Finally, the slides were put in a clean slide box and were stored for scanning.

HI and OF experiments

(1) cDNA synthesis

cDNAs were synthesized from total RNA with the **3DNA Array 900MPX Expression Array Detection Kit** (Genisphere, Hatfield, PA). This kit was also developed based on 3DNA dendrimer technology. Compared to 3DNA Array 350 Expression Array Detection Kit, it requires small amount of starting eukaryotic total RNA (0.5-2 μg). One microgram of total RNA was combined with 2 μl of random primer, 1 μl of MPX dT primer in a final volume of 11 μl. The mixture was incubated at 80°C for 10 min and cooled on ice for 2 min. Four microliters of 5x SuperScript II first strand buffer, 1 μl of dNTP mix, 2 μl of 0.1M dithiothreitol and 1 μl of Superase-In RNase inhibitor were added to the RNA sample along with 1 μl of SuperScript II reverse transcriptase (200 U/μl) (Invitrogen, Carlsbad, CA). The reaction was incubated at 42°C for 2 hours. After that, 3.5 μl of 0.5M NaOH/50mM EDTA was added to degrade the RNA with a 15 min incubation at 65°C. The reaction was neutralized with 5 μl of 1 M Tris-HCl (pH 7.5). At the end, 21.5 μl of 1x TE buffer was added to the reaction.

(2) cDNA purification, tailing and ligation

The cDNA was purified using the Qiagen MinElute PCR purification kit (Qiagen, Valencia, CA) according to the manufacturer's protocol. Briefly, 250 μl of buffer PB was added to the cDNA sample obtained above, mixed, and then applied to the MinElute column for centrifugation at 13,000 rpm for 1 min. The flow through was

discarded. Seven hundred microliters of ethanol-containing buffer PE was added to the MinElute column and centrifuged at 13,000 rpm for 1 min. The flow through was discarded. In order to get rid of the residual ethanol, the MinElute column was placed on the same collection tube and centrifuged at 13,000 rpm for additional 2 min. After centrifugation, 10 µl of buffer EB was added into the MinElute column placed on a 1.5 ml nuclease-free tube to elute cDNA. The MinElute column tube was incubated for 2 min at room temperature and centrifuged at 13,000 rpm for 2 min. Then nuclease-free water was added to the purified cDNA isolated in the 1.5 ml nuclease-free tube to a volume of 16.5 µl. The cDNA was incubated at 95°C for 10 min in a PCR thermal cycler and cooled on ice for 2 min.

The cDNA was tailed by terminal deoxynucleotidyl transferase (TdT) enzyme in a reaction of 25 µl. Purified cDNA was mixed with 2.5 µl of 10x tailing buffer, 4 µl of 10 mM dTTP, and 2 µl of TdT enzyme. The mixture was incubated at 37°C for 30 min and ligated to 3DNA capture sequence. The ligation steps were as follows: The tailed DNA was incubated at 95°C for 10 min in a PCR thermal cycler and cooled on ice for 2 min. Five microliters of 6x ligation mix and 2 µl of T4 DNA ligase were added to the tailed DNA and were incubated at room temperature for 30 min. Then, 3.5 µl of 0.5M EDTA was added to the ligation reaction and vortexed. Subsequently 14.5 µl of 1xTE buffer was added to the reaction to bring the total volume to 50 µl. The 50 µl tagged DNA was purified again using the Qiagen MinElute PCR purification kit (Qiagen, Valencia, CA) according to the manufacturer's protocol. The purified 10 µl of cDNAs were combined according to the experimental design of hybridization.

(3) Microarray tagged cDNA hybridization and wash

A 543 µl reaction was used for the tagged cDNA hybridization mix. Hybridization buffer (2x enhanced) was thawed and resuspended by heating at 70°C for 10 min. Then the buffer was vortexed and centrifuged at 4000 rpm for 1 min. The hybridization mix was constituted as follows: 10 µl of Cy3-cDNA and 10 µl of Cy5-cDNA were mixed with 2 µl of LNA dT blocker, 201 µl of nuclease-free water, 30 µl of 1x TE buffer and 290 µl of hybridization buffer (2x enhanced). The hybridization mix (543 µl) was gently vortexed, microfuged, and incubated at 75°C for 10 min. The mixture was again vortexed, microfuged and applied to the gasket slide of an Agilent microarray hybridization chamber. Considerable care was taken to prevent the mixture from splashing under the edges of the gasket slide.

The microarray slide (array side down) was laid on top of the gasket slide and the hybridization chamber was subsequently assembled tightly. The hybridization chamber was rotated to make sure the gasket slide was wet and the bubbles moved to the side and were removed. The slides were then incubated at 55°C while gently rotating at a speed of 5 rpm in a hybridization oven (Agilent Technologies, Santa Clara, CA) for 16 hours. After overnight incubation, the hybridization chamber was taken out of the incubator and disassembled. The "microarray-gasket slide sandwich" was soaked in a Wheaton jar with pre-warmed (42°C) 2x SSC-0.2% SDS wash buffer for 3 min while gently agitating up and down by hand. The array slide always remained in the solution. Then a tweezer was used to separate the microarray slide from the gasket slide until the gasket slide fell off.

The slides were transferred to another Wheaton jar with pre-warmed (42°C) 2x SSC-0.2% SDS wash buffer and the holder with slides was agitated up and down for 10 times and then incubated at 42°C for 15 min. Following this, the slides were transferred to a new Wheaton jar with 2x SSC wash buffer and the holder with slides was agitated up and down for 10 times and incubated at room temperature for 15 min. Following this, the slides were transferred to a new Wheaton jar with 0.2x SSC wash buffer and incubated and gently rinsed at room temperature for 15 min. The slides (label side up) were dried in a 50 ml conical tube with cap off and centrifuged at 1000 rpm for 4 min. Finally, the slides were put in a clean slide box and were stored prior to second hybridization.

(4) 3DNA hybridization and wash

3DNA Array 900MPX capture reagents were thawed in the dark for 20 min at room temperature. The capture reagents were then vortexed, microfuged and incubated at 50°C for 10 min. At the same time, 2x SDS-based hybridization buffer was thawed and resuspended by heating at 70°C for 10 min. 3DNA hybridization master mix was prepared by combining 2.5 µl of 3DNA Array 900MPX capture reagent 1 (Cy3, red cap tube), 2.5 µl of 3DNA Array 900MPX capture reagent 2 (Cy5, blue cap tube), 20 µl of nuclease-free water and 25 µl of 2x SDS-based hybridization buffer. The 3DNA hybridization mix was incubated at 75-80°C for 10 min, applied to the array (label side) and covered with a coverslip in the dark. Care was taken to avoid any bubbles under the coverslip. The slide was placed in a 50 ml conical tube with 400 µl of nuclease-free water and incubated horizontally at 55°C in a hybridization oven (Agilent technologies,

Santa Clara, CA) for 4 hours in the dark. The cap of the tube was closed to maintain humidity.

All washing steps following 3DNA hybridization step were conducted in the dark. The 50 ml conical tube with the slide was taken out of the incubator and immersed in a Wheaton jar with the pre-warmed (42°C) 2x SSC-0.2% SDS wash buffer. The cover slip was removed from the array slide by gently agitating the slide up and down without touching the bottom of the jar. The array slides were transferred to another Wheaton jar with pre-warmed (42°C) 2x SSC-0.2% SDS wash buffer and the holder with slides was agitated up and down for 10 times and incubated at 42°C for 15 min. The slides were then transferred to a new Wheaton jar with 2x SSC wash buffer and the holder with slides was agitated up and down for 10 times and incubated at room temperature for 15 min. Following this, the slides were transferred to a new Wheaton jar with 0.2x SSC wash buffer and incubated and gently rinsed at room temperature for 15 min. The slides (label side up) were dried in a 50 ml conical tube with the cap off and centrifuged at 1000 rpm for 4 min. Finally, the slides were put in a clean slide box and were stored for scanning.

MICROARRAY IMAGE PROCESSING

The slides were scanned with a GenePix Personal 4000B microarray scanner (Molecular Devices Corporation, Sunnyvale, CA) at 5 μm resolution and the images were saved in 16-bit multi-image Tagged Image Format File (TIFF) format. A preview scan was conducted to view the entire slide and select the area on the array that will be scanned at high resolution. During the preview scan, the photomultiplier tube (PMT)

voltage setting was adjusted so that the ratio of the intensities of both channels (635 nm and 532 nm) is around 1. Channel Cy5 is excited by 635 nm red laser light and channel Cy3 is excited by 532 nm green laser light. The histogram tab in the GenePix Pro 6.0 program (Molecular Devices Corporation, Sunnyvale, CA) for GenePix microarray scanners can be used as reference for PMT adjustment. The PMT voltage is optimal when the lines representing both channels approximately overlap in the histogram tab. Once the array was scanned, a GenePix Array List (GAL) file was loaded into the GenePix Pro 6.0 program. The GAL file provided position and identity information of each spot on the array. Each spot was visually inspected by manual gridding. All aberrant (e.g., high background, dust, and scratch) and empty spots were flagged and excluded from further analysis. The fluorescence intensities of all spots from each array were quantified using GenePix Pro 6.0 program and saved as GenePix Results (GPR) file.

DIFFERENTIAL EXPRESSION DATA ANALYSIS

CHO experiment

The subset signal intensity data of GPR file including the median of signal intensity and local background of both channels (F635 median, F532 median, B635, and B532, F635 median: the foreground median intensity value of all pixels at the red channel (635 nm), F532 median: the foreground median intensity value of all pixels at the green channel (532 nm), B635: the background intensity value of all pixels at the red channel, B532: the background intensity value of all pixels at the green channel) were used as input into R statistical computing environment R.10.0 (Ihaka and Gentleman,

1996) (http://www.r-project.org/). LOWESS normalization was applied to the signal intensity data to eliminate intensity-dependent dye bias (Yang et al., 2002). It is based on the fact that the quantified signal intensities are usually related nonlinearly to the expression level of the corresponding genes (Ramdas et al., 2001). The efficiency of LOWESS normalization was evaluated by checking Cy5 intensity-Cy3 intensity plot for data from each array before and after LOWESS normalization. The normalized data was then analyzed using a mixed model approach in SAS (SAS 9.1.3) (SAS Institute Inc. Cary, NC). The mixed model including treatment (fixed effect), dye (fixed effect), and array (random effect) was used to identify significantly differentially expressed genes. The SAS estimate function was used to test the statistical significance between conditions and the output file with P value and natural logarithms of fold change of each gene was obtained.

HI and OF experiments

The microarray data were analyzed using the bioconductor (http://www.bioconductor.org/) (Gentleman et al., 2004) LIMMA (linear models for microarray data) package version 3.4 in the R statistical computing environment R.10.0 (Ihaka and Gentleman, 1996) (http://www.r-project.org/). LIMMA is a software package that uses linear models to assess differential expression (Smyth, 2004). The signal intensity file including the median of signal intensity and local background of both channels (F635 median, F532 median, B635, and B532) was used as input into LIMMA program. The foreground median signal intensity was background corrected for each spot. Those spots with negative background corrected intensity in both channels across

all replicated slides were filtered. The default print-tip loess normalization was then applied to each array as recommended by Smyth and Speed (Smyth and Speed, 2003). Scale normalization was performed between arrays if there was evidence of a scale difference. The quality of the microarray data was evaluated by examining the MA plot, in which log-transformed ratios of fluorescence intensities ($M=\log_2(R/G)$ were plotted against log-transformed multiples of intensities ($A=\log_2(R*G)/2$) before and after normalization. R represents the background adjusted fluorescence intensity in the red channel and G represents the background adjusted fluorescence intensity in the green channel. In addition, the boxplot of background intensities of each array was checked to assess the microarray quality. After normalization, a linear model was applied to the normalized data and a design matrix was specified. The design matrix indicated the RNA targets which hybridized into the arrays (including dye swaps). The columns of the design matrix represent the parameters to be evaluated (e.g., M values for HI/CON comparison) and the rows correspond to the arrays in the experiment. Empirical Bayes moderated F statistics was used to assess differential expression. The advantage of the empirical Bayes method implemented in LIMMA is that it can borrow information from the replicates and make stable inference about each gene (Ritchie et al., 2007; Smyth, 2004). An output file containing a P value, t-statistic, average $\log_2$ expression level, $\log_2$-based fold change of each gene was generated.

FUNCTIONAL ANNOTATION ANALYSIS

Gene ontology analysis

Gene ontology (GO) was performed to classify the differentially expressed genes based on biological process (BP), molecular function (MF), and cellular component (CC) (http://www.geneontology.org/). GO analysis can provide information about the overrepresented categories among the genes. The list of DE genes ($P<0.01$ and fold change>2) was selected and separated based on the direction of regulation. The Database for Annotation, Visualization and Integrated Discovery (DAVID version 6.7) (Dennis et al., 2003; Huang et al., 2009) (http://david.abcc.ncifcrf.gov/), based on a Fisher Exact statistic methodology, was used to obtain GO terms within up and down-regulated genes. The RefSeq protein IDs from human orthologs were used as input and human database as background (DAVID default setting). We chose RefSeq protein ID as identifier because protein ID is unique. An output file in Functional Annotation Chart of DAVID containing GO term, count, percent and P value of each category was generated. The column labeled with count means the total number of genes from the input list that belong to the corresponding GO term. The column labeled with percent corresponds to the number of count divided by the number of input genes. The enrichment P value in Functional Annotation Chart is calculated based on EASE score (Hosack et al., 2003). P value of 0.05 was used as a cutoff for determining statistical significance as recommended by Huang et al. (Huang et al., 2009). GO terms are in a tree structure and GO_ALL were used for analysis because the GO terms at this level are more specific.

Pathway and network analysis

Initial pathway analysis was conducted using GenMAPP version 2.1 (Salomonis et al., 2007) (http://www.genmapp.org/) and Kyoto Encyclopedia of Genes and Genomes (KEGG) pathway databases (Kanehisa et al., 2008) (http://www.genome.jp/kegg/). To expand upon these results, we utilized a more robust pathway and associated network detection program, Ingenuity Pathways Analysis program (Ingenuity Systems, http://www.ingenuity.com/, version 8.7).

Networks, relevant biofunctions and canonical (i.e., known or established) pathways were generated through the use of Ingenuity Pathways Analysis program in order to understand the potential pathways and associated networks involved in laminitis pathogenesis. A dataset containing gene identifier (RefSeq protein IDs from human orthologs), corresponding P value ($P<0.01$) and fold change (fold change>2) from microarray expression analysis were uploaded into the application as input dataset. Each gene identifier was mapped to its corresponding gene object in the Ingenuity Knowledge Base. These genes, called focus genes, were overlaid onto a global molecular network developed from information contained in the Ingenuity Pathway Knowledge Base. Networks of these focus genes were then algorithmically generated based on their connectivity. Ingenuity will generate several analysis results include one summary file, networks, canonical pathways, and function tables. Only top biological functions, associated diseases, top canonical pathways and top network based on P value that were most significant to the dataset are presented in this study.

The functional analysis identified the biological functions and diseases that were most significant to the dataset. Genes from the dataset that were associated with biological functions and diseases in the Ingenuity Pathway Knowledge Base were considered for further analysis. Fisher's exact test was used to calculate a P value determining the probability that each biological function and disease assigned to that data set is due to chance alone. The functional analysis of a network identified the biological functions and diseases that were most significant to the genes in the network. The network genes associated with biological functions and diseases in the Ingenuity Pathways Knowledge Base were considered for the analysis. Fisher's exact test was used to calculate a P value determining the probability that each biological function and disease assigned to that network is due to chance alone.

Canonical pathways analysis identified the pathways from the Ingenuity Pathways Analysis library of canonical pathways that were most significant to the dataset. Genes from the dataset that were associated with a canonical pathway in the Ingenuity Pathway Knowledge Base were considered for analysis. The significance of the association between the dataset and the canonical pathway was measured in two ways: first, a ratio of the number of genes from the dataset that map to the pathway divided by the total number of genes that map to the canonical pathway was obtained. Second, Fisher's exact test was used to calculate a P value describing the probability that the association between the genes in the dataset and the canonical pathway is explained by chance alone.

Pathways were constructed using both direct and indirect relationships that provided graphical representation of the molecular relationships between genes (Merico et al., 2009). In these representations genes or gene products are shown as nodes, and the biological relationship between two nodes is presented as a line. All lines are supported by at least one reference from the literature. The intensity of the node color indicates the degree of up- (red) or down- (green) regulation. Nodes are displayed using various shapes that represent the functional class of the gene product. Lines are displayed with various labels that describe the nature of the relationship between the nodes.

QUANTITATIVE REAL TIME PCR

Although microarray technology is powerful, low-level gene expression is difficult to quantify because of low signal intensity which is sensitive to interference from factors (e.g., background noise) other than the samples themselves (Provenzano and Mocellin, 2007). Quantitative real-time PCR has been used in gene expression profiling to overcome the disadvantages encountered in microarray analysis (Dallas et al., 2005). To validate the differential expression of microarray results, a subset of DE genes (both up and down regulated) were examined by quantitative reverse transcriptase PCR (qRT-PCR). Most of DE genes with a small P value and large fold change were selected. The fold change of all selected genes is larger than 2. Some DE genes whose expression patterns and functional relevance link them to laminitis were also chosen for confirmation by qRT-PCR. Many genes that fit the criteria could not be used for real time PCR. Primer sets did not produce amplification, formed primer dimers, were not specific (as shown by multiple peaks in the melting curve), or had poor efficiency.

Primer 3 software (Rozen and Skaletsky, 2000) was used to design gene specific primers (http://frodo.wi.mit.edu/primer3/) and the designed primer pairs were checked by BLAST program (http://blast.ncbi.nlm.nih.gov/) for specificity. Each of the designed amplicons was 100-250 bp in length and each pair of primers were designed to span intron and exon boundaries whenever possible. We could not design primers for some genes because of an incomplete sequence (can't generate gene specific primers) or no associated annotation information (e.g., hypothetical protein).

The cDNA was synthesized using TaqMan® Reverse Transcriptase reagents (Applied Biosystems, Carlsbad, CA) according to the manufacturer's protocol. In a 10 µl reverse transcription reaction, 0.2 µl of RNase inhibitor (20 units/µl), 2 µl of dNTP mix (10 mM), 0.25 µl of oligo $d(T)_{16}$ (50 µM), 0.25 µl of random hexamer (50 µM), 1 µl of 10x RT buffer, 2.2 µl of $MgCl_2$ (25 mM), 0.25 µl of reverse transcriptase (50 units/µl), and 2.85 µl of nuclease-free water were mixed with 1 µl of total RNA (250 ng/µl). The reaction was gently vortexed and briefly centrifuged to collect the mixture at the bottom of a PCR tube. The reaction was incubated in a thermal cycler under the following conditions: 25ºC for 10 min, 48ºC for 30 min and 5 min at 95ºC at the end.

The synthesized cDNA, horse genomic DNA, and nuclease-free water, were used as templates in a PCR reaction. In a 10 µl PCR reaction, the following components were added: 1.0 µl of 10x PCR buffer (containing 15 mM $MgCl_2$), 0.1 µl of dNTP mix (20 mM), 0.6 µl of forward and reverse primer mix (10 µM), 0.25 µl of JumpStart REDTaq DNA polymerase, 6.05 µl nuclease-free water with 2 µl of cDNA (25 ng/µl)/genomic DNA (25 ng/µl)/nuclease-free water. The cycling conditions for routine PCR

amplification were as follows: 1 cycle at 95ºC for 5 min, 30 cycles of 94ºC for 30 sec, 58 ºC for 30 sec, 72ºC for 30 sec and 10 min at 72ºC at the end. The amplified DNA fragment of each gene was run in 2% agarose gel electrophoresis in order to check gene specific PCR product.

Real time PCR amplification was carried out in 96-well plates on a LightCycler 480 (Roche Diagnostics, Indianapolis, IN). Amplification reactions were performed in duplicate from individual laminar cDNA samples from each horse. One hundred nanograms of cDNA were used in a total volume of 20 µl with 10 µl 2x LightCycler ® 480 SYBR Green I master mix (Roche Diagnostics, Indianapolis, IN), 9 µl of water (PCR grade) and 1 µl of forward and reverse primers (10 µM). To calculate the PCR amplification efficiencies of target and reference genes, a serial dilution of laminar cDNA template at different concentrations (200 ng/µl, 100 ng/µl, 50 ng/µl, 25 ng/µl, 12.5 ng/µl, and 6.25 ng/µl) was made and used as a template for the real time PCR amplification reaction. The PCR efficiency was determined from the slope of the line along the concentrations as calculated by LightCycler 480 basic software version 1.2 (Roche Applied Science, Indianapolis, IN). Crossing point (Cp) value is the fluorescence signal point where background fluorescence is exceeded and is inversely related to the cDNA concentration. The real-time PCR amplification program was 5 min at 95ºC, followed by 45 cycles of 10 sec at 95ºC, 5 sec at optimal annealing temperature for each specific set of primers and 10 sec at 72ºC. At the end, melting curves of PCR products were acquired by increasing the temperature from 65ºC to 95ºC. The primer set was

evaluated through the melting curve of the amplification product. The average Cp of the two duplicates was used for relative quantification.

geNorm

Because of the inherent variation in expression of reference genes (Piehler et al., 2010; Radonic et al., 2004), qRT-PCR was carried out for several horse reference genes. The average expression stability and the optimal number of control genes for normalization were calculated using the geNorm computer program version 3.5 (http://medgen.ugent.be/~jvdesomp/genorm/) (Vandesompele et al., 2002). geNorm is a Visual Basic program that evaluates the gene expression stability measure M for the reference genes. M is the mean pairwise variation of a reference gene compared with all other tested reference genes. For each reference gene, the pairwise variation with all other reference genes is calculated as the standard deviation of the logarithmic 2 transformed expression ratios. Genes with higher M values have greater variation in expression. The stepwise exclusion of the gene with the highest M value leads to the ranking of the tested genes based on their expression stability. geNorm can also allow the determination of the optimal number of reference genes based on the pairwise variation V value. In order to determine the optimal number of reference genes, a normalization factor (NF) was calculated based on the geometric mean of Cp values of the multiple reference genes according to Vandesompele et al. (Vandesompele et al., 2002). The pairwise variation was determined between two NFs for all samples ($V_{n/n+1}$=standard deviation of NF_n and NF_{n+1}). A large V value means that the additional reference gene should be included for NF calculation. A V value of 0.15 was generally

used to determine the optimal number of reference genes. The selection of 0.15 cut-off value is based on the finding that the inclusion of additional reference gene has less effect on the normalization when the pairwise variation between the sequential NFs is less than 0.15 (Hellemans et al., 2007).

In order to get the most stable reference genes for real time PCR data normalization, Cp values across all samples obtained from real time PCR need to be transformed into relative quantification (Q) data using delta-Cq method. An input file containing sample and gene names with Q values was used for geNorm analysis. geNorm generated two output figures. First output chart gave information about the most stably expressed reference genes in the system. Second output chart gave information about how many reference genes needed for optimal normalization.

qBasePlus

qRT-PCR data was analyzed by the delta-Cq method (Hellemans et al., 2007). This method not only considered the difference of PCR amplification efficiency between the gene of interest and the reference gene, but also allowed to use more than one reference gene for qRT-PCR data normalization (Hellemans et al., 2007). Therefore it is much more accurate and reliable than the comparative Ct method (Livak and Schmittgen, 2001) or the Pfaffl method (Pfaffl, 2001). The qBase*Plus* software version 1.0 (Biogazelle, Ghent, Belgium) was used to evaluate gene expression difference among experimental conditions. The input file containing Cp values, gene name and sample information was loaded into qBase*Plus* program. qBase*Plus* program converts the Cp values into normalized relative quantities (NRQs) based on both the differences

in PCR amplification efficiency between target genes and reference genes and multiple reference gene factors. It also calculates the calibrated normalized relative quantity (CNRQ), which equals the NRQ of the target gene divided by the geometric mean of NRQ of the reference genes. The output file of qBase*Plus* program has CNRQ value of each gene across all samples. It also provides the histograms showing the expression level and corresponding error bars of each gene across all samples under study. The statistical significance of the normalized CNRQ values between two groups was determined by nonparametric Mann-Whitney test in SPSS 17.0 statistics software (SPSS Inc, Chicago, IL). As gene expression levels often do not follow a normal distribution even after normalization (Purdom and Holmes, 2005), Mann-Whitney test is a good choice for comparing 2 unpaired groups since this test does not require a normal distribution (Motulsky, 2010). A P value less than 0.05 (95% confidence level) was considered statistically significant.

CLUSTER ANALYSIS

Cluster analysis is an exploratory data analysis approach for gene expression experiments. There are four types of clustering: "hierarchical clustering, k-means clustering, self organizing maps (SOMs), and principle component analysis (PCA)" (Eisen et al., 1998). Methods such as hierarchical clustering can allow us to cluster genes and samples respectively based on the expression pattern similarity and generate heat maps for visualization (Chipman and Tibshirani, 2006; D'Haeseleer, 2005). MultiExperiment viewer and R (MeV/R) program version 4.6 (Chu et al., 2008; Saeed et al., 2003) (http://expression.washington.edu/mevr/) was used for hierarchical cluster

analysis. The input tab-delimited text file containing gene name and expression values was loaded into MeV/R program and an expression image was generated. Then a commonly used clustering algorithm hierarchical clustering was performed on the expression values with default settings (euclidean distance metric and average linkage clustering method) and a heat map was constructed. In the heat map, each column corresponds to a sample and each row corresponds to a gene. The green to red color scale indicates the level of expression, where red corresponds to higher expression, green corresponds to lower expression. In the color scale limits default setting, the low end is 0 and midpoint is median value and high end is the value that 80% of the data below this value (http://www.tm4.org/documentation/MeV_Manual.pdf).

CHAPTER III

GENOME-WIDE TRANSCRIPTOME ANALYSIS OF LAMINAR TISSUE DURING THE DEVELOPMENTAL STAGE AND THE ONSET OF CARBOHYDRATE OVERLOAD INDUCED EQUINE LAMINITIS

INTRODUCTION

Equine laminitis is a painful and debilitating condition that has an enormous impact on the economy of the horse industry as well as on quality of life for afflicted horses. Acute laminitis often results in the failure of the dermal-epidermal laminae and dorsopalmar rotation of the distal phalanx, causing extreme pain and many times leading to permanent lameness. The molecular triggers that cause laminitis are still unknown, although there are many suspected predisposing factors (Hood, 1999a). Excess grain intake, lush pasture, colitis and metritis can all lead to laminitis (Colles and Jeffcott, 1977). Gastrointestinal disease is the most common problem occurring just prior to the onset of acute laminitis (Slater et al., 1995) and it has been suggested that "gastrointestinal derived factors are potential triggers for acute equine laminitis" (Elliott and Bailey, 2006). Experimentally induced models of laminitis have been established through the administration of CHO (Garner et al., 1975), BWE (Minnick et al., 1987), OF (van Eps and Pollitt, 2006) and a hyperinsulinemic/euglycemic clamp (Asplin et al., 2007; de Laat et al., 2010).

We currently have a limited ability to prevent and treat this devastating disease, which reflects a lack of understanding of its pathogenesis. Elucidation of the molecular

mechanisms responsible for the development and progression of laminitis may lead to improved strategies for early prevention or treatment of this disease. Although an equine-specific 3076 element cDNA microarray (Noschka et al., 2008) and a bovine 15K oligoarray (Budak et al., 2009) have been used to investigate equine laminitis, they have inherent limitations that prevent detailed studies aimed at understanding the potential genetic pathways and networks associated with the pathogenesis and progression of laminitis on a genome-wide scale.

We recently developed a comprehensive equine-specific ~21,000 element whole genome expression microarray for functional analysis of the equine genome (Bright et al., 2009). This oligoarray was constructed based on a 2.4 Gb whole genome sequence of the horse genome (EquCab2; http://www.broad.mit.edu/mammals/horse/), combined with RefSeq release 26, UniGene build#3, SwissProt release 12 and ~43,000 unpublished ESTs, making it by far the most representative functional analysis tool for examining the equine transcriptome. Because the initial stages of laminitis are critical in understanding the progression of the disease, we sought to identify differentially expressed genes and their likely interactions that could lead to observed pathological changes during these stages. To accomplish this aim, we used a 70-mer equine whole-genome oligoarray to investigate the laminar gene expression profile during the developmental stage (defined as the onset of fever) and the onset (Obel grade 1) of experimental carbohydrate induced laminitis.

MATERIALS AND METHODS

Experimental design

Experimental protocols were approved by the Animal Care and Use Committee at the Ohio State University. Fifteen Quarter horses (3-12 years of age) were confirmed to be healthy and without any history of metabolic-endocrine disorders. Five horses were used for each category (developmental, Obel grade 1 and control). Horses in the developmental (DEV) and the Obel grade 1 (OG1) groups were administered carbohydrate in the form of corn starch (17.6 g/kg body weight) via nasogastric tube. Control group horses (CON) received saline injection. This method is an effective, repeatable means by which to induce laminitis (Garner et al., 1975). Laminar samples were obtained from the control group at 24 h (CON, n=5), a developmental group at the onset of fever (DEV, n=5), or when the onset of lameness was observed (OG1, n=5). Laminar tissue was rapidly obtained from the hoof and distal phalanx, snap frozen immediately in liquid nitrogen, and stored at -80 °C.

A two channel, balanced block design was used for genome-wide transcriptional analysis. Three different comparisons were carried out (DEV vs. CON, OG1 vs. CON, and DEV vs. OG1). Dye swaps were incorporated into the hybridization scheme of the experiment to eliminate dye bias. The microarray hybridization experiment conducted in this study is shown in Fig. 3.1.

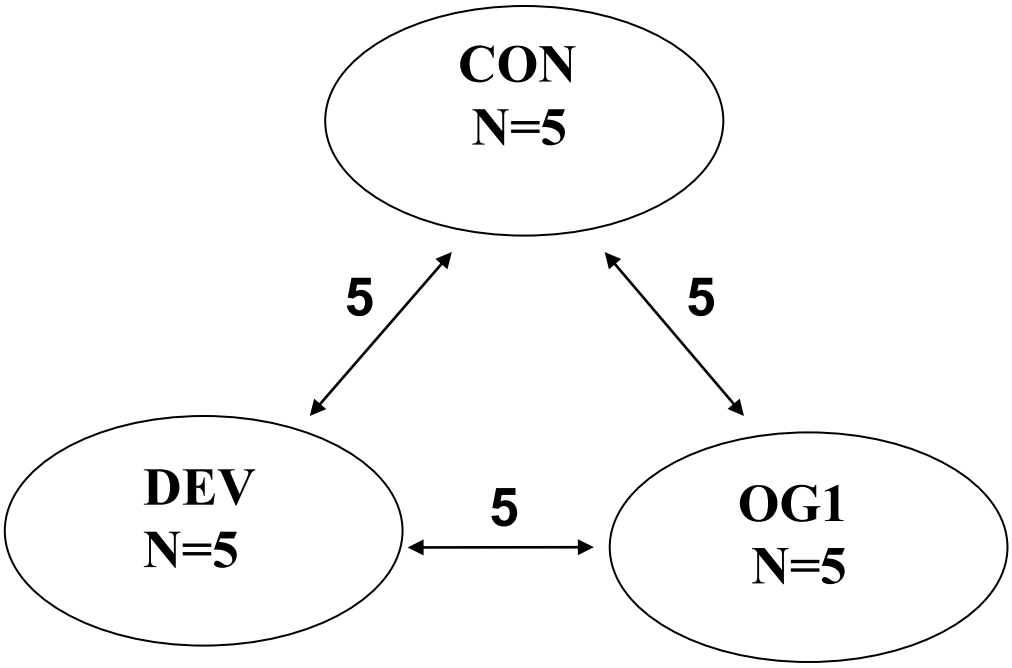

Fig. 3.1. Diagram of the CHO model laminitis experimental design. Fifteen hybridizations were performed. Arrows represent the hybridization between the laminar samples from different groups (n=5). CON: laminar samples from control horses; DEV: laminar samples from horses at the developmental stage; OG1: laminar samples from horses with Obel grade 1 laminitis.

Equine 21K oligonucleotide microarray

The 70-mer oligoarray was constructed based on a 2.4 Gb EquCab2 of horse genome (http://www.broadinstitute.org/mammals/horse), combined with RefSeq release 26, UniGene build#3, SwissProt release 12 and ~43,000 unpublished ESTs (Bright et al., 2009). Alignments of transcript and protein sequences to the genomic sequence were performed and analyzed in order to group all sequences representing the same gene into the same entity. Genes can thus be defined as intervals on the genome and can be given a type identified by the nature of sequences that define it (for example, RNA + EST). The proportion of transcript sequences represented in the genome assembly serves as an

indication of the genome sequence coverage. The genome coverage appears near complete (female genome), and supports restricting oligo design to genes present on the genome sequence. Genes with RNA, UniGene or EST in their type represent 97.5% of all genes (22414 out of 23012) and 13191 of these contain an EST. The other 2.5% of genes (598) are documented solely by a protein hit and could represent pseudogenes as well as genes. The 70-mer oligo design process resulted in 21351 probes, which were synthesized (Invitrogen, Carlsbad, CA) and spotted on amino-silane coated slides (Corning Incorporated, Corning, NY).

RNA isolation and cDNA synthesis

Total RNA was isolated from 80-100 mg of frozen laminar tissue, which was mechanically disrupted in the presence of Tri reagent (MRC, Cincinnati, OH). This was followed by RNA cleanup with RNase-free DNase treatment (RNeasy Mini Kit, Qiagen, Valencia, CA) of the isolate according to the manufacturer's protocol. RNA was eluted with 35 µl RNase-free water. RNA concentration was quantified using a spectrophotometer (NanoDrop Technologies, Wilmington, DE) and the quality was evaluated with an Agilent 2100 Bioanalyzer and RNA Lab Chip (RNA 6000 Nano Assay, Agilent Technologies, Palo Alto, CA). Labeled cDNAs were synthesized from total RNA with the 3DNA Array 350 Expression Array Detection Kit (Genisphere, Hatfield, PA) using SuperScript II reverse transcriptase (Invitrogen, Carlsbad, CA). Three micrograms of total RNA was combined with oligo-d(T) primers, incubated at 80°C for 10 min, and cooled on ice for 2 min. Finally, 0.5M NaOH/50mM EDTA was

added to degrade any remaining RNA; this reaction was neutralized with 1 M Tris-HCl (pH 7.5).

Pre-hybridization treatment of microarray slide

Rehydration and crosslinking of the microarray slide was performed to ensure that the probe was spread evenly in the spot and immobilized on the slide. The slides were rehydrated by holding the slide label side down over the steam from a 50°C water bath for 10 s. The slides were dried for 5 s at 65°C and then brought to room temperature (20°C) for 1 min. This process was repeated up to four times. After rehydration, the slides were subjected to UV crosslinking at 750 MJ/cm^2 for 2 minutes.

Microarray cDNA hybridization

A 580 µl reaction was used for the cDNA hybridization mix, which was prepared according to the manufacturer's instructions (Genisphere, Hatfield, PA). The mixture was applied to the gasket slide of an Agilent microarray hybridization chamber and the microarray slide (array side down) was laid on top of the gasket slide. The hybridization chamber was assembled and the slides were then incubated at 55°C while rotating at 5 rpm in a hybridization oven (Agilent Technologies, Santa Clara, CA) for 16 hours. The "microarray-gasket slide sandwich" was then washed once with pre-warmed (42°C) 2x SSC-0.2% SDS wash buffer, disassembled, and washed again. The array slide was then washed with 2x SSC and 0.2x SSC wash buffers. Slides were dried at room temperature, centrifuged at 1000 rpm for 4 min, and then stored in a dry box prior to the second hybridization.

3DNA hybridization and wash

3DNA hybridization master mix was prepared according to the manufacturer's instructions (Genisphere, Hatfield, PA), applied to the array, and covered with a coverslip in the dark. The slide was placed in a 50 ml conical tube with 400 µl of nuclease-free water and incubated horizontally at 55°C in a hybridization oven (Agilent Technologies, Santa Clara, CA) for 4 hours in the dark. All washing steps following 3DNA hybridization were conducted in the dark. The slide was taken out of the incubator and washed with pre-warmed (42°C) 2x SSC-0.2% SDS wash buffer. The cover slip was removed and the slide was washed again with 2x SSC-0.2% SDS buffer. The slide was then washed with 2x SSC and 0.2x SSC wash buffers. Finally, the slide was dried at room temperature, centrifuged at 1000 rpm for 4 min, and stored for scanning.

Microarray image processing and data analysis

The slides were scanned with a GenePix Personal 4000B microarray scanner (Molecular Devices Corporation, Sunnyvale, CA) at a resolution of 5 µm. The fluorescence intensities from each array were quantified using GenePix Pro 6.0 (Molecular Devices Corporation, Sunnyvale, CA). Each spot was inspected by manual gridding and empty spots were flagged out. The LOWESS normalization method (Yang et al., 2002) was used to normalize the signal intensity of each gene in the R statistical computing environment (http://www.r-project.org/). The normalized natural logarithms of the intensities were then analyzed using a mixed model in SAS 9.1.3 (SAS Institute Inc, Cary, NC). The SAS estimate function was used to test for differential expression.

Gene ontology analysis

Gene ontology (GO) is used to functionally annotate gene products. It has three categories: biological process (BP), cellular component (CC) and molecular function (MF). The Database for Annotation, Visualization and Integrated Discovery (DAVID 6.7) (Dennis et al., 2003; Huang et al., 2009) (http://david.abcc.ncifcrf.gov/) was used to obtain GO terms, associated diseases, and related KEGG pathways for DE genes for the three comparisons: DEV vs. CON, OG1 vs. CON, and DEV vs. OG1. RefSeq protein IDs from human orthologs were used as input and Fisher's Exact P value of 0.05 was used as a cutoff for determining statistical significance. Gene ontology terms of all levels were included in the analysis.

Pathway analysis

Networks, relevant biofunctions and canonical pathways were generated through the use of Ingenuity Pathways Analysis program (Ingenuity Systems, version 8.7) in order to understand the potential pathways and associated networks involved in laminitis pathogenesis. A data set containing gene identifiers and corresponding expression values from the microarray expression analysis was uploaded into the application. Functional analysis identified the biological functions and diseases that were most significant to the dataset. Fisher's Exact test was used to calculate a P value determining the probability that each biological function and disease assigned to that data set (or network) is due to chance alone.

Quantitative real time PCR

To further explore microarray results, a subset of DE genes from each comparison were examined by quantitative reverse transcription PCR (qRT-PCR). cDNA was synthesized using TaqMan® Reverse Transcriptase reagents (Applied Biosystems, Carlsbad, CA) according to the manufacturer's protocol. Real time PCR amplification of each gene was carried out in duplicate on a LightCycler ® 480 (Roche Diagnostics, Indianapolis, IN) using 2x LightCycler ® 480 SYBR Green I master mix (Roche Diagnostics, Indianapolis, IN). To calculate the PCR amplification efficiencies of target and reference genes, a serial dilution of laminar cDNA was made (200 ng/µl, 100 ng/µl, 50 ng/µl, 25 ng/µl, 12.5 ng/µl, and 6.25 ng/µl) and used as a template. PCR efficiency of each gene was determined from the slope of the line along the concentrations as calculated by LightCycler ® 480 basic software version 1.2 (Roche Applied Science, Indianapolis, IN). Each individual sample was run in duplicate and the average crossing point (Cp) value was used for relative quantification.

Quantitative real time PCR data analysis

Because of the inherent variation in expression of reference genes (Piehler et al., 2010; Radonic et al., 2004), qRT-PCR was carried out for seven horse reference genes: ACTB, B2M, PPIA, GAPDH, GNB2L1, EEF1A1, and RPLP0. The average expression stability and the optimal number of control genes for normalization were calculated using the geNorm computer program version 3.5 (http://medgen.ugent.be/~jvdesomp/genorm/) (Vandesompele et al., 2002). geNorm is a Visual Basic program that evaluates the gene expression stability measure M for the

reference genes. M is the mean pairwise variation of a reference gene compared with all other tested reference genes; genes with higher M values have greater variation in expression. The stepwise exclusion of the gene with the highest M value leads to the ranking of the tested genes based on their expression stability. The optimal number of reference genes was determined based on the pairwise variation V value according to the methods of Vandesompele et al. (Vandesompele et al., 2002). A V value of 0.15 was selected as a cut-off value (Hellemans et al., 2007). The two most stable genes were used for normalization of qRT-PCR data.

qRT-PCR data was analyzed by the delta-Cq method (Hellemans et al., 2007) in qBase*Plus* version 1.0 (Biogazelle, Ghent, Belgium). In brief, the qBase*Plus* program converts Cp values into normalized relative quantities (NRQs) based on both the differences in PCR amplification efficiency between target genes and reference genes and multiple reference gene factors. It also calculates the calibrated normalized relative quantity (CNRQ), which is the NRQ of the target gene normalized to the geometric mean of the NRQ of the reference genes. The statistical significance of the derived CNRQ values between two groups was determined by nonparametric Mann-Whitney test in SPSS 17.0 statistics software (SPSS Inc, Chicago, IL). A P value less than 0.05 was considered statistically significant.

Hierarchical cluster analysis

To identify gene clusters with similar expression pattern among CON, DEV and OG1 conditions, hierarchical clustering was performed on the mean values of selected

DE genes from qRT-PCR to construct a heat map using MultiExperiment viewer and R (MeV/R) program version 4.6 (Chu et al., 2008; Saeed et al., 2003).

RESULTS

Differential gene expression profile

Differential gene expression was determined for the pairwise comparisons among the three groups: developmental vs. control (DEV/CON), Obel grade 1 vs. control (OG1/CON), and developmental vs. Obel grade 1 (DEV/OG1). There were 68, 149, and 160 genes differentially expressed ($P<0.01$, fold change>2) in the DEV/CON, OG1/CON and DEV/OG1 comparisons, respectively. Of these, 56, 114, and 135 were annotated (Table 3.1). Fold changes ranged from 0.33 to 2.80 (DEV/CON), 0.22 to 38.4 (OG1/CON), and 0.03 to 5.30 (DEV/OG1). A general predominance of down-regulation was seen among differentially expressed (DE) genes in the DEV group, whereas up-regulated genes were predominant in the OG1 group. The DE genes with the largest fold changes are shown in Tables 3.2, 3.3, and 3.4 for each of the three comparisons, respectively. Complete lists of DE genes ($P<0.01$, fold change>2) are shown in Tables A.1, A.2, and A.3.

Table 3.1
Distribution of differentially expressed genes among comparisons.

	Upregulated	Downregulated	Total
DEV/CON	11 (19.6%)	45 (80.4%)	56
OG1/CON	82 (71.9%)	32 (29.1%)	114
DEV/OG1	30 (22.2%)	105 (77.8%)	135

Table 3.2
Top differentially expressed genes (11 upregulated and 15 downregulated; P < 0.01 and fold change> 2) for the DEV/CON comparison. Unannotated genes are labelled as NULL. Asterisks denote genes selected for confirmation with PCR.

Gene Name	Description	Public Accession	P	Fold Change	PCR
Upregulated					
NULL		BM734930	0.0026	3.35	
CCL2	C-C motif chemokine 2	AJ251189	0.0056	3.00	*
NULL		BI961659	0.0000	2.79	*
MFAP5	Microfibrillar associated protein 5	NULL	0.0071	2.68	
HOPX	Homeodomain-only protein	XM_001491312	0.0096	2.45	*
RSPH3	Radial spoke protein homolog 3	XM_001491976	0.0042	2.35	
CRYAB	Alpha crystallin B chain	XM_001501779	0.0031	2.35	*
NULL		CX602928	0.0068	2.31	
CLEC2L	C-type lectin 2L (CD69)	XM_001496572	0.0099	2.28	
USP44	Ubiquitin carboxyl-terminal hydrolase 44	XM_001495993	0.0095	2.07	
NULL		DN505910	0.0052	2.03	
Downregulated					
PIGR	Polymeric IgG receptor	XM_001492298	0.0001	0.33	
SNF8	Vacuole protein VPS22	XM_001502240	0.0012	0.34	*
NULL		XM_001498378	0.0028	0.35	
FLRT3	Fibronectin leucine rich transmembrane protein 3	XM_001491950	0.0072	0.37	
NULL		CX604746	0.0001	0.37	
SEPP1	Selenoprotein P, plasma, 1	XR_036255	0.0014	0.39	*
ZDHHC6	Zinc finger, DHHC-type containing 6	XM_001498439	0.0050	0.39	
PTPN6	Protein tyrosine phosphatase, non-receptor type 6	XM_001497706	0.0079	0.40	
TIGD1	Tigger transposable element derived 1	XM_001503915	0.0032	0.40	

Table 3.2 continued

Gene Name	Description	Public Accession	P	Fold Change	PCR
Downregulated					
C11orf59		XM_001499308	0.0080	0.40	
CA5B	Carbonic anhydrase VB	XM_001490349	0.0071	0.40	
CILP2	Cartilage intermediate layer protein 2	XR_036360	0.0007	0.41	
CDK5RAP2	CDK5 regulatory subunit associated protein 3	XM_001501690	0.0022	0.42	
C8orf70		XM_001491870	0.0079	0.43	
PRR15	Proline rich 15	XM_001500279	0.0050	0.43	

Table 3.3

Top differentially expressed genes (15 upregulated and 15 downregulated; $P < 0.01$ and fold change > 2) for the OG1/CON comparison. Unannotated genes are labelled as NULL. Asterisks denote genes selected for confirmation with PCR.

Gene Name	Description	Public Accession	P	Fold Change	PCR
Upregulated					
S100A8	S100 calcium binding protein A8	XM_001493589	0.0000	38.36	*
S100A12	S100 calcium binding protein A12	CD535886	0.0000	36.47	*
DEFB4	Beta-defensin 4	AY170305	0.0000	31.68	*
NULL		BM734930	0.0000	22.85	
SOD2	Superoxide dismutase 2, mitochondrial	AB001693	0.0000	20.09	
S100A8	S100 calcium binding protein A8	XM_001494358	0.0000	16.90	
NULL		CD467650	0.0000	16.27	
PI3	Peptidase inhibitor 3, skin-derived	BM734843	0.0001	15.34	

Table 3.3 continued

Gene Name	Description	Public Accession	P	Fold Change	PCR
SAA1	Serum amyloid A1	NM_001081853	0.0002	12.03	
S100A9	S100 calcium binding protein A9	XM_001493530	0.0003	10.42	*
CCL2	Chemokine (C-C motif) ligand 2	AJ251189	0.0000	9.72	
SERPINB3	Serpin peptidase inhibitor, clade B (ovalbumin), member 3	XM_001491507	0.0001	8.72	
NULL		CX605648	0.0000	8.11	
NULL		BI961659	0.0000	7.31	
ING5	Inhibitor of growth family, member 5	NULL	0.0000	5.97	
Downregulated					
SELENBP1	Selenium binding protein 1	NULL	0.0004	0.23	
OR7A10	Olfactory receptor, family 7, subfamily A, member 10	NULL	0.0002	0.25	
CD69	CD69 molecule	XM_001499388	0.0008	0.25	
CXCL14	Chemokine (C-X-C motif) ligand 14	XM_001502713	0.0022	0.25	
NULL		CD465749	0.0000	0.25	
TPPP3	Tubulin polymerization-promoting protein family member 3	CX596053	0.0005	0.26	
NULL		CX604746	0.0001	0.32	
NULL		CX603968	0.0026	0.32	
CD28	CD28 molecule	NM_001100179	0.0068	0.34	
MATN2	Matrilin 2	XM_001490965	0.0006	0.34	
FIBIN	Fin bud initiation factor homolog (zebrafish)	AB302195	0.0050	0.36	*
MNAT1	Menage a trois homolog 1, cyclin H assembly factor	XM_001497949	0.0004	0.36	*
ACBD7	Acyl-Coenzyme A binding domain containing 7	XM_001498628	0.0029	0.37	
FLRT3	Fibronectin leucine rich transmembrane protein 3	XM_001491950	0.0087	0.38	
SNRPN	Small nuclear ribonucleoprotein polypeptide N	XM_001492702	0.0099	0.42	*

Table 3.4
Top differentially expressed genes (15 upregulated and 15 downregulated; $P < 0.01$ and fold change > 2) for the DEV/OG1 comparison. Unannotated genes are labelled as NULL. Asterisks denote genes selected for confirmation with PCR.

Gene Name	Description	Public Accession	P	Fold Change	PCR
Upregulated					
TPPP3	Tubulin polymerization-promoting protein family member 3	CX596053	0.0000	5.31	
NULL		CX601554	0.0074	4.95	
CD69	CD69 molecule	XM_001499388	0.0000	4.84	
NDUFA4L2	NADH dehydrogenase (ubiquinone) 1 alpha subcomplex, 4-like 2	XM_001488582	0.0036	3.77	
CXCL14	Chemokine (C-X-C motif) ligand 14	XM_001502713	0.0015	3.76	
HOPX	HOP homeobox	XM_001491312	0.0004	3.73	*
FAM82C		XM_001501075	0.0047	3.64	
CALCB	Calcitonin-related polypeptide beta	AF257470	0.0009	3.59	*
FLJ36070		XM_001489063	0.0020	3.29	
MFAP5	Microfibrillar associated protein 5	NULL	0.0017	3.25	
IGFBP7	Insulin-like growth factor binding protein 7	XM_001491171	0.0004	3.19	
SLC22A12	Solute carrier family 22 (organic anion/urate transporter), member 12	XM_001489840	0.0031	3.18	
OR7A10	Olfactory receptor, family 7, subfamily A, member 10	NULL	0.0016	3.18	
PPP2R3B	Protein phosphatase 2 (formerly 2A), regulatory subunit B'', beta	XM_001488015	0.0004	3.09	
NULL		CD465749	0.0000	3.09	
Downregulated					
S100A8	S100 calcium binding protein A8	XM_001493589	0.0000	0.03	
S100A12	S100 calcium binding protein A12	CD535886	0.0000	0.05	*
S100A8	S100 calcium binding protein A8	XM_001494358	0.0000	0.07	*
S100A9	S100 calcium binding protein A9	XM_001493530	0.0001	0.08	*
SOD2	Superoxide dismutase 2, mitochondrial	AB001693	0.0000	0.09	
DEFB4	Beta-defensin 4	AY170305	0.0001	0.10	*
NULL		CD467650	0.0000	0.12	
NULL		CX605648	0.0000	0.15	

Table 3.4 continued

Gene Name	Description	Public Accession	P	Fold Change	PCR
Downregulated					
NULL		BM734930	0.0000	0.15	
SERPINB3	Serpin peptidase inhibitor, clade B (ovalbumin), member 3	XM_001491507	0.0003	0.15	*
ING5	Inhibitor of growth family, member 5	NULL	0.0000	0.15	
PI3	Peptidase inhibitor 3, skin-derived	BM734843	0.0037	0.19	
SAA1	Serum amyloid A1	NM_001081853	0.0021	0.16	
CITED1	Cbp/p300-interacting transactivator, with Glu/Asp-rich carboxy-terminal domain, 1	XM_001488044	0.0000	0.17	
PI3	Peptidase inhibitor 3, skin-derived	BM734843	0.0037	0.19	

Only 11 genes were up-regulated in the DEV group as compared with controls (Table 3.1). The 7 annotated genes within this list represented a wide range of functions, including inflammation/immune response, regulation of transcription, and protein folding and ubiquitination. Though the remaining up-regulated genes lack annotation data, some share sequence homology with other species to allow a tentative identification. The most up-regulated gene, BM734930, is 99% similar to superoxide dismutase 2 (*Equus caballus* SOD2, 63% coverage), a superoxide scavenger. Likewise, BI961659 shares 76% homology with transmembrane protein 49 (*Pan troglodytes* TMEM49/VSP1, 99% coverage), which is associated with intracellular vesicle formation during autophagy. Intracellular vesicles and vacuoles have been described in CHO model of laminitis (Morgan et al., 2003; Pollitt, 1996; Pollitt and Daradka, 1998). The 44 down-regulated genes in the DEV/CON comparison (Table A.1) included 4 genes with immunoglobulin-like domains, 7 genes encoding proteins with hydrolase function, and 9 genes for zinc binding proteins. Among the down-regulated genes with the largest fold changes were those expressed by immune effector cells, components of the extracellular matrix, a regulator of transcription, and a gene involved in mitochondrial nitrogen metabolism. A summary of the differentially expressed genes with the largest fold changes is provided in Table 3.2. The names, fold changes, and associated P values of fifteen down-regulated genes, as well as all 11 up-regulated genes, are presented in this table.

Many genes that were up-regulated in the OG1 group as compared to the controls are involved in the innate immune response; these include 4 S100 calcium binding

proteins, 1 acute phase protein, 2 chemokines, and 2 anti-microbial peptides. Eleven of the 15 genes with the largest fold changes were annotated and of these 11, 8 are immune-related (Table 3.3). In addition, SOD2 was overexpressed (two unannotated genes, BM734930 and CD467650, share 99 and 78% homology with equine and porcine SOD2, respectively), as was the serine protease inhibitor SERPINB3 (Table 3.3) and two other SERPINs (Table A.2). Down-regulated genes of the OG1/CON comparison included a number of genes associated with cellular proliferation and apoptosis, as well as several genes involved in regulation of transcription. Of note, ADAM metallopeptidase with thrombospondin type 1 motif, 1 (ADAMTS1), a metalloproteinase that is associated with extracellular matrix (ECM) degradation, was up-regulated. Matrilin 2 (MATN2), an ECM adaptor protein that is specifically involved in the keratinocyte response to wounding, was down-regulated. Up-regulated gene matrix metalloproteinase 13 (MMP13) has collagenase activity and can degrade collagen, which is a component of basement membrane (BM) of equine hoof laminae.

As a result of the general trend towards transcriptional down-regulation in the developmental stage and the widespread up-regulation in the Obel grade 1 stage, the DEV/OG1 comparison exhibited a predominance of down-regulated genes (Table 3.1). Genes that were more highly expressed in the DEV group included tubulin polymerization-promoting protein family member 3, CD 69 molecule, and homeodomain protein HOPX (Table 3.4). Down-regulated genes of this comparison consisted primarily of those genes that were dramatically increased in the OG1 group (S100 genes, SOD2, DEFB4; Table 3.4), as well as genes encoding 4 zinc finger

proteins, 7 solute carriers, and 5 serine protease inhibitors (Table A.3). Results from this comparison thus validate the data generated by the DEV/CON and OG1/CON comparisons in addition to highlighting the more subtle changes occurring during the transition from the developmental stage to the clinical onset of lameness.

In addition to genes that were differentially expressed between the two laminitis groups, we also found 22 genes that were consistently up- or down-regulated in both the DEV and OG1 groups (Table 3.5). Significantly overexpressed genes included inflammatory mediators, the antioxidant SOD2, and the vacuole-associated protein TMEM49, as well as several unannotated genes. Eight of the 9 up-regulated genes were more highly expressed in the OG1 group than in the DEV group; the remaining gene KIAA0391 had a slightly higher expression level in the DEV group. Many of the strongly overexpressed genes of the OG1/CON comparison, such as the S100 genes, were not differentially expressed in the DEV group, indicating a time-dependence of this transcriptional response. CCL2, however, showed a large fold change in both the DEV and OG1 groups (Tables 3.2 and 3.3). Notably, down-regulated genes included multiple DNA binding proteins, a potassium channel, an aldo-keto reductase, and a regulator of apoptosis (Table 3.5). The consistent change in expression level suggests that these 22 genes may be reflective of ongoing processes during the early stages of the progression of laminitis.

Table 3.5
List of differentially expressed genes common to both the DEV and OG1 stages.

Gene Name	Public Accession	Human Protein	pDEV	DEVfold	pOG1	Obelfold
Up-regulation						
KIAA0391	XM_001491047	NP_055487.2	0.0181882	2.2809171	0.0395235	2.0322141
NULL	DN505910	NULL	0.0052354	2.0308402	0.0070953	2.1287296
NULL	CX602004	NULL	0.0143219	2.176123	0.0095785	2.2898602
RSPH3	XM_001491976	NP_114130.3	0.0042391	2.3534586	0.0019278	3.0788139
PPA1	XM_001502747	NP_066952.1	0.0177216	2.0092664	1.628E-05	4.2789416
TMEM49	BI961659	NULL	1.498E-05	2.7866203	7.63E-10	7.3082392
CCL2	AJ251189	NP_002973.1	0.0056063	3.0044443	8.76E-06	9.7152828
SOD2	BM734930	NULL	0.0026373	3.3508285	4.40E-09	22.847298
DEFB4	AY170305	NP_004933.1	0.0318583	3.1619832	3.16E-07	31.678786
Down-regulation						
SELENBP1	NULL	NP_003935.2	0.0339868	0.4732622	0.0004266	0.230477
NULL	CX604746	NULL	0.0001236	0.3730017	5.79E-05	0.3204686
NULL	CX603968	NULL	0.0220934	0.4816291	0.0026067	0.3230924
FLRT3	XM_001491950	NP_037413.1	0.0071702	0.372587	0.0087306	0.3831077
SMARCA1	XM_001500518	NP_003060.2	0.0116903	0.4169139	0.0144975	0.3984922
BFAR	XM_001490098	NP_057645.1	0.0098486	0.4386322	0.0117411	0.4188644
TMEM38A	XM_001499622	NP_076979.1	0.0297946	0.4471773	0.0370885	0.4326369
EXOSC8	XM_001495546	NP_852480.1	0.0120244	0.4183502	0.0256852	0.4383527
AKR1C1	XM_001500743	NP_001344.2	0.0240601	0.483199	0.0249889	0.4611078
C1orf125	XM_001488358	NP_653297.3	0.0229755	0.4616029	0.0452853	0.4802466
KIAA1377	XM_001498604	NP_065853.2	0.0326062	0.4788407	0.0492041	0.4803119
ANKRD35	XM_001499402	NP_653299.3	0.0093994	0.4375781	0.0294139	0.4820767
ZDHHC6	XM_001498439	NP_071939.1	0.0050028	0.3948714	0.0456295	0.5008687

Gene ontology

Overrepresented gene ontologies within up- and down-regulated genes were determined using the NIH-DAVID bioinformatics database. The list of DE genes ($P< 0.01$, fold change>2) of the DEV/CON comparison did not yield any significantly overrepresented gene ontologies, pathways, or diseases, with the exception of the biological process GO terms such as response to heat, response to temperature stimulus, and negative regulation of cellular process among up-regulated genes and cellular component GO term extracellular region part among down-regulated genes.

When the number of DE genes was expanded by relaxing the P value cut off to 0.05 (220 genes: 48 up-regulated and 172 down-regulated), a number of significant associations were generated (Table A.4). GO terms associated with biological processes shared several common genes, including CCL2, alpha crystallin chains CRYAA and CRYAB, and insulin-like growth factor binding proteins IGFBP2 and IGFBP7. The biological process categories containing the greatest number of DE genes were response to stimulus, response to chemical stimulus, and response to stress. The two overrepresented cellular component terms were both extracellular, suggesting a transcriptional up-regulation of matrix constituents during the developmental stage of laminitis. Interestingly, despite the large number of down-regulated genes in the DEV/CON comparison, no GO term was significantly overrepresented. Molecular functions were limited to neuronal Cdc2-like kinase binding, hydrolase activity and carbon-oxygen lyase activity.

Up-regulated genes from the OG1/CON comparison yielded a number of overrepresented GO terms (Table A.5). Of the 92 biological processes significantly associated with these genes, most were involved in cellular ion regulation, inflammation/wounding, or negative regulation of apoptosis. As in the DEV/CON comparison of differentially expressed genes, many were found to belong to more than one GO term; however, this may be expected given the known interactions between intracellular ion concentration, initiation of apoptosis, and control of inflammation (Fox et al., 2010; Wessling-Resnick, 2010; Yu et al., 2001). Cellular component terms all pointed to changes in the extracellular matrix and molecular functions were associated with peptidase inhibition and binding of G-protein coupled receptors, glycosaminoglycans and polysaccharides. Among down-regulated genes, regulation of cell cycle was the only overrepresented biological process, although all molecular functions related to fatty acid metabolism.

Few GO terms were overrepresented among up-regulated genes of the DEV/OG1 comparison (Table A.6) and included responses to inorganic substance and heat (biological processes), involvement of extracellular proteins (cellular component), and cytoskeletal protein binding (molecular function). In contrast, 98 biological processes were overrepresented among down-regulated genes. Most of these 98 processes related to inflammation/wound healing, regulation of apoptosis, cell motility and migration, and intracellular ion homeostasis. Whereas many of the GO terms found in this comparison were also found in the DEV/CON and OG1/CON comparisons, the appearance of two new terms describing synthesis of interleukin 6 (IL6) and two terms associated with

leukocyte trafficking is noteworthy. Most of cellular components in this comparison dealt with the extracellular space, while molecular functions were associated with peptidase inhibition and protein binding.

Pathway analysis

Initial pathway analysis was conducted using the KEGG pathway database (Kanehisa et al., 2008) linked through the DAVID database. Two pathways were detected for both the OG1/CON and DEV/OG1 comparisons when all genes, both up and down-regulated, were included. These pathways were cytokine-cytokine receptor signaling, which is in fact a collection of many unrelated receptor-ligand interactions, and the nucleotide binding oligomerization domain (NOD)-like receptor signaling pathway, which is involved in recognition of intracellular bacteria. To expand upon these results, we utilized a more robust pathway detection program, Ingenuity Pathways Analysis (IPA) version 8.7 (http://www.ingenuity.com/), to establish relationships among DE genes ($P<0.01$ and fold change>2) for the DEV/CON, OG1/CON and DEV/OG1 comparisons. In addition to identifying canonical pathways that include differentially expressed genes, Ingenuity also develops regulatory networks that show interactions among gene products. Like the gene ontology analysis, it identifies overrepresented biofunctions and associated diseases.

For the DEV/CON comparison, IPA analysis was performed on genes that were differentially expressed at $P<0.01$ with a fold change of 2 or higher. The *top biofunctions* determined by IPA were carbohydrate metabolism, inflammatory response, and hematopoiesis (Table 3.6). The *associated diseases* were nutritional disease, cancer

(inflammatory disease), ophthalmic disease, and connective tissue disorders (Table 3.12). Sixty-three canonical pathways were detected and the *top canonical pathways* determined through the IPA library were liver X receptor/retinoid X receptor (LXR/RXR) activation and triggering receptor expressed on myeloid cells (TREM) 1 signaling. LXR/RXR activation is involved in a variety of cellular functions ranging from cholesterol metabolism to inhibition of the inflammatory response. The TREM1 signaling pathway is stimulated by and negatively regulates TLR4 signal transduction in response to ligation of bacterial wall components (Ornatowska et al., 2007; Zheng et al., 2010). The *top network* with a score of 33 is shown (Fig. 3.2). The *network function* was gene expression, carbohydrate metabolism, and small molecule biochemistry. This network included 35 genes, 15 of which were identified as DE in the differential expression analysis of the DEV/CON comparison. Among these 15 genes, RSPH3, USP44, CCL2 and CRYAB were up-regulated.

For the OG1/CON comparison, the *top biofunctions* were inflammatory response, antigen presentation, hematological system development and function (Table 3.6). The *associated diseases* were inflammatory disease, cancer, dermatological diseases and conditions, and hematological diseases. The *top canonical pathways* were IL17 signaling and vitamin D receptor/retinoid X receptor (VDR/RXR) activation. The *top network* with a score of 39 exhibited a central importance of p38 MAPK and NF-κB pathway molecules (Fig. 3.3). This network included 33 genes, 20 of which were DE. In the network, DEFB4, S100A8 and S100A12 showed up-regulation while CD69 showed

down-regulation. The top associated *network functions* were inflammatory response, antigen presentation, and cellular movement.

For the DEV/OG1 comparison, the *top biofunctions* were cellular movement, antigen presentation, hematological system development and function, and immune cell trafficking (Table 3.6). The *associated diseases* were metabolic disease, cancer, inflammatory disease, connective tissue disorders (arthritis) and immunological disease. Laminitis is also a connective tissue disease (Mobasheri et al., 2004). One hundred and twenty-eight canonical pathways were detected among DE genes of the DEV/OG1 comparison; the *top canonical pathways* were LXR/RXR activation and IL-17 signaling and these pathways are associated with hormone transcriptional activation and immune response. The *top network* with a score of 37 is shown (Fig. 3.4) and its *functions* were cell cycle, DNA replication, recombination, and repair, and nucleic acid metabolism. This network included 20 DE genes and displayed the presence of p38 MAPK pathway molecule. Furthermore, CALCB was up-regulated and SOD2 was down-regulated within the network.

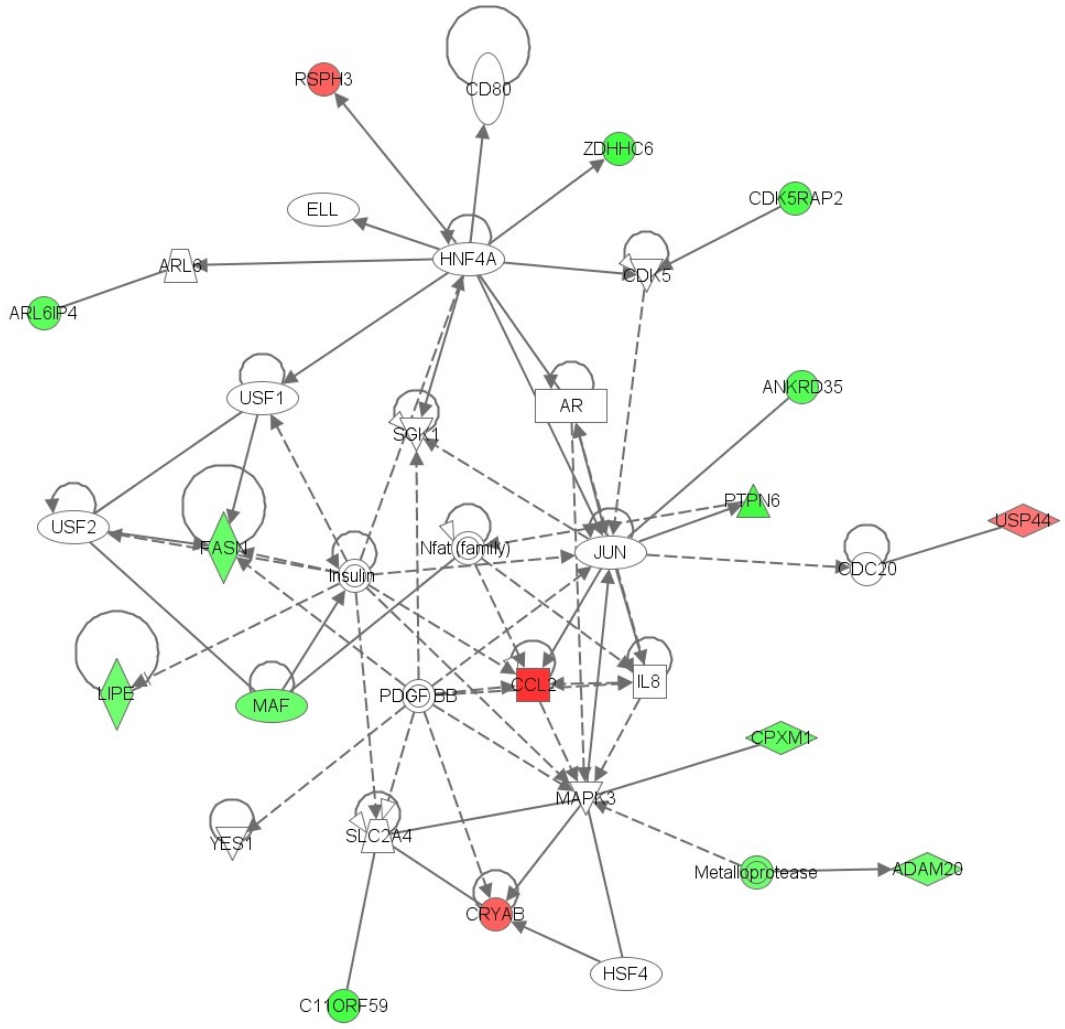

Fig. 3.2. Ingenuity network analysis of DEV compared to control. The top network identified by IPA with a significant score of 33. Both direct (solid line) and indirect (dashed line) interactions among genes (including IL8, CRYAB, and CCL2) were shown in the network. This analysis was performed on the DE genes of $P<0.01$ and $FC>2$ in the DEV/CON comparison. The intensity of the node color are depicted as down-regulated (green) or up-regulated (red). Square: cytokine/growth factor; vertical diamond: enzyme; horizontal diamond: peptidase; circle: other; parallelogram: transporter; circle-in-circle: complex; oval: transmembrane receptor; shaded circle-in-circle: group.

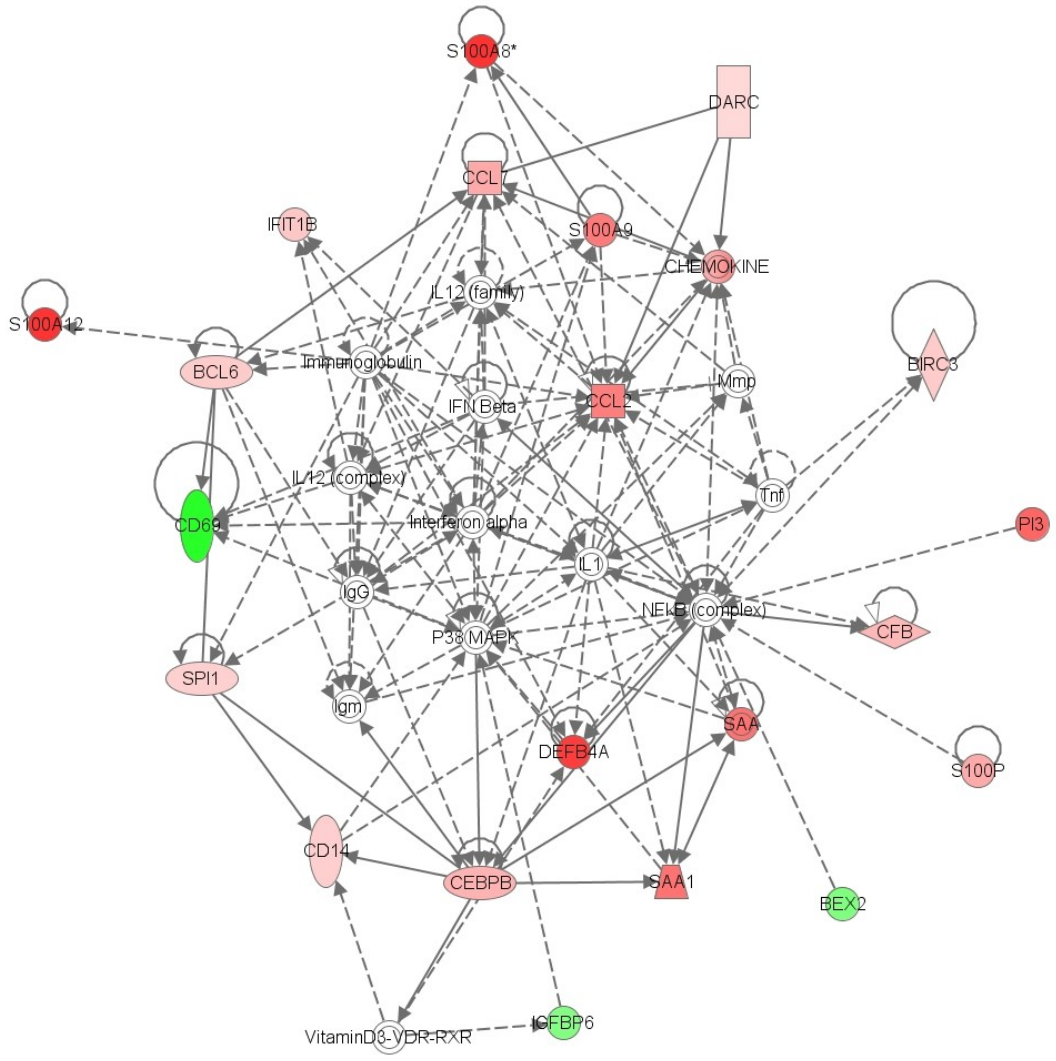

Fig. 3.3. Ingenuity network analysis of OG1 compared to control. The top network identified by IPA with a significant score of 39. Both direct (solid line) and indirect (dashed line) interactions among genes were shown in the network. This network showed the central position of p38 MAPK and NF-κB. This analysis was performed on the differentially expressed genes of P<0.01 and FC>2 in the OG1/CON comparison. The significant biofunctions associated with this network are inflammatory disease/connective disorders/skeletal and muscular disorders. The intensity of the node color are depicted as down-regulated (green) or up-regulated (red). Square: cytokine/growth factor; vertical diamond: enzyme; horizontal diamond: peptidase; circle: other; parallelogram: transporter; circle-in-circle: complex; oval: transmembrane receptor; shaded circle-in-circle: group.

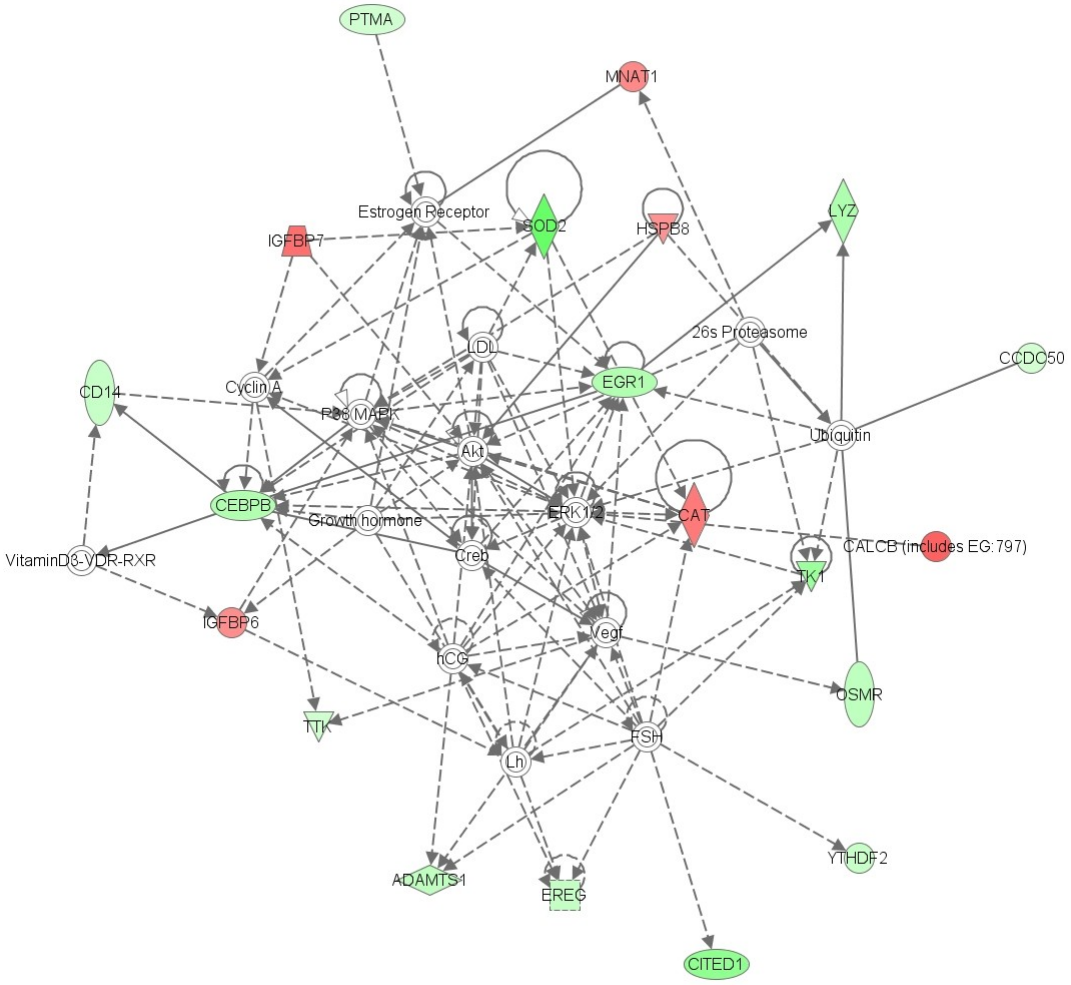

Fig. 3.4. Ingenuity network analysis of DEV compared to OG1. The top network identified by IPA with a significant score of 37. Both direct (solid line) and indirect (dashed line) interactions among genes were shown in the network. This network showed the central position of p38 MAPK. This analysis was performed on the differentially expressed genes of P<0.01 and FC>2 in the DEV/OG1 comparison. The highest scoring biofunctions associated with this network are inflammatory disease/connective disorders/skeletal and muscular disorders. The intensity of the node color are depicted as down-regulated (green) or up-regulated (red). Square: cytokine/growth factor; vertical diamond: enzyme; horizontal diamond: peptidase; circle: other; parallelogram: transporter; circle-in-circle: complex; oval: transmembrane receptor; shaded circle-in-circle: group.

Table 3.6
The top biofunctions, associated diseases, canonical pathways, and network functions that were most significant to the data set of CHO laminitis experiment. The DE genes at the level of P<0.01 and FC>2 were used as input data set for DEV/CON, OG1/CON and DEV/OG1 comparison respectively.

	Biological functions	**Associated diseases**	**Top canonical pathways**	**Top network function**
DEV/CON	Carbohydrate metabolism, inflammatory response, and hematopoiesis	Nutritional disease, cancer, ophthalmic disease, and connective tissue disorders	LXR/RXR activation and TREM1 signaling	Gene expression, carbohydrate metabolism, and small molecule biochemistry
OG1/CON	Inflammatory response, antigen presentation, and hematological system development and function	Inflammatory disease, cancer, dermatological diseases and conditions, and hematological diseases	IL-17 signaling and VDR/RXR activation	Inflammatory response, antigen presentation, and cellular movement
DEV/OG1	Cellular movement, antigen presentation, hematological system development and function, and immune cell trafficking	Metabolic disease, cancer, inflammatory disease, connective tissue disorders (arthritis), and immunological disease	LXR/RXR activation and IL-17 signaling	Cell cycle, DNA replication, recombination, and repair, and nucleic acid metabolism

Quantitative real time PCR

In order to select the best reference gene for normalization of qRT-PCR data, expression of seven reference control genes (ACTB, B2M, PPIA, GAPDH, GNB2L1, EEF1A1, and RPLP0) was analyzed. The selection of stable reference genes can minimize the variation in expression between tissues. Gene expression stability among all laminar samples (CON, DEV and OG1) was determined using geNorm software version 3.5 (Vandesompele et al., 2002). We found that two reference genes were sufficient for normalization as the pairwise variation V for the two genes was less than the 0.15 cut-off value recommended by Hellemans et al. (Hellemans et al., 2007). When the 7 candidate reference genes were ranked based on their calculated M values, we found that EEF1A1 and RPLP0 had less variation in expression among the laminar samples compared to the other 5 reference genes. We thus chose EEF1A1 and RPLP0 for normalization of qRT-PCR data.

To confirm the differential expression of microarray results, a total of 30 DE genes were selected for qRT-PCR validation. Based on the microarray analysis, we select most of the DE genes with a small P value and large fold change. The fold change of all selected genes is larger than 2. Three additional genes, each of which was differentially expressed in at least one of the three comparisons, were also selected based on their likely functional relevance to laminitis. LOXL1 is a member of lysyl oxidase family, which plays a role in the oxidation of ECM structural proteins (e.g., collagen and elastin) (Lucero and Kagan, 2006). MMP13 is a member of matrix metalloproteinase family, which is important in tissue remodeling and ECM degradation (Amalinei et al., 2007).

Basement membrane (BM) is a thin layer of ECM and its degradation is believed to be involved in the initiation of laminar failure in the pathogenesis of acute laminitis (Pollitt, 1996). KRT17 is a keratin and keratins are structural component of the hoof wall and keratinization is essential for equine hoof integrity (Grosenbaugh and Hood, 1992). qRT-PCR was performed on 30 genes across all laminar tissues (CON, DEV, and OG1 stages).

The primers used for qRT-PCR are listed in Table 3.7. Of the 8 genes analyzed by qRT-PCR for the DEV/CON comparison, six (CCL2, CPXM1, CRYAB, FASN, HOPX, and TMEM49) had significantly different expression between the two groups (Fig. 3.5). Notably, CCL2, CRYAB, HOPX, and TMEM49 were among the 11 up-regulated genes identified by microarray analysis. SEPP1 and SNF8, both identified by microarray as being down-regulated, were not significantly different from controls. ADAMTS1, CCL7, CD14, IL10RB, LOXL1, MATN2, NP, S100A8, S100A9, S100A12 and DEFB4 were confirmed to be significantly different between OG1 and CON groups (Fig. 3.6). Expression levels of the two down-regulated genes, FIBIN and MNAT1, were not similar to those found with microarray: FIBIN was not increased, whereas MNAT1 increased significantly ($P<0.05$). The direction of expression change of SNRPN gene was the same as the microarray result but did not show statistical significance at the level of $P<0.05$.

Eleven genes were chosen for qRT-PCR analysis from the DEV/OG1 comparison (Fig. 3.7). Both up-regulated genes (CALCB and HOPX), as well as all down-regulated genes, were confirmed to be significantly different between the two groups. Both GSN

and NDEL1 had the same direction of changes in expression as in the microarray analysis but the difference shown by real time PCR did not reach statistical significance.

A heat map was constructed using MeV/R software for the 30 selected DE genes based on qRT-PCR results across all conditions (CON, DEV and OG1) (Fig. 3.8). Cluster analysis showed a distinct transition in expression pattern among the conditions (CON, DEV and OG1). Moreover, the pattern of gene expression in the CON group was more similar to that of DEV than OG1, where more genes were up-regulated. Cluster 1 and cluster 4 had increased expression at the OG1 stage compared to the CON and DEV conditions. These genes play essential roles in immunity, inflammation, calcium signaling transduction (i.e., S100A8, S100A9 and S100A12) and BM turnover (i.e., ADAMTS1 and MMP13). Based on the analysis, five genes in cluster 2 had relatively high expression at the DEV stage. These genes have different biological functions but are mainly relevant to the maintenance of cell growth. Most of the genes in cluster 3 were up-regulated at the CON and DEV stage but their expression decreased at the OG1 stage. Many genes involved in the formation of actin filaments/collagen, such as GSN, MATN2, and LOXL1 were in this group.

Table 3.7
Primers of selected genes used for quantitative RT-PCR of CHO laminitis experiment.

Gene Symbol	Accession No.	Forward Sequence (5'-3')	Reverse Sequence (5'-3')	PCR Product Size (bp)	Tm(°C) *
CCL2	AJ251189	TCCAGTCACCTGCTGCTATAC	ATTCTTGGCTTTTGGAGTAGG	235	58
DEFB4	AY170305	ACTTGCCTTCCTCATTGTCTT	AGCAGTTTCTCCGCTTTCTAT	195	58
SEPP1	XR_036255	AGTGTGGAAACTGCTCTCTCA	TTGCTGATTCTCTGAAAGCTG	179	58
ADAMTS1	AF541975	AGGCTCACAATGAATTTTCG	CACAGCCAGCTTTTACACACT	225	58
CCL7	XM_001501551	TCAATAAGAAGATCCCCATCC	TCTTGTCCAGGTAGTTCGTGA	162	58
IL10RB	XM_001498211	TTACCATACCTTGCGAGTCAG	CAGGTTCATTCTCAATTTTGG	173	58
CD14	AF200416	CAGCTCTTTCCAGAGTCCAC	AGTTCTCATCGTCCACCTCA	144	60
MMP13	AF034087	CTTGAGCTGGACTCGTTGTT	CAGCAGGATTAAGGGGATAGT	131	55
GSN	U31699	TTACGGAGACTTCTTCACAGG	TGTACTTGAGGCCAGACTTGA	248	58
CALCB	AF257470	TCAGCATCTTGGTCCTGTG	ATTGGTCTTCCTCTGCACATA	155	58
MNAT1	XM_001497949	TGAAGCTGATGGTGAATGTGT	CCTAATCTCAACCTCCTTGTCA	170	58
TIMP1	CX602739	AGAAGTCAACCAGACCACCTT	TCTCCGACCTGTGGAAGTATC	152	58

Table 3.7 continued

Gene Symbol	Accession No.	Forward Sequence (5'-3')	Reverse Sequence (5'-3')	PCR Product Size (bp)	Tm(°C) *
SNF8	XM_001502240	AGCAGGTGTTGAAAGGAAGG	CCACCCACAGGGATGATAC	118	58
CRYAB	XM_001501779	AAGGTGCTGGGAGATGTGATT	CTGGGATTCGGTACTTCCTGT	103	58
S100A8	XM_001493589	ACGGATCTGGAGAATGCTATC	TGATGTCCAACTCTTTGAACC	175	58
SERPINB3	XM_001491507	CGTGCAGATGATGAAACAAAT	TTCTGTGAGCTTGTCCACTCT	195	58
NP	XM_001505137	AGCTACAGGAAGGCACTTACG	TTCTCCAGGCTTTCATAATCC	205	58
MATN2	XM_001490965	CTTTCTGCTGATTCTTGGACA	AATGAACTCCTTGACCTTTGC	217	58
FIBIN	AB302195	CTTTGTGGTGGTGACGTATTC	CCAATAAGCAAACAGAAGCAA	181	58
SNRPN	XM_001492702	TTACACCTGAGACGGACTACG	AGGTATTTGCTGTTGCTGAGA	132	58
LOXL1	CX605389	TGCATGTGAACCCGAAGTA	CTGTCTGTCCACCCTCTCC	145	58
S100A9	XM_001493485	CGACCTAGAGACCATCATCAA	TGCTTGTCCTCATTAGTGTCC	189	58
TMEM49	XM_001503742	TTACAGAAGCCATTCCAAGAA	TGGAGTTAATGATGGACAGGA	160	58
OSMR	XM_001496993	CGTGTCCACAGTCTTGCTTAT	TCGTCCACCCTACTCCTTATC	203	58
NDEL1	XM_001504824	AGGAAACTGCTTATTGGAAGG	TGCCTCCACTTCATATTTCAG	194	58
HOPX	XM_001491312	TTCAACAAGGTCAACAAGCA	AGGAGAGAAACAGCAGATGGT	219	58

Table 3.7 continued

Gene Symbol	Accession No.	Forward Sequence (5'-3')	Reverse Sequence (5'-3')	PCR Product Size (bp)	Tm(°C) *
KRT17	XM_001496441	TGAAGATCCGAGACTGGTACA	ACGAAGCTGGCATTGTCC	127	58
FASN	XM_001491292	AAGCAGGCACACACTATGGAT	AGGTCGAAGAAGAAGGAGAGG	242	55
S10012	CD535886	TCATCAACATCTTCCACCAGT	ACCTTGCACACCAGGACTAC	211	58
CPXM1	XM_001497131	AACCAGGACTTCTCCTTGCAT	TCATTCTCGTGAGGGAACTTG	149	55
EEF1A1[a]	NM_001081781	TGGAAAGAAGCTGGAAGATG	CAACCGTCTGTCTCATGTCA	132	58
RPLP0[a]	BC107717	TTGCATCAGTACCCCATTCT	ACCAAATCCCATATCCTCGT	242	58
ACTB[c]	AF035774	CCAGCACGATGAAGATCAAG	GTGGACAATGAGGCCAGAAT	88	58
GAPDH[c]	AF157626	GATGCCCCAATGTTTGTGA	AAGCAGGGATGATGTTCTGG	250	61
B2M	X69083	CGAGACCTCTAACCAGCATC	AGACATAGCGGCCAAAGTAG	186	58
PPIA	NM_021130	TGGGGAGAAAGGATTTGGTT	CATGGACAAGATGCCAGGAC	178	58
GNB2L1	CD469980	CAGGGATGAGACCAACTACG	ATGCCACACTCAGCACATC	200	58

*The optimal annealing temperature
[a]EEF1A1 and RPLP0 were used for normalization of quantitative RT-PCR data
[c] Information about the primers from (Bogaert et al., 2006)

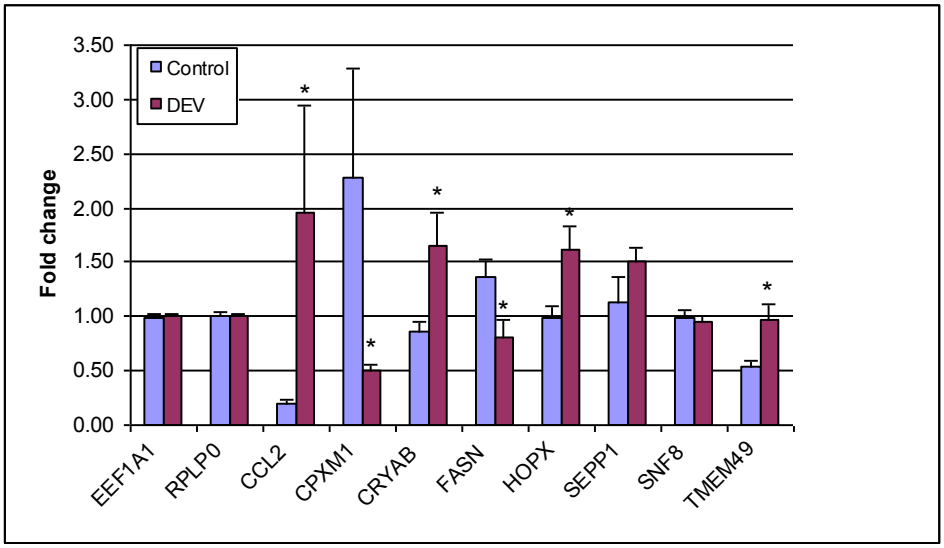

Fig. 3.5. Real time PCR validation of the microarray results of the DEV/CON comparison. EEF1A1 and RPLP0 are reference genes used for normalization. Eight DE genes from the microarray analysis were selected for real time PCR confirmation. Data are presented as mean ± SEM. Those genes marked with asterisks are significantly different from CON.

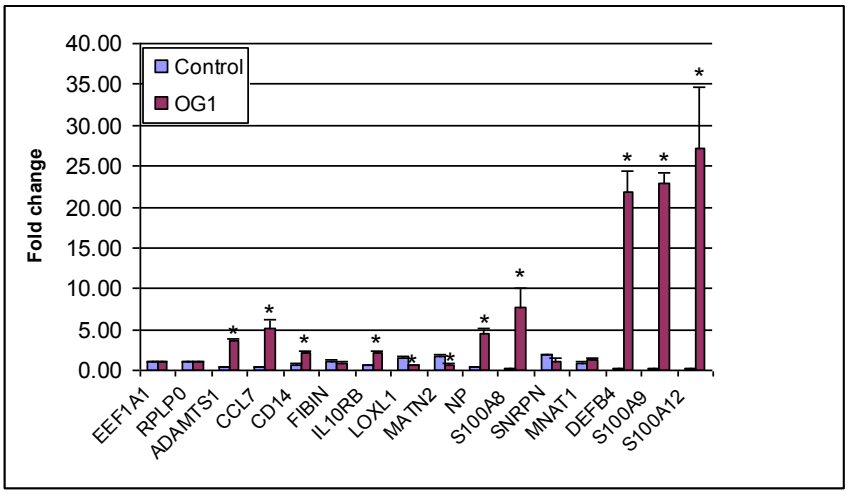

Fig. 3.6. Real time PCR validation of the microarray results of the OG1/CON comparison. EEF1A1 and RPLP0 are reference genes used for normalization. Fourteen DE genes from the microarray analysis were selected for real time PCR confirmation. Data are presented as mean ± SEM. Those genes marked with asterisks are significantly different from CON.

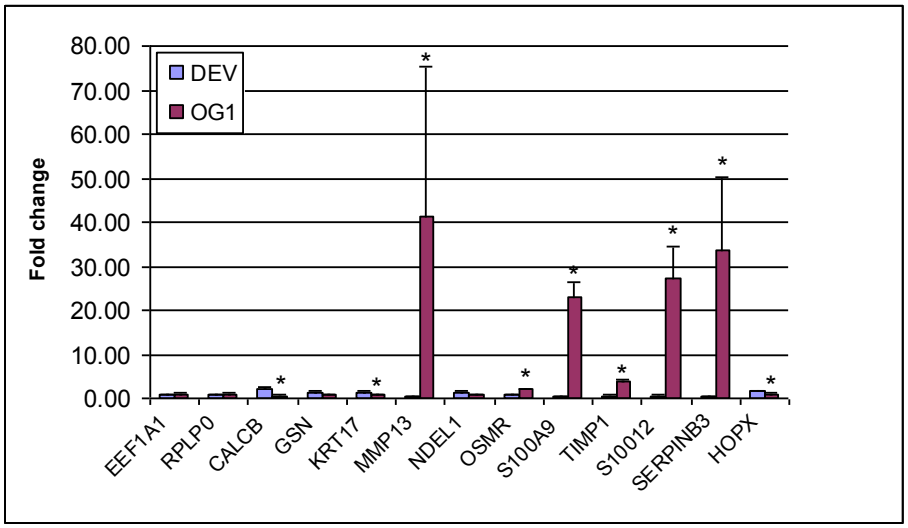

Fig. 3.7. Real time PCR validation of the microarray results of the DEV/OG1 comparison. EEF1A1 and RPLP0 are reference genes used for normalization. Eleven DE genes from the microarray analysis were selected for real time PCR confirmation. Data are presented as mean ± SEM. Those genes marked with asterisks are significantly between DEV and OG1.

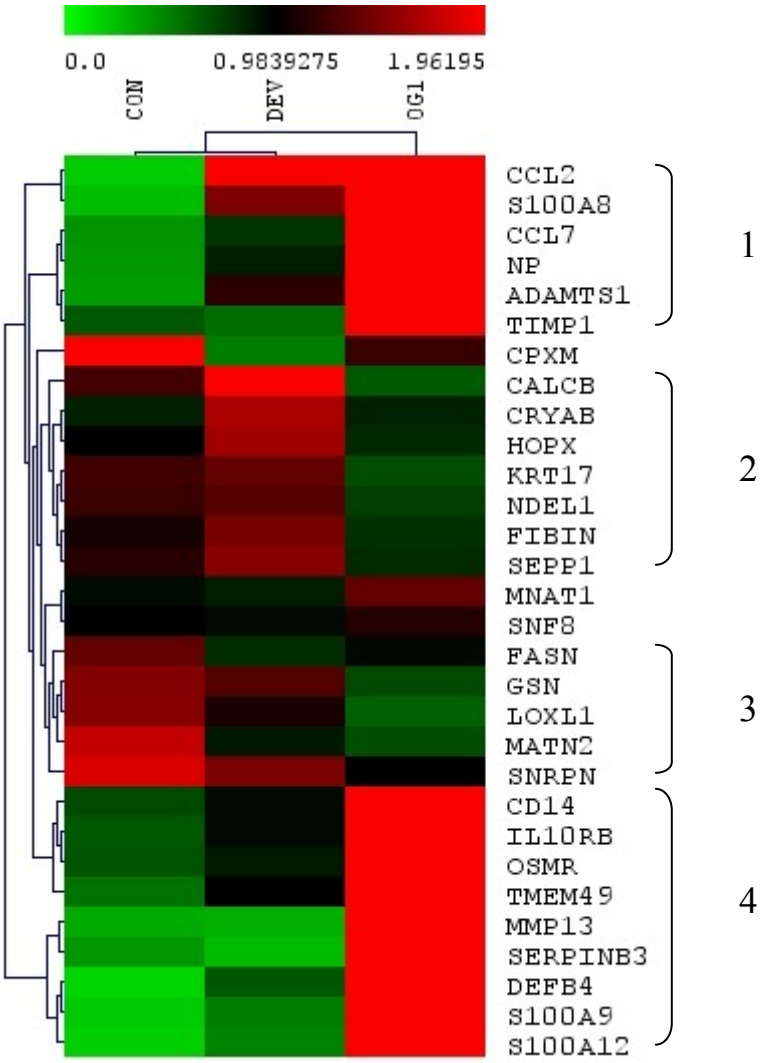

Fig. 3.8. Cluster diagram of the mean of calibrated normalized relative quantities **(**CNRQ) values at control, developmental and Obel grade 1 stage as determined by qRT-PCR. The green to red color scale demonstrates the expression value of mean of CNRQ. EEF1A1 and RPLP0 were used as reference genes to calculate normalized ΔCq.

DISCUSSION

Our goal in this study was to identify changes in the gene expression profile during the developmental stage and the onset of equine laminitis using an equine whole genome oligoarray. Oligoarrays have become a popular technique for exploring the transcriptome in domestic animals such as pigs (Zhao et al., 2006), dogs (Higgins et al., 2003), cattle (Wilson et al., 2005), and chickens (Heidari et al., 2008). We identified differential expression of 68 and 149 genes at the DEV and OG1 stages, respectively, as well as associated pathways and networks during the initiation and progression of laminitis.

Development of laminitis

In order to determine genes and regulatory pathways that might be involved in the development of laminitis, we performed transcriptional profiling and quantitative real time PCR on laminar samples obtained at the onset of fever following carbohydrate overload. Rectal temperature begins to increase linearly upon administration of starch, with fever generally occurring between 12 and 22 h. At this stage, horses also exhibit an elevated heart rate, sweating or nervousness, and signs of gastrointestinal discomfort, but show no signs of foot pain associated with laminitis (Garner et al., 1975). In the developmental stage, we found few differentially expressed annotated genes (56), and the majority of these (80%) were down-regulated when compared to controls (Table 3.1). This, in conjunction with no significantly overrepresented GO term found for down-regulated genes, suggests that the pathophysiological process leading to laminitis may first cause non-specific transcriptional suppression of seemingly unrelated genes.

This is supported by the down-regulation of 8 genes involved in the regulation of transcription. Conversely, only 11 genes were significantly overexpressed at the developmental stage, indicating that these genes may be "first responders" and could be involved in disease progression. In particular, the up-regulation of SOD2 points to oxidative stress and an excess of reactive oxygen species (ROS), presumably within the mitochondria. ROS have been proposed to cause tissue damage in joint diseases and SOD enzyme can reduce the ROS production (Afonso et al., 2007). One cause of ROS accumulation in the mitochondria is the uncoupling of the respiratory chain, although none of the DE genes at the developmental stage encode respiratory chain proteins. Another indication of disrupted metabolism is the overexpression of TMEM49, which is a component of the membrane of the intracellular vacuoles created during starvation-induced autophagy (Ropolo et al., 2007). This type of autophagy is initiated when cellular energy sources are scarce; the cell begins to catabolize intracellular molecules for energy. Importantly, the formation of intracellular vacuoles is a common feature of equine laminitis (Morgan et al., 2003; Pollitt, 1996), although it is not known whether TMEM49 localizes to these vacuoles. Differential expression was not seen, however, among members of the Atg family of autophagy-associated genes, making interpretation of this result difficult.

Two genes encoding different units of alpha-crystallin, a heat shock protein, were up-regulated in the DEV group. Alpha-crystallin are mainly expressed in the lens of the eye (Horwitz et al., 1999) and sequesters misfolded proteins that accumulate during periods of thermal, oxidative, or metabolic stress (Sun and MacRae, 2005), further

suggesting that changes seen during the developmental stage result from a prior cellular stressor. Interestingly, the transcription factor HOPX, which is elevated in differentiating human keratinocytes (Yang et al., 2010), was up-regulated, possibly as a part of the terminal differentiation and apoptosis of keratinocytes as they become part of the stratum corneum. Thus, the initiation of laminitis may involve an alteration in the rate of programmed cell death in keratinocytes.

Perhaps the most intriguing DE gene during this stage is CCL2, also known as macrophage chemotactic protein 1 (MCP-1). CCL2 is a chemoattractant for macrophages but not for neutrophils (Patterson et al., 2002) and may be up-regulated by bacterial endotoxin, glucose, trauma, or hypoxia, all of which have been postulated as causes of laminitis. Epithelial cells in other species and anatomical locations have been shown to be accessory immune cells and are capable of producing CCL2 when stimulated (Barker et al., 1991; Chui and Dorovini-Zis, 2010). We therefore hypothesize that CCL2 might represent the beginning of a common unifying pathway that connects the various proposed triggers of laminitis (i.e., hypoxia, infection, trauma, glucose/insulin) with the ultimate disintegration of the laminae.

Progression of laminitis

In contrast to the developmental stage of laminitis, samples taken at the onset of clinical symptoms (Obel grade 1 lameness) show a strong transcriptional response and a dramatic up-regulation of inflammatory genes. In addition to SOD2 and CCL2, which were seen at the earlier time point, the acute phase protein (APP) serum amyloid A (SAA1) was also overexpressed at the OG1 stage. APPs are generally produced by the

liver and their abundance may be increased several hundred-fold following acute infection (Zhang et al., 2005). Genes encoding several members of the S100 family of proteins were also significantly up-regulated (Table 3.3). S100 proteins, members of the damage-associated molecular pattern (DAMP) family of molecules, are important in both calcium signaling transduction and in the regulation of inflammation (Foell et al., 2007a). A recent study has immunolocalized the S100A8/S100A9 complex in the laminar tissue of normal and experimentally induced laminitic horses; the complex was overexpressed 106 fold at the onset of lameness (Faleiros et al., 2009). The significant up-regulation of these genes could amplify the inflammatory response and lead to laminar tissue damage. Alternatively, their calcium-binding properties could counteract the disruption of cellular ion homeostasis that was suggested by GO analysis (Table A.5). The strong induction of S100 proteins in our study and the report of overexpression of the S100A8/S100A9 protein complex in a different model of laminitis indicate that S100 proteins may play a common role in many forms of laminitis. Perhaps more telling than the elevation of the S100 gene expression, however, is the indication of a transcriptional response to microbial infection. Beta-defensin 2 (DEFB4) and peptidase inhibitor 3 (also called PI3, elafin, or SKALP) are both expressed in keratinocytes and have direct anti-microbial properties (Sallenave, 2010; Schneider et al., 2005). Likewise, the down-regulation of chemokine CXCL14, particularly in keratinocytes, is taken as evidence of bacterial infection (Maerki et al., 2009). It is thought that CXCL14 is up-regulated immediately following exposure to bacterial components and that, because of its potency and potential to cause collateral damage, its expression is quickly suppressed

(Maerki et al., 2009; Yang et al., 2003). In this study, the hypothesis of an infection is also supported by the overrepresentation members (DEFB4, CCL2, TIMP1, and CEBPB) of the IL17 signaling pathway within the group of up-regulated genes. IL17 is produced by T lymphocytes in response to dendritic cell presentation of bacterial antigens (Peck and Mellins, 2010).

The negative regulation of apoptosis was also a common finding in the GO analysis of up-regulated genes in the OG1 stage, as was intracellular ion homeostasis. Apoptosis often involves a large influx of calcium into the cell, but it is unclear whether these two processes are related in this study. Signs of apoptosis have been noted in laminar keratinocytes following administration of black walnut extract, another experimental model of laminitis (Faleiros et al., 2004). The stimulus for the attempted suppression of apoptosis, as well as the reason for the assumed failure of this suppression, is unknown. As apoptotic cells inhibit inflammation (Fadok et al., 1998) whereas necrotic cells are pro-inflammatory (El Mezayen et al., 2007), one determinant of the clinical outcome of acute laminitis may be the relative percentages of these two types of cell death, although this remains speculative.

Transition from developmental to clinical laminitis

To a certain extent, direct comparison of the early and later stages of laminitis recapitulates results found when comparing each stage to the control group. For example, GO terms involving inflammation, apoptosis, and ion homeostasis found among down-regulated genes of the DEV/OG1 comparison reflect the strong up-regulation of these genes at the OG1 stage. However, this comparison yielded two new

results: the overrepresentation of leukocyte trafficking and IL6 synthesis GO terms. It is unclear whether this is due to an up-regulation at the OG1 stage, a down-regulation at the DEV stage, or a combination of both. We may postulate that the leukocyte chemotaxis terms directly relate to the influx of neutrophils (and presumably other inflammatory cell types) into the laminae during this stage. The synthesis of IL6 is interesting, however, in light of the conspicuous lack of differential expression of "typical" proinflammatory cytokines such as tumor necrosis factor α (TNFα), interleukin 1 (IL1), and interferon γ (IFNγ). The overrepresentation of different peptidase inhibitor molecular function terms suggests a strong anti-protease response that could perhaps counteract the induction of various matrix metalloproteinases (MMPs) seen in previous studies (Kyaw-Tanner et al., 2008; Loftus et al., 2006; Loftus et al., 2009; Riggs et al., 2007).

A second type of comparison that may be equally enlightening is the identification of differentially expressed genes common to both stages. This search found 22 common genes and, while many were not annotated, DEFB4, SOD2, CCL2, and TMEM49 were consistently up-regulated, suggesting a central importance of these genes (Table 3.5). Likewise, SELENBP1, the apoptosis regulator EXOSC8, and the potassium channel TMEM38A were persistently down-regulated. It remains unknown whether these genes cause the pathological changes seen in laminitis or are merely a physiological reaction to tissue damage that has already occurred.

Comparison to previous studies

Recently, Noschka and colleagues used an equine-specific 3,076 element cDNA microarray to investigate changes in laminar gene expression during black walnut extract induced laminitis (Noschka et al., 2008). Similar to our study, these authors found up-regulation of CCL2, CCL7, S100P, SAA, SOD2, beta-defensin 1 (BD1), and SKALP (PI3), suggesting a role for these genes in laminitis independent of the mechanism of induction. Noschka and colleagues did not identify changes in apoptosis regulators or ion channels, perhaps due to the limited number of genes represented in the microarray used. For comparison, Budak and colleagues used a 15,000 bovine microarray chip to study the oligofructose induction model of laminitis (Budak et al., 2009), which is similar to the carbohydrate overload model used in this study. Although the platform used by Budak et al. had more complete coverage than the one used by Noschka, only three genes (BIRC3, CCL2, and DARC) were differentially expressed both in our study and in Budak's. The consistent up-regulation of CCL2 among three different models of laminitis highlights this molecule's likely importance to the pathogenesis of this disease.

Relevance to current hypotheses

Currently, the three most popular hypotheses regarding the initiation of laminitis implicate vasoconstriction/hypoxia, MMPs, and escape of bacteria from the hindgut into the bloodstream (Bailey et al., 2004). Hypoxia typically stimulates expression of response factors such as hypoxia-inducible factor (HIF1α) (Semenza, 1998), vascular endothelial growth factor (VEGF) (Shweiki et al., 1992), endothelial nitric oxide synthase (eNOS) (Thompson et al., 2000), and heat shock protein 90 (HSP90) (Almgren

and Olson, 1999). We saw no evidence of differential expression of these genes and thus cannot hypothesize that hypoxia plays a role in this model of laminitis. However, we saw evidence of transcriptional up-regulation of MMP13. Therefore, as with the vasoconstriction/hypoxia hypothesis, we did not generate new data supporting this theory but we cannot rule it out as a possibility. We did, however, find evidence to support the hypothesis that bacteria or bacterial components escape from the hindgut and cause laminar inflammation. The differential expression of anti-microbial peptides such as DEFB4, PI3, and CXCL14 is suggestive of the presence of bacterial antigens, although microarray data necessarily need to be confirmed at the protein and functional levels.

CONCLUSION

We have used a 21,000 equine oligoarray to investigate changes in the transcriptional profile of laminar tissue during carbohydrate overload induced laminitis. This array is both genome-wide and species-specific, making our dataset the most reliable and complete picture of gene expression during laminitis. We discovered what appear to be central roles of apoptosis and intracellular ion homeostasis pathways and identified a small set of consistently differentially expressed genes that are likely to play a role in the development and progression of this disease. Of these, CCL2 is arguably the most prominent and could integrate signals from a variety of stimuli (infection, hypoxia, elevated glucose) into a common pathway leading to laminar failure. Pathway and network analysis revealed biological relationships among DE genes relevant to equine laminitis and the presence of p38 MAPK and NF-κB pathway molecules. In addition, the

overexpression of several anti-microbial genes supports the hypothesis that bacterial components might play a role in the pathogenesis of the carbohydrate overload model of laminitis. Transcriptional analysis of other models of laminitis and identification of common differentially expressed genes will provide further insight into the cause of this devastating disease.

CHAPTER IV

GENE EXPRESSION PROFILING IN INDUCED LAMINITIC HORSES BY PROLONGED HYPERINSULINAEMIA (HI) USING AN EQUINE WHOLE GENOME OLIGOARRAY

INTRODUCTION

Equine laminitis is an extremely painful hoof disease that affects the laminar tissue. The condition is defined as the separation that occurs between the coffin bone and the hoof wall (Pollitt, 2004b). Laminitis has been linked to many factors such as grain overload, gastrointestinal tract disease and endotoxemia. Studies have shown that metabolic and endocrine abnormalities are risk factors for laminitis in horses and ponies (Geor and Frank, 2008; Geor, 2008; Johnson, 2002; Treiber et al., 2006b). Experimentally induced models of laminitis have been established through the administration of CHO (Garner et al., 1975), BWE (Minnick et al., 1987), OF (van Eps and Pollitt, 2006) and prolonged HI with euglycaemia (Asplin et al., 2007; de Laat et al., 2010).

HI induced laminitis is considered to be a model of endocrinopathic laminitis. Constant infusion of insulin and glucose while maintaining euglycaemia causes laminitis in healthy ponies (Asplin et al., 2007) and healthy Standardbred horses (de Laat et al., 2010). Naturally occurring HI is a condition of high levels of insulin in the bloodstream and is proposed to be caused by insulin resistance (IR) (Frank, 2009; Johnson et al., 2004b). IR is the core component of equine metabolic syndrome (EMS) and equine

Cushing's disease (ECD) (Frank, 2009; Geor, 2009; Johnson et al., 2004a) and is defined as failure of tissues to take up glucose via insulin-dependent glucose transporters. Due to IR, glucose remains in the blood and the pancreas continues to secret insulin, which causes HI (Kronfeld, 2005; Shanik et al., 2008). Laminar lesions in the hoof were demonstrated in HI induced laminitis using light and transmission electron microscopy (TEM) (Nourian et al., 2009). There was no global BM separation in affected ponies following HI (Nourian et al., 2009).

EMS is a term used to describe a cluster of conditions, including obesity, IR and HI (Johnson, 2002; Johnson et al., 2009). This syndrome is similar to the metabolic syndrome in humans, which is primarily associated with cardiovascular disease and type 2 diabetes mellitus (T2DM) (Caballero, 2004; Miranda et al., 2005). It is a neurodegenerative disease (McFarlane, 2007) and has been shown to be associated with laminitis (Donaldson et al., 2004). Recent studies have shown a connection between high insulin and laminitis with IR in pony breeds (Welsh and Dartmoor) (Kronfeld et al., 2005; Treiber et al., 2006b). A study using a cohort of ponies demonstrated the importance of monitoring insulin concentration and obesity to determine risk of laminitis (Carter et al., 2009). Currently, there are several theories regarding the contribution of IR/HI to laminitis. One theory states that IR predisposes horses to laminitis by altering vascular dynamics and endothelial function (Geor and Frank, 2008; Treiber et al., 2006a). Another theory states that endocrinopathic laminitis is the result of inflammation (McGowan, 2008). Asplin and co-workers suggested that it is not IR but insulin toxicity that causes endocrinopathic laminitis (Asplin et al., 2007). Research in the horse has

demonstrated that there is an interconnection between IR, altered lipid metabolism, inflammation and obesity (Vick et al., 2007). At present, there are two competing theories regarding IR in humans: the inflammation theory and the lipid overload theory (Taubes, 2009). The lipid overload theory states that IR is associated with the level of fatty acids in the bloodstream and that the accumulation of fat promotes IR. On the other hand, the inflammatory theory states that the overexpression of inflammatory cytokines can induce IR (Taubes, 2009). Human research findings in regard to the relationship between obesity, inflammation, and IR may give insight into the association of these conditions to laminitis in horses with EMS (de Luca and Olefsky, 2008).

Because the early stages of laminitis are critical in understanding the progression of the disease, we sought to identify differentially expressed genes and their likely interactions that may lead to observed pathological changes in the HI model of laminitis. Knowing the gene expression changes within the laminar tissue during the development and progression of laminitis could lead to new ways to predict disease outcome and design therapies for treatment/prevention. The overall objective of this study was to determine global gene expression profile and identify differentially expressed genes and their likely interactions in laminar tissue 48 h after HI induction using the 70-mer equine-specific ~21,000 element whole genome expression microarray (Bright et al., 2009).

MATERIALS AND METHODS

Experimental design

Eight clinically normal Standardbred horses (7 geldings, 1 filly) were used for this study. The horses were divided into control and experimental groups, with 4 horses in each group. The horses were examined and confirmed to be healthy and had no history of metabolic-endocrine disorders. Laminitis was induced in the experimental horses (labeled TH) using a prolonged euglycemic-hyperinsulinemic clamp (EHC) technique (DeFronzo et al., 1979). Each treatment horse was paired with a control horse (labeled CH), which had a saline infusion and was then euthanized. The laminar samples were rapidly collected from the hoof and distal phalanx, snap frozen in liquid nitrogen, and stored at -80°C. The Animal Ethics Committee of the University of Queensland approved the experimental protocol.

A two channel, balanced block design was used to compare HI and control samples. Dye swaps were incorporated into the hybridization scheme of the experiment to eliminate dye bias. A total of 4 whole genome equine microarray slides were used. The microarray hybridization experiment conducted in this study is shown in Fig. 4.1.

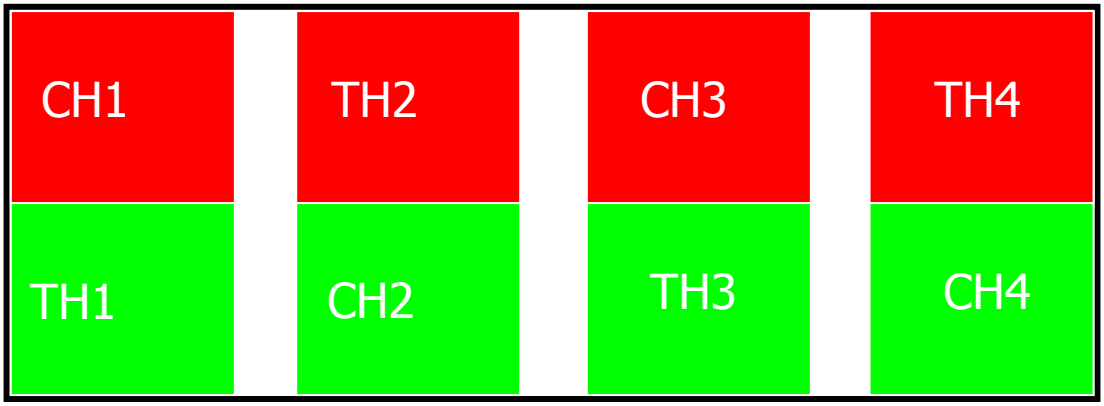

Fig. 4.1. Diagram of the HI model laminitis experimental design. Four hybridizations were performed. The green color represents Cy3 and the red color represents Cy5. The laminar samples labeled with CH1, CH2, CH3, and CH4 were from control horses. The laminar samples labeled with TH1, TH2, TH3, and TH4 were from HI induced horses. Half of the samples from the control group were labeled with Cy3 and the other half were labeled with Cy5. Half of the samples from the HI laminitis group were labeled with Cy3 and the other half were labeled with Cy5.

Equine 21K oligonucleotide microarray

The 70-mer oligoarray was constructed based on a 2.4 Gb EquCab2 of the horse genome, combined with RefSeq release 26, UniGene build#3, SwissProt release 12 and ~43,000 unpublished ESTs (Bright et al., 2009). Probes were synthesized (Invitrogen, Carlsbad, CA) and printed into amino-silane coated slides (Corning Incorporated, Corning, NY).

RNA isolation and cDNA synthesis

Total RNA was extracted from 80-100 mg of frozen laminar tissue, which was disrupted and homogenized in the presence of Tri reagent (MRC, Cincinnati, OH) as described in (Chomczynski, 1993). This was followed by RNA cleanup with RNase-free DNase treatment (RNeasy Mini Kit, Qiagen, Valencia, CA) of the isolate according to

the manufacturer's protocol. RNA concentration was quantified using a spectrophotometer (NanoDrop Technologies, Wilmington, DE) and the quality was evaluated with an Agilent 2100 Bioanalyzer and RNA Lab Chip (RNA 6000 Nano Assay, Agilent Technologies, Palo Alto, CA). cDNAs were synthesized from total RNA with the 3DNA Array 900MPX Expression Array Detection Kit (Genisphere, Hatfield, PA) using SuperScript II reverse transcriptase (Invitrogen, Carlsbad, CA). One microgram of total RNA was combined with random primer and MPX dT primer, incubated at 80°C for 10 min, and cooled on ice for 2 min. Finally, 0.5M NaOH/50mM EDTA was added to degrade any remaining RNA; this reaction was neutralized with 1 M Tris-HCl (pH 7.5).

cDNA purification, tailing and ligation

The cDNA was purified using the Qiagen MinElute PCR purification kit (Qiagen, Valencia, CA) according to the manufacturer's protocol. Then nuclease-free water was added to the purified cDNA to a volume of 16.5 µl. The cDNA was incubated at 95°C for 10 min in a PCR thermal cycler and cooled on ice for 2 min. The cDNA was tailed by terminal deoxynucleotidyl transferase (TdT) enzyme and ligated to 3DNA capture sequence. The ligated DNA was purified again using the Qiagen MinElute PCR purification kit (Qiagen, Valencia, CA) according to the manufacturer's protocol.

Pre-hybridization treatment of microarray slide

Rehydration and crosslinking of the microarray slide was performed to ensure that the probe was spread evenly in the spot and immobilized on the slide. The slides were rehydrated by holding the slide label side down over the steam from a 50°C water

bath for 10 s. The slides were dried for 5 s at 65°C and then brought to room temperature (20°C) for 1 min. This process was repeated up to four times. After rehydration, the slides were subjected to UV crosslinking at 750 MJ/cm^2 for 2 minutes.

Microarray cDNA hybridization

A 543 µl reaction was used for the tagged cDNA hybridization mix, which was prepared according to the manufacturer's instructions (Genisphere, Hatfield, PA). The mixture was applied to the gasket slide of an Agilent microarray hybridization chamber and the microarray slide (array side down) was laid on top of the gasket slide. The hybridization chamber was assembled and the slides were then incubated at 55°C while rotating at 5 rpm in a hybridization oven (Agilent Technologies, Santa Clara, CA) for 16 hours. The "microarray-gasket slide sandwich" was then washed once with pre-warmed (42°C) 2x SSC-0.2% SDS wash buffer, disassembled, and washed again. The array slide was then washed with 2x SSC and 0.2x SSC wash buffers. Slides were dried at room temperature, centrifuged at 1000 rpm for 4 min, and then stored in a dry box prior to the second hybridization.

3DNA hybridization and wash

3DNA hybridization master mix was prepared according to the manufacturer's instructions (Genisphere, Hatfield, PA), applied to the array, and covered with a coverslip in the dark. The slide was placed in a 50 ml conical tube with 400 µl of nuclease-free water and incubated horizontally at 55°C in a hybridization oven (Agilent Technologies, Santa Clara, CA) for 4 hours in the dark. All washing steps following 3DNA hybridization were conducted in the dark. The slide was taken out of the

incubator and washed with pre-warmed (42°C) 2x SSC-0.2% SDS wash buffer. The cover slip was removed and the slide was washed again with 2x SSC-0.2% SDS buffer. The slide was then washed with 2x SSC and 0.2x SSC wash buffers. Finally, the slide was dried at room temperature, centrifuged at 1000 rpm for 4 min, and stored for scanning.

Microarray image processing and data analysis

The slides were scanned with a GenePix Personal 4000B microarray scanner (Molecular Devices Corporation, Sunnyvale, CA) at a resolution of 5 μm. The fluorescence intensities from each array were quantified using GenePix Pro 6.0 program (Molecular Devices Corporation, Sunnyvale, CA). Each spot was inspected by manual gridding and empty spots were flagged out. The median signal intensity and local background intensity of each gene were normalized by print-tip loess normalization using the bioconductor LIMMA package (Gentleman et al., 2004) in the R statistical computing environment (http://www.r-project.org/). Linear models and empirical Bayes moderated F statistics (Smyth, 2004) were applied to obtain the P value and $\log_2$-based fold change for each gene.

Gene ontology analysis

The Database for Annotation, Visualization and Integrated Discovery (DAVID version 6.7) (Dennis et al., 2003; Huang et al., 2009) (http://david.abcc.ncifcrf.gov/) was used to obtain gene ontology (GO) terms of biological process (BP), cellular component (CC) and molecular function (MF) for DE genes of the HI/CON comparison. RefSeq protein IDs from human orthologs were used as input and Fisher's Exact P value of 0.05

was used as a cutoff for determining statistical significance. Gene ontology terms of all levels were included in the analysis.

Pathway analysis

Ingenuity Pathways Analysis program (Ingenuity Systems, version 8.7) was used to obtain networks, relevant biofunctions and canonical pathways pertinent to laminitis. A data set containing gene identifiers and corresponding expression values from the microarray expression analysis was uploaded into the application. Functional analysis identified the biological functions and diseases that were most significant to the dataset. Fisher's Exact test was used to calculate the P value determining the probability that each biological function and disease assigned to that data set (or network) is due to chance alone.

Quantitative real time PCR

To validate microarray results, the expression of a subset of DE genes from the HI/CON comparison were examined by quantitative reverse transcription PCR (qRT-PCR). cDNA was synthesized from total RNA (250 ng) of each sample (HI and CON) using TaqMan® Reverse Transcriptase reagents (Applied Biosystems, Carlsbad, CA) according to the manufacturer's protocol. The cDNAs were quantified by qRT-PCR on a LightCycler ® 480 thermocycler (Roche Diagnostics, Indianapolis, IN) using 2x LightCycler ® 480 SYBR Green I master mix (Roche Diagnostics, Indianapolis, IN). Primers for selected genes were designed by Primer 3 program. To calculate the PCR amplification efficiencies of target and reference genes, a serial dilution of laminar cDNA was made (200 ng/µl, 100 ng/µl, 50 ng/µl, 25 ng/µl, 12.5 ng/µl, and 6.25 ng/µl)

and used as a template. PCR efficiency of each gene was determined from the slope of the line along the concentrations as calculated by LightCycler ® 480 basic software (Roche Applied Science, Indianapolis, IN). Each individual sample was run in duplicate and the average crossing point (Cp) value was used for further analysis.

Quantitative real time PCR data analysis

In order to select appropriate reference genes for qRT-PCR data normalization, qRT-PCR was carried out for eleven equine genes ACTB, B2M, PPIA, GAPDH, GNB2L1, EEF1A1, HPRT1, TUBA1, UBB, RPL32 and RPLP0. The average expression stability and the optimal number of control genes for normalization were determined using the geNorm computer program (http://medgen.ugent.be/~jvdesomp/genorm/) (Vandesompele et al., 2002). The two most stable genes from those tested were used for normalization of the qRT-PCR data. The data was analyzed by the delta-Cq method (Hellemans et al., 2007) in qBase*Plus* (Biogazelle, Ghent, Belgium). The statistical significance of the derived CNRQ values between the two groups was determined by nonparametric Mann-Whitney test in SPSS 17.0 statistics software (SPSS Inc, Chicago, IL). A P value less than 0.05 was considered statistically significant.

Hierarchical cluster analysis

The mean values of selected DE genes from qRT-PCR were used to do hierarchical clustering analysis as well as heat map construction using MultiExperiment viewer and R (MeV/R) program version 4.6 (Chu et al., 2008; Saeed et al., 2003).

RESULTS

All horses (n=4) in the treatment group developed laminitis (Obel grade 2), whereas the control horses (n=4) did not show any signs of clinical laminitis. TH4 was the most insulin sensitive horse but all horses treated with insulin were more sensitive than ponies and also compared to horses used in previous studies with EHC (Asplin et al., 2007; Rijnen and van der Kolk, 2003). Changes in other parameters (e.g., body temperature, heart rate and respiration rate) and various clinical outcomes of the horses during the study have been described by de Laat et al. (2010).

Identification of differentially expressed genes in laminar tissue following HI

Differential gene expression analysis was performed by comparing gene expression profiles between laminar tissues from 48 h HI treated and control horses. There were 106, 242, and 772 genes differentially expressed (DE) at the cut-off of $P<0.005$, $P<0.01$ and $P< 0.05$ respectively (Table 4.1). The fold change range of gene expression difference was 38.1 to 0.07 for each cut-off P value. Genes with a P value less than 0.01 and fold change larger than 2 were used for subsequent analysis. This category contained 242 genes; of which 116 were up-regulated and 126 were down-regulated (Table 4.1).

Table 4.1
Distribution of differentially expressed genes at different significance level and fold change larger than 2.

	Upregulated	Downregulated	Total
P<0.005	57 (53.8%)	49 (46.2%)	106
P<0.01	116 (47.9%)	126 (52.1%)	242
P<0.05	342 (44.3%)	430 (55.7%)	772

Table 4.2
Top differentially expressed genes (14 upregulated and 14 downregulated; P<0.01 and fold change>2) for the HI/CON comparison. Unannotated genes are labelled as NULL. Asterisks denote genes selected for confirmation with PCR.

Gene Name	Description	Public Accession	P	Fold Change	PCR
Upregulated					
CRTAC1	Cartilage acidic protein 1	XM_001501238	0.0008	7.65	
SUGT1	SGT1, suppressor of G2 allele of SKP1	XM_001492933	0.0042	7.58	*
RILPL2	Rab interacting lysosomal protein-like 2	DN504908	0.0047	7.06	
MORN3	MORN repeat containing 3	XM_001496205	0.0008	6.86	
PTPRQ	Protein tyrosine phosphatase, receptor type,Q	XM_001492869	0.0001	6.66	
EIF1AX	Eukaryotic translation initiation factor 1A, X-linked	XM_001492752	0.0066	6.60	*
HEMGN	Hemogen	XM_001504109	0.0008	5.93	
C16orf44	Chromosome 16 open reading frame 44	XM_001502352	0.0021	5.59	
C17orf79	Chromosome 17 open reading frame 79	CX605748	0.0074	5.48	
S100A2	S100 calcium binding protein A2	CX598422	0.0064	5.39	*
LMOD2	Leiomodin 2	XM_001502348	0.0082	5.18	
TULP3	Tubby like protein 3	XM_001490880	0.0017	5.04	*
ZNF75A	Zinc finger protein 75a	XM_001499142	0.0019	4.99	
MAPK14	Mitogen-activated protein kinase 14	XM_001494719	0.0002	4.95	*
Downregulated					
MYBPC2	Myosin binding protein C	XM_001494408	0.0017	0.07	
SLC24A2	Solute carrier family 24, member 2	XM_001495010	0.0049	0.14	
TIMM9	Translocase of inner mitochondrial membrane 9 homolog	XM_001497047	0.0017	0.15	

Table 4.2 continued

Gene Name	Description	Public Accession	P	Fold Change	PCR
Downregulated					
SDF2L1	Stromal cell-derived factor 2-like 1	XM_001493091	0.0057	0.16	*
RER1	RER1 retention in endoplasmic reticulum 1 homolog	NULL	0.0065	0.17	*
RNF32	Ring finger protein 32	XM_001504692	0.0095	0.18	
NULL	NULL	CX603169	0.0078	0.19	
FANCF	Fanconi anemia, complementation group F	NULL	0.0079	0.19	
C17orf64	Chromosome 17 open reading frame 64	XM_001501083	0.0026	0.19	
PSMD1	Proteasome (prosome, macropain) 26S subunit, non-ATPase, 1	XM_001498019	0.0027	0.19	*
C16orf77	Chromosome 16 open reading frame 77	XM_001500794	0.0026	0.20	*
C16orf46	Chromosome 16 open reading frame 46	XM_001501937	0.0081	0.21	
NULL	NULL	CX593149	0.0094	0.21	
PACSIN3	Protein kinase C and casein kinase substrate in neurons 3	XM_001490695	0.0017	0.21	

A total of 28 DE genes with the largest fold changes (up and down regulated) are shown in Table 4.2. Among these 28 genes, the most up-regulated gene CRTAC1 is a cartilage-related extracellular matrix protein (Redruello et al., 2010). The degradation of extracellular matrix proteins (e.g., collagen and laminin) has been described in acute laminitis (Pollitt and Daradka, 1998). SUGT1, HEMGN and MAPK14 are up-regulated and are signal transduction regulators and genes maintaining homeostasis. Three genes encode adaptor proteins (RILPL2, ZNF75A, and MYBPC2) also changed their expression. Additionally, down-regulated gene SLC24A2 is a sodium-calcium exchanger (Prinsen et al., 2000).

The list of all differentially expressed genes ($P<0.01$ and fold change>2) is shown in Table A.7. It is noteworthy that three extracellular matrix proteins encoded by KRT15, ADAMTS1 and CRTAC1 were all up-regulated. KRT15 is a member of the keratin family and keratins are a structural component of the equine hoof. ADAMTS1 is a member of the ADAMTS family and ADAMTSs play an important role in ECM components cleavage. The up-regulated gene MAPK14 (also called p38 MAPKα) is a member of the mitogen-activated protein kinase (MAPK) subfamily. P38 MAPK is associated with neutrophil migration during acute laminitis (Eckert et al., 2008). Among other DE genes, PROM2 and STC1 encode glycoproteins and glycoproteins are main component of the BM of the lamina. Next, OR7G2, OR5M3, and OR5AK2 are among the DE genes that belong to the olfactory receptor family, which is a superfamily of G-protein coupled receptors (GPCRs). Further, three genes encoding S100 calcium binding proteins were differentially expressed, including S100PBP, S100A1 and S100A2. The

presence and overexpression of S100A8 and S100A9 have been described in the black walnut extract model of laminitis (Faleiros et al., 2009). Metalloproteinase carboxypeptidase A6 (CPA6), ADAM-like, decysin 1 (ADAMDEC1) and ADAMTS1 were all dysregulated. Among these genes, only ADAMTS1 was up-regulated. ADAMDEC1 and ADAMTS1 have metalloendopeptidase activity. Both of ADAM and ADAMTS family play role in the degradation of ECM components (Cawston and Wilson, 2006). CPA6 has carboxypeptidase activity. Carboxypeptidase is a zinc metalloenzyme and is important for the keratinization process (Parisi and Vallee, 1969; Tomlinson et al., 2004). Keratin is a structural protein of equine hoof and the keratinization is essential for the hoof structure integrity (Grosenbaugh and Hood, 1992).

GO analysis

Gene ontology analysis was performed within the up and down-regulated DE genes ($P<0.01$ and $FC>2$) discovered between the 48 h HI and control laminar tissue comparison using the NIH-DAVID Bioinformatics Resources version 6.7 software (Dennis et al., 2003; Huang et al., 2009). Only enriched GO terms ($P<0.05$) are shown (Table A.8). The biological process categories containing the greatest number of DE genes were response to stimulus (31%) and immune response (11%).

It is noteworthy that there is only one major histocompatibility complex (MHC) gene (HLA-DQA1, MHC class II, DQ alpha 1) in the input gene list, however, DAVID algorithm matched it to six different isoforms (the column labeled ‘Count” is 6 in the overrepresented category). DAVID database integrates multiple resources together and attempts to remove redundancy and cross linking among resources. However, in each original database, many gene accessions could represent the same gene or its different isoforms. Thus one MHC gene was counted 6 times. The majority of the GO terms of BP category, including immune response (BNIP3, VSIG4, POLM and HLA-DQA1), regulation of cell cycle and negative regulation of cell proliferation were found in the up-regulated genes (Table A.8). Cellular component terms pointed to changes in cytosol and nuclear part. Molecular functions were associated with molecular transducer activity and signal transducer activity, suggesting a transcriptional up-regulation of genes associated with signal transduction during the OG2 stage of HI associated laminitis. On the other hand, genes involved in proteolysis and cellular response to stimulus were down-regulated. Two overrepresented cellular components were both intracellular and molecular functions related to signal transduction regulation and protein binding.

Pathway analysis

We utilized the GenMAPP version 2.1 (Salomonis et al., 2007), KEGG (Kanehisa et al., 2008), and Ingenuity Pathways Analysis (Ingenuity Systems, http://www.ingenuity.com/, version 8.7) applications to establish relationships among DE genes ($P<0.01$ with $FC>2$) and to predict pathways potentially associated with the pathogenesis of laminitis. When we mapped the full set of DE genes into the metabolic process category in GenMAPP, two up-regulated genes, GAPDH and PGAM1, were linked to glycolysis and gluconeogenesis pathway (Fig. 4.2). Another up-regulated gene, GALM, was also in the glycolysis and gluconeogenesis pathway but was not mapped by GenMAPP program since the MAPP category metabolic process doesn't contain this gene. Spliceosome pathway was detected using KEGG pathway database linked through the DAVID database.

Network analysis

Ingenuity analysis was performed on genes that were differentially expressed at $P<0.01$ with a fold change of 2 or higher. The *top biofunctions* based on P value determined by IPA were DNA replication, recombination, repair, cell cycle, organ morphology, cardiovascular system development and function (Table 4.3). The *associated diseases* identified through the analysis were cancer (Hu et al., 2010), dermatological diseases (Dourmishev and Draganov, 2009) and endocrine system disorders (Maser et al., 2006). Essentially, all these conditions have gastrointestinal tract involvement (Table 4.3). Many dermatological diseases have been associated with an underlying malignancy of gastrointestinal tract (Dourmishev and Draganov, 2009). One

hundred and forty-four *canonical pathways* were detected and the top canonical pathways based on P value determined through the IPA library were Parkinson's signaling and maturity onset diabetes of young (MODY) signaling. Parkinson's disease is a neurodegenerative disorder that is associated with impairment of insulin signaling (Cardoso et al., 2009; Moroo et al., 1994). MODY is a form of diabetes that often occurs at young age (Nyunt et al., 2009). The *top network* with a score of 48 and the second network with a score of 37 are shown (Fig. 4.3 A and B). The top *network function* was DNA replication, recombination, repair, cell death, skeletal and muscular system development and function. There were 35 genes in the top network, which included 27 of the genes we identified as DE in the HI/CON comparison. Therefore, additional 8 genes were found to interact with DE genes through the network. Of the DE genes in the network, 17 genes were up-regulated and 10 genes were down-regulated. Furthermore, among these 27 genes, SUGT1 had a high degree of up-regulation with a fold change of 8. Additionally, the network showed the central position of p38 MAPK, MAPK14, and NF-κB (not DE) in the pathways, as well as the peripheral role of PSMD1 and HSPA8. The second network with a score of 37 had 35 genes, which included 21 genes we identified as DE. Another 14 genes had biological relationships with those DE genes through the network. Of the DE genes in the network, 13 genes were up-regulated and 8 genes were down-regulated. The associated *network functions* were nervous system development and function, tissue development and small molecule biochemistry. In the network, FOSL1 had a high degree of up-regulation with a fold change of 5.

Fig. 4.2. Glycolysis and gluconeogenesis pathways generated by GenMAPP program.
The DE genes (P<0.01 and FC>2) of HI/CON comparison were used as input to GenMAPP. The gene database used was Hs_std_20070817.gdb. The gene identifier used was the human ortholog protein ID. Those genes linked to MAPPs representing the metabolic process (i.e. glycolysis and gluconeogenesis) in GenMAPP are color coded (red: up-regulation, green: down-regulation).

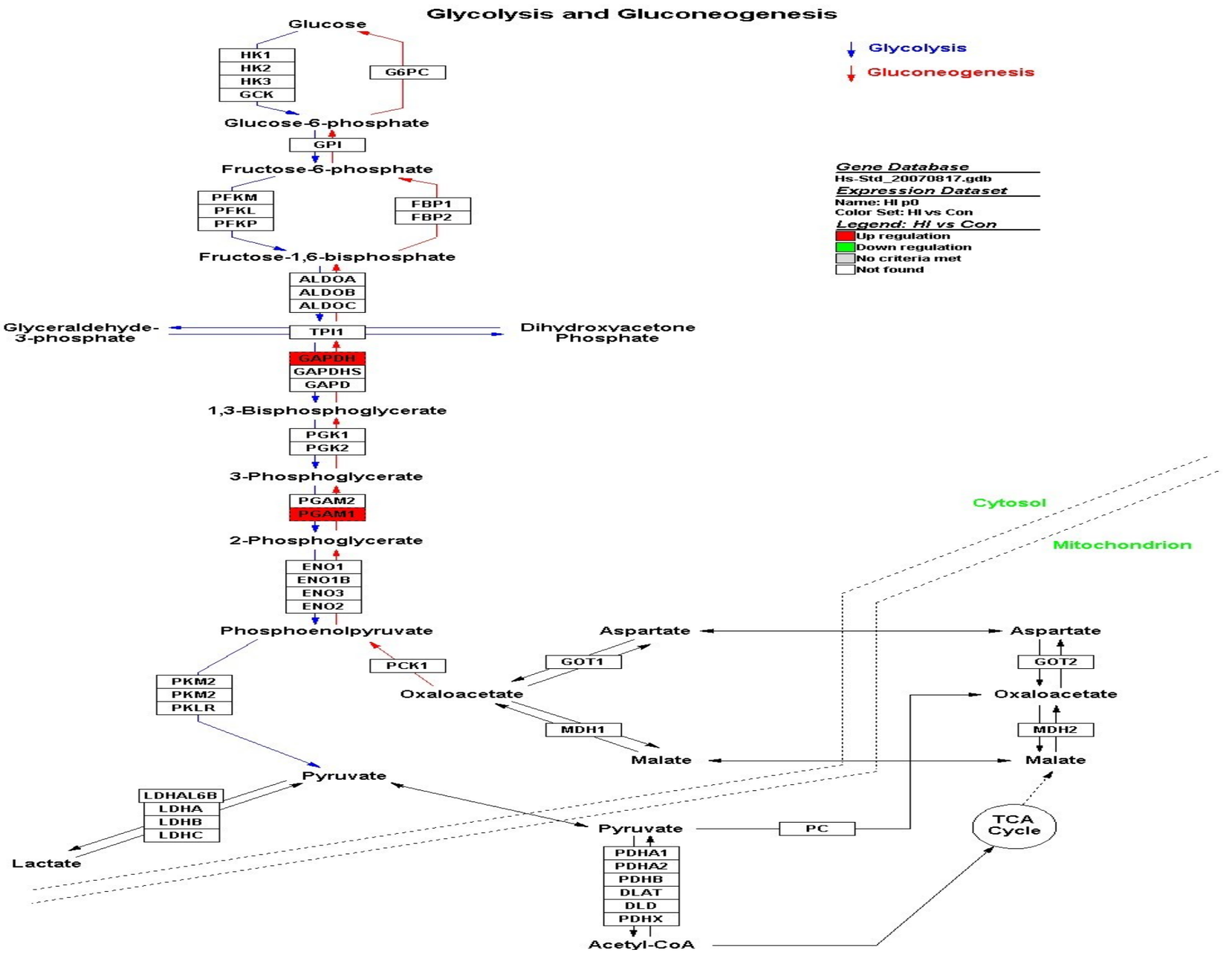
Glycolysis and Gluconeogenesis
Glycolysis
Gluconeogenesis
Gene Database
Hs-Std_20070817.gdb
Expression Dataset
Name: HI p0
Color Set: HI vs Con
Legend: HI vs Con
Up regulation
Down regulation
No criteria met
Not found
Glucose
HK1
HK2
HK3
GCK
G6PC
Glucose-6-phosphate
GPI
Fructose-6-phosphate
PFKM
PFKL
PFKP
FBP1
FBP2
Fructose-1,6-bisphosphate
ALDOA
ALDOB
ALDOC
Glyceraldehyde-3-phosphate
TPI1
Dihydroxyacetone Phosphate
GAPDH
GAPDHS
GAPD
1,3-Bisphosphoglycerate
PGK1
PGK2
3-Phosphoglycerate
PGAM2
PGAM1
2-Phosphoglycerate
ENO1
ENO1B
ENO3
ENO2
Phosphoenolpyruvate
PCK1
PKM2
PKM2
PKLR
Pyruvate
LDHAL6B
LDHA
LDHB
LDHC
Lactate
Cytosol
Mitochondrion
Aspartate
GOT1
Oxaloacetate
MDH1
Malate
Aspartate
GOT2
Oxaloacetate
MDH2
Malate
TCA Cycle
Pyruvate
PC
PDHA1
PDHA2
PDHB
DLAT
DLD
PDHX
Acetyl-CoA

Table 4.3
The top biofunctions, associated diseases, canonical pathways, and network functions that were most significant to the data set of HI laminitis experiment. The DE genes at the level of P<0.01 and FC>2 were used as input data set for HI/CON comparison.

	Biological functions	**Associated diseases**	**Top canonical pathways**	**Top network function**
HI/CON	DNA replication, recombination, and repair, cell cycle, cardiovascular system development and function	Cancer, dermatological diseases and endocrine system disorders	Parkinson's signaling, maturity onset diabetes of young (MODY) signaling	DNA replication, recombination, and repair, cell death, skeletal and muscular system development and function

A

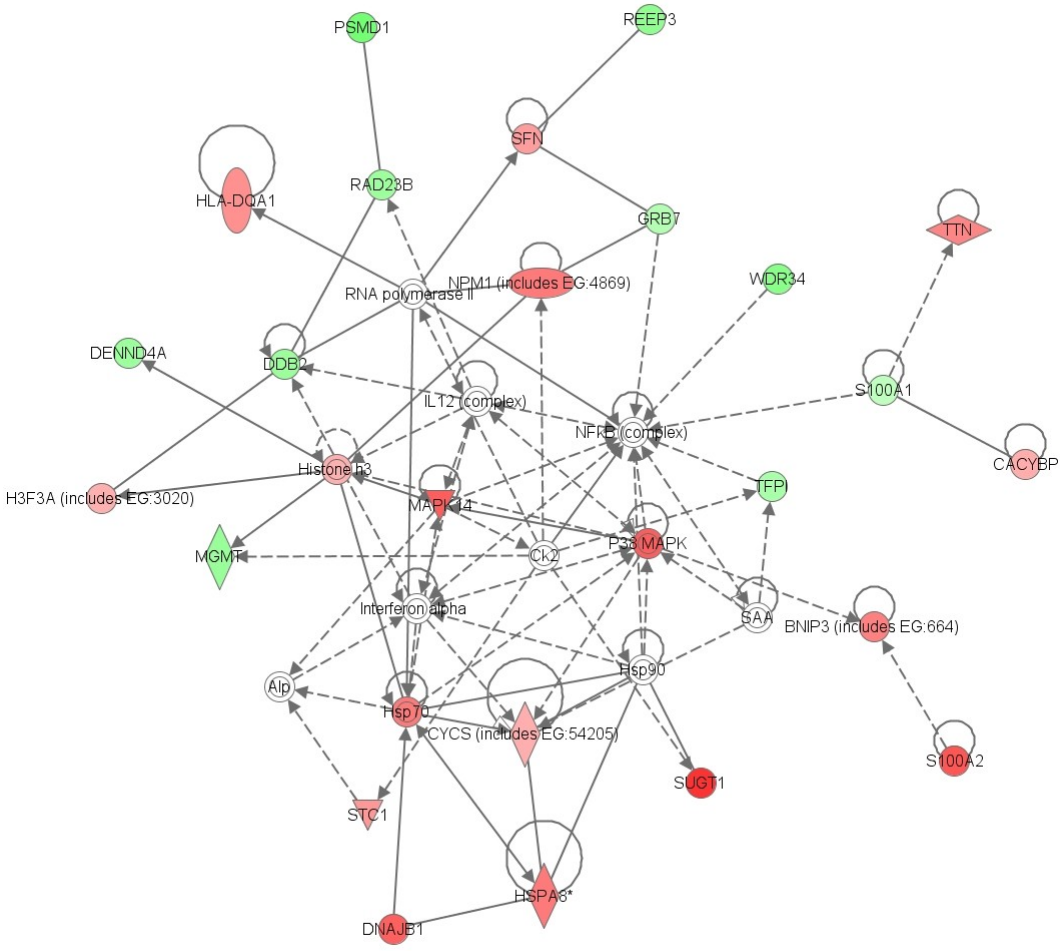

Fig. 4.3. Ingenuity network analysis of HI 48 h compared to CON. The top network identified by IPA with a significant score of 48 (A) and 37 (B). Both direct (solid line) and indirect (dashed line) interactions among genes were shown in the network. This analysis was performed on the DE genes of P<0.01 and FC>2. In A, this network showed the central position of p38 MAPK and NF-κB. In B, This network showed ERK and AP-1 linked to many genes we identified as DE. The intensity of the node color are depicted as down-regulated (green) or up-regulated (red). Square: cytokine/growth factor; vertical diamond: enzyme; horizontal diamond: peptidase; circle: other; parallelogram: transporter; circle-in-circle: complex; oval: transmembrane receptor; shaded circle-in-circle: group.

B

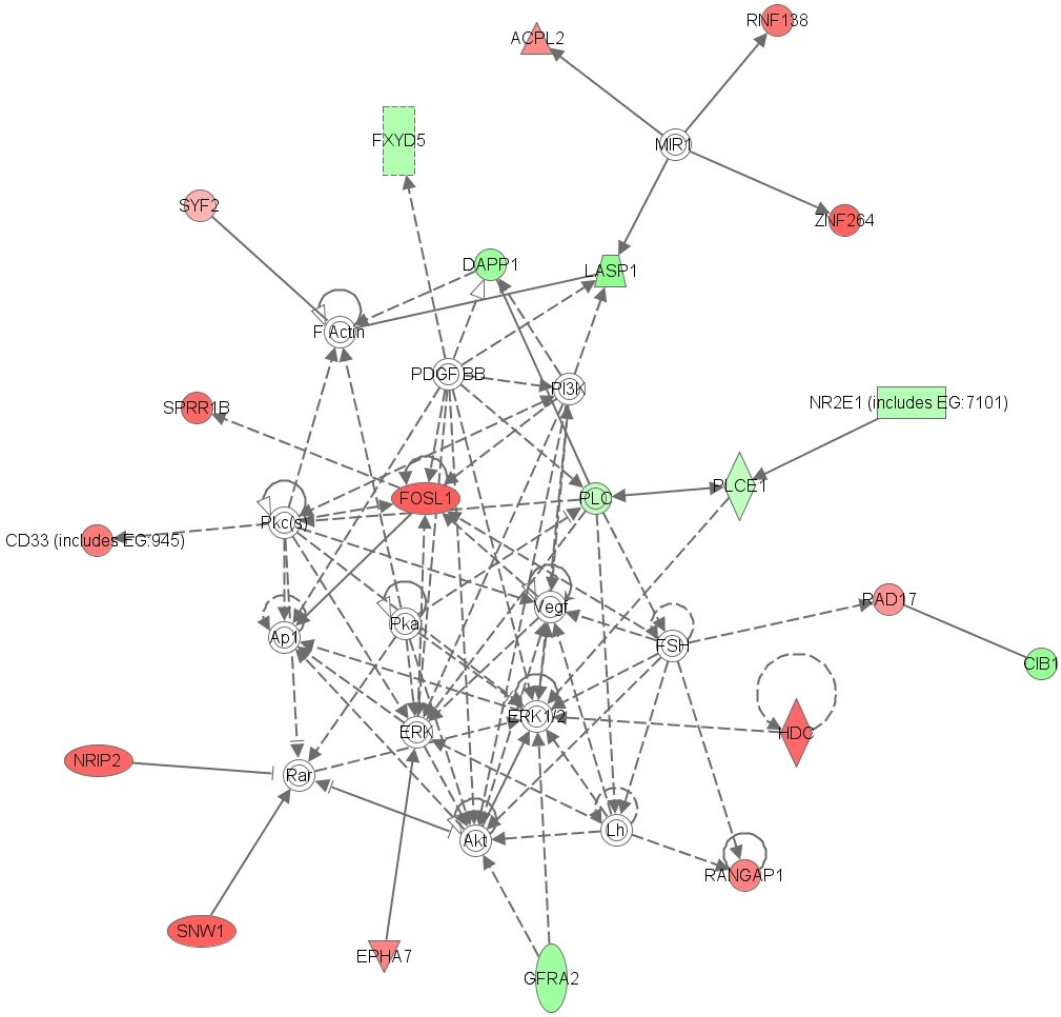

Fig. 4.3. continued

Quantitative real time PCR

To select the best reference gene for qRT-PCR data normalization, qRT-PCR was carried out for eleven horse reference genes (ACTB, B2M, PPIA, GAPDH, GNB2L1,

EEF1A1, HPRT1, TUBA1, UBB, RPL32 and RPLP0). Gene expression stability among the laminar samples (HI and CON) was determined according to the geNorm software (Vandesompele et al., 2002). We found that GNB2L1 and RPL32 were the most stable genes in the HI laminitis.

To confirm the differential expression results suggested by microarray, 16 genes (up-regulated and down-regulated) were selected for qRT-PCR validation. We select most of the DE genes based on a small P value and large fold change. The fold change of all selected genes was larger than 2. For the HI/CON comparison, there were only 5 annotated DE genes with a P value less than 0.001 and fold change larger than 2. Therefore most of genes were selected from Table 4.2 and have a P value between 0.001 and 0.01 (shown with an asterisk). Real time PCR was performed on 16 DE genes across tissues (CON and HI).

Three additional genes with P values between 0.01 and 0.05 (CD14, TNFRSF11B, and S100PBP) were also chosen based on their probable functional relevance to laminitis. CD14 is a lipopolysaccharide (LPS) binding protein that facilitates the recognition of pathogen associated molecular patterns (PAMPs) in the innate immune response (Akira et al., 2006). It has been shown that the expression of CD14 was increased in laminitic horses (Stokes et al., 2010). TNFRSF11B (osteoprotegerin, OPG) is a member of the tumor necrosis factor receptor superfamily and is important in bone homeostasis (Ueland et al., 2001). Engiles et al. have recently suggested that the digital bone microenvironment underlying the laminae may be affected by laminitis (Engiles, 2010). S100PBP is a member of the S100 protein family, which play a role in the

inflammatory response (Foell et al., 2007b). S100A8 and S100A9, members of S100 protein family, have been recently detected in laminar epidermis and shown to be up-regulated in BWE model of laminitis (Faleiros et al., 2009).

The primers used for qRT-PCR are listed in Table 4.4. qRT-PCR results showed that 11 genes (C16orf77, CD14, CXCL14, EIF1AX, GAPDH, MAPK14, S100A2, S100PBP, TNFRSF11B, TULP3, and ADAMTS1) had significantly different expression between HI and CON groups (Fig. 4.4). Of note, ADAMTS1 and TNFRSF11B genes had a high fold difference of 22 and 8, respectively, between the experimental and control groups in qRT-PCR.

To visualize the expression patterns of laminar tissue following HI induction, A heat map was constructed using MeV/R software for the 16 DE genes based on qRT-PCR results across the two conditions (CON and HI) (Fig. 4.5). Hierarchical clustering classified the genes based on their expression similarity between conditions. Cluster analysis showed a distinct expression pattern between the conditions (CON and HI). Moreover, the up-regulated group (ADAMTS1, CD14, GAPDH, S100A2, and TNFRSF11B) and the down-regulated group (CXCL14, PSMD1, C16orf77, and S100A1) were distinctly separated.

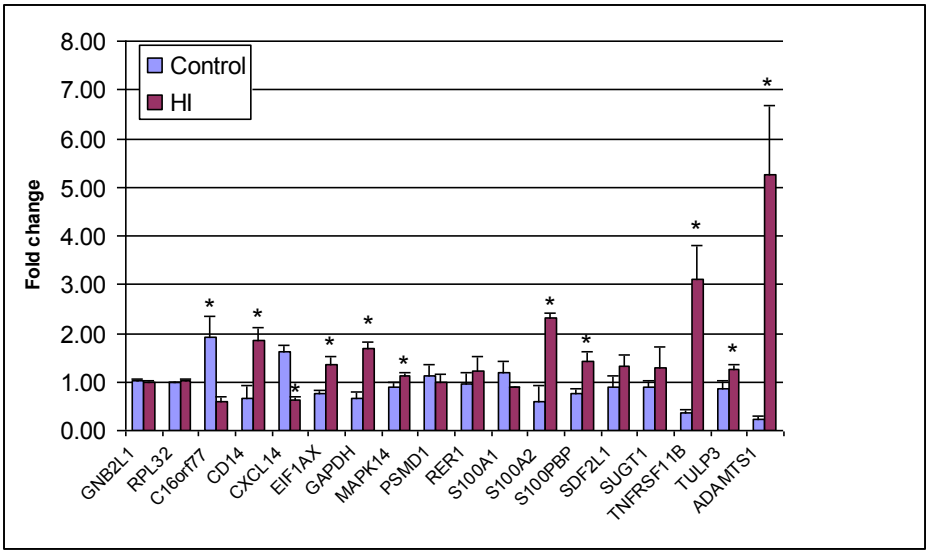

Fig. 4.4. Real time PCR validation of the microarray results of the HI/CON comparison. GNB2L1 and RPL32 are reference genes used for normalization. Sixteen DE genes from the microarray analysis were selected for real time PCR confirmation. Data are presented as mean ± SEM. Those genes marked with asterisks are significantly different from CON.

Table 4.4
Primers of genes used for quantitative RT-PCR of HI laminitis experiment.

Gene Symbol	Accession No.	Forward Sequence (5'-3')	Reverse Sequence (5'-3')	PCR Product Size (bp)	Tm(°C) *
ADAMTS1	AF541975	AGGCTCACAATGAATTTTCG	CACAGCCAGCTTTTACACACT	225	58
CXCL14	XM_001502713	ACTGCGAGGAGAAGATGGTTA	CTCGTTCCAGGCGTTGTA	128	58
S100A1	XM_001494870	AGGGGACAAGTACAAGCTGAG	TCTCGTCTAGCTCCTTCATCA	125	58
CD14	AF200416	CAGCTCTTTCCAGAGTCCAC	AGTTCTCATCGTCCACCTCA	144	60
S100A2	CX598422	GCGACAAGTTCAAGCTGAGTA	ATAGTGATGAGGGCCAGAAAA	181	58
TNFRSF11B	XR_036157	CGTCATCTAAAGCACCCTGTA	CTGAGCCAATTAGGGGTAAAC	202	58
GAPDH[c]	AF157626	GATGCCCCAATGTTTGTGA	AAGCAGGGATGATGTTCTGG	250	61
S100PBP	XM_001499793	GCCTCTCCAAACTACCTCAAC	CCTTATCAAGCACAGCATCAC	156	58
MAPK14	XM_001494719	AAGAGGATTACAGCAGCACAA	CGGGATCAAGAGAACAGAAAT	229	58
TULP3	XM_001490880	CACCATATTCAGAGGCAGAGA	TCATCCTTTTCCAAGTGCATA	244	58
SUGT1	XM_001492933	CTAGAGGGGCAAGGAGATGT	CCAACCAATTTATCCCAATTT	107	58
EIF1AX	XM_001492752	ACGAAATCCAGTTTGATGACA	CAACAGATCACAGCCAAAATC	130	58
SDF2L1	XM_001493091	CTGCACACGCACCACTTC	CATACTGCTCGCCGGTAACT	193	58

Table 4.4 continued

Gene Symbol	Accession No.	Forward Sequence (5'-3')	Reverse Sequence (5'-3')	PCR Product Size (bp)	Tm(°C) *
RER1	XM_001503365	TCTTTGAGGCTTTCAACGTC	CTCCTTGCCCTTGTACGTC	155	58
PSMD1	XM_001498019	CCAGTGAAGACATTGAAGAGC	AATAGCAGGTCTCAGCATGAA	190	58
C16orf77	XM_001500794	TGGAAGTACCTGGAGGAGGT	CATGACCCGGAAGCAGTT	171	58
GNB2L1[a]	AY246708	CAGGGATGAGACCAACTACG	ATGCCACACTCAGCACATC	269	58
RPL32[ac]	CX594263	AGCCATCTACTCGGCGTCA	TCCAATGCCTCTGGGTTTC	149	58
UBB [c]	AF506969	GCAAGACCATCACCCTGGA	CTAACAGCCACCCCTGAGAC	206	61
HPRT1 [c]	AY372182	GGCAAAACAATGCAAACCTT	CAAGGGCATATCCTACGACAA	163	61
TUBA1[c]	AW260995	GCCCTACAACTCCATCCTGA	ATGGCTTCATTGTCCACCA	78	60
EEF1A1	NM_001081781	TGGAAAGAAGCTGGAAGATG	CAACCGTCTGTCTCATGTCA	132	58
RPLP0	BC107717	TTGCATCAGTACCCCATTCT	ACCAAATCCCATATCCTCGT	242	58
ACTB[c]	AF035774	CCAGCACGATGAAGATCAAG	GTGGACAATGAGGCCAGAAT	88	58
B2M	X69083	CGAGACCTCTAACCAGCATC	AGACATAGCGGCCAAAGTAG	186	58
PPIA	NM_021130	TGGGGAGAAAGGATTTGGTT	CATGGACAAGATGCCAGGAC	178	58

* The optimal annealing temperature
[a] GNB2L1 and RPL32 were used for normalization during quantitative RT- PCR
[c] Information about the primers from (Bogaert et al., 2006)

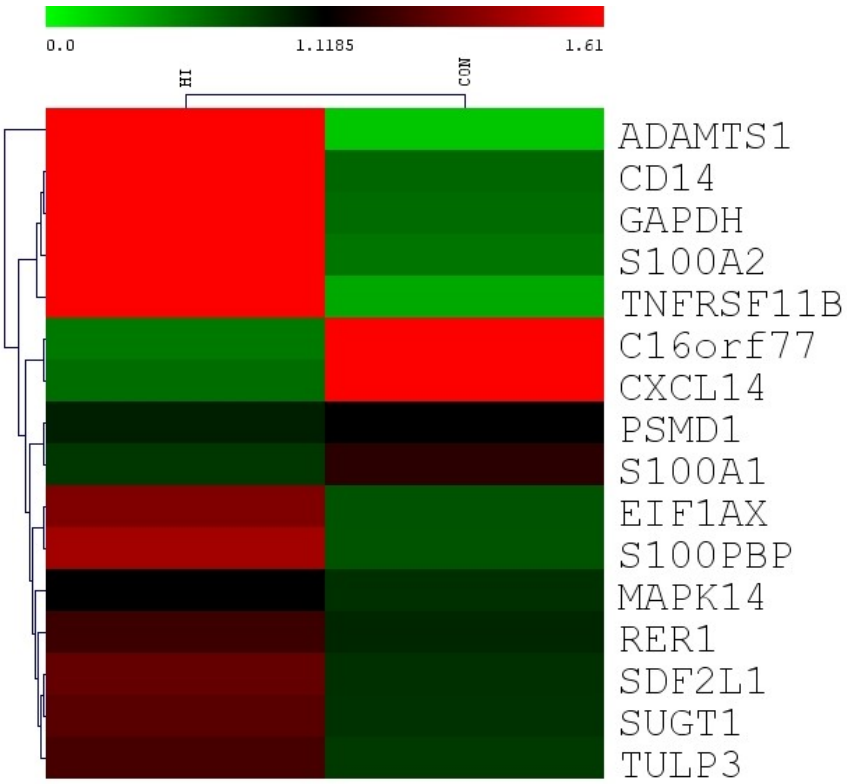

Fig. 4.5. Cluster diagram of the mean of CNRQ values at HI 48 h time point and control as determined by qRT-PCR. The green to red color scale demonstrates expression value of mean of CNRQ. GNB2L1 and RPL32 were used as reference genes to calculate normalized ΔCq.

DISCUSSION

Whole genome expression oligoarray has served as an extremely useful technique for exploring the transcriptome (Hardiman, 2004; Hughes et al., 2001; Woo et al., 2004). While previous investigations using microarray technology focused on the OF and BWE models of laminitis (Budak et al., 2009; Noschka et al., 2008), our study is the first to investigate genome-wide transcriptome profiling in endocrinopathic laminitis at

the Obel grade 2 stage of acute laminitis using an equine whole-genome long oligonucleotide microarray (Bright et al., 2009).

Analysis of differentially expressed genes

Equine whole-genome oligoarray identified differential expression of 242 genes ($P<0.01$ and $FC>2$) between the experimental and control groups (Table 4.1). Among these genes, CXCL14, CD1C, CD33, and SIGLEC10 are involved in inflammation and immune response. CXCL14 is a regulator of glucose metabolism and is associated with obesity-induced IR in mice (Nara et al., 2007; Tanegashima et al., 2010). CD1C, a member of CD1 family, is an antigen presenting molecule and involved in T cell recognition of lipid (Moody et al., 2000). SIGLEC10, a member of sialic-acid binding immunoglobulin-like lectins (SIGLECS) of the immunoglobulin superfamily, is a ligand for vascular adhension protein 1 (VAP-1) and their interaction can mediate leukocyte trafficking (Kivi et al., 2009). CD33 is another member of SIGLECS and has been shown to modulate leukocyte function (Crocker et al., 2007). The up-regulated inflammatory mediators CD33 and SIGLEC10 are potential target genes to develop treatments to reduce inflammation associated with endocrinopathic laminitis.

We also identified the differential expression of other groups of genes, such as extracellular matrix proteins KRT15 and keratinocyte protein SPRR1B (Li et al., 2008). Keratin is an important component of the epidermis of equine hoof. Furthermore, some genes encoding adaptor proteins changed expression following HI induction (Table A.7). Adaptor proteins have been demonstrated to play important role in signal transduction (Flynn, 2001), hence these proteins are potentially related to the pathogenesis of

endocrinopathic laminitis through signal transduction regulation. Three up-regulated genes are signal transduction regulators and genes maintaining homeostasis (SUGT1, HEMGN, and MAPK14) (Table 4.2). Because HI affects the endocrine system and metabolism of the body (i.e., insulin-glucose signal transduction and lipid metabolism) (Lovegrove, 2005; Sam, 2000), the up-regulation of these genes in the HI model of laminitis may be an attempt to compensate for the endocrine and metabolic effects caused by HI. OR7G2, OR5M3, and OR5AK2, members of olfactory receptor family were up-regulated. Olfactory receptors are mainly expressed in the nose, but also expressed in other tissue types such as the kidney and sperm (Kaupp, 2010; Pluznick et al., 2009; Spehr et al., 2003). The expression of olfactory receptors in the foot and their possible function in laminitis remain to be investigated.

Three calcium binding proteins, S100PBP, S100A1, and S100A2, were dysregulated in HI relative to control horses in our study. S100 proteins play an important role in innate immunity through inflammatory response mediation and leukocyte recruitment (Foell et al., 2007b). They also play a role in the maintenance of Ca^{2+} homeostasis in the body (Mandinova et al., 1998). These genes may contribute to the pathogenesis of the HI model of laminitis by regulating the inflammatory response and leukocyte activation. The strong induction of calcium binding proteins in the HI model of equine laminitis has not been previously reported.

In this study, we also identified the differential expression of ADAMDEC1 and ADAMTS1 at 48 h time point following HI induction. ADAMDEC1 is associated with atherosclerosis (Papaspyridonos et al., 2006) and ADAMTS1 is also up-regulated in the

OG1 stage of the CHO model of laminitis (Chapter III). The ADAMs belong to the family of metalloproteinases which also includes the adamalysin subfamily ADAMTS (Reiss et al., 2006). Both ADAMs and ADAMTSs play an important role in the turnover of ECM proteins (e.g., collagen and aggrecan) and their differential expression has been implicated in various cancers and arthritis (Tortorella et al., 2009). Another study of the comparison of expression between normal and painful tendons further suggests that many ADAMTS members might play key role in the pathology of connective tissues through the degradation of ECM components (Jones and Riley, 2005). Laminitis is also a connective tissue disease and the site of disease occurs at the laminar tissue, which is the connective tissue between the hoof wall and coffin bone. Therefore, metalloproteinases ADAMTS1 and ADAMDEC1 have potential role in laminitis progression through ECM cleavage. Most importantly, ADAMTS1 is a potential target of therapeutic intervention for equine laminitis. The inhibition of ADAMTS1 activity could reduce ECM components degradation. BM (a thin layer of ECM) degradation is the early pathological change during the pathogenesis of equine acute laminitis (Pollitt, 1996). The down-regulation of CPA6 gene at the OG2 stage may potentially affect the equine hoof structure integrity.

Comparison to previous studies

Similar to results seen using a 15,000 bovine microarray chip in laminar tissue from the OF model of laminitis (Budak et al., 2009), we identified the differential expression of FOS and PSMD genes. Compared to the work carried out by an equine-specific 3,076 element cDNA microarray in laminar tissue of the BWE model laminitis

(Noschka et al., 2008), we also identified the differential expression of SERPINF2. Additionally, we identified the differential expression of interferon regulatory factor IRF4 instead of IRF1, S100 protein S100PBP instead of S100P, and RAS oncogene family member RAB3A instead of RAB1A. Differential expression of IRF1, S100P and RAB1A were identified in laminar tissue from the BWE model laminitis (Noschka et al., 2008).

GO functional enrichment analysis

GO analysis provides information about the overrepresented categories (i.e., BP, MF and CC) among the DE genes. The BP GO terms response to stimulus and immune response were significantly enriched among up-regulated genes (Table A.8). During HI induced laminitis, these up-regulated genes might counteract the effects of excess insulin in an attempt to maintain the body's homeostasis. It is noteworthy that one gene involved in adaptive immune response HLA-DQA1 was up-regulated. On the other hand, genes associated with molecular transducer activity and signal transducer activity increased their expression, suggesting a signal transduction regulation following HI during the progression of the disease.

Pathway and network relevance to laminitis

Pathway analysis identified three DE genes involved in glycolysis and gluconeogenesis processes (GALM was not mapped) (Fig. 4.2). Although this is limited evidence, differential expression of these genes may disrupt glucose metabolism, which could contribute to the pathogenesis of HI laminitis. There is evidence that changes in glucose uptake can induce laminar failure *in vitro* (Pass et al., 1998; Wattle and Pollitt,

2004). It has also been shown that abnormal glucose metabolism in horses with ECD could cause laminitis (Keen et al., 2004). Interestingly, another study has demonstrated the expression of glucose transporter-1 (GLUT-1) and GLUT-4 proteins in equine keratinocytes and the expression of GLUT-4 decreased with the progression of laminitis (Mobasheri et al., 2004). It remains to be investigated if abnormal glucose metabolism is due to the varied expression of GLUT-4 in these studies. Insulin can regulate glucose metabolism through the inhibition of gluconeogenesis process (Barthel and Schmoll, 2003). Although Asplin and co-workers suggested that it is not IR but insulin toxicity that causes endocrinopathic laminitis (Asplin et al., 2007), it is also possible that HI contributes to laminitis through the disruption of glucose metabolism.

Pathway analysis of DE genes in the HI/CON comparison showed the central role of p38 MAPK and NF-κB pathway molecules and the biological interactions among the genes in the networks (Fig. 4.3). The dysregulation of the DE genes in the network may affect the activity of other relevant genes. Therefore the biological interactions between these genes were disrupted indirectly, which may contribute to the pathogenesis of laminitis. Many DE genes are also linked to AP-1. Studies have shown p38 MAPK induction in equine neutrophil activation and suggested that p38 MAPK inhibition may help decrease the inflammatory response in the affected laminae (Eckert et al., 2008). In human medicine, the NF-κB family of transcription factors have been shown to be involved in rheumatoid arthritis (RA) (Simmonds and Foxwell, 2008). Interestingly, in people with metabolic syndrome and type 2 diabetes, there is an interaction between the insulin signaling cascade and obesity-induced inflammation through NF-κB and AP-1

(de Luca and Olefsky, 2008). Together, these results indicate the potential molecular mechanisms (i.e., p38 MAPK and NF-κB) associated with endocrinopathic laminitis and give insight into laminitis cases associated with endocrine dysfunctions.

Relevance to current theories of hyperinsulinemic laminitis

There are several theories regarding the pathogenesis of hyperinsulinemic laminitis, including vascular dysfunction (Geor and Frank, 2008), inflammation (McGowan, 2008) and insulin toxicity (Asplin et al., 2007). Differential expression results of this study showed that some genes involved in inflammation changed their expression (e.g., CXCL14 and CD33) during the progression of laminitis. Insulin is not only a hormone but also a vasoactive mediator (Johnson et al., 2004b). It can affect the blood flow through the modulation of endothelin-1 (ET-1) and nitric oxide (NO) production (Muniyappa et al., 2007). ET-1 is a potent vasoconstrictor that may be involved in equine laminitis (Katwa et al., 1999). HI has been shown to cause endothelial dysfunction in humans (Arcaro et al., 2002) and is associated with the impairment of endothelium-dependent vasodilation as well as enhanced production of ET-1 (Potenza et al., 2005). ET-1 can induce endothelial dysfunction by reducing NO availability in mice (Iglarz and Clozel, 2007). Additionally, it has been suggested that endothelial dysfunction is involved in the pathogenesis of diabetic foot disease in humans (La Fontaine et al., 2006). Therefore, it is likely that the combination of these effects (i.e., vascular dysfunction, inflammation and glucose metabolism changes) contributes to the pathogenesis of HI laminitis.

CONCLUSION

Overall, this is the first investigation of genome-wide transcriptome profiling of the laminar tissue at 48 h time point after HI induction using an equine-whole genome 21,000 long oligonucleotide microarray approach. We identified the differential expression of several S100 gene family members, signal transduction regulators and genes maintaining homeostasis, extracellular matrix proteins, adaptor proteins, glycoproteins, and ADAMTS1 and ADAMDEC1 metalloproteinases during the progression of HI model laminitis. These genes will be good candidates for further functional study in insulin-associated laminitis. Pathway and network analysis revealed genes, gene-gene interactions relevant to equine laminitis and the presence of p38 MAPK and NF-κB pathway molecules. Furthermore, it is possible that HI contributes to hyperinsulinemic laminitis through glucose metabolism disruption. These findings will be critical in paving the way for predicting and developing improved preventatives and treatments for endocrinopathic laminitis in the future.

CHAPTER V

TRANSCRIPTOME PROFILING OF LAMINAR TISSUE DURING THE EARLY STAGES OF OLIGOFRUCTOSE INDUCED LAMINITIS IN THE HORSE

INTRODUCTION

Equine laminitis is a serious disease of the equine foot that is characterized by basement membrane (BM) degradation as well as laminar separation at the dermal-epidermal interface (Pollitt, 2004b). The exact mechanisms by which laminar separation occurs need further investigation. However, laminitis has been linked to many factors such as grain overload, gastrointestinal (GI) tract disease and endotoxemia. Studies have shown that metabolic and endocrine abnormalities are risk factors for the development of laminitis in horses and ponies (Geor and Frank, 2008; Geor, 2008; Johnson, 2002; Treiber et al., 2006b). In order to study the initiation and progression of equine laminitis, four experimentally induced models have been established using the administration of CHO (Garner et al., 1975), BWE (Minnick et al., 1987), OF (van Eps and Pollitt, 2006) and prolonged HI with euglycaemia (Asplin et al., 2007; de Laat et al., 2010).

Fructan is a form of oligofructose and OF induced laminitis is a model of pasture associated laminitis (van Eps and Pollitt, 2006). It is still unknown which factors trigger the onset of OF induced laminitis. Recent work has demonstrated a diverse bacterial community in the horse hindgut (Al Jassim and Andrews, 2009). It has been shown that changes in the bacterial populations of the GI tract occur during OF induced laminitis

(Milinovich et al., 2006). The majority of microbes in the equine hindgut of OF induced laminitis are in the genus *Streptococcus.* Furthermore, microbe *S. infantarius* ssp. *coli* was overrepresented in the bacterial population before the onset of laminitis (Milinovich et al., 2006). Additionally, two novel species of the genus *Streptococcus* were identified in the horse hindgut in the OF induced model of laminitis (Milinovich et al., 2008a). Equine hindgut streptococcal species (EHSS) have been proposed as an etiological agent and the released cellular components in the GI tract may initiate laminitis (Milinovich et al., 2008b).

Although an equine-specific 3,076 element cDNA microarray (Noschka et al., 2008), bovine 15,000 oligoarray (Budak et al., 2009) applied in equine laminitis, they have inherent limitations that prevent detailed studies aimed at understanding the potential genetic pathways and gene networks associated with the pathogenesis and progression of equine laminitis on a genome-wide scale. Because early stages of laminitis are critical in understanding the initiation of the disease, we sought to identify genes and their likely interactions that may lead to observed pathological changes in the early time points of the OF model of laminitis. The overall objective of this study was to identify transcriptomic profiling and associated pathways in laminar tissue at 12 h and 24 h time points after OF induction using the 70-mer equine whole-genome oligoarray (Bright et al., 2009).

MATERIALS AND METHODS

Experimental design

Eighteen clinically normal Standardbred horses (2-12 years of age, 15 geldings and 3 mares) were used in this study. The horses were examined and confirmed to be healthy and without a history of metabolic-endocrine disorders. Six horses were used for each category (12 h, 24 h and control). Horses grouped in the '12 h' and the '24 h' stages were administered OF (10 g/kg of body weight) via nasogastric tube. Control group horses received water via nasogastric tube. The induction of laminitis using OF was carried out according to the method of van Eps and Pollitt (van Eps and Pollitt, 2006). Laminar samples were obtained from control horses (CON, n=6) at the 24 h time point and laminitic horses at 12 h (12 h, n=6) and 24 h (24 h, n=6). The Animal Ethics Committee of the University of Queensland approved the experimental protocol.

A two channel, balanced block design was used for microarray hybridizations. Three different comparisons were carried out (12 h vs. control, 24 h vs. control, and 12 h vs. 24 h). Dye balance was performed during the experiment to eliminate dye bias. A total of 18 slides (6 slides per comparison) were used. The microarray hybridization experiment conducted in this study is shown in Fig.5.1.

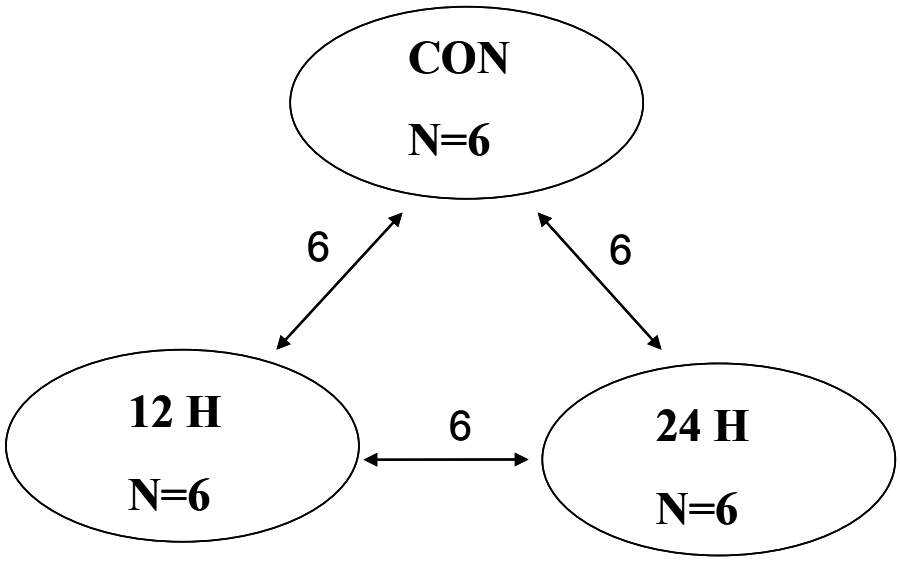

Fig. 5.1. Diagram of the OF model laminitis experimental design**.** Eighteen hybridizations were performed. Arrows represent the hybridization between the laminar samples from different groups. Six animals were included in each group (N=6). CON: laminar samples from control horses; 12 H: laminar samples from 12 h OF induced horses; 24 H: laminar samples from 24 h OF induced horses.

Equine 21K oligonucleotide microarray

The 70-mer oligoarray was constructed based on a 2.4 Gb EquCab2 of the horse genome, combined with RefSeq release 26, UniGene build#3, SwissProt release 12 and ~43,000 unpublished ESTs (Bright et al., 2009). Probes were synthesized (Invitrogen, Carlsbad, CA) and printed into amino-silane coated slides (Corning Incorporated, Corning, NY).

RNA isolation and cDNA synthesis

Total RNA was extracted from 80-100 mg of frozen laminar tissue, which was disrupted and homogenized in the presence of Tri reagent (MRC, Cincinnati, OH) as described in (Chomczynski, 1993). This was followed by RNA cleanup with RNase-free

DNase treatment (RNeasy Mini Kit, Qiagen, Valencia, CA) of the isolate according to the manufacturer's protocol. RNA concentration was quantified using a spectrophotometer (NanoDrop Technologies, Wilmington, DE) and the quality was evaluated with an Agilent 2100 Bioanalyzer and RNA Lab Chip (RNA 6000 Nano Assay, Agilent Technologies, Palo Alto, CA). cDNAs were synthesized from total RNA with the 3DNA Array 900MPX Expression Array Detection Kit (Genisphere, Hatfield, PA) using SuperScript II reverse transcriptase (Invitrogen, Carlsbad, CA). One microgram of total RNA was combined with random primer and MPX dT primer, incubated at 80°C for 10 min, and cooled on ice for 2 min. Finally, 0.5M NaOH/50mM EDTA was added to degrade any remaining RNA; this reaction was neutralized with 1 M Tris-HCl (pH 7.5).

cDNA purification, tailing and ligation

The cDNA was purified using the Qiagen MinElute PCR purification kit (Qiagen, Valencia, CA) according to the manufacturer's protocol. Then nuclease-free water was added to the purified cDNA to a volume of 16.5 µl. The cDNA was incubated at 95°C for 10 min in a PCR thermal cycler and cooled on ice for 2 min. The cDNA was tailed by terminal deoxynucleotidyl transferase (TdT) enzyme and ligated to 3DNA capture sequence. The ligated DNA was purified again using the Qiagen MinElute PCR purification kit (Qiagen, Valencia, CA) according to the manufacturer's protocol. The purified cDNAs were combined according to the experimental design of hybridization.

Pre-hybridization treatment of microarray slide

Rehydration and crosslinking of the microarray slide was performed to ensure that the probe was spread evenly in the spot and immobilized on the slide. The slides were rehydrated by holding the slide label side down over the steam from a 50°C water bath for 10 s. The slides were dried for 5 s at 65°C and then brought to room temperature (20°C) for 1 min. This process was repeated up to four times. After rehydration, the slides were subjected to UV crosslinking at 750 MJ/cm^2 for 2 minutes.

Microarray cDNA hybridization

A 543 µl reaction was used for the tagged cDNA hybridization mix, which was prepared according to the manufacturer's instructions (Genisphere, Hatfield, PA). The mixture was applied to the gasket slide of an Agilent microarray hybridization chamber and the microarray slide (array side down) was laid on top of the gasket slide. The hybridization chamber was assembled and the slides were then incubated at 55°C while rotating at 5 rpm in a hybridization oven (Agilent Technologies, Santa Clara, CA) for 16 hours. The "microarray-gasket slide sandwich" was then washed once with pre-warmed (42°C) 2x SSC-0.2% SDS wash buffer, disassembled, and washed again. The array slide was then washed with 2x SSC and 0.2x SSC wash buffers. Slides were dried at room temperature, centrifuged at 1000 rpm for 4 min, and then stored in a dry box prior to the second hybridization.

3DNA hybridization and wash

3DNA hybridization master mix was prepared according to the manufacturer's instructions (Genisphere, Hatfield, PA), applied to the array, and covered with a

coverslip in the dark. The slide was placed in a 50 ml conical tube with 400 µl of nuclease-free water and incubated horizontally at 55°C in a hybridization oven (Agilent Technologies, Santa Clara, CA) for 4 hours in the dark. All washing steps following 3DNA hybridization were conducted in the dark. The slide was taken out of the incubator and washed with pre-warmed (42°C) 2x SSC-0.2% SDS wash buffer. The cover slip was removed and the slide was washed again with 2x SSC-0.2% SDS buffer. The slide was then washed with 2x SSC and 0.2x SSC wash buffers. Finally, the slide was dried at room temperature, centrifuged at 1000 rpm for 4 min, and stored for scanning.

Microarray image processing and data analysis

The slides were scanned with a GenePix Personal 4000B microarray scanner (Molecular Devices Corporation, Sunnyvale, CA) at a resolution of 5 µm. The fluorescence intensities from each array were quantified using GenePix Pro 6.0 program (Molecular Devices Corporation, Sunnyvale, CA). Each spot was inspected by manual gridding and empty spots were flagged out. The median signal intensity and local background intensity of each gene were normalized by print-tip loess normalization using the bioconductor LIMMA package (Gentleman et al., 2004) in the R statistical computing environment (http://www.r-project.org/). Linear models and empirical Bayes moderated F statistics (Smyth, 2004) were applied to obtain the P value and $\log_2$-based fold change of each gene.

Gene ontology analysis

Gene ontology (GO) is used to functionally annotate gene products. It has three categories: biological process (BP), cellular component (CC), and molecular function (MF). The Database for Annotation, Visualization and Integrated Discovery (DAVID version 6.7) (Dennis et al., 2003; Huang et al., 2009) (http://david.abcc.ncifcrf.gov/) was used to obtain GO terms and related KEGG pathways for differentially expressed genes for the three comparisons: 12 h vs. CON, 24 h vs. CON, and 12 h vs. 24 h. RefSeq protein IDs of human orthologs were used as input and Fisher's Exact P value of 0.05 was used as a cutoff for determining statistical significance. Gene ontology terms of all levels were included in the analysis.

Pathway analysis

Ingenuity Pathways Analysis program (Ingenuity Systems, version 8.7) was used to obtain networks, biofunctions and canonical pathways relevant to laminitis. A data set containing gene identifiers and corresponding expression values from the microarray expression analysis was uploaded into the application. Functional analysis identified the biological functions and diseases that were most significant to the dataset. Fisher's Exact test was used to calculate the P value determining the probability that each biological function and disease assigned to that data set (or network) is due to chance alone.

Quantitative real time PCR

To further explore microarray results, a subset of DE genes from each comparison were examined by quantitative reverse transcription PCR (qRT-PCR). cDNA was synthesized from total RNA (250 ng) of each sample (CON, 12 h, and 24 h) using

TaqMan® Reverse Transcriptase reagents (Applied Biosystems, Carlsbad, CA) according to the manufacturer's protocol. The cDNAs were quantified by qRT-PCR using a LightCycler®480 Real-Time PCR System (Roche Diagnostics, Indianapolis, IN) with 2x LightCycler®480 SYBR Green I master mix (Roche Diagnostics, Indianapolis, IN). To calculate the PCR amplification efficiencies of target and reference genes, a serial dilution of laminar cDNA was made (200 ng/µl, 100 ng/µl, 50 ng/µl, 25 ng/µl, 12.5 ng/µl, and 6.25 ng/µl) and used as a template. PCR efficiency of each gene was determined from the slope of the line along the concentrations as calculated by LightCycler ® 480 basic software version 1.2 (Roche Applied Science, Indianapolis, IN). Each individual sample was run in duplicate and the average crossing point (Cp) value was used for further analysis.

Quantitative real time PCR data analysis

In order to select appropriate reference genes for qRT-PCR data normalization, qRT-PCR was carried out for ten equine reference genes: ACTB, B2M, PPIA, GAPDH, GNB2L1, EEF1A1, HPRT1, TUBA1, UBB and RPL32. The average expression stability and the optimal number of control genes for normalization were determined using the geNorm computer program (http://medgen.ugent.be/~jvdesomp/genorm/) (Vandesompele et al., 2002). The two most stable genes from those tested were used for normalization of the qRT-PCR data. The data was analyzed by the delta-Cq method (Hellemans et al., 2007) in qBase*Plus* (Biogazelle, Ghent, Belgium). The statistical significance of the derived CNRQ values between two groups was determined by

nonparametric Mann-Whitney test in SPSS 17.0 statistics software (SPSS Inc, Chicago, IL). A P value less than 0.05 was considered statistically significant.

Hierarchical cluster analysis

To get an overview of gene expression pattern of qRT-PCR data among CON, 12 h and 24 h conditions, hierarchical clustering was performed on the mean values of selected DE genes from qRT-PCR to construct a heat map using MultiExperiment viewer and R (MeV/R) program version 4.6 (Chu et al., 2008; Saeed et al., 2003).

RESULTS

Clinical observations

No control horses showed clinical evidence of laminitis before euthanasia. While there were individual differences, horses in the treatment group didn't show clinical signs of laminitis at 12 h or 24 h after OF administration. Shortly before euthanasia one horse (24 h treatment group) showed lameness.

Identification of DE genes in laminar tissue following OF

Differential gene expression was determined by comparing gene expression profiles among three different groups (CON, 12 h and 24 h). There were 71, 151, 251 genes differentially expressed (DE) in each comparison of 12 h/CON, 24 h/CON and 12 h/24 h at the cut-off of $P<0.01$ and fold change>2 (Table 5.1). The ranges of fold change in differential expression were 5.16 to 0.23, 24.8 to 0.10, and 14.6 to 0.03 in each comparison of 12 h/CON, 24 h/CON and 12 h/24 h. A general trend of up-regulation was seen among DE genes in the 24 h/CON comparison, whereas down-regulated genes were predominant in the 12 h/24 h comparison (Table 5.1). The DE genes with the

largest fold changes (up and down regulated) are shown in Table 5.2, 5.3, and 5.4 for each of the three comparisons, respectively. Complete lists of DE genes at the p value less than 0.01 and fold change larger than 2 are presented in Table A.9, A.10 and A.11.

Table 5.1
Distribution of differentially expressed genes among comparisons.

	Upregulated	Downregulated	Total
12 h/CON	33 (46.5%)	38 (53.5%)	71
24 h/CON	105 (69.5%)	46 (30.5%)	151
12 h/24 h	92 (36.7%)	159 (63.3%)	251

Among the up-regulated genes with the largest fold changes at the 12 h time point compared to control (Table 5.2), XR_035808 shares 97% homology with equine leukocyte immunoglobulin-like receptor, subfamily A, member 6. Interesting, chemokine CXCL2 (macrophage inflammatory protein 2-alpha) was consistently up-regulated at 12 h and 24 h compared to controls. CXCL2 is essential chemoattractant for neutrophils and neutrophils are primary cell type for host defense against invading pathogens at the site of infection. Neutrophil activation has been described in BWE model of laminitis (Black et al., 2006). Down-regulated genes included four genes (CKM, DHRS2, TAOK3, and RPS6KB2) encoding enzymes. BAX, a member of BCL2 protein family, plays a role in the regulation of apoptosis (Green and Chipuk, 2008). OR7A10, a member of olfactory receptor family, also belonged to the group of down-regulated genes and is involved in odorant signal transduction.

Table 5.2
Top differentially expressed genes (15 upregulated and 15 downregulated; P<0.01 and fold change>2) for the 12 h/CON comparison. Unannotated genes are labelled as NULL. Asterisks denote genes selected for confirmation with PCR.

Gene Name	Description	Public Accession	P	Fold Change	PCR
Upregulated					
IFI30	interferon, gamma-inducible protein 30	XM_001500556	0.0059	4.66	*
GLMN	glomulin	XM_001492771	0.0034	4.37	*
PSIP1	PC4 and SFRS1 interacting protein 1	DQ873682	0.0081	3.96	
MITD1	microtubule interacting and transport, domain containing 1	XM_001490447	0.0013	3.73	*
BAIAP3	BAI1-associated protein 3	XM_001497570	0.0041	3.61	
NULL	NULL	XR_035808	0.0023	3.45	
NULL	NULL	CX601068	0.0007	3.38	
NULL	NULL	CX596707	0.0023	3.32	
CXCL2	chemokine (C-X-C motif) ligand 2	AF053497	0.0023	3.21	*
PARP6	poly (ADP-ribose) polymerase family, member 6	XM_001494491	0.0041	3.19	
CBARA1	calcium binding atopy-related autoantigen 1	XM_001503797	0.0025	3.10	
CCDC67	coiled-coil domain containing 67	XM_001491708	0.0030	2.89	
NULL	NULL	CX593986	0.0073	2.88	
EZH2	enhancer of zeste homolog 2	XM_001504629	0.0081	2.65	
ZNF30	zinc finger protein 30	XM_001493964	0.0042	2.63	
Downregulated					
NULL	NULL	DN510842	0.0010	0.23	
CKM	creatine kinase, muscle	XM_001502522	0.0011	0.25	
LOC284890		XM_001489526	0.0081	0.25	

Table 5.2 continued

Gene Name	Description	Public Accession	P	Fold Change	PCR
Downregulated					
PTGFR	prostaglandin F receptor (FP)	DQ385610	0.0083	0.26	*
COMMD2	COMM domain containing 2	DN509689	0.0086	0.26	*
OR7A10	olfactory receptor, family 7, subfamily A, member 10	XM_001492035	0.0028	0.26	
ZNF451	zinc finger protein 451	XM_001499700	0.0093	0.27	
DHRS2	dehydrogenase/reductase member 2	XM_001489482	0.0017	0.27	
LOC26010	viral DNA polymerase-transactivated protein 6	XM_001502795	0.0032	0.29	
NULL	NULL	CX604266	0.0005	0.30	
TAOK3	TAO kinase 3	XM_001490545	0.0021	0.30	
LGALS4	lectin, galactoside-binding, soluble, 4	XM_001497350	0.0062	0.34	
RPS6KB2	ribosomal protein S6 kinase, 70kDa, polypeptide 2	XM_001497573	0.0029	0.34	
MAGED2	melanoma antigen family D, 2	XM_001496158	0.0037	0.36	
BAX	BCL2-associated X protein	NULL	0.0011	0.36	

Many genes that were up-regulated at the 24 h time point as compared to controls are involved in the immune response; these include acute phase protein SAA1, interleukin IL12A, anti-microbial peptides DEFB4 and PI3, calcium binding protein S100A8 and S100A9, and antioxidant enzyme SOD2. The differentially expressed genes with the largest fold changes at the 24 h time point compared to control are shown in Table 5.3. The up-regulated gene, CD467650, is 71% similar to superoxide dismutase 2 (*Canis familiaris* SOD2, 81% coverage), which is associated with oxidative stress. Oxidative stress has been described in affected laminar tissue of BWE model of laminitis (Yin et al., 2009). Likewise, BI961659 shares 76% homology with transmembrane protein 49 (*Pan troglodytes*, TMEM49, 99% coverage), which is associated with the formation of intracellular vacuoles in autophagy (Ropolo et al., 2007). The presence of intracellular vacuoles has been detected in the laminar epidermis of CHO model of laminitis (Morgan et al., 2003). Chemokine CCL2 was also up-regulated at 24 h. The down-regulated genes with the largest fold changes included 2 genes encoding cytoskeletal matrix proteins, 2 genes for enzymes, and a solute carrier transporter protein. Of note, ADAMTS1, a metalloproteinase that involved in the degradation of extracellular matrix (ECM) components, was up-regulated at 24 h compared to control (Table A.10).

Table 5.4 shows a total of 30 DE genes with the largest fold changes at the 12 h time point compared to 24 h time point. CD467650, has 78% homology with superoxide dismutase 2 (*Sus scrofa*, SOD2, 56% coverage), increased its expression at 24 h time point. Among these genes, S100A8, S100A9, S100A12, SOD2, PI3, DEFB4, and SAA1 dramatically increased their expression at 24 h time point. MMP26, a member of MMP family was up-regulated (Table A.11) and MMP26 has been shown the role in ECM cleavage in human (Lee et al., 2006). BM (a thin layer of ECM) degradation has been described as early pathological change in equine laminitis (Pollitt, 1996). The up-regulated genes with the largest fold changes included 3 genes associated with body homeostasis and 2 genes encoding transcription factors. FREM1, an ECM related protein that is involved in epidermal differentiation, was also up-regulated. Of note, OR5M9, OR5AR1, OR7A5, OR56B1, and OR2J3, members of olfactory receptor superfamily of GPCRs, had differential expression during the transition from the 12 h time point to 24 h time point.

Table 5.3

Top differentially expressed genes (15 upregulated and 15 downregulated; P<0.01 and fold change>2) for the 24 h/CON comparison. Unannotated genes are labelled as NULL. Asterisks denote genes selected for confirmation with PCR.

Gene Name	Description	Public Accession	P	Fold Change	PCR
Upregulated					
S100A8	S100 calcium binding protein A8	XM_001493589	0.0000	24.76	*
SOD2	Superoxide dismutase 2	AB001693	0.0000	11.28	
DEFB4	Defensin, beta 4	AY170305	0.0000	10.57	*
EREG	Epiregulin	XM_001490281	0.0001	6.91	*
SAA1	Serum amyloid A1	NM_001081853	0.0018	6.77	
NULL	NULL	CD467650	0.0002	4.79	
FTH1	Ferritin, heavy polypeptide 1	XM_001489262	0.0048	4.77	
NULL	NULL	XM_001498707	0.0002	4.47	
S100A9	S100 calcium binding protein A9	XM_001493530	0.0047	4.46	*
IL12A	Interleukin 12A	Y11130	0.0032	4.45	
NULL	NULL	CD535521	0.0012	4.38	
NULL	NULL	BI961659	0.0001	4.31	
HINT2	Histidine triad nucleotide binding protein 2	NULL	0.0073	4.04	
GLUL	Glutamate-ammonia ligase	XM_001489235	0.0005	4.02	
KIAA1524	KIAA1524	XM_001503233	0.0037	3.99	
Downregulated					
NDUFB3	NADH dehydrogenase 1 beta subcomplex, 3	XM_001503625	0.0009	0.10	*
NULL	NULL	CX592434	0.0038	0.19	
PSMA4	Proteasome subunit, alpha type, 4	XM_001489071	0.0062	0.20	*
NKX3-1	NK3 homeobox 1	XM_001491242	0.0066	0.24	
SLC5A6	Solute carrier family 5, member 6	XM_001502487	0.0020	0.25	

Table 5.3 continued

Gene Name	Description	Public Accession	P	Fold Change	PCR
Downregulated					
LOC650780		CD466835	0.0081	0.26	
NEB	Nebulin	NULL	0.0018	0.27	
ANKRD26	Ankyrin repeat domain 26	CX601264	0.0015	0.31	
EIF2AK4	Eukaryotic translation initiation factor 2 alpha kinase 4	XM_001501267	0.0042	0.32	
TNNT1	Troponin T type 1	NULL	0.0048	0.32	
NRBF2	Nuclear receptor binding factor 2	XM_001502366	0.0041	0.32	
NPHP4	Nephronophthisis 4	XM_001497162	0.0009	0.33	
ISCU	Iron-sulfur cluster scaffold homolog	NULL	0.0057	0.34	
NULL	NULL	CX601609	0.0069	0.36	
GMPS	Guanine monphosphate synthetase	XM_001488228	0.0070	0.36	

Table 5.4
Top differentially expressed genes (15 upregulated and 15 downregulated; P<0.01 and fold change>2) for the 12 h/24 h comparison. Unannotated genes are labelled as NULL. Asterisks denote genes selected for confirmation with PCR.

Gene Name	Description	Public Accession	P	Fold Change	PCR
Upregulated					
NULL	NULL	DN508706	0.0001	14.59	
C3orf26	Chromosome 3 open reading frame 26	XM_001502207	0.0037	5.76	
ARHGAP11A	Rho GTPase activating protein 11A	XM_001503656	0.0092	4.32	*
LGALS4	Lectin, galactoside-binding, soluble, 4	XM_001497350	0.0005	4.18	
HMGN3	High mobility group nucleosomal binding domain 3	XM_001499096	0.0020	4.12	
BBS7	Bardet-Biedl syndrome 7	XM_001503097	0.0005	4.04	
COCH	Coagulation factor C homolog, cochlin	XM_001489788	0.0046	3.95	
RNF113A	Ring finger protein 113A	XM_001491814	0.0031	3.83	
NULL	NULL	CX603542	0.0001	3.79	
STAT4	Signal transducer and activator of transcription 4	XM_001502206	0.0019	3.74	
C17orf70	Chromosome 17 open reading frame 70	XM_001489884	0.0028	3.60	
FREM1	FRAS1 related extracellular matrix 1	XM_001493917	0.0050	3.40	
SPAG17	Sperm associated antigen 17	XM_001500885	0.0068	3.23	
P2RY13	Purinergic receptor P2Y,G-protein coupled,13	XM_001489171	0.0041	3.22	
NULL	NULL	DN506907	0.0052	3.13	
Downregulated					
S100A12	S100 calcium binding protein A12	CD535886	0.0003	0.03	*
S100A8	S100 calcium binding protein A8	XM_001494358	0.0000	0.04	*
S100A8	S100 calcium binding protein A8	XM_001493589	0.0001	0.06	
NULL	NULL	CD467650	0.0000	0.06	

Table 5.4 continued

Gene Name	Description	Public Accession	P	Fold Change	PCR
Downregulated					
SOD2	Superoxide dismutase 2	AB001693	0.0000	0.07	*
S100A9	S100 calcium binding protein A9	XM_001493530	0.0045	0.12	*
PI3	Peptidase inhibitor 3	BM734843	0.0007	0.12	
DEFB4	Defensin, beta 4	AY170305	0.0001	0.12	
SAA1	Serum amyloid A1	NM_001081853	0.0004	0.16	
OR5M9	Olfactory receptor, family 5, subfamily M, member 9	XM_001488291	0.0009	0.19	
THBS1	Thrombospondin 1	XM_001503599	0.0008	0.19	
SLA	Src-like-adaptor	XM_001498789	0.0066	0.20	
ORMDL1	ORM1-like 1	XM_001501956	0.0018	0.20	
HSPA8	Heat shock 70kDa protein 8	NULL	0.0069	0.21	
MORC3	MORC family CW-type zinc finger 3	XM_001493319	0.0073	0.21	

GO analysis

Gene ontology was performed for each comparison using NIH-DAVID software version 6.7. Overrepresented GO terms of BP, CC and MF within up and down-regulated genes (P value less than 0.01 and fold change larger than 2) were determined. Only enriched ($P<0.05$) GO terms are presented.

There were no significant GO terms of CC and MF categories found when using the DE genes of $P<0.01$ and $FC>2$ as input data for the 12 h/CON comparison. The GO term immune system process was found in the up-regulated genes in the 12 h/CON comparison (Table A.12). On the other hand, GO terms, including hemopoiesis, hemopoietic or lymphoid organ development, immune system development, immune system process, and leukocyte differentiation were found in the down-regulated genes at the 12 h time point.

Up-regulated genes from the 24 h/CON comparison yielded a number of overrepresented GO terms (Table A.13). Of the 29 biological processes significantly associated with these genes, most genes were involved in defense response, inflammation/wounding or regulation of cell proliferation/adhesion/death. The BP category containing the greatest number of DE genes was response to stress. The two overrepresented cellular component terms were mitochondrial intermembrane space and organelle envelope lumen.

Among down-regulated genes, cellular amino acid metabolic process and cellular response to starvation were the only overrepresented biological processes. Interestingly, most of cellular components dealt with the intracellular part, while all molecular functions were related to transferase activity.

Most GO terms were overrepresented in down-regulated genes of the 12 h/24 h comparison (Table A.14). Of the 127 biological processes significantly overrepresented among these genes, many were associated with response to stress/stimulus, inflammation/wounding or chemotaxis. In contrast, 7 biological processes were overrepresented among up-regulated genes. Most were involved in sensory perception and system process. Cell component was limited to plasma membrane and molecular function related to olfactory receptor activity. Although many of the GO terms found in this comparison were also found in the 24 h/CON comparison, the appearance of eleven new terms associated with cellular ion homeostasis and two new terms describing synthesis of interleukin 1 (IL1) is noteworthy. Cellular components dealt with both of intracellular and extracellular and the molecular function containing most of DE genes was protein binding.

Pathway analysis

Pathway analysis was conducted using the KEGG pathway database (Kanehisa et al., 2008) (http://www.genome.jp/kegg/) linked through the NIH-DAVID database. Totally two pathways were detected for both the 24 h/CON and 12 h/24 h comparisons when the full set of DE genes ($P<0.01$ with $FC>2$) were included. These pathways were Huntington's disease (24 h/CON) and nucleotide binding oligomerization domain (NOD)-like receptor (NLR) signaling pathway (12 h/24 h). NLR can recognize intracellular pathogens and play essential role in the innate immunity (Shaw et al., 2010). To expand on these results, we utilized the Ingenuity Pathways Analysis (IPA; Ingenuity Systems, http://www.ingenuity.com/, version 8.7) application to establish relationships between the full set of DE genes ($P<0.01$ with $FC>2$) for 12 h/CON, 24 h/CON and 12 h/24 h comparisons and predict potential pathways associated with laminitis pathogenesis.

The *top biofunctions* determined by IPA were cellular growth and proliferation, nervous system development and function, and inflammatory response for the 12 h/CON comparison (Table 5.5). The *associated diseases* identified through the analysis were cancer, dermatological diseases and reproductive diseases. The *top canonical pathways* were urea cycle, metabolism of amino groups and primary immunodeficiency signaling. The *top network* with a score of 23 is shown (Fig. 5.2). The *network function* was embryonic development, inflammatory response, cell to cell signaling and interaction. This network included 35 genes, 14 of which were identified as DE in the 12 h/CON

comparison. Five DE genes were up-regulated (IGLL1, ZBP1, MED7, CXCL2, and SLC27A2).

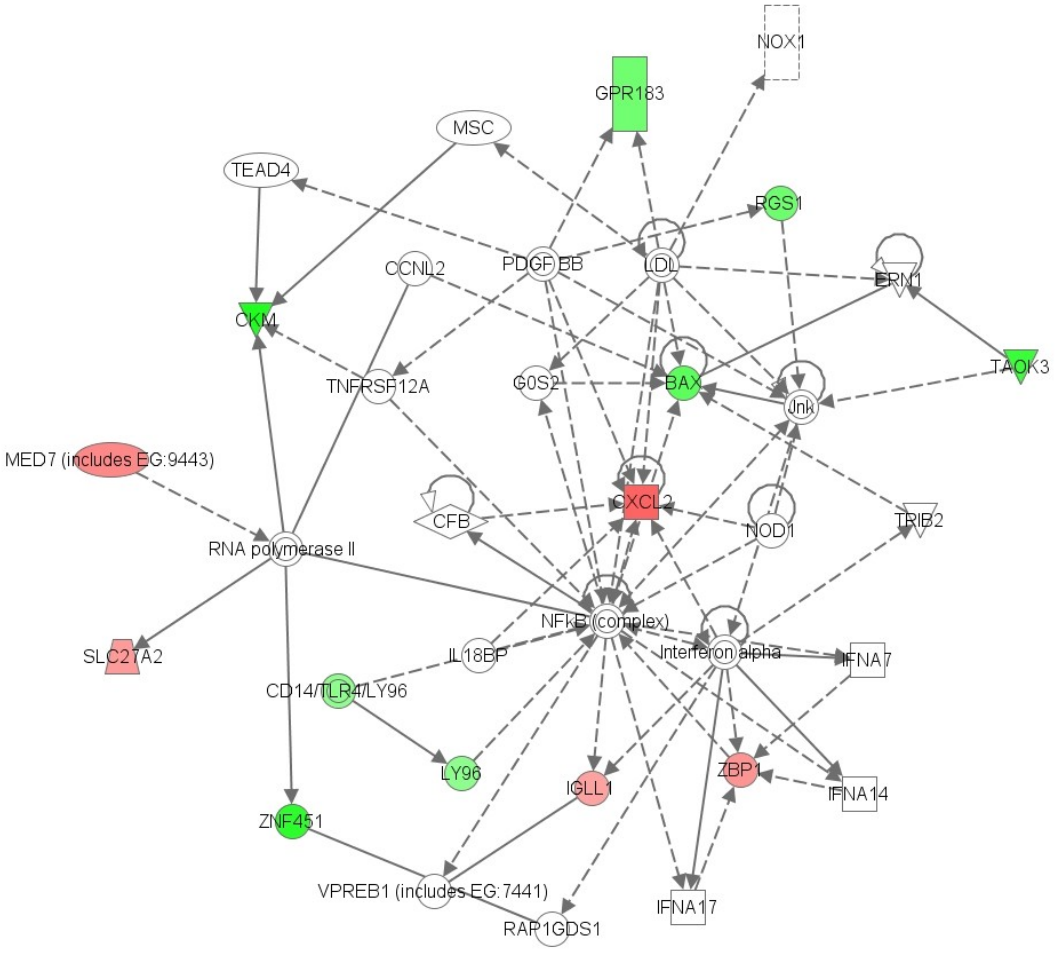

Fig. 5.2. Ingenuity network analysis of 12 h time point compared to control. The top network identified by IPA with a significant score of 23. Both direct (solid line) and indirect (dashed line) interactions among genes (including CXCL2, BAX, and IGLL1) were shown in the network. This analysis was performed on the DE genes of P<0.01 and FC>2 in the 12 h/CON comparison. The intensity of the node color are depicted as down-regulated (green) or up-regulated (red). Square: cytokine/growth factor; vertical diamond: enzyme; horizontal diamond: peptidase; circle: other; parallelogram: transporter; circle-in-circle: complex; oval: transmembrane receptor; shaded circle-in-circle:group.

Additionally, NF-κB, CXCL2 and BAX were in the central positions of network. The dysregulation of DE genes potentially affected the activity of other genes and associated pathways (e.g., core molecule NF-κB in NF-κB pathway) during the pathogenesis of laminitis due to the biological interactions among the genes in the network.

For the 24 h/CON comparison, the *top biofunctions* were inflammatory response, cell death, and free radical scavenging (Table 5.5). The *associated diseases* were connective tissue disorders, immunological disease, inflammatory disease, skeletal and muscular disorders. Laminitis is also a connective tissue disease. The *top canonical pathways* were VDR/RXR activation (Sanchez-Martinez et al., 2006), glucocorticoid receptor signaling (Smoak and Cidlowski, 2004) and TNF-like weak inducer of apoptosis (TWEAK) signaling (Kumar et al., 2009). VDR/RXR signaling is the heterodimer formed between vitamin D receptor (VDR) and retinoid receptor (RXR) can regulate gene expression (Sanchez-Martinez et al., 2006). These pathways are associated with gene expression regulation at the transcriptional level. The *top network* with a score of 34 is shown (Fig. 5.3). The *network function* was inflammatory response, free radical scavenging and lipid metabolism. This network included 34 genes, of which 19 were identified as DE in the 24 h/CON comparison. Therefore an additional 15 genes were related to DE genes through biological interactions. The network also showed a central role of non DE genes p38 MAPK, PI3K, ERK, Akt, and NF-κB and the peripheral role of DE genes PI3 and FAIM. In the network, both S100A8 and SOD2 had higher expression level with fold changes of 24.76 and 11.28, respectively. Also all 19 DE

genes (except NKX3-1) in the network were up-regulated and they were connected directly or indirectly based on their biological relationships.

The *top biofunctions* associated with DE genes of the 12 h/24 h comparison were inflammatory response, protein degradation, antigen presentation, cell to cell signaling and interaction, and hematological system development and function (Table 5.5). The *associated diseases* were dermatological disease, hematological disease, cancer, and connective tissue disease. The *top canonical pathways* that were most significant to the dataset were calcium signaling (Marambaud et al., 2009), role of nuclear factor of activated T cells (NFAT) in cardiac hypertrophy (Molkentin, 2004), IL-17 signaling (Henness et al., 2006) and aldosterone signaling in epithelial cells (Stockand, 2002). Essentially, these pathways are associated with MAPK signaling transduction, suggesting the likely involvement of MAPK signaling pathway in the early stage of OF model of laminitis. The *top network* with a score of 33 is shown (Fig. 5.4). The associated *network functions* were tissue development, cancer, dermatological diseases and conditions. This network included 23 DE genes and all of them linked to non DE gene p38 MAPK through direct and indirect interactions. Among these DE genes, SYNE2, HDAC9, and SLC12A6 were up-regulated and were in peripheral positions in the network.

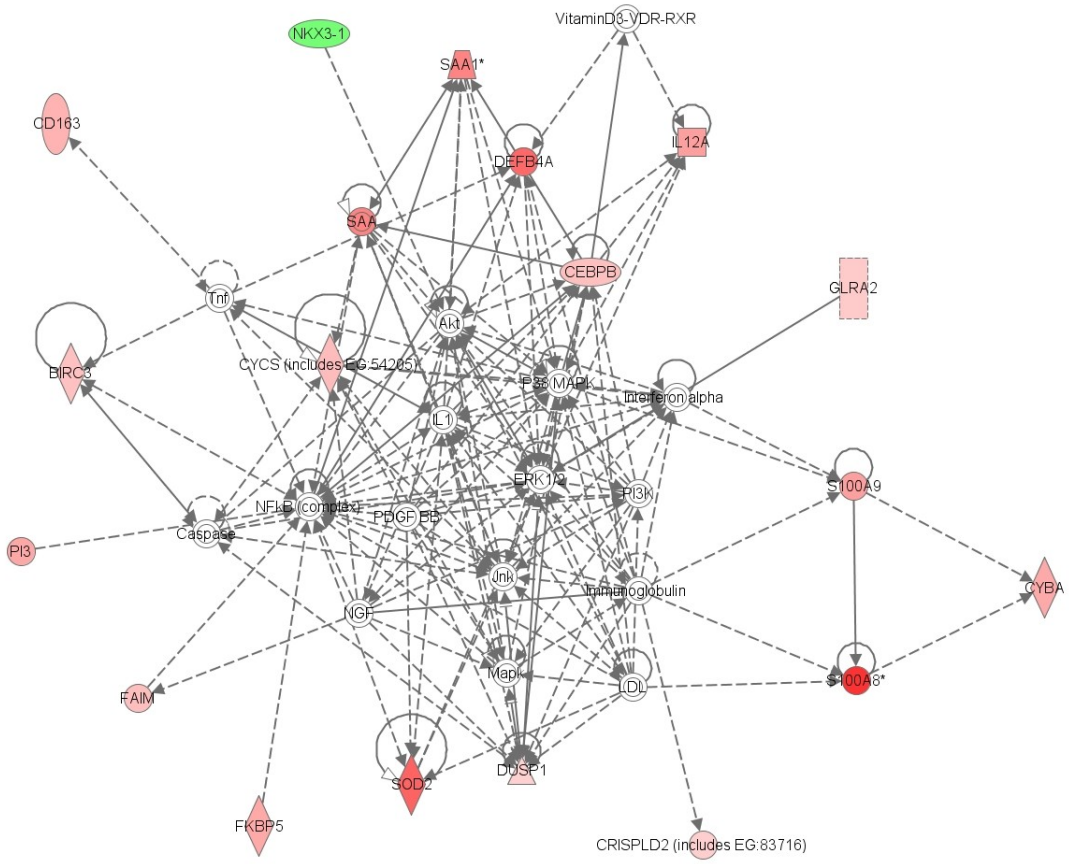

Fig. 5.3. Ingenuity network analysis of 24 h time point compared to control. The top network identified by IPA with a significant score of 34. Both direct (solid line) and indirect (dashed line) interactions among genes were shown in the network. This analysis was performed on the DE genes of $P<0.01$ and $FC>2$ in the 24 h/CON comparison. This network showed the central position of p38 MAPK and NF-κB. The intensity of the node color are depicted as down-regulated (green) or up-regulated (red). Square: cytokine/growth factor; vertical diamond: enzyme; horizontal diamond: peptidase; circle: other; parallelogram: transporter; circle-in-circle: complex; oval: transmembrane receptor; shaded circle-in-circle: group.

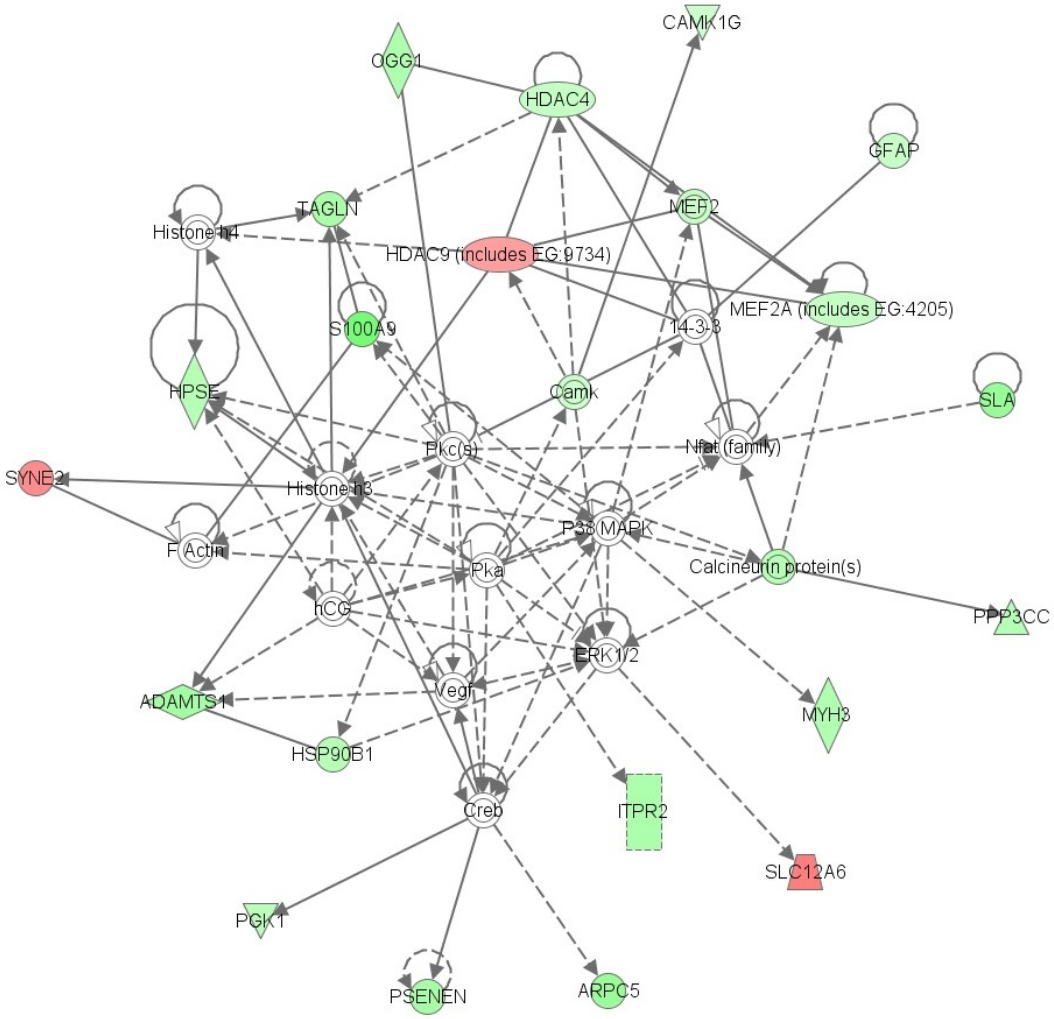

Fig. 5.4. Ingenuity network analysis of 12 h time point compared to 24 h time point. The top network identified by IPA with a significant score of 33. Both direct (solid line) and indirect (dashed line) interactions among genes were shown in the network. This network showed the central position of p38 MAPK. This analysis was performed on the DE genes of $P<0.01$ and $FC>2$ in the 12 h/24 h comparison. The highest scoring biofunctions associated with this network are inflammatory disease/connective disorders/skeletal and muscular disorders. The intensity of the node color are depicted as down-regulated (green) or up-regulated (red). Square: cytokine/growth factor; vertical diamond: enzyme; horizontal diamond: peptidase; circle: other; parallelogram: transporter; circle-in-circle: complex; oval: transmembrane receptor; shaded circle-in-circle: group.

Table 5.5
The top biofunctions, associated diseases, canonical pathways, and network functions that were most significant to the data set of OF laminitis experiment. The DE genes at the level of P<0.01 and FC>2 were used as input data set for 12 h/CON, 24 h/CON and 12 h/24 h comparison respectively.

	Biological functions	**Associated diseases**	**Top canonical pathways**	**Top network function**
12 h/CON	Cellular growth and proliferation, nervous system development and function, and Inflammatory response	Cancer, dermatological diseases, and reproductive system diseases	Urea cycle and metabolism of amino groups, primary immunodeficiency signaling	Embryonic development, inflammatory response, and cell to cell signaling and interaction
24 h/CON	Inflammatory response, cell death, free radical scavenging	Connective tissue disorders (such as rheumatoid arthritis), immunological disease, inflammatory disease and skeletal and muscular disorders (collagen-induced arthritis)	VDR/RXR activation, glucocorticoid receptor signaling, and TWEAK signaling	Inflammatory response, free radical scavenging, and lipid metabolism
12 h/24 h	Inflammatory response, protein degradation, antigen presentation, cell to cell signaling and interaction, and hematological system development and function	Dermatological disease, hematological disease, cancer and connective tissue disease	Calcium signaling, role of NFAT in cardiac hypertrophy, IL-17 signaling and aldosterone signaling in epithelial cells	Tissue development, cancer, dermatological diseases and conditions

Quantitative real time PCR

To select the best reference gene for qRT-PCR data normalization, qRT-PCR was performed for ten reference control genes, including ACTB, B2M, PPIA, GAPDH, GNB2L1, EEF1A1, HPRT1, TUBA1, UBB and RPLP32. The gene expression stability among the laminar samples (CON, 12 h and 24 h) of OF model laminitis was determined

according to the geNorm software (Vandesompele et al., 2002). The 2 reference genes that received best score (EEF1A1 and UBB) from those tested were used for qRT-PCR data normalization.

To validate the differential expression of microarray results, a total of 28 DE genes (up-regulated and down-regulated) were selected for qRT-PCR confirmation. Based on the microarray analysis, we selected most of the DE genes based on a small P value and large fold change. The fold change of all selected genes was larger than 2. Four additional genes with P values between 0.01 and 0.05 were also chosen based on their likely functional relevance to laminitis. ADAMTSL2 is a member of ADAMTS-like protein subfamily and plays a key role in transforming growth factor beta (TGF-β) signaling (Le Goff et al., 2008). TGF-β can regulate the expression of integrin ligands (Margadant and Sonnenberg, 2010). Integrins are ligands of ECM proteins (e.g., laminin, fibronectin and collagen) (Friedl and Brocker, 2000). ECM is the component of equine hoof laminar tissue. BM (a thin layer of ECM) degradation is an early event of pathological changes in the pathogenesis of equine laminitis (Pollitt, 1994). S100A2 and S100A4 are members of S100 protein family, which are involved in the inflammatory response (Foell et al., 2009). The presence and overexpression of other S100 protein members (i.e., S100A8 and S100A9) have been described in the BWE model of laminitis (Faleiros et al., 2009). TMEM38A is an important molecule for calcium signaling. Calcium signaling has been demonstrated to mediate intracellular adhesion in connective tissue (Ko et al., 2001). Laminitis is a disease of the connective tissue laminae of the hoof.

The primers used for qRT-PCR are listed in Table 5.6. Of the 10 genes analyzed by qRT-PCR for the 12 h/CON comparison, CXCL2, IFI30 and TMEM38A had statistically different expression between the two groups (Fig. 5.5). Among the inconsistencies, GLMN, COMMD2, PTGFR, ARPC5L and ADAMTSL1 had the same direction of expression change as in the microarray but the difference shown by real time PCR did not reach statistical significance. For genes MITD1 and CD19, the direction of change in expression was different from the microarray analysis and did not show statistical significance at the level of $P<0.05$. ADAMTS1, DEFB4, S100A8, S100A9, PI3, TMEM49, PSMA4 and EREG were significantly different between 24 h and CON groups and were consistent with microarray results (Fig. 5.6). OF the 11 genes tested by qRT-PCR for the 12 h/24 h comparison, eight (CCL2, CXCL14, S100A8, S100A9, S100A12, SERPINB3, TLR4, and SOD2) were significantly different between the two groups (Fig. 5.7). SOD2, S100A12, and SERPINB3 had fold changes of 17.74, 17.87, and 17.58, respectively. S100A4 had the same direction of change in expression as in the microarray analysis for the 12 h/24 h comparison but was not significantly increased at 12 h time point.

Cluster analysis was performed for the 28 differentially expressed genes based on their mean values among (CON, 12 h and 24 h) groups and a heat map was constructed (Fig. 5.8). The result showed a distinct expression pattern among the conditions (CON, 12 h and 24 h). Moreover, the pattern of gene expression in CON was closer to the 12 h time point than that of the 24 h time point. Most of the genes were up-regulated at the 24 h time point compared to either the CON or the 12 h time point.

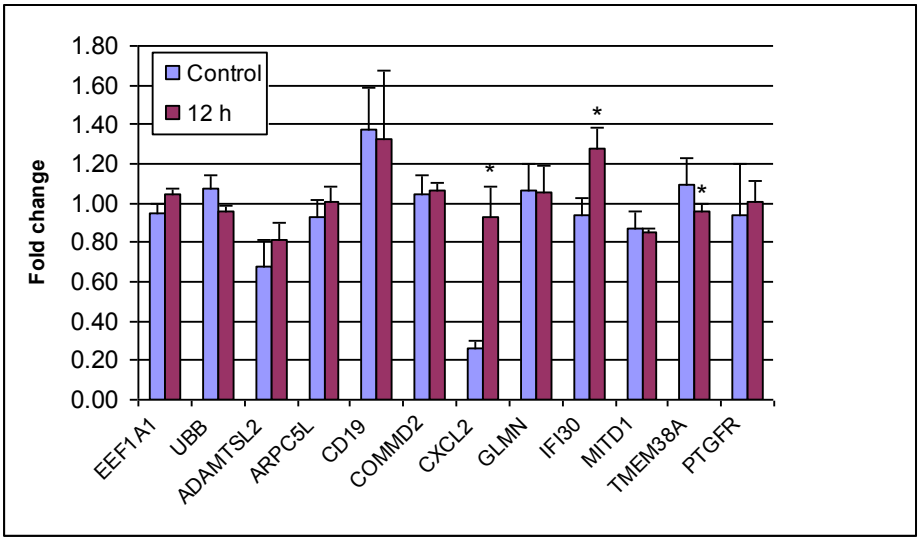

Fig. 5.5. Real time PCR validation of the microarray results of the 12 h/CON comparison. EEF1A1 and UBB are reference genes used for normalization. Ten DE genes from the microarray analysis were selected for real time PCR confirmation. Data are presented as mean ± SEM. Those genes marked with asterisks are significantly different from CON.

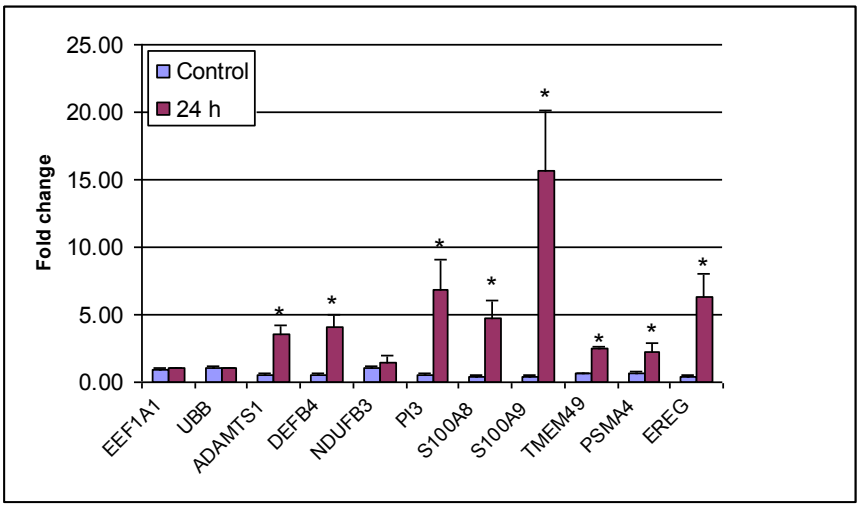

Fig. 5.6. Real time PCR validation of the microarray results of the 24 h/CON comparison. EEF1A1 and UBB are reference genes used for normalization. Nine DE genes from the microarray analysis were selected for real time PCR confirmation. Data are presented as mean ± SEM. Those genes marked with asterisks are significantly different from CON.

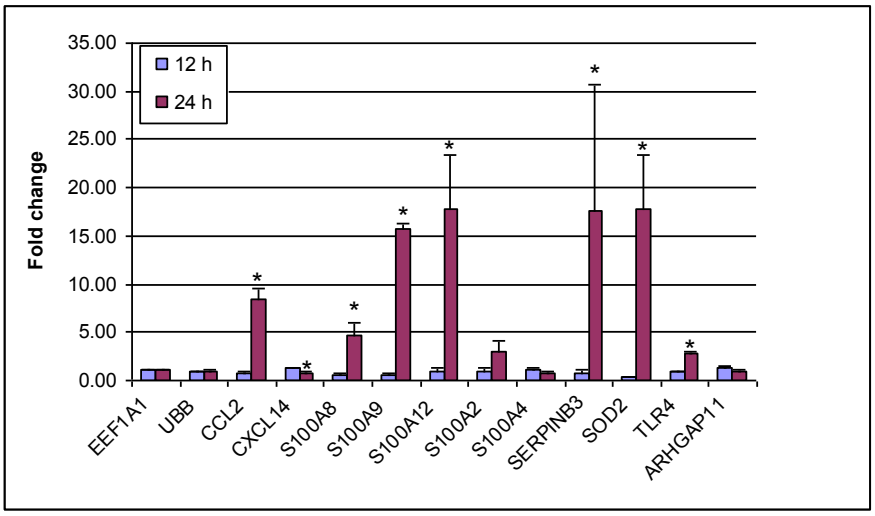

Fig. 5.7. Real time PCR validation of the microarray results of the 12 h/24 h comparison. EEF1A1 and UBB are reference genes used for normalization. Eleven DE genes from the microarray analysis were selected for real time PCR confirmation. Data are presented as mean ± SEM. Those genes marked with asterisks are significantly different between 12 h and 24 h.

Table 5.6
Primers of genes used for quantitative RT-PCR of OF laminitis experiment.

Gene Symbol	Accession No.	Forward Sequence (5'-3')	Reverse Sequence (5'-3')	PCR Product Size (bp)	Tm(°C) *
CCL2	AJ251189	TCCAGTCACCTGCTGCTATAC	ATTCTTGGCTTTTGGAGTAGG	235	58
DEFB4	AY170305	ACTTGCCTTCCTCATTGTCTT	AGCAGTTTCTCCGCTTTCTAT	195	58
ADAMTS1	AF541975	AGGCTCACAATGAATTTTCG	CACAGCCAGCTTTTACACACT	225	58
S100A8	XM_001493589	ACGGATCTGGAGAATGCTATC	TGATGTCCAACTCTTTGAACC	175	58
SERPINB3	XM_001491507	CGTGCAGATGATGAAACAAAT	TTCTGTGAGCTTGTCCACTCT	195	58
S100A9	XM_001493485	CGACCTAGAGACCATCATCAA	TGCTTGTCCTCATTAGTGTCC	189	58
TMEM49	XM_001503742	TTACAGAAGCCATTCCAAGAA	TGGAGTTAATGATGGACAGGA	160	58
S100A12	CD535886	TCATCAACATCTTCCACCAGT	ACCTTGCACACCAGGACTAC	211	58
CXCL14	XM_001502713	ACTGCGAGGAGAAGATGGTTA	CTCGTTCCAGGCGTTGTA	128	58
S100A2	CX598422	GCGACAAGTTCAAGCTGAGTA	ATAGTGATGAGGGCCAGAAAA	181	58
TLR4	AY005808	GGCCAGTGATTTTCCAGTATT	AGGGTGGTCAGGTTAGTCATC	195	58
TMEM38A	XM_001499622	TGGTACTTGGTTTTCTTCTGC	GACTCTCACCACCTCCTTCAT	102	58
SOD2	AB001693	ACTTTGGTTCCTTCGACAAAT	CAGGGGAATAAGACCTGTTGT	167	58
S100A4	CX604383	GGATGTGATGGTATCCACCTT	GCAGGACAGGAAGACACAGTA	217	58
NDUFB3	XM_001503625	GGAAGATAGAAGGGACACCAT	TCCTACAGCTACCACAAATGC	185	58

Table 5.6 continued

Gene Symbol	Accession No.	Forward Sequence (5'-3')	Reverse Sequence (5'-3')	PCR Product Size (bp)	Tm(°C) *
PI3	BM734843	CTTCTTGATCCTGGTGGTGTT	ACTGAATCTTGCCCTTTGACT	162	58
ADAMTSL2	XM_001497636	ACACCCACCTTGGTTACTCTC	TGCCGTTGAAGAAGTAGTAGC	132	58
CD19	CX592103	AGACTCCTTCTCCAACGGTAA	CCACCTCTTCATCCTCATTCT	157	58
CXCL2	AF053497	AACCGAAGTCATAGCCACTCT	CCTTTTCTCCAGGTTAGTTGG	125	58
ARPC5L	XM_001502042	CTATGCCTTTGTCCACGAGTA	AAACAAGCTCTCCCTCTACCA	161	58
GLMN	XM_001492771	CATAGATGAAGGGCACGTAGA	ATTCCATAAAAGGCATCGAAC	121	58
MITD1	XM_001490447	AAGGCAGTAGGAGAGAACAGC	TAATCAAGTCCCCTTCCAATC	163	58
IFI30	XM_001500556	CAGCTCCTGTACCTCGTCTG	CTGGACTTCATGGAATGTGTC	222	58
COMMD2	DN509689	AGACCTTCCCAGTTACCACAG	TTGTTTTCATCTCCTCCAGTG	210	58
PTGFR	DQ385610	TGCCATCACAGGAATTACACT	AGCGTTGTTTCACAGGTCTC	201	58
EREG	XM_001490281	ACATGAATGGCTACTGTTTGC	AGTATATGGAACCGGCGACTA	204	58
PSMA4	XM_001489071	TGAAGTCAGCACTTGCTCTTG	CTCACGCTCAGCTTTAGCTTC	194	58
ARHGAP11	XM_001503656	CAGGTTGCTTCTCTCCTAAAA	TCGACCAACATTTTCACATCT	134	58
EEF1A1[a]	NM_001081781	TGGAAAGAAGCTGGAAGATG	CAACCGTCTGTCTCATGTCA	132	58
UBB[a]	AF506969	GCAAGACCATCACCCTGGA	CTAACAGCCACCCCTGAGAC	206	61
HPRT1[c]	AY372182	GGCAAAACAATGCAAACCTT	CAAGGGCATATCCTACGACAA	163	61
TUBA1[c]	AW260995	GCCCTACAACTCCATCCTGA	ATGGCTTCATTGTCCACCA	78	60

Table 5.6 continued

Gene Symbol	Accession No.	Forward Sequence (5'-3')	Reverse Sequence (5'-3')	PCR Product Size (bp)	Tm(°C) *
RPLP0	BC107717	TTGCATCAGTACCCCATTCT	ACCAAATCCCATATCCTCGT	242	58
ACTB[c]	AF035774	CCAGCACGATGAAGATCAAG	GTGGACAATGAGGCCAGAAT	88	58
B2M	X69083	CGAGACCTCTAACCAGCATC	AGACATAGCGGCCAAAGTAG	186	58
PPIA	NM_021130	TGGGGAGAAAGGATTTGGTT	CATGGACAAGATGCCAGGAC	178	58
GNB2L1	AY246708	CAGGGATGAGACCAACTACG	ATGCCACACTCAGCACATC	269	58
RPL32[c]	CX594263	AGCCATCTACTCGGCGTCA	TCCAATGCCTCTGGGTTTC	149	58
GAPDH[c]	AF157626	GATGCCCCAATGTTTGTGA	AAGCAGGGATGATGTTCTGG	250	61

* The optimal annealing temperature
[a] EEF1A1 and UBB were used for normalization during quantitative RT- PCR
[c] Information about the primers from (Bogaert et al., 2006)

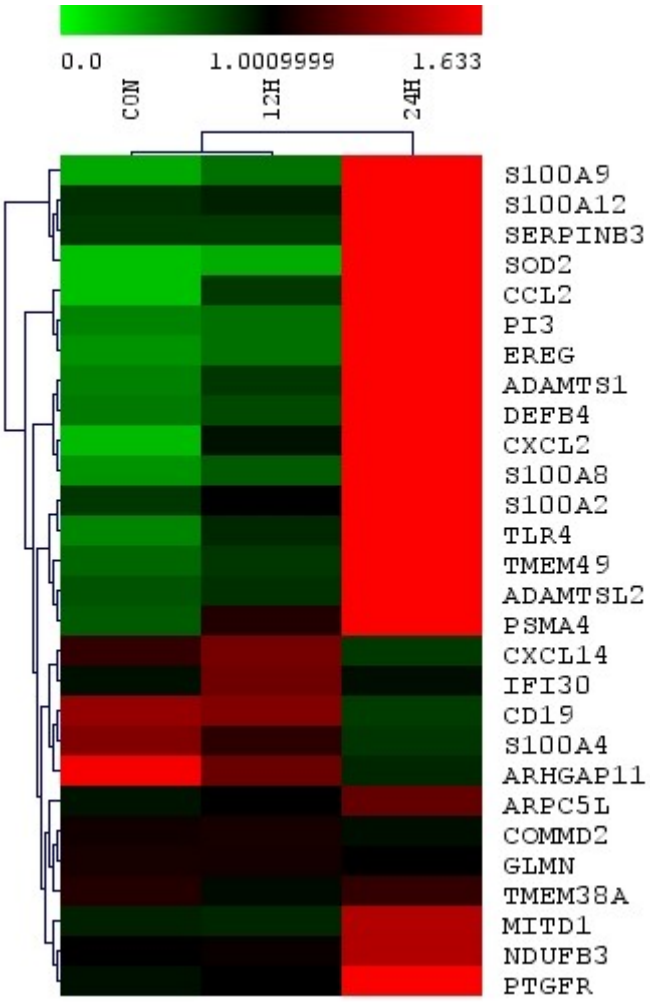

Fig. 5.8. Cluster diagram of the mean of CNRQ values at control, 12 h and 24 h time point as determined by qRT-PCR. The green to red color scale demonstrates the expression value of mean of CNRQ. EEF1A1 and UBB were used as reference genes to calculate normalized ΔCq.

DISCUSSION

This is the first study to investigate the genome wide transcriptome profiling during the early time points of OF induced equine laminitis using an equine whole genome long oligonucleotide microarray. Equine whole genome oligoarray identified differential expression of 71 and 151 genes at 12 h and 24 h time points (Table 5.1) as well as associated pathways and networks accompanying the initiation of laminitis.

Initiation of laminitis

In order to determine genes and relevant pathways that might be associated with the initiation of laminitis, we performed transcriptomic profiling on laminar tissue samples collected at 12 h and 24 h time points following oligofructose administration. Most of horses used (3 mares, 15 geldings) are geldings in this study. On the other hand, most of horses used in CHO model laminitis (Chapter III) are mares (10 mares, 5 geldings). There was no stallion used in the study. Alford and coworkers found age, sex, and breed were risk factors for acute laminitis (Alford et al., 2001). This same study found mares (not stallions) had greater risk for acute laminitis when compared with geldings. In addition, the Thoroughbred (TB) is at decreased risk of laminitis compared to other breeds (Alford et al., 2001). In contrast, other epidemiological studies have reported that there was no significant association between age, breed, sex or weight and the development of acute laminitis (Polzer and Slater, 1997; Slater et al., 1995). At 24 h, horses exhibit an increased rectal temperature and heart rate. Horses at 12 h and 24 h time points show no clinical sign of lameness except one horse developed Obel grade 2 lame at 24 h.

We identified differential expression of genes involved in signal transduction, immune response, genes encoding transcription factors and enzymes (Table 5.2, 5.3 and 5.4). At 12 h time point, few differentially expressed genes were identified when compared to controls (Table 5.1). Overrepresented GO term of immune system process found from both of up and down-regulated genes (Table A.12), suggesting that the immune response that contributing to/affected by laminitis likely occur at least at 12 h before any clinical evidence of laminitis. Among the DE genes, BAX was down-regulated (Table 5.2). BAX has been shown to enhance apoptosis (Green and Chipuk, 2008). Therefore apoptosis may be associated with early histological changes of laminitis.

Perhaps the most intriguing DE gene during this stage is CXCL2, also known as macrophage inflammatory protein 2 (MIP-2). This chemokine was consistently overexpressed at 12 h and 24 h. CXCL2 is a crucial chemoattractant for neutrophils (polymorphonuclear leukocytes) and has been shown to be up-regulated by bacterial LPS in enterocytes (De Plaen et al., 2006). Neutrophils provide the first line of host defense against invading microbial pathogens through phagocytosis process (Kobayashi et al., 2003). In addition to neutralize pathogens through the release of ROS and proteases at the site of infection/inflammation, neutrophils cause host tissue destruction (Brown et al., 2006). It has been indicated that the control of neutrophil apoptosis following phagocytosis is essential to minimize the tissue damage (Haslett, 1999; Kobayashi et al., 2003; Weiss, 1989). The presence and activation of neutrophil has been reported in the developmental stage and the onset of different model of laminitis (Black

et al., 2006). It remains unknown whether the up-regulation of CXCL2 is the potential cause or a result of neutrophil activation in this study. However, together with the fact that the up-regulation of CXCL2 occurs (i.e., 12 h time point) before the horses exhibit clinical sign of laminitis (i.e., foot pain), we therefore hypothesize that CXCL2 may play initialing role in neutrophil accumulation in the OF induced laminitis. Of course the role of neutrophil in laminitis pathology needs further investigation.

Development of laminitis

In contrast to 12 h time point, samples taken at the 24 h time point show a strong transcriptomic response and a dramatic up-regulation of inflammatory genes. This is also supported by GO analysis and most of significantly enriched GO terms of 24 h/CON comparison are associated with inflammation and immune response (Table A.13). Among the DE genes with largest fold changes at the 24 h time point, SAA1, EREG, DEFB4, SOD2 and S100A8 were highly up-regulated genes with large fold changes in expression (Table 5.3). SAA1 has been shown to induce cytokine production and inhibit neutrophil apoptosis in inflammation (Christenson et al., 2008). EREG, a member of epidermal growth factor family, plays a regulatory role in human keratinocyte growth (Hashimoto, 2000). Keratinocytes are the main cell type in the hoof epidermis and their growth is essential for the hoof's structural integrity. DEFB4 is an antimicrobial peptide and plays antimicrobial role in innate immunity (Ganz, 2003). It has recently been suggested that S100A8 may have an anti-oxidant function (Perera et al., 2010) and regulate oxidative modification (Lim et al., 2009). SOD2 is an antioxidant enzyme and is also up-regulated at the developmental stage of CHO model laminitis (Chapter III). It remains unknown that

whether S100A8 and SOD2 may contribute to the early pathological change of laminitis or are merely a physiological reaction to underlying tissue damage that has already occurred at cellular level. It is noteworthy that five members of the olfactory receptor superfamily showed differential expression during the transition from the 12 h time point to 24 h time point (Table A.11). Olfactory receptors are mainly expressed in the nose but have been shown to be expressed in other tissue types such as the kidney and sperm (Kaupp, 2010; Pluznick et al., 2009; Spehr et al., 2003). Further study is needed to investigate their possible function in laminitis.

Metalloproteinase ADAMTS1 was overexpressed at the 24 h time point (Table 5.6) and had no differential expression at the 12 h time point. Based on our findings, ADAMTS1 has been up-regulated in three different models of laminitis investigated (Chapter III and IV). ADAMTSs have been shown to play an essential role in ECM components (e.g., collagen) degradation (Apte, 2009) and their differential expression has been found in cancer and arthritis (Tortorella et al., 2009). Therefore ADAMTS1 may be essential for equine laminitis pathogenesis.

Genes encoding calcium binding proteins S100A8, S100A9, and S100A12 were up-regulated at 24 h time point relative to control horses, and S100A4, S100A8, S100A9, and S100A12 were up-regulated at 24 h time point relative to 12 h time point. This gene family has been shown to play an essential role in the inflammatory response during arthritis (Perera et al., 2010), leukocyte recruitment during inflammation (Roth et al., 2003) and calcium homeostasis (Heizmann et al., 2002). S100 proteins may also play a regulatory role in oxidative stress (Lim et al., 2009). Oxidative stress had been shown

to be essential for laminar tissue damage in laminitic horses (Yin et al., 2009). Therefore, their regulatory role in oxidative stress could control the production of hydrogen peroxide and superoxide anion as indicated by GO analysis (Table 5.9). S100A4 is correlated with the progression of rheumatoid arthritis (RA) (Oslejskova et al., 2009). S100A8 and S100A9 have been shown to play a role in cartilage destruction in osteoarthritis (OA) (Zreiqat et al., 2010). RA is both a joint (Diarra et al., 2007) and connective tissue disease (Bateman et al., 2009; Vincenti and Brinckerhoff, 2001). Laminitis is a connective tissue disease (Mobasheri et al., 2004). The differential expression of the S100 family of genes could promote inflammation and regulate oxidative stress in the laminae through leukocyte activation and migration, which may lead to laminar tissue damage. Furthermore, the strong induction of S100 family of proteins in CHO (Chapter III), HI (Chapter IV) and OF models of laminitis indicated that the overexpression of S100 proteins is likely a common scenario of laminitis pathogenesis.

Interestingly, an indication of a transcriptional response to microbial infection was observed. The protein encoded by SAA1 is an acute phase protein and opsonizes Gram-negative bacteria (Shah et al., 2006). CXCL2 is a critical chemokine for neutrophils and neutrophils are the first line of defense against bacterial infection. Beta-defensin 2 (DEFB4) and peptidase inhibitor 3 (PI3) are both expressed in keratinocytes and have direct anti-microbial properties (Sallenave, 2010; Schneider et al., 2005). Likewise, the down-regulation of chemokine CXCL14, particularly in keratinocytes, is taken as evidence of bacterial infection (Maerki et al., 2009). The identification of metabolic

pathway of NOD-like receptor signaling, which is involved in recognition of intracellular bacteria and detection of bacterial components in the cytosol (Franchi et al., 2006; Kanneganti et al., 2007), also indicated a bacterial infection. The hypothesis of an infection is also supported by the overrepresented GO terms of response to external stimulus, defense response and leukocyte chemotaxis within the group of up-regulated genes.

Transition from 12 h to 24 h of developmental laminitis

Direct comparison of the 12 h and 24 h time points of laminitis generates some results found when comparing each stage to the control group. For example, GO terms involving inflammatory response, regulation of apoptosis, and response to external stimulus found among down-regulated genes of the 12 h/24 h comparison reflect the strong up-regulation of these genes at the 24 h stage compared to controls. However, this comparison yielded two new results: the overrepresentation of cellular ion homeostasis and synthesis of IL1 GO terms. It is unclear whether this is due to an up-regulation at the 24 h stage, a down-regulation at the 12 h stage, or a combination of both. Ion homeostasis has been linked to inflammatory response and infection (Wessling-Resnick, 2010). IL1 is a "typical" cytokine in inflammatory response and can be produced by macrophages, neutrophils, and epithelial cells (e.g., keratinocytes).

The common DE inflammatory mediators between the 24/CON comparison and 12 h/24 h comparison included SAA1, S100A8, SOD2, and DEFB4 (Table 5.3 and 5.4). These genes are potential targets for anti-inflammatory treatment through the design of antagonists to counteract their inflammatory effect. A recent review has indicated that a

critical point of inflammation control is at the transcriptional level (Medzhitov and Horng, 2009). Those transcription factors, transcriptional activator/repressor, and chromatin remodeling involved in the toll like receptor (TLR) induced inflammatory response were inflammation control points (Medzhitov and Horng, 2009).

Comparison to previous studies

Similar to results seen using an equine-specific 3,076 element cDNA microarray in laminar tissue of the black walnut extract model of laminitis (Noschka et al., 2008), we identified the up-regulation of CCL2 and SAA1 at the 24 h time point, suggesting the role of these genes in laminitis pathogenesis regardless of the mechanism of induction. We also identified the up-regulation of DEFB4, IL16, CXCL4, CXCL2, TLR4, CD19, COX17, and ADAMTS1 as well as several S100 family members. Differential expression of these genes was not detected (except S100P) at any time point of BWE model laminitis (Noschka et al., 2008). Compared to the work carried out by 15 K bovine microarray chip in the OF model laminitis (Budak et al., 2009), we identified the up-regulation of CCL2. However, we didn't find many common differentially expressed genes. This may be due to the different time points we used. In Budak's study, the authors euthanatized the OF horses after 24-30 h (Budak et al., 2009). In our study, we collected tissue at 12 h and 24 h. Therefore the laminar tissue samples we collected may be at different phase of laminitis pathogenesis, which could cause differences in gene expression.

Pathway and network study of laminitis

Pathway and network analysis of DE genes in the 12 h/CON, 24 h/CON and 12 h/24 h comparisons indicated that many DE genes were linked to p38 MAPK and NF-κB pathway molecules at both the 12 h and 24 h time points (Fig. 5.2, 5.3, and 5.4). Similar results were found in the CHO and HI models of laminitis, as shown in previous chapters of the dissertation. Inhibition of the NF-κB and the MAPK signaling pathways has been investigated in OA and RA (Murphy and Nagase, 2008; Sweeney and Firestein, 2007). Laminitis is also a connective tissue disease as RA and hence they may share common features of pathogenesis (e.g., pathway) (Zhernakova et al., 2009). The inhibition of p38 MAPK and NF-κB can suppress cytokine production (Matsumori et al., 2004; Smith et al., 2006b). It is likely that the design of NF- κB and p38 MAPK inhibitors can alleviate the laminar tissue destruction at the site of inflammation by reducing cytokine production. The analysis of top biofunctions and associated diseases also demonstrated that laminitis has many similarities with other connective tissue diseases such as RA.

Relevance to current hypotheses

Currently, the three most popular hypotheses regarding the initiation of laminitis implicate vasoconstriction/hypoxia, MMPs, and escape of bacteria from the hindgut into the bloodstream (Bailey et al., 2004). We saw no evidence of differential expression of these genes and thus cannot hypothesize that hypoxia/MMP play a role in this model of laminitis. However, we found evidence support the hypothesis that bacteria or bacterial components escape from the hindgut and cause laminar inflammation. It has been shown

that changes in microbial populations of equine GI tract occur in the OF model of laminitis (Milinovich et al., 2006). The differential expression of anti-microbial peptides such as DEFB4, PI3, and CXCL14 and critical chemokine CXCL2 for neutrophil accumulation at the site of infection is suggestive of the presence of bacterial antigens, although microarray data necessarily need to be confirmed at the protein and functional levels.

Our qRT-PCR validation experiments showed that most of the qRT-PCR results were consistent with those generated using the microarray (Fig. 5.4, 5.5 and 5.6) except the 12 h/CON comparison. It is possible due to the experimental condition that the subtle difference in gene expression of laminar tissue occurs between 12 h time point and control. Microarray has an inherent limitation to detect small changes between conditions because of the "noise" from different variations during experiments (Yao et al., 2004). Together with qRT-PCR validation of CHO and HI microarray experiments, for those genes that did not correlate with microarray analysis, most of them did not reach statistical significance by qRT-PCR. Microarray is hybridization-based technology and it tends to produce false positives (Pawitan et al., 2005). On the other hand, qRT-PCR is much more sensitive and specific than microarray (Sinicropi et al., 2007). Large variation between biological replicates was seen in qRT-PCR, which caused higher P value. It is also possible the non-specific primers used (e.g., located at different cDNA) although we have checked the specificity of primer sets with BLAST search. Another possibility of inconsistency is that qRT-PCR primer sets did not target the same transcript as the microarray probe (Dallas et al., 2005).

CONCLUSION

In conclusion, this is the first investigation of genome-wide transcriptome profiling of the laminar tissue at two early time points (i.e., 12 h and 24 h) following OF administration using an equine whole genome microarray. The genes with differential expression we identified are more comprehensive compared to the two expression arrays used previously in laminitis. We identified the differential expression of genes encoding enzymes, olfactory receptors, extracellular matrix proteins, and genes involved in signal transduction, homeostasis, apoptosis and immune response in the initiation of equine laminitis. We also identified the differential expression of S100 family members and metalloproteinase ADAMTS1. These genes will be good candidates for further functional investigation in laminitis. We performed pathway and network analysis on the DE genes of each comparison and elucidated the gene-gene interactions relevant to equine laminitis and the pertinent p38 MAPK and NF-κB pathway molecules. In addition, the overexpression of several anti-microbial genes and chemoattractant CXCL2 for neutrophils supports the hypothesis that bacterial components might play a role in the pathogenesis of the OF model of laminitis. These discoveries may contribute to better understanding of the molecular mechanism underlying the initiation of laminitis. Our results provide better understanding of equine laminitis pathogenesis and these findings will be critical in paving the way for developing improved preventatives and treatments for equine laminitis in the future.

CHAPTER VI

SUMMARY AND FUTURE DIRECTIONS

SUMMARY

This is the first genome-wide transcriptome analysis of laminar tissue during the early stages of CHO, HI and OF induced equine laminitis using an equine 21,000 70-mer long oligoarray approach. The work described in this dissertation substantially improved current knowledge regarding molecular underpinnings of the pathogenesis of equine laminitis and helped identify DE genes, potential pathways, and genetic networks associated with the initiation and progression of the disease. The findings in this study gave us a better comparative understanding of the genes associated with the interplay that occurs during early stages of the progression of the disease compared to the two previous arrays used (Budak et al., 2009; Noschka et al., 2008) in laminitis. Additionally, we verified earlier results describing gene expression analysis in laminar tissue that have been focused on selected genes considered central in disease progression.

The identified DE genes will be good candidates for further functional study in equine laminitis. Furthermore, we identified the presence of NOD-like receptor signaling metabolic pathway, which is involved in recognition of intracellular bacteria in both of CHO and OF models of laminitis. *The most important finding of this study is the implication of laminitis initiation: the overexpression of anti-microbial genes supports*

the hypothesis that bacterial components might play a role in the pathogenesis of the CHO and OF models of laminitis.

We investigated three models of laminitis: carbohydrate overload, a common cause of naturally occurring laminitis, oligofructose, a specific type of nonstructural carbohydrate, representation of pasture-associated laminitis, and hyperinsulinemic laminitis, usually associated with endocrine dysfunctions. The comparative study of gene expression during the early stages of CHO, HI and OF models of laminitis showed common features as well as differences among all three models.

Common changes of gene expression patterns among three models

Although the laminar tissue samples obtained from different time points of early stages of acute laminitis, common functional categories of DE genes were found among these models, which include genes involved in signal transduction, immune response, enzymes, enzyme inhibitors, transcription factors, extracellular matrix proteins, and S100 calcium binding proteins. Between CHO and OF models of laminitis, there were more shared genes.

The strong induction of inflammatory mediators such as SOD2, SAA1, DEFB4, SERPINB3, SERPINB11, PI3, CCL2, CXCL2, S100A8, S100A9, and S100A12, vacuole-associated transmembrane protein TMEM49, epidermal growth factor EREG, the up-regulation of BIRC3, CEBPB, CYCS, and SEC11C and the down-regulation of the potassium channel TMEM38A were observed between CHO and OF models of laminitis.

The consistent up-regulation of ADAMTS1, apoptosis-associated molecule cytochrome c (CYCS), and down-regulation of CXCL14 among CHO, HI and OF models of laminitis highlight these molecules' likely importance to the pathogenesis of equine laminitis. Another unexpected result from this study was the differential expression of olfactory receptors. Olfactory receptors were mainly expressed in the nose and play essential role in sensory perception. Their possible function in equine laminitis needs further investigation.

Differential expression also showed the likely involvement of S100 calcium binding proteins in the progression of equine laminitis. S100P, S100A8, S100A9 and S100A12, were up-regulated at OG1 stage relative to control horses in the CHO model of laminitis. S100PBP, S100A1, and S100A2 were dysregulated at OG2 stage relative to control horses in the HI model of laminitis. S100A8, S100A9, and S100A12 were up-regulated at 24 h time point relative to control horses in the OF model of laminitis. S100A2, S100A4, S100A8, S100A9, and S100A12 (S100A4 was down-regulated) were up-regulated at the 24 h time point relative to the 12 h time point in the OF model of laminitis. The up-regulation of S100 proteins in laminitis and their known function in other diseases suggest that they may promote inflammation, regulate ion homeostasis and control oxidative stress, which could lead to laminar tissue destruction during the pathogenesis of equine laminitis. To the best of our knowledge, the strong induction of S100 calcium binding proteins in CHO, HI and OF models of equine laminitis has not been previously reported.

Furthermore, we discovered convergent pathway core molecules potentially associated with equine laminitis: p38 MAPK and NF-κB in the CHO, HI and OF models of laminitis. Pathway and genetic network analysis revealed DE genes and the likely gene-gene biological interactions relevant to the pathogenesis of equine laminitis. It also allowed us to link primary gastrointestinal disease or other systemic diseases (e.g., rheumatoid arthritis) to laminitis. This is a key advancement of current limited knowledge of molecular mechanisms of laminitis. The inhibition of these cell signaling molecules can be evaluated for laminitis therapy in the future.

Different features of gene expression patterns among three models

On the other hand, there were different features of expression patterns among these models of laminitis. Most DE genes were different among these three models. The number of DE genes associated with immune response in HI model is smaller than that of either CHO or OF model at the same statistical confidence level. This may be due to the fact that the laminar tissue samples we collected at different time points (i.e., OG2 stage in HI model). Another interesting feature is that the associated top canonical pathways and diseases were different among these three models even though CHO and OF models shared some common associated diseases (e.g., connective tissue disease).

One prominent difference is the differential expression of CCL2 and CXCL2 between CHO and OF models of laminitis. Chemokine CCL2 was consistently overexpressed at DEV (12-18 h) and OG1 stages (20-48 h) of CHO model of laminitis. It showed no differential expression at 12 h time point and up-regulated at 24 h time point (P value 0.03 and fold change 2.90) of OF model of laminitis. For CXCL2 gene, it

was consistently up-regulated at 12 and 24 h time point of OF model of laminitis. However it did not show differential expression at DEV and OG1 stages of CHO model of laminitis. The different model and time point/stage may be the possible reasons for the expression difference. The time for laminar tissue samples collected at DEV stage (onset of fever) of CHO model ranged from 12 to 18 h. It is suggested that the up-regulation of CXCL2 may occur at very early developmental stage (i.e., 12 h time point) and possibly initiate neutrophil accumulation and followed by the up-regulation of CCL2.

The most stable reference genes were different in expression among three models in qRT-PCR. Only one reference gene such as GAPDH or ACTB was used in most published real time PCR studies in horse and human medicine. Because the expression level of reference genes has been demonstrated to vary among different conditions (Suzuki et al., 2000), the selection of reliable reference genes is essential for the accurate interpretation of qRT-PCR data. We not only consider the difference of PCR amplification efficiency between gene of interest and reference gene but use more than one reference gene for qRT-PCR data normalization as well. The data suggested that EEF1A1 and RPLP0 can be used in the CHO model laminitis, GNB2L1 and RPL32 may be used in the HI model laminitis, and EEF1A1 and UBB are good reference genes for the OF model of laminitis expression studies.

Overall, the studies described advanced our current understanding of the equine laminitis pathogenesis. The common gene expression changes of early stages of CHO, HI and OF models of laminitis data will be potentially useful to design antagonist or

agonist that targets the key gene receptor, inhibitor, activator of the target enzyme, or anti-inflammatory therapies for use in the developmental stage of laminitis.

FUTURE DIRECTIONS

One direction for future laminitis study is to study this disease at protein level. The validation and functional significance of the identified DE genes in this study may be evaluated using proteomic techniques (e.g., western blotting). Proteomic approaches have been proposed to predict the onset of laminitis and help elucidate the molecular causes of laminitis (Mankowski and Graham, 2008).

The primary laminar basal epithelial cell (LBEC) culture within BM or cell line needs to be established and the study of functional aspects of the DE genes identified through this study at cellular level will be essential. The better understanding of the mechanism of laminar failure is impossible without the knowledge of events occurring at cellular level. Recently a primary culture of keratinocyte has been established for horses and will be a valuable tool to study the ECM components in laminitis (Visser and Pollitt, 2010). Another attempt to isolate epidermal cells from equine hoof is underway (Galantino-Homer et al., 2010).

Another direction for future study is to identify the trigger that initiates laminitis. Several DE genes common to both of CHO and OF models of laminitis have antimicrobial property and therefore support the bacterial components trigger theory. Laminitis has been associated with CHO overload (i.e., excess lush pasture or excess grain). The natural place to look for the trigger is the GI tract. GI disease is the most common disease associated with laminitis (Cohen and Woods, 1999; Slater et al., 1995).

This is supported by several studies that have suggested that the origin of the trigger for laminitis is in the hindgut (Bailey et al., 2004; Milinovich et al., 2010). Understanding the events that occur in the gastrointestinal tract (i.e., hindgut) during laminitis pathogenesis may help us to identify the trigger that causes laminitis. The elucidation of the equine gut microbiome in the future will eventually contribute to the better understanding of the pathogenesis of laminitis.

Furthermore, the identification of many inflammatory mediators and p38 MAPK/NF-κB pathway molecules in this study will enable the design of gene specific anti-inflammatory drugs (e.g., anticytokine therapy) as well as p38 MAPK/NF-κB inhibitors (Dinarello, 2010). The *in vitro* assays of testing (e.g., with an antibody, or siRNA) and evaluation of these targets as well as clinical trial will be essential. This therapeutics has been investigated in connective tissue diseases such as rheumatoid arthritis (RA). For example, p38 MAPK inhibitor has been investigated in RA (Chopra et al., 2010). The application of therapeutic strategy for RA treatment through NF-κB inhibition (Criswell, 2010) has been proposed.

The availability of the draft sequence of horse genome generates a single nucleotide polymorphism (SNP) map as well as enables the development of an equine whole genome SNP chip (Swinburne, 2009; Wade et al., 2009). This tool will be valuable for genome wide association study (GWAS) in laminitis to investigate disease susceptibility. Recent studies using the Illumina equine 50K SNP chip has led to the identification of a haplotype associated with lordosis (Cook et al., 2009), and a causative mutation in Lavender Foal Syndrome (LFS) (Brooks et al., 2010) in horses.

Overall, the outcome and significance of the findings expanded the current knowledge about equine laminitis and can lead to new ways to help develop potential preventions and therapeutic strategies. As the mission " To Conquer Laminitis by 2020", postulated by Equine Laminitis Research Community (Orsini and Moore, 2010), the unified information from diverse components of laminitis such as gene expression, association study, histological, pathological, endocrinological, and immunological aspects will help elucidate the disease pathogenesis and provide a more effective treatment strategy.

REFERENCES

Afonso, V., Champy, R., Mitrovic, D., Collin, P., Lomri, A., 2007, Reactive oxygen species and superoxide dismutases: role in joint diseases. Joint Bone Spine 74, 324-329.

Akira, S., Uematsu, S., Takeuchi, O., 2006, Pathogen recognition and innate immunity. Cell 124, 783-801.

Al Jassim, R.A.M., Andrews, F.M., 2009, The bacterial community of the horse gastrointestinal tract and its relation to fermentative acidosis, laminitis, colic, and stomach ulcers. Vet Clin North Am Equine Pract 25, 199-215.

Alford, P., Geller, S., Richrdson, B., Slater, M., Honnas, C., Foreman, J., Robinson, J., Messer, M., Roberts, M., Goble, D., Hood, D., Chaffin, M., 2001, A multicenter, matched case-control study of risk factors for equine laminitis. Preventive Veterinary Medicine 49, 209-222.

Allen, D., Jr., Clark, E.S., Moore, J.N., Prasse, K.W., 1990, Evaluation of equine digital Starling forces and hemodynamics during early laminitis. Am J Vet Res 51, 1930-1934.

Almgren, C.M., Olson, L.E., 1999, Moderate hypoxia increases heat shock protein 90 expression in excised rat aorta. Journal of Vascular Research 36, 363-371.

Amalinei, C., Caruntu, I.D., Balan, R.A., 2007, Biology of metalloproteinases. Rom J Morphol Embryol 48, 323-334.

Apte, S.S., 2009, A disintegrin-like and metalloprotease (reprolysin-type) with thrombospondin type 1 motif (ADAMTS) superfamily: functions and mechanisms. J Biol Chem 284, 31493-31497.

Arcaro, G., Cretti, A., Balzano, S., Lechi, A., Muggeo, M., Bonora, E., Bonadonna, R.C., 2002, insulin causes endothelial dysfunction in humans: sites and mechanisms. Circulation 105, 576-582.

Asplin, K.E., Sillence, M.N., Pollitt, C.C., McGowan, C.M., 2007, Induction of laminitis by prolonged hyperinsulinaemia in clinically normal ponies. Vet J 174, 530-535.

Bailey, S.R., Marr, C.M., Elliott, J., 2004, Current research and theories on the pathogenesis of acute laminitis in the horse. Vet J 167, 129-142.

Barker, J., Jones, M., Swenson, C., Sarma, V., Mitra, R., Ward, P., Johnson, K., Fantone, J., Dixit, V., Nickoloff, B., 1991, Monocyte chemotaxis and activating factor production by keratinocytes in response to IFN-gamma. J Immunol 146, 1192-1197.

Barrett, J.C., Kawasaki, E.S., 2003, Microarrays: the use of oligonucleotides and cDNA for the analysis of gene expression. Drug Discovery Today 8, 134-141.

Barrey, E., Mucher, E., Robert, C., Amiot, F., Gidrol, X., 2006, Gene expression profiling in blood cells of endurance horses completing competition or disqualified due to metabolic disorder. Equine Vet J Suppl, 43-49.

Barthel, A., Schmoll, D., 2003, Novel concepts in insulin regulation of hepatic gluconeogenesis. Am J Physiol Endocrinol Metab 285, E685-692.

Bateman, J.F., Boot-Handford, R.P., Lamande, S.R., 2009, Genetic diseases of connective tissues: cellular and extracellular effects of ECM mutations. Nat Rev Genet 10, 173-183.

Baxter, G.M., Morrison, S., 2008, Complications of unilateral weight bearing. Vet Clin North Am Equine Pract 24, 621-642.

Belknap, J.K., 2010, The pharmacologic basis for the treatment of developmental and acute laminitis. Vet Clin North Am Equine Pract 26, 115-124.

Belknap, J.K., Giguere, S., Pettigrew, A., Cochran, A.M., Van Eps, A.W., Pollitt, C.C., 2007, Lamellar pro-inflammatory cytokine expression patterns in laminitis at the

developmental stage and at the onset of lameness: innate vs. adaptive immune response. Equine Vet J 39, 42-47.

Benes, V., Muckenthaler, M., 2003, Standardization of protocols in cDNA microarray analysis. Trends Biochem Sci 28, 244-249.

Black, S.J., 2009, Extracellular matrix, leukocyte migration and laminitis. Vet Immunol Immunopathol 129, 161-163.

Black, S.J., Lunn, D.P., Yin, C., Hwang, M., Lenz, S.D., Belknap, J.K., 2006, Leukocyte emigration in the early stages of laminitis. Vet Immunol Immunopathol 109, 161-166.

Bogaert, L., Van Poucke, M., De Baere, C., Peelman, L., Gasthuys, F., Martens, A., 2006, Selection of a set of reliable reference genes for quantitative real-time PCR in normal equine skin and in equine sarcoids. BMC Biotechnology 6, 24.

Bolstad, B.M., Irizarry, R.A., Astrand, M., Speed, T.P., 2003, A comparison of normalization methods for high density oligonucleotide array data based on variance and bias. Bioinformatics 19, 185-193.

Borradori, L., Sonnenberg, A., 1999, Structure and function of hemidesmosomes: more than simple adhesion complexes. J Invest Dermatol 112, 411-418.

Branham, W., Melvin, C., Han, T., Desai, V., Moland, C., Scully, A., Fuscoe, J., 2007, Elimination of laboratory ozone leads to a dramatic improvement in the reproducibility of microarray gene expression measurements. BMC Biotechnology 7, 8.

Bright, L., Burgess, S., Chowdhary, B., Swiderski, C., McCarthy, F., 2009, Structural and functional-annotation of an equine whole genome oligoarray. BMC Bioinformatics 10, S8.

Brooks, S.A., Gabreski, N., Miller, D., Brisbin, A., Brown, H.E., Streeter, C., Mezey, J., Cook, D., Antczak, D.F., 2010, Whole-Genome SNP association in the horse:

identification of a deletion in myosin va responsible for lavender foal syndrome. PLoS Genet 6, e1000909.

Brown, K.A., Brain, S.D., Pearson, J.D., Edgeworth, J.D., Lewis, S.M., Treacher, D.F., 2006, Neutrophils in development of multiple organ failure in sepsis. The Lancet 368, 157-169.

Brown, P.O., Botstein, D., 1999, Exploring the new world of the genome with DNA microarrays. Nat Genet 21, 33-37.

Budak, M.T., Orsini, J.A., Pollitt, C.C., Rubinstein, N.A., 2009, Gene expression in the lamellar dermis-epidermis during the developmental phase of carbohydrate overload-induced laminitis in the horse. Vet Immunol Immunopathol 131, 86-96.

Caballero, A., 2004, Endothelial dysfunction, inflammation, and insulin resistance: A focus on subjects at risk for type 2 diabetes. Current Diabetes Reports 4, 237-246.

Cardoso, S., Correia, S., Santos, R.X., Carvalho, C., Santos, M.S., Oliveira, C.R., Perry, G., Smith, M.A., Zhu, X., Moreira, P.I., 2009, Insulin is a two-edged knife on the brain. J Alzheimers Dis 18, 483-507.

Carter, D.W., Ben Renfroe, J., 2009, A novel approach to the treatment and prevention of laminitis: botulinum toxin type A for the treatment of laminitis. Journal of Equine Veterinary Science 29, 595-600.

Carter, R.A., Treiber, K.H., Geor, R.J., Douglass, L., Harris, P.A., 2009, Prediction of incipient pasture-associated laminitis from hyperinsulinaemia, hyperleptinaemia and generalised and localised obesity in a cohort of ponies. Equine Vet J 41, 171-178.

Cawston, T.E., Wilson, A.J., 2006, Understanding the role of tissue degrading enzymes and their inhibitors in development and disease. Best Practice & Research Clinical Rheumatology 20, 983-1002.

Chen, J.J., Delongchamp, R.R., Tsai, C.A., Hsueh, H.M., Sistare, F., Thompson, K.L., Desai, V.G., Fuscoe, J.C., 2004, Analysis of variance components in gene expression data. Bioinformatics 20, 1436-1446.

Chiogna, M., Massa, M.S., Risso, D., Romualdi, C., 2009, A comparison on effects of normalisations in the detection of differentially expressed genes. BMC Bioinformatics 10, 61.

Chipman, H., Tibshirani, R., 2006, Hybrid hierarchical clustering with applications to microarray data. Biostatistics 7, 286-301.

Chomczynski, P., 1993, A reagent for the single-step simultaneous isolation of RNA, DNA and proteins from cell and tissue samples. Biotechniques 15, 532-534, 536-537.

Chopra, P., Kulkarni, O., Gupta, S., Bajpai, M., Kanoje, V., Banerjee, M., Bansal, V., Visaga, S., Chatterjee, M., Chaira, T., Shirumalla, R.K., Verma, A.K., Dastidar, S.G., Sharma, G., Ray, A., 2010, Pharmacological profile of AW-814141, a novel, potent, selective and orally active inhibitor of p38 MAP kinase. International Immunopharmacology 10, 467-473.

Chowdhary, B.P., Raudsepp, T., 2008, The horse genome derby: racing from map to whole genome sequence. Chromosome Res 16, 109-127.

Christenson, K., Bjorkman, L., Tangemo, C., Bylund, J., 2008, Serum amyloid A inhibits apoptosis of human neutrophils via a P2X7-sensitive pathway independent of formyl peptide receptor-like 1. J Leukoc Biol 83, 139-148.

Chu, V.T., Gottardo, R., Raftery, A.E., Bumgarner, R.E., Yeung, K.Y., 2008, MeV+R: using MeV as a graphical user interface for Bioconductor applications in microarray analysis. Genome Biol 9, R118.

Chuaqui, R.F., Bonner, R.F., Best, C.J., Gillespie, J.W., Flaig, M.J., Hewitt, S.M., Phillips, J.L., Krizman, D.B., Tangrea, M.A., Ahram, M., Linehan, W.M., Knezevic, V., Emmert-Buck, M.R., 2002, Post-analysis follow-up and validation of microarray experiments. Nat Genet 32 Suppl, 509-514.

Chui, R., Dorovini-Zis, K., 2010, Regulation of CCL2 and CCL3 expression in human brain endothelial cells by cytokines and lipopolysaccharide. Journal of Neuroinflammation 7, 1.

Churchill, G.A., 2002, Fundamentals of experimental design for cDNA microarrays. Nat Genet 32 Suppl, 490-495.

Cohen, N.D., Woods, A.M., 1999, Characteristics and risk factors for failure of horses with acute diarrhea to survive: 122 cases (1990-1996). J Am Vet Med Assoc 214, 382-390.

Colles, C.M., Jeffcott, L.B., 1977, Laminitis in the horse. Vet Rec 100, 262-264.

Cook, D., Gallagher, P., Bailey, E., 2009, Illumina equine SNP50 bead chip investigation of adolescent idiopathic lordosis among American Saddlebred horses. Journal of Equine Veterinary Science 29, 315-316.

Coppée, J.-Y., 2008, Do DNA microarrays have their future behind them? Microbes and Infection 10, 1067-1071.

Coyne, M.J., Cousin, H., Loftus, J.P., Johnson, P.J., Belknap, J.K., Gradil, C.M., Black, S.J., Alfandari, D., 2008, Cloning and expression of ADAM-related metalloproteases in equine laminitis. Vet Immunol Immunopathol 129, 231-241.

Crawford, C., Sepulveda, M.F., Elliott, J., Harris, P.A., Bailey, S.R., 2007, Dietary fructan carbohydrate increases amine production in the equine large intestine: implications for pasture-associated laminitis. J Anim Sci 85, 2949-2958.

Criswell, L.A., 2010, Gene discovery in rheumatoid arthritis highlights the CD40/NF-312B signaling pathway in disease pathogenesis. Immunological Reviews 233, 55-61.

Crocker, P.R., Paulson, J.C., Varki, A., 2007, Siglecs and their roles in the immune system. Nat Rev Immunol 7, 255-266.

Cui, X., Churchill, G., 2003, Statistical tests for differential expression in cDNA microarray experiments. Genome Biology 4, 210.

D'Haeseleer, P., 2005, How does gene expression clustering work? Nat Biotech 23, 1499-1501.

Dabney, A.R., Storey, J.D., 2007, A new approach to intensity-dependent normalization of two-channel microarrays. Biostatistics 8, 128-139.

Dallas, P.B., Gottardo, N.G., Firth, M.J., Beesley, A.H., Hoffmann, K., Terry, P.A., Freitas, J.R., Boag, J.M., Cummings, A.J., Kees, U.R., 2005, Gene expression levels assessed by oligonucleotide microarray analysis and quantitative real-time RT-PCR -- how well do they correlate? BMC Genomics 6, 59.

de la Rebiere, G., Franck, T., Deby-Dupont, G., Salciccia, A., Grulke, S., Peters, F., Serteyn, D., 2008, Effects of unfractionated and fractionated heparins on myeloperoxidase activity and interactions with endothelial cells: possible effects on the pathophysiology of equine laminitis. Vet J 178, 62-69.

de Laat, M.A., McGowan, C.M., Sillence, M.N., Pollitt, C.C., 2010, Equine laminitis: induced by 48 h hyperinsulinaemia in Standardbred horses. Equine Vet J 42, 129-135.

de Luca, C., Olefsky, J.M., 2008, Inflammation and insulin resistance. FEBS Lett 582, 97-105.

De Plaen, I.G., Han, X.B., Liu, X., Hsueh, W., Ghosh, S., May, M.J., 2006, Lipopolysaccharide induces CXCL2/macrophage inflammatory protein-2 gene expression in enterocytes via NF-κB activation: independence from endogenous TNF-α and platelet-activating factor. Immunology 118, 153-163.

DeFronzo, R.A., Tobin, J.D., Andres, R., 1979, Glucose clamp technique: a method for quantifying insulin secretion and resistance. Am J Physiol 237, E214-223.

Denhardt, D.T., Feng, B., Edwards, D.R., Cocuzzi, E.T., Malyankar, U.M., 1993, Tissue inhibitor of metalloproteinases (TIMP, aka EPA): structure, control of expression and biological functions. Pharmacol Ther 59, 329-341.

Dennis, G., Jr., Sherman, B.T., Hosack, D.A., Yang, J., Gao, W., Lane, H.C., Lempicki, R.A., 2003, DAVID: Database for Annotation, Visualization, and Integrated Discovery. Genome Biol 4, P3.

Diarra, D., Stolina, M., Polzer, K., Zwerina, J., Ominsky, M.S., Dwyer, D., Korb, A., Smolen, J., Hoffmann, M., Scheinecker, C., van der Heide, D., Landewe, R., Lacey, D., Richards, W.G., Schett, G., 2007, Dickkopf-1 is a master regulator of joint remodeling. Nat Med 13, 156-163.

Dinarello, C.A., 2010, Anti-inflammatory agents: present and future. Cell 140, 935-950.

Divers, T.J., 2003, Prevention and treatment of thrombosis, phlebitis, and laminitis in horses with gastrointestinal diseases. Vet Clin North Am Equine Pract 19, 779-790.

Do, J.H., Choi, D.K., 2006, Normalization of microarray data: single-labeled and dual-labeled arrays. Mol Cells 22, 254-261.

Dobbin, K., Simon, R., 2002, Comparison of microarray designs for class comparison and class discovery. Bioinformatics 18, 1438-1445.

Dobbin, K.K., Kawasaki, E.S., Petersen, D.W., Simon, R.M., 2005, Characterizing dye bias in microarray experiments. Bioinformatics 21, 2430-2437.

Donaldson, M.T., Jorgensen, A.J., Beech, J., 2004, Evaluation of suspected pituitary pars intermedia dysfunction in horses with laminitis. J Am Vet Med Assoc 224, 1123-1127.

Dourmishev, L.A., Draganov, P.V., 2009, Paraneoplastic dermatological manifestation of gastrointestinal malignancies. World J Gastroenterol 15, 4372-4379.

Eades, S.C., 2010, Overview of current laminitis research. Vet Clin North Am Equine Pract 26, 51-63.

Eades, S.C., M.S., H., Moore, R.M., 2002, A review of the pathophysiology and treatment of acute laminitis: pathophysiologic and therapeutic implications of endothelin-1. AAEP Proceedings 48, 353-361.

Eades, S.C., Stokes, A.M., Johnson, P.J., LeBlanc, C.J., Ganjam, V.K., Buff, P.R., Moore, R.M., 2007, Serial alterations in digital hemodynamics and endothelin-1 immunoreactivity, platelet-neutrophil aggregation, and concentrations of nitric oxide, insulin, and glucose in blood obtained from horses following carbohydrate overload. Am J Vet Res 68, 87-94.

Eades, S.C., Stokes, A.M., Moore, R.M., 2006, Effects of an endothelin receptor antagonist and nitroglycerin on digital vascular function in horses during the prodromal stages of carbohydrate overload-induced laminitis. Am J Vet Res 67, 1204-1211.

Eaton, S.A., Allen, D., Eades, S.C., Schneider, D.A., 1995, Digital starling forces and hemodynamics during early laminitis induced by an aqueous extract of black walnut (Juglans nigra) in horses. Am J Vet Res 56, 1338-1344.

Eckert, R.E., Sharief, Y., Jones, S.L., 2008, p38 mitogen-activated kinase (MAPK) is essential for equine neutrophil migration. Vet Immunol Immunopathol 129, 181-191.

Eisen, M.B., Spellman, P.T., Brown, P.O., Botstein, D., 1998, Cluster analysis and display of genome-wide expression patterns. Proc Natl Acad Sci U S A 95, 14863-14868.

El Mezayen, R., El Gazzar, M., Seeds, M.C., McCall, C.E., Dreskin, S.C., Nicolls, M.R., 2007, Endogenous signals released from necrotic cells augment inflammatory responses to bacterial endotoxin. Immunology Letters 111, 36-44.

Elliott, J., Bailey, S.R., 2006, Gastrointestinal derived factors are potential triggers for the development of acute equine laminitis. J. Nutr. 136, 2103S-2107.

Engiles, J.B., 2010, Pathology of the distal phalanx in equine laminitis: more than just skin deep. Vet Clin North Am Equine Pract 26, 155-165.

Erkert, R.S., Macallister, C.G., 2002, Isoxsuprine hydrochloride in the horse: a review. J Vet Pharmacol Ther 25, 81-87.

Fadok, V.A., Bratton, D.L., Konowal, A., Freed, P.W., Westcott, J.Y., Henson, P.M., 1998, Macrophages that have ingested apoptotic cells in vitro inhibit proinflammatory cytokine production through autocrine/paracrine mechanisms involving TGF-beta, PGE2, and PAF. The Journal of Clinical Investigation 101, 890-898.

Fagliari, J.J., McClenahan, D., Evanson, O.A., Weiss, D.J., 1998, Changes in plasma protein concentrations in ponies with experimentally induced alimentary laminitis. Am J Vet Res 59, 1234-1237.

Faleiros, R.R., Nuovo, G.J., Belknap, J.K., 2009, Calprotectin in myeloid and epithelial cells of laminae from horses with black walnut extract-induced laminitis. J Vet Intern Med 23, 174-181.

Faleiros, R.R., Stokes, A.M., Eades, S.C., Kim, D.Y., Paulsen, D.B., Moore, R.M., 2004, Assessment of apoptosis in epidermal lamellar cells in clinically normal horses and those with laminitis. Am J Vet Res 65, 578-585.

Fare, T., Coffey, E., Dai, H., He, Y., Kessler, D., Kilian, K., Koch, J., LeProust, E., Marton, M., Meyer, M., Stoughton, R., Tokiwa, G., Wang, Y., 2003, Effects of atmospheric ozone on microarray data quality. Anal Chem 75, 4672 - 4675.

Fingleton, B., 2008, MMPs as therapeutic targets--still a viable option? Semin Cell Dev Biol 19, 61-68.

Flynn, D.C., 2001, Adaptor proteins. Oncogene 20, 6270-6272.

Foell, D., Wittkowski, H., Roth, J., 2007a, Mechanisms of disease: a 'DAMP' view of inflammatory arthritis. Nat Clin Pract Rheumatol 3, 382-390.

Foell, D., Wittkowski, H., Roth, J., 2009, Monitoring disease activity by stool analyses: from occult blood to molecular markers of intestinal inflammation and damage. Gut 58, 859-868.

Foell, D., Wittkowski, H., Vogl, T., Roth, J., 2007b, S100 proteins expressed in phagocytes: a novel group of damage-associated molecular pattern molecules. J Leukoc Biol 81, 28-37.

Fontaine, G.L., Belknap, J.K., Allen, D., Moore, J.N., Kroll, D.L., 2001, Expression of interleukin-1beta in the digital laminae of horses in the prodromal stage of experimentally induced laminitis. Am J Vet Res 62, 714-720.

Foster, W.R., Huber, R.M., 2002, Current themes in microarray experimental design and analysis. Drug Discov Today 7, 290-292.

Fox, S., Leitch, A.E., Duffin, R., Haslett, C., Rossi, A.G., 2010, Neutrophil apoptosis: relevance to the innate immune response and inflammatory disease. Journal of Innate Immunity 2, 216-227.

Franchi, L., McDonald, C., Kanneganti, T.-D., Amer, A., Nunez, G., 2006, Nucleotide-binding oligomerization domain-like receptors: intracellular pattern recognition molecules for pathogen detection and host defense. J Immunol 177, 3507-3513.

Frank, N., 2009, Equine metabolic syndrome. Journal of Equine Veterinary Science 29, 259-267.

Frank, N., Elliott, S.B., Brandt, L.E., Keisler, D.H., 2006, Physical characteristics, blood hormone concentrations, and plasma lipid concentrations in obese horses with insulin resistance. Journal of the American Veterinary Medical Association 228, 1383-1390.

French, K.R., Pollitt, C.C., 2004a, Equine laminitis: glucose deprivation and MMP activation induce dermo-epidermal separation in vitro. Equine Vet J 36, 261-266.

French, K.R., Pollitt, C.C., 2004b, Equine laminitis: loss of hemidesmosomes in hoof secondary epidermal lamellae correlates to dose in an oligofructose induction model: an ultrastructural study. Equine Vet J 36, 230-235.

Friedl, P., Brocker, E.B., 2000, The biology of cell locomotion within three-dimensional extracellular matrix. Cell Mol Life Sci 57, 41-64.

Gadgil, M., Lian, W., Gadgil, C., Kapur, V., Hu, W.S., 2005, An analysis of the use of genomic DNA as a universal reference in two channel DNA microarrays. BMC Genomics 6, 66.

Galantino-Homer, H., Megee, S., Senoo, M., 2010, Isolation of equine hoof epidermal cells for in vitro studies. Journal of Equine Veterinary Science 30, 107-107.

Galey, F.D., Whiteley, H.E., Goetz, T.E., Kuenstler, A.R., Davis, C.A., Beasley, V.R., 1991, Black walnut (Juglans nigra) toxicosis: a model for equine laminitis. J Comp Pathol 104, 313-326.

Ganz, T., 2003, Defensins: antimicrobial peptides of innate immunity. Nat Rev Immunol 3, 710-720.

Garner, H.E., Coffman, J.R., Hahn, A.W., Hutcheson, D.P., Tumbleson, M.E., 1975, Equine laminitis of alimentary origin: an experimental model. Am J Vet Res 36, 441-444.

Gentleman, R.C., Carey, V.J., Bates, D.M., Bolstad, B., Dettling, M., Dudoit, S., Ellis, B., Gautier, L., Ge, Y., Gentry, J., Hornik, K., Hothorn, T., Huber, W., Iacus, S., Irizarry, R., Leisch, F., Li, C., Maechler, M., Rossini, A.J., Sawitzki, G., Smith, C., Smyth, G., Tierney, L., Yang, J.Y., Zhang, J., 2004, Bioconductor: open software development for computational biology and bioinformatics. Genome Biol 5, R80.

Geor, R., Frank, N., 2008, Metabolic syndrome-From human organ disease to laminar failure in equids. Vet Immunol Immunopathol 129, 151-154.

Geor, R.J., 2008, Metabolic predispositions to laminitis in horses and ponies: obesity, insulin resistance and metabolic syndromes. Journal of Equine Veterinary Science 28, 753-759.

Geor, R.J., 2009, Pasture-associated laminitis. Vet Clin North Am Equine Pract 25, 39-50.

Geor, R.J., Harris, P., 2009, Dietary management of obesity and insulin resistance: countering risk for laminitis. Vet Clin North Am Equine Pract 25, 51-65.

Gilhooly, M.H., Eades, S.C., Stokes, A.M., Moore, R.M., 2005, Effects of topical nitroglycerine patches and ointment on digital venous plasma nitric oxide concentrations and digital blood flow in healthy conscious horses. Vet Surg 34, 604-609.

Glaser, K.E., Sun, Q., Wells, M.T., Nixon, A.J., 2009, Development of a novel equine whole transcript oligonucleotide GeneChip microarray and its use in gene expression profiling of normal articular-epiphyseal cartilage. Equine Vet J 41, 663-670.

Green, D.R., Chipuk, J.E., 2008, Apoptosis: stabbed in the BAX. Nature 455, 1047-1049.

Grosenbaugh, D.A., Hood, D.M., 1992, Keratin and associated proteins of the equine hoof wall. Am J Vet Res 53, 1859-1863.

Gu, W., Bertone, A.L., 2004, Generation and performance of an equine-specific large-scale gene expression microarray. Am J Vet Res 65, 1664-1673.

Hardiman, G., 2004, Microarray platforms--comparisons and contrasts. Pharmacogenomics 5, 487-502.

Harkema, J.R., Robinson, N.E., Scott, J.B., 1978, Cardiovascular, acid-base, electrolyte, and plasma volume changes in ponies developing alimentary laminitis. Am J Vet Res 39, 741-744.

Harman, J., Ward, M., 2001, The role of nutritional therapy in the treatment of equine Cushing's syndrome and laminitis. Altern Med Rev 6 Suppl, S4-S16.

Harris, P., Bailey, S.R., Elliott, J., Longland, A., 2006, Countermeasures for pasture-associated laminitis in ponies and horses. J Nutr 136, 2114S-2121S.

Hashimoto, K., 2000, Regulation of keratinocyte function by growth factors. Journal of Dermatological Science 24, S46-S50.

Haslett, C., 1999, Granulocyte apoptosis and its role in the resolution and control of lung inflammation. American Journal of Respiratory and Critical Care Medicine 160, S5-S11.

Heidari, M., Huebner, M., Kireev, D., Silva, R.F., 2008, Transcriptional profiling of Marek's disease virus genes during cytolytic and latent infection. Virus Genes 36, 383-392.

Heizmann, C.W., Fritz, G., Schafer, B.W., 2002, S100 proteins: structure, functions and pathology. Front Biosci 7, d1356-d1368.

Hellemans, J., Mortier, G., De Paepe, A., Speleman, F., Vandesompele, J., 2007, qBase relative quantification framework and software for management and automated analysis of real-time quantitative PCR data. Genome Biol 8, R19.

Henness, S., van Thoor, E., Ge, Q., Armour, C.L., Hughes, J.M., Ammit, A.J., 2006, IL-17A acts via p38 MAPK to increase stability of TNF-{alpha}-induced IL-8 mRNA in human ASM. Am J Physiol Lung Cell Mol Physiol 290, L1283-L1290.

Higgins, M.A., Berridge, B.R., Mills, B.J., Schultze, A.E., Gao, H., Searfoss, G.H., Baker, T.K., Ryan, T.P., 2003, Gene expression analysis of the acute phase response using a canine microarray. Toxicol Sci 74, 470-484.

Hood, D.M., 1999a, Laminitis as a systemic disease. Vet Clin North Am Equine Pract 15, 481-494.

Hood, D.M., 1999b, The pathophysiology of developmental and acute laminitis. Vet Clin North Am Equine Pract 15, 321-343.

Hood, D.M., Grosenbaugh, D.A., Mostafa, M.B., Morgan, S.J., Thomas, B.C., 1993, The role of vascular mechanisms in the development of acute equine laminitis. J Vet Intern Med 7, 228-234.

Horwitz, J., Bova, M.P., Ding, L.L., Haley, D.A., Stewart, P.L., 1999, Lens alpha-crystallin: function and structure. Eye (Lond) 13 (Pt 3b), 403-408.

Hosack, D., Dennis, G., Sherman, B., Lane, H., Lempicki, R., 2003, Identifying biological themes within lists of genes with EASE. Genome Biology 4, P4.

Hu, Y., Lu, X., Luo, G., 2010, Effect of Recql5 deficiency on the intestinal tumor susceptibility of Apc(min) mice. World J Gastroenterol 16, 1482-1486.

Huang, D.W., Sherman, B.T., Lempicki, R.A., 2009, Systematic and integrative analysis of large gene lists using DAVID bioinformatics resources. Nat Protoc 4, 44-57.

Hughes, T.R., Mao, M., Jones, A.R., Burchard, J., Marton, M.J., Shannon, K.W., Lefkowitz, S.M., Ziman, M., Schelter, J.M., Meyer, M.R., Kobayashi, S., Davis, C., Dai, H., He, Y.D., Stephaniants, S.B., Cavet, G., Walker, W.L., West, A., Coffey, E., Shoemaker, D.D., Stoughton, R., Blanchard, A.P., Friend, S.H., Linsley, P.S., 2001, Expression profiling using microarrays fabricated by an ink-jet oligonucleotide synthesizer. Nat Biotech 19, 342-347.

Iglarz, M., Clozel, M., 2007, Mechanisms of ET-1-induced endothelial dysfunction. J Cardiovasc Pharmacol 50, 621-628.

Ihaka, R., Gentleman, R., 1996, R: A Language for data analysis and graphics. Journal of Computational and Graphical Statistics 5, 299-314.

Ing, N.H., Laughlin, A.M., Varner, D.D., Welsh, T.H., Jr., Forrest, D.W., Blanchard, T.L., Johnson, L., 2004, Gene expression in the spermatogenically inactive "dark" and maturing "light" testicular tissues of the prepubertal colt. J Androl 25, 535-544.

Ingle-Fehr, J.E., Baxter, G.M., 1999, The effect of oral isoxsuprine and pentoxifylline on digital and laminar blood flow in healthy horses. Vet Surg 28, 154-160.

Ivan Stamenkovic, 2003, Extracellular matrix remodelling: the role of matrix metalloproteinases. The Journal of Pathology 200, 448-464.

Johnson, P.J., 2002, The equine metabolic syndrome peripheral Cushing's syndrome. Vet Clin North Am Equine Pract 18, 271-293.

Johnson, P.J., Kreeger, J.M., Keeler, M., Ganjam, V.K., Messer, N.T., 2000, Serum markers of lamellar basement membrane degradation and lamellar histopathological changes in horses affected with laminitis. Equine Vet J 32, 462-468.

Johnson, P.J., Messer, N.T., Ganjam, V.K., 2004a, Cushing's syndromes, insulin resistance and endocrinopathic laminitis. Equine Vet J 36, 194-198.

Johnson, P.J., Messer, N.T., Slight, S.H., Wiedmeyer, C., Buff, P., Ganjam, V.K., 2004b, Endocrinopathic laminitis in the horse. Clinical Techniques in Equine Practice 3, 45-56.

Johnson, P.J., Tyagi, S.C., Katwa, L.C., Ganjam, V.K., Moore, L.A., Kreeger, J.M., Messer, N.T., 1998, Activation of extracellular matrix metalloproteinases in equine laminitis. Vet Rec 142, 392-396.

Johnson, P.J., Wiedmeyer, C.E., Messer, N.T., Ganjam, V.K., 2009, Medical implications of obesity in horses-lessons for human obesity. J Diabetes Sci Technol 3, 163-174.

Jones, G.C., Riley, G.P., 2005, ADAMTS proteinases: a multi-domain, multi-functional family with roles in extracellular matrix turnover and arthritis. Arthritis Res Ther 7, 160-169.

Kalck, K.A., Frank, N., Elliott, S.B., Boston, R.C., 2009, Effects of low-dose oligofructose treatment administered via nasogastric intubation on induction of laminitis and associated alterations in glucose and insulin dynamics in horses. Am J Vet Res 70, 624-632.

Kanehisa, M., Araki, M., Goto, S., Hattori, M., Hirakawa, M., Itoh, M., Katayama, T., Kawashima, S., Okuda, S., Tokimatsu, T., Yamanishi, Y., 2008, KEGG for linking genomes to life and the environment. Nucleic Acids Res 36, D480-484.

Kanneganti, T.-D., Lamkanfi, M., Núñez, G., 2007, Intracellular NOD-like receptors in host defense and disease. Immunity 27, 549-559.

Kashiwagi, M., Enghild, J.J., Gendron, C., Hughes, C., Caterson, B., Itoh, Y., Nagase, H., 2004, Altered proteolytic activities of ADAMTS-4 expressed by C-terminal processing. Journal of Biological Chemistry 279, 10109-10119.

Katwa, L.C., Johnson, P.J., Ganjam, V.K., Kreeger, J.M., Messer, N.T., 1999, Expression of endothelin in equine laminitis. Equine Vet J 31, 243-247.

Kaupp, U.B., 2010, Olfactory signalling in vertebrates and insects: differences and commonalities. Nat Rev Neurosci 11, 188-200.

Keen, J.A., McLaren, M., Chandler, K.J., McGorum, B.C., 2004, Biochemical indices of vascular function, glucose metabolism and oxidative stress in horses with equine Cushing's disease. Equine Vet J 36, 226-229.

Kendziorski, C., Irizarry, R.A., Chen, K.S., Haag, J.D., Gould, M.N., 2005, On the utility of pooling biological samples in microarray experiments. Proc Natl Acad Sci U S A 102, 4252-4257.

Kerr, M.K., 2003, Design considerations for efficient and effective microarray studies. Biometrics 59, 822-828.

Kerr, M.K., Churchill, G.A., 2001a, Experimental design for gene expression microarrays. Biostatistics 2, 183-201.

Kerr, M.K., Churchill, G.A., 2001b, Statistical design and the analysis of gene expression microarray data. Genet Res 77, 123-128.

Kerr, M.K., Martin, M., Churchill, G.A., 2000, Analysis of variance for gene expression microarray data. J Comput Biol 7, 819-837.

Kim, H., Zhao, B., Snesrud, E.C., Haas, B.J., Town, C.D., Quackenbush, J., 2002, Use of RNA and genomic DNA references for inferred comparisons in DNA microarray analyses. Biotechniques 33, 924-930.

Kivi, E., Elima, K., Aalto, K., Nymalm, Y., Auvinen, K., Koivunen, E., Otto, D.M., Crocker, P.R., Salminen, T.A., Salmi, M., Jalkanen, S., 2009, Human siglec-10 can bind to vascular adhesion protein-1 and serves as its substrate. Blood 114, 5385-5392.

Ko, K., Arora, P., Bhide, V., Chen, A., McCulloch, C., 2001, Cell-cell adhesion in human fibroblasts requires calcium signaling. J Cell Sci 114, 1155-1167.

Kobayashi, S.D., Voyich, J.M., DeLeo, F.R., 2003, Regulation of the neutrophil-mediated inflammatory response to infection. Microbes and Infection 5, 1337-1344.

Kronfeld, D.S., 2005, Insulin signaling, laminitis, and exercise. Journal of Equine Veterinary Science 25, 404-407.

Kronfeld, D.S., Treiber, K.H., Byrd, B.M., Staniar, W.B., Splan, R.K., 2005, Laminitic metabolic profile in genetically predisposed ponies involves exaggerated compensated insulin resistance. Journal of Animal Physiology and Animal Nutrition 89, 431-431.

Kronfeld, D.S., Treiber, K.H., Hess, T.M., Splan, R.K., Byrd, B.M., Staniar, W.B., White, N.W., 2006, Metabolic syndrome in healthy ponies facilitates nutritional countermeasures against pasture laminitis. J Nutr 136, 2090S-2093S.

Kumar, M., Makonchuk, D.Y., Li, H., Mittal, A., Kumar, A., 2009, TNF-like weak inducer of apoptosis (TWEAK) activates proinflammatory signaling pathways and gene expression through the activation of TGF-{beta}-activated kinase 1. J Immunol 182, 2439-2448.

Kyaw-Tanner, M., Pollitt, C.C., 2004, Equine laminitis: increased transcription of matrix metalloproteinase-2 (MMP-2) occurs during the developmental phase. Equine Vet J 36, 221-225.

Kyaw-Tanner, M.T., Wattle, O., van Eps, A.W., Pollitt, C.C., 2008, Equine laminitis: membrane type matrix metalloproteinase-1 (MMP-14) is involved in acute phase onset. Equine Vet J 40, 482-487.

La Fontaine, J., Harkless, L.B., Davis, C.E., Allen, M.A., Shireman, P.K., 2006, Current concepts in diabetic microvascular dysfunction. J Am Podiatr Med Assoc 96, 245-252.

Le Goff, C., Morice-Picard, F., Dagoneau, N., Wang, L.W., Perrot, C., Crow, Y.J., Bauer, F., Flori, E., Prost-Squarcioni, C., Krakow, D., Ge, G., Greenspan, D.S., Bonnet, D., Le Merrer, M., Munnich, A., Apte, S.S., Cormier-Daire, V., 2008, ADAMTSL2 mutations in geleophysic dysplasia demonstrate a role for ADAMTS-like proteins in TGF-[beta] bioavailability regulation. Nat Genet 40, 1119-1123.

Lee, M.L., Kuo, F.C., Whitmore, G.A., Sklar, J., 2000, Importance of replication in microarray gene expression studies: statistical methods and evidence from repetitive cDNA hybridizations. Proc Natl Acad Sci U S A 97, 9834-9839.

Lee, S., Desai, K.K., Iczkowski, K.A., Newcomer, R.G., Wu, K.J., Zhao, Y.-G., Tan, W.W., Roycik, M.D., Sang, Q.-X.A., 2006, Coordinated peak expression of MMP-26 and TIMP-4 in preinvasive human prostate tumor. Cell Res 16, 750-758.

Leise, B.S., Fugler, L.A., Stokes, A.M., Eades, S.C., Moore, R.M., 2007, Effects of intramuscular administration of acepromazine on palmar digital blood flow, palmar digital arterial pressure, transverse facial arterial pressure, and packed cell volume in clinically healthy, conscious horses. Vet Surg 36, 717-723.

Leung, Y.F., Cavalieri, D., 2003, Fundamentals of cDNA microarray data analysis. Trends in Genetics 19, 649-659.

Li, J., Pankratz, M., Johnson, J.A., 2002, Differential gene expression patterns revealed by oligonucleotide versus long cDNA arrays. Toxicol Sci 69, 383-390.

Li, S., Nikulina, K., DeVoss, J., Wu, A.J., Strauss, E.C., Anderson, M.S., McNamara, N.A., 2008, Small proline-rich protein 1B (SPRR1B) is a biomarker for squamous metaplasia in dry eye disease. Invest. Ophthalmol. Vis. Sci. 49, 34-41.

Lim, S.Y., Raftery, M.J., Goyette, J., Hsu, K., Geczy, C.L., 2009, Oxidative modifications of S100 proteins: functional regulation by redox. J Leukoc Biol 86, 577-587.

Livak, K.J., Schmittgen, T.D., 2001, Analysis of relative gene expression data using real-time quantitative PCR and the 2(-Delta Delta C(T)) Method. Methods 25, 402-408.

Lizarraga, I., Castillo, F., Valderrama, M.E., 2004, An analgesic evaluation of isoxsuprine in horses. J Vet Med A Physiol Pathol Clin Med 51, 370-374.

Loftus, J.P., Belknap, J.K., Black, S.J., 2006, Matrix metalloproteinase-9 in laminae of black walnut extract treated horses correlates with neutrophil abundance. Vet Immunol Immunopathol 113, 267-276.

Loftus, J.P., Black, S.J., Pettigrew, A., Abrahamsen, E.J., Belknap, J.K., 2007, Early laminar events involving endothelial activation in horses with black walnut-induced laminitis. Am J Vet Res 68, 1205-1211.

Loftus, J.P., Johnson, P.J., Belknap, J.K., Pettigrew, A., Black, S.J., 2009, Leukocyte-derived and endogenous matrix metalloproteinases in the lamellae of horses with naturally acquired and experimentally induced laminitis. Vet Immunol Immunopathol 129, 221-230.

Lombard, M.A., Wallace, T.L., Kubicek, M.F., Petzold, G.L., Mitchell, M.A., Hendges, S.K., Wilks, J.W., 1998, Synthetic matrix metalloproteinase inhibitors and tissue inhibitor of metalloproteinase (TIMP)-2, but not TIMP-1, inhibit shedding of tumor necrosis factor-alpha receptors in a human colon adenocarcinoma (Colo 205) cell line. Cancer Res 58, 4001-4007.

Lovegrove, C., 2005, Early hyperinsulinemia predicts gestational diabetes mellitus in high-risk patients. Nat Clin Pract End Met 1, 69-69.

Lucero, H., Kagan, H., 2006, Lysyl oxidase: an oxidative enzyme and effector of cell function. Cellular and Molecular Life Sciences 63, 2304-2316.

Maerki, C., Meuter, S., Liebi, M., Muhlemann, K., Frederick, M.J., Yawalkar, N., Moser, B., Wolf, M., 2009, Potent and broad-spectrum antimicrobial activity of CXCL14 suggests an immediate role in skin infections. J Immunol 182, 507-514.

Mandinova, A., Atar, D., Schafer, B., Spiess, M., Aebi, U., Heizmann, C., 1998, Distinct subcellular localization of calcium binding S100 proteins in human smooth muscle cells and their relocation in response to rises in intracellular calcium. J Cell Sci 111, 2043-2054.

Mankowski, J.L., Graham, D.R., 2008, Potential proteomic-based strategies for understanding Laminitis: predictions and pathogenesis. Journal of Equine Veterinary Science 28, 484-487.

Marambaud, P., Dreses-Werringloer, U., Vingtdeux, V., 2009, Calcium signaling in neurodegeneration. Molecular Neurodegeneration 4, 20.

Margadant, C., Sonnenberg, A., 2010, Integrin-TGF-[beta] crosstalk in fibrosis, cancer and wound healing. EMBO Rep 11, 97-105.

Martin-Magniette, M.L., Aubert, J., Cabannes, E., Daudin, J.J., 2005, Evaluation of the gene-specific dye bias in cDNA microarray experiments. Bioinformatics 21, 1995-2000.

Maser, C., Toset, A., Roman, S., 2006, Gastrointestinal manifestations of endocrine disease. World J Gastroenterol 12, 3174-3179.

Matsumori, A., Nunokawa, Y., Yamaki, A., Yamamoto, K., Hwang, M.-W., Miyamoto, T., Hara, M., Nishio, R., Kitaura-Inenaga, K., Ono, K., 2004, Suppression of cytokines and nitric oxide production, and protection against lethal endotoxemia and viral myocarditis by a new NF-κB inhibitor. European Journal of Heart Failure 6, 137-144.

McFarlane, D., 2007, Advantages and limitations of the equine disease, pituitary pars intermedia dysfunction as a model of spontaneous dopaminergic neurodegenerative disease. Ageing Research Reviews 6, 54-63.

McGowan, C., 2008, The Role of insulin in endocrinopathic laminitis. Journal of Equine Veterinary Science 28, 603-607.

McGowan, C.M., 2010, Endocrinopathic laminitis. Vet Clin North Am Equine Pract 26, 233-237.

Medzhitov, R., Horng, T., 2009, Transcriptional control of the inflammatory response. Nat Rev Immunol 9, 692-703.

Merico, D., Gfeller, D., Bader, G.D., 2009, How to visually interpret biological data using networks. Nat Biotech 27, 921-924.

Mienaltowski, M., Huang, L., Frisbie, D., McIlwraith, C.W., Stromberg, A., Bathke, A., MacLeod, J., 2009, Transcriptional profiling differences for articular cartilage and repair tissue in equine joint surface lesions. BMC Medical Genomics 2, 60.

Mienaltowski, M., Huang, L., Stromberg, A., MacLeod, J., 2008, Differential gene expression associated with postnatal equine articular cartilage maturation. BMC Musculoskeletal Disorders 9, 149.

Milinovich, G.J., Burrell, P.C., Pollitt, C.C., Bouvet, A., Trott, D.J., 2008a, Streptococcus henryi sp. nov. and Streptococcus caballi sp. nov., isolated from the hindgut of horses with oligofructose-induced laminitis. Int J Syst Evol Microbiol 58, 262-266.

Milinovich, G.J., Burrell, P.C., Pollitt, C.C., Klieve, A.V., Blackall, L.L., Ouwerkerk, D., Woodland, E., Trott, D.J., 2008b, Microbial ecology of the equine hindgut during oligofructose-induced laminitis. ISME J 2, 1089-1100.

Milinovich, G.J., Klieve, A.V., Pollitt, C.C., Trott, D.J., 2010, Microbial events in the hindgut during carbohydrate-induced equine laminitis. Vet Clin North Am Equine Pract 26, 79-94.

Milinovich, G.J., Trott, D.J., Burrell, P.C., Eps, A.W.v., Thoefner, M.B., Blackall, L.L., Jassim, R.A.M.A., Morton, J.M., Pollitt, C.C., 2006, Changes in equine hindgut bacterial populations during oligofructose-induced laminitis. Environmental Microbiology 8, 885-898.

Minnick, P.D., Brown, C.M., Braselton, W.E., Meerdink, G.L., Slanker, M.R., 1987, The induction of equine laminitis with an aqueous extract of the heartwood of black walnut (Juglans nigra). Vet Hum Toxicol 29, 230-233.

Miranda, P.J., DeFronzo, R.A., Califf, R.M., Guyton, J.R., 2005, Metabolic syndrome: definition, pathophysiology, and mechanisms. Am Heart J 149, 33-45.

Mobasheri, A., Critchlow, K., Clegg, P.D., Carter, S.D., Canessa, C.M., 2004, Chronic equine laminitis is characterised by loss of GLUT1, GLUT4 and ENaC positive laminar keratinocytes. Equine Vet J 36, 248-254.

Molkentin, J.D., 2004, Calcineurin–NFAT signaling regulates the cardiac hypertrophic response in coordination with the MAPKs. Cardiovascular Research 63, 467-475.

Moody, D.B., Ulrichs, T., Muhlecker, W., Young, D.C., Gurcha, S.S., Grant, E., Rosat, J.-P., Brenner, M.B., Costello, C.E., Besra, G.S., Porcelli, S.A., 2000, CD1c-mediated T-cell recognition of isoprenoid glycolipids in *Mycobacterium tuberculosis* infection. Nature 404, 884-888.

Moore, J.N., Garner, H.E., Coffman, J.R., 1981, Haematological changes during development of acute laminitis hypertension. Equine Vet J 13, 240-242.

Moore, R.M., 2008, Evidence-based treatment for laminitis--what works? Journal of Equine Veterinary Science 28, 176-179.

Moore, R.M., 2010, Vision 20/20 - conquer laminitis by 2020. Journal of Equine Veterinary Science 30, 74-76.

Moore, R.M., Eades, S.C., Stokes, A.M., 2004, Evidence for vascular and enzymatic events in the pathophysiology of acute laminitis: which pathway is responsible for initiation of this process in horses? Equine Vet J 36, 204-209.

Morgan, S.J., Hood, D.M., Wagner, I.P., Postl, S.P., 2003, Submural histopathologic changes attributable to peracute laminitis in horses. Am J Vet Res 64, 829-834.

Moroo, I., Yamada, T., Makino, H., Tooyama, I., McGeer, P., McGeer, E., Hirayama, K., 1994, Loss of insulin receptor immunoreactivity from the substantia nigra pars compacta neurons in Parkinson's disease. Acta Neuropathologica 87, 343-348.

Motulsky, H., 2010, Intuitive biostatistics: a nonmathematical guide to statistical thinking. Oxford University Press, New York.

Mucher, E., Jayr, L., Rossignol, F., Amiot, F., Gidrol, X., Barrey, E., 2006, Gene expression profiling in equine muscle tissues using mouse cDNA microarrays. Equine Vet J Suppl, 359-364.

Mungall, B.A., Pollitt, C.C., 1999, Zymographic analysis of equine laminitis. Histochem Cell Biol 112, 467-472.

Muniyappa, R., Montagnani, M., Koh, K.K., Quon, M.J., 2007, Cardiovascular actions of insulin. Endocr Rev 28, 463-491.

Murphy, G., Nagase, H., 2008, Reappraising metalloproteinases in rheumatoid arthritis and osteoarthritis: destruction or repair? Nat Clin Pract Rheumatol 4, 128-135.

Nara, N., Nakayama, Y., Okamoto, S., Tamura, H., Kiyono, M., Muraoka, M., Tanaka, K., Taya, C., Shitara, H., Ishii, R., Yonekawa, H., Minokoshi, Y., Hara, T., 2007, Disruption of CXC motif chemokine ligand-14 in mice ameliorates obesity-induced insulin resistance. Journal of Biological Chemistry 282, 30794-30803.

Nomura, M., Hosaka, Y., Kasashima, Y., Ueda, H., Takehana, K., Kuwano, A., Arai, K., 2007, Active expression of matrix metalloproteinase-13 mRNA in the granulation tissue of equine superficial digital flexor tendinitis. J Vet Med Sci 69, 637-639.

Noschka, E., Vandenplas, M.L., Hurley, D.J., Moore, J.N., 2008, Temporal aspects of laminar gene expression during the developmental stages of equine laminitis. Vet Immunol Immunopathol 129, 242-253.

Nourian, A.R., Asplin, K.E., McGowan, C.M., Sillence, M.N., Pollitt, C.C., 2009, Equine laminitis: Ultrastructural lesions detected in ponies following hyperinsulinaemia. Equine Vet J 41, 671-677.

Nourian, A.R., Baldwin, G.I., van Eps, A.W., Pollitt, C.C., 2007, Equine laminitis: ultrastructural lesions detected 24-30 hours after induction with oligofructose. Equine Vet J 39, 360-364.

Novoradovskaya, N., Whitfield, M.L., Basehore, L.S., Novoradovsky, A., Pesich, R., Usary, J., Karaca, M., Wong, W.K., Aprelikova, O., Fero, M., Perou, C.M., Botstein, D., Braman, J., 2004, Universal reference RNA as a standard for microarray experiments. BMC Genomics 5, 20.

Nyunt, O., Wu, J.Y., McGown, I.N., Harris, M., Huynh, T., Leong, G.M., Cowley, D.M., Cotterill, A.M., 2009, Investigating maturity onset diabetes of the young. Clin Biochem Rev 30, 67-74.

Obel, N., 1948, Studies on the histopathology of acute laminitis.Almquist and Wiksells Boktryckteri, AK, Uppsala, Sweden.

Ornatowska, M., Azim, A.C., Wang, X., Christman, J.W., Xiao, L., Joo, M., Sadikot, R.T., 2007, Functional genomics of silencing TREM-1 on TLR4 signaling in macrophages. Am J Physiol Lung Cell Mol Physiol 293, L1377-1384.

Orsini, J., Galantino-Homer, H., Pollitt, C.C., 2009, Laminitis in horses: through the lens of systems theory. Journal of Equine Veterinary Science 29, 105-114.

Orsini, J.A., 2008, Ten topics to remember from the Third International Equine Conference on Laminitis and Diseases of the Foot: a detailed summary. Journal of Equine Veterinary Science 28, 180-183.

Orsini, J.A., Moore, R.M., 2010, Lessons learned from the 2nd American Association of Equine Practitioners Foundation's Equine Laminitis Research Workshop. Journal of Equine Veterinary Science 30, 87-92.

Oslejskova, L., Grigorian, M., Hulejova, H., Vencovsky, J., Pavelka, K., Klingelhofer, J., Gay, S., Neidhart, M., Brabcova, H., Suchy, D., Senolt, L., 2009, Metastasis-inducing S100A4 protein is associated with the disease activity of rheumatoid arthritis. Rheumatology 48, 1590-1594.

Papakonstantis, I., Diakakis, N., Patsikas, M., Desiris, A., 2007, Equine laminitis: a retrospective study of 55 cases (2000-2004). Journal of the Hellenic Veterinary Medical Society 58, 107-123.

Papaspyridonos, M., Smith, A., Burnand, K.G., Taylor, P., Padayachee, S., Suckling, K.E., James, C.H., Greaves, D.R., Patel, L., 2006, Novel candidate genes in unstable areas of human atherosclerotic plaques. Arterioscler Thromb Vasc Biol 26, 1837-1844.

Parisi, A.F., Vallee, B.L., 1969, Zinc Metalloenzymes: characteristics and significance in biology and medicine. Am J Clin Nutr 22, 1222-1239.

Parks, A., O'Grady, S.E., 2003, Chronic laminitis: current treatment strategies. Vet Clin North Am Equine Pract 19, 393-416, vi.

Parks, A.H., 2003, Treatment of acute laminitis. Equine Vet. Educ. 15(5), 273-280.

Parks, W.C., Wilson, C.L., Lopez-Boado, Y.S., 2004, Matrix metalloproteinases as modulators of inflammation and innate immunity. Nat Rev Immunol 4, 617-629.

Parsons, C.S., Orsini, J.A., Krafty, R., Capewell, L., Boston, R., 2007, Risk factors for development of acute laminitis in horses during hospitalization: 73 cases (1997-2004). J Am Vet Med Assoc 230, 885-889.

Pass, M.A., Pollitt, S., Pollitt, C.C., 1998, Decreased glucose metabolism causes separation of hoof lamellae in vitro: a trigger for laminitis? Equine Vet J Suppl, 133-138.

Patterson, A., Schmutz, C., Davis, S., Gardner, L., Ashton, B., Middleton, J., 2002, Differential binding of chemokines to macrophages and neutrophils in the human inflamed synovium. Arthritis Res 4, 209 - 214.

Patterson, T.A., Lobenhofer, E.K., Fulmer-Smentek, S.B., Collins, P.J., Chu, T.M., Bao, W., Fang, H., Kawasaki, E.S., Hager, J., Tikhonova, I.R., Walker, S.J., Zhang, L., Hurban, P., de Longueville, F., Fuscoe, J.C., Tong, W., Shi, L., Wolfinger, R.D., 2006, Performance comparison of one-color and two-color platforms within the MicroArray Quality Control (MAQC) project. Nat Biotechnol 24, 1140-1150.

Pavlidis, P., Li, Q., Noble, W.S., 2003, The effect of replication on gene expression microarray experiments. Bioinformatics 19, 1620-1627.

Pawitan, Y., Michiels, S., Koscielny, S., Gusnanto, A., Ploner, A., 2005, False discovery rate, sensitivity and sample size for microarray studies. Bioinformatics 21, 3017-3024.

Peck, A., Mellins, E.D., 2010, Precarious balance: Th17 cells in host defense. Infect. Immun. 78, 32-38.

Perera, C., McNeil, H.P., Geczy, C.L., 2010, S100 Calgranulins in inflammatory arthritis. Immunol Cell Biol 88, 41-49.

Petersen, D., Chandramouli, G.V., Geoghegan, J., Hilburn, J., Paarlberg, J., Kim, C.H., Munroe, D., Gangi, L., Han, J., Puri, R., Staudt, L., Weinstein, J., Barrett, J.C., Green, J., Kawasaki, E.S., 2005, Three microarray platforms: an analysis of their concordance in profiling gene expression. BMC Genomics 6, 63.

Pfaffl, M.W., 2001, A new mathematical model for relative quantification in real-time RT-PCR. Nucleic Acids Res 29, e45.

Pham, C.T., 2008, Neutrophil serine proteases fine-tune the inflammatory response. Int J Biochem Cell Biol 40, 1317-1333.

Piehler, A., Grimholt, R., Ovstebo, R., Berg, J., 2010, Gene expression results in lipopolysaccharide-stimulated monocytes depend significantly on the choice of reference genes. BMC Immunology 11, 21.

Pluznick, J.L., Zou, D.-J., Zhang, X., Yan, Q., Rodriguez-Gil, D.J., Eisner, C., Wells, E., Greer, C.A., Wang, T., Firestein, S., Schnermann, J., Caplan, M.J., 2009, Functional expression of the olfactory signaling system in the kidney. Proc Natl Acad Sci USA 106, 2059-2064.

Pollitt, C.C., 1994, The basement membrane at the equine hoof dermal epidermal junction. Equine Vet J 26, 399-407.

Pollitt, C.C., 1996, Basement membrane pathology: a feature of acute equine laminitis. Equine Vet J 28, 38-46.

Pollitt, C.C., 1999, Equine laminitis: A revised pathophysiology. Proceedings of the 45th annual convention of the American Association of Equine Practitioners 45, 188–192.

Pollitt, C.C., 2004a, Anatomy and physiology of the inner hoof wall. Clinical Techniques in Equine Practice 3, 3-21.

Pollitt, C.C., 2004b, Equine laminitis. Clinical Techniques in Equine Practice 3, 34-44.

Pollitt, C.C., Daradka, M., 1998, Equine laminitis basement membrane pathology: loss of type IV collagen, type VII collagen and laminin immunostaining. Equine Vet J Suppl, 139-144.

Pollitt, C.C., Daradka, M., 2004, Hoof wall wound repair. Equine Vet J 36, 210-215.

Pollitt, C.C., Davies, C.T., 1998, Equine laminitis: its development coincides with increased sublamellar blood flow. Equine Vet J Suppl, 125-132.

Pollitt, C.C., Pass, M.A., Pollitt, S., 1998, Batimastat (BB-94) inhibits matrix metalloproteinases of equine laminitis. Equine Vet J Suppl, 119-124.

Pollitt, C.C., Visser, M.B., 2010, Carbohydrate alimentary overload laminitis. Vet Clin North Am Equine Pract 26, 65-78.

Polzer, J., Slater, M.R., 1997, Age, breed, sex and seasonality as risk factors for equine laminitis. Preventive Veterinary Medicine 29, 179-184.

Potenza, M.A., Marasciulo, F.L., Chieppa, D.M., Brigiani, G.S., Formoso, G., Quon, M.J., Montagnani, M., 2005, Insulin resistance in spontaneously hypertensive rats is associated with endothelial dysfunction characterized by imbalance between NO and ET-1 production. Am J Physiol Heart Circ Physiol 289, H813-822.

Prinsen, C.F.M., Szerencsei, R.T., Schnetkamp, P.P.M., 2000, Molecular cloning and functional expression of the potassium-dependent sodium-calcium exchanger from human and chicken retinal cone photoreceptors. J. Neurosci. 20, 1424-1434.

Provenzano, M., Mocellin, S., 2007, Complementary techniques: validation of gene expression data by quantitative real time PCR. Adv Exp Med Biol 593, 66-73.

Purdom, E., Holmes, S.P., 2005, Error distribution for gene expression data. Stat Appl Genet Mol Biol 4, Article16.

Quackenbush, J., 2001, Computational analysis of microarray data. Nat Rev Genet 2, 418-427.

Quackenbush, J., 2002, Microarray data normalization and transformation. Nat Genet 32 Suppl, 496-501.

Radonic, A., Thulke, S., Mackay, I.M., Landt, O., Siegert, W., Nitsche, A., 2004, Guideline to reference gene selection for quantitative real-time PCR. Biochem Biophys Res Commun 313, 856-862.

Ramdas, L., Coombes, K., Baggerly, K., Abruzzo, L., Highsmith, W.E., Krogmann, T., Hamilton, S., Zhang, W., 2001, Sources of nonlinearity in cDNA microarray expression measurements. Genome Biology 2, research0047.0041 - research0047.0047.

Ramery, E., Closset, R., Art, T., Bureau, F., Lekeux, P., 2009, Expression microarrays in equine sciences. Vet Immunol Immunopathol 127, 197-202.

Ramery, E., Closset, R., Bureau, F., Art, T., Lekeux, P., 2008, Relevance of using a human microarray to study gene expression in heaves-affected horses. Vet J 177, 216-221.

Ramnath, N., Creaven, P.J., 2004, Matrix metalloproteinase inhibitors. Curr Oncol Rep 6, 96-102.

Redruello, B., Louro, B., Anjos, L., Silva, N., Greenwell, R.S., Canario, A.V.M., Power, D.M., 2010, CRTAC1 homolog proteins are conserved from cyanobacteria to man and secreted by the teleost fish pituitary gland. Gene 456, 1-14.

Reiss, K., Ludwig, A., Saftig, P., 2006, Breaking up the tie: disintegrin-like metalloproteinases as regulators of cell migration in inflammation and invasion. Pharmacology & Therapeutics 111, 985-1006.

Riggs, L.M., Franck, T., Moore, J.N., Krunkosky, T.M., Hurley, D.J., Peroni, J.F., de la Rebière, G., Serteyn, D.A., 2007, Neutrophil myeloperoxidase measurements in plasma, laminar tissue, and skin of horses given black walnut extract. Am J Vet Res 68, 81-86.

Rijnen, K.E., van der Kolk, J.H., 2003, Determination of reference range values indicative of glucose metabolism and insulin resistance by use of glucose clamp techniques in horses and ponies. Am J Vet Res 64, 1260-1264.

Ritchie, M.E., Silver, J., Oshlack, A., Holmes, M., Diyagama, D., Holloway, A., Smyth, G.K., 2007, A comparison of background correction methods for two-colour microarrays. Bioinformatics 23, 2700-2707.

Ropolo, A., Grasso, D., Pardo, R., Sacchetti, M.L., Archange, C., Re, A.L., Seux, M., Nowak, J., Gonzalez, C.D., Iovanna, J.L., Vaccaro, M.I., 2007, The pancreatitis-induced vacuole membrane protein 1 triggers autophagy in mammalian cells. Journal of Biological Chemistry 282, 37124-37133.

Rose, R.J., Allen, J.R., Hodgson, D.R., Kohnke, J.R., 1983, Studies on isoxsuprine hydrochloride for the treatment of navicular disease. Equine Vet J 15, 238-243.

Roth, J., Vogl, T., Sorg, C., Sunderkötter, C., 2003, Phagocyte-specific S100 proteins: a novel group of proinflammatory molecules. Trends in Immunology 24, 155-158.

Rozen, S., Skaletsky, H., 2000, Primer3 on the WWW for general users and for biologist programmers. Methods Mol Biol 132, 365-386.

Saeed, A.I., Sharov, V., White, J., Li, J., Liang, W., Bhagabati, N., Braisted, J., Klapa, M., Currier, T., Thiagarajan, M., Sturn, A., Snuffin, M., Rezantsev, A., Popov, D., Ryltsov, A., Kostukovich, E., Borisovsky, I., Liu, Z., Vinsavich, A., Trush, V., Quackenbush, J., 2003, TM4: a free, open-source system for microarray data management and analysis. Biotechniques 34, 374-378.

Sallenave, J.-M., 2010, Secretory leukocyte protease inhibitor and elafin/trappin-2: versatile mucosal antimicrobials and regulators of immunity. Am. J. Respir. Cell Mol. Biol. 42, 635-643.

Salomonis, N., Hanspers, K., Zambon, A.C., Vranizan, K., Lawlor, S.C., Dahlquist, K.D., Doniger, S.W., Stuart, J., Conklin, B.R., Pico, A.R., 2007, GenMAPP 2: new features and resources for pathway analysis. BMC Bioinformatics 8, 217.

Sam, J.B., 2000, Relationship between fatty acids and the endocrine system. BioFactors 13, 35-39.

Sanchez-Martinez, R., Castillo, A.I., Steinmeyer, A., Aranda, A., 2006, The retinoid X receptor ligand restores defective signalling by the vitamin D receptor. EMBO Rep 7, 1030-1034.

Sasik, R., Woelk, C., Corbeil, J., 2004, Microarray truths and consequences. J Mol Endocrinol 33, 1-9.

Schena, M., Shalon, D., Davis, R.W., Brown, P.O., 1995, Quantitative monitoring of gene expression patterns with a complementary DNA microarray. Science 270, 467-470.

Schneider, J.J., Unholzer, A., Schaller, M., Schafer-Korting, M., Korting, H.C., 2005, Human defensins. J Mol Med 83, 587-595.

Semenza, G.L., 1998, Hypoxia-inducible factor 1 and the molecular physiology of oxygen homeostasis. Journal of Laboratory and Clinical Medicine 131, 207-214.

Shah, C., Hari-Dass, R., Raynes, J.G., 2006, Serum amyloid A is an innate immune opsonin for Gram-negative bacteria. Blood 108, 1751-1757.

Shanik, M.H., Xu, Y., Skrha, J., Dankner, R., Zick, Y., Roth, J., 2008, Insulin resistance and hyperinsulinemia: is hyperinsulinemia the cart or the horse? Diabetes Care 31 Suppl 2, S262-268.

Shaw, P.J., Lamkanfi, M., Kanneganti, T.D., 2010, NOD-like receptor (NLR) signaling beyond the inflammasome. European Journal of Immunology 40, 624-627.

Shweiki, D., Itin, A., Soffer, D., Keshet, E., 1992, Vascular endothelial growth factor induced by hypoxia may mediate hypoxia-initiated angiogenesis. Nature 359, 843-845.

Silver, I.A., 2008, Laminitis: drink deep, or taste not the Pierian Spring. Equine Vet J 40, 431-432.

Simmonds, R.E., Foxwell, B.M., 2008, Signalling, inflammation and arthritis: NF-{kappa}B and its relevance to arthritis and inflammation. Rheumatology 47, 584-590.

Simon, R.M., Dobbin, K., 2003, Experimental design of DNA microarray experiments. Biotechniques Suppl, 16-21.

Sinicropi, D., Cronin, M., Liu, M.-L., 2007, Gene expression profiling utilizing microarray technology and RT-PCR, In: Ferrari, M., Ozkan, M., Heller, M.J. (Eds.) BioMEMS and biomedical nanotechnology. Springer, New York, pp. 23-46.

Slater, M.R., Hood, D.M., Carter, G.K., 1995, Descriptive epidemiological study of equine laminitis. Equine Vet J 27, 364-367.

Smith, K.J., Bertone, A.L., Weisbrode, S.E., Radmacher, M., 2006a, Gross, histologic, and gene expression characteristics of osteoarthritic articular cartilage of the metacarpal condyle of horses. Am J Vet Res 67, 1299-1306.

Smith, S.J., Fenwick, P.S., Nicholson, A.G., Kirschenbaum, F., Finney-Hayward, T.K., Higgins, L.S., Giembycz, M.A., Barnes, P.J., Donnelly, L.E., 2006b, Inhibitory effect of p38 mitogen-activated protein kinase inhibitors on cytokine release from human macrophages. Br J Pharmacol 149, 393-404.

Smoak, K.A., Cidlowski, J.A., 2004, Mechanisms of glucocorticoid receptor signaling during inflammation. Mechanisms of Ageing and Development 125, 697-706.

Smyth, G.K., 2004, Linear models and empirical bayes methods for assessing differential expression in microarray experiments. Stat Appl Genet Mol Biol 3, Article3.

Smyth, G.K., Speed, T., 2003, Normalization of cDNA microarray data. Methods 31, 265-273.

Spehr, M., Gisselmann, G., Poplawski, A., Riffell, J.A., Wetzel, C.H., Zimmer, R.K., Hatt, H., 2003, Identification of a testicular odorant receptor mediating human sperm chemotaxis. Science 299, 2054-2058.

Staudt, L.M., Brown, P.O., 2000, Genomic views of the immune system. Annu Rev Immunol 18, 829-859.

Stears, R.L., Getts, R.C., Gullans, S.R., 2000, A novel, sensitive detection system for high-density microarrays using dendrimer technology. Physiol Genomics 3, 93-99.

Steinmetz, L.M., Davis, R.W., 2004, Maximizing the potential of functional genomics. Nat Rev Genet 5, 190-201.

Stewart, A.J., Pettigrew, A., Cochran, A.M., Belknap, J.K., 2009, Indices of inflammation in the lung and liver in the early stages of the black walnut extract model of equine laminitis. Vet Immunol Immunopathol 129, 254-260.

Stockand, J.D., 2002, New ideas about aldosterone signaling in epithelia. Am J Physiol Renal Physiol 282, F559-576.

Stokes, A.M., Keowen, M.L., McGeachy, M., Carlisle, K., Garza, F., 2010, Potential role of the toll-like receptor signaling pathway in equine laminitis. Journal of Equine Veterinary Science 30, 113-114.

Sun, Y., MacRae, T.H., 2005, Small heat shock proteins: molecular structure and chaperone function. Cell Mol Life Sci 62, 2460-2476.

Suzuki, T., Higgins, P.J., Crawford, D.R., 2000, Control selection for RNA quantitation. Biotechniques 29, 332-337.

Sweeney, S.E., Firestein, G.S., 2007, Primer: signal transduction in rheumatic disease--a clinician's guide. Nat Clin Pract Rheumatol 3, 651-660.

Swinburne, J., 2009, Inherited disease in the horse: Mapping complex disease variants is on the horizon. The Veterinary Journal 179, 317-318.

Tanegashima, K., Okamoto, S., Nakayama, Y., Taya, C., Shitara, H., Ishii, R., Yonekawa, H., Minokoshi, Y., Hara, T., 2010, CXCL14 deficiency in mice attenuates obesity and inhibits feeding behavior in a novel environment. PLoS ONE 5, e10321.

Taubes, G., 2009, Prosperity's plague. Science 325, 256-260.

Thompson, L.P., Aguan, K., Pinkas, G., Weiner, C.P., 2000, Chronic hypoxia increases the NO contribution of acetylcholine vasodilation of the fetal guinea pig heart. Am J Physiol Regul Integr Comp Physiol 279, R1813-1820.

Tomlinson, D.J., Mulling, C.H., Fakler, T.M., 2004, Invited Review: formation of keratins in the bovine claw: roles of hormones, minerals, and vitamins in functional claw integrity. J. Dairy Sci. 87, 797-809.

Tortorella, M.D., Malfait, F., Barve, R.A., Shieh, H.S., Malfait, A.M., 2009, A review of the ADAMTS family, pharmaceutical targets of the future. Curr Pharm Des 15, 2359-2374.

Treiber, K.H., Kronfeld, D.S., Geor, R.J., 2006a, Insulin resistance in equids: possible role in laminitis. J. Nutr. 136, 2094S-2098.

Treiber, K.H., Kronfeld, D.S., Hess, T.M., Byrd, B.M., Splan, R.K., Staniar, W.B., 2006b, Evaluation of genetic and metabolic predispositions and nutritional risk factors for pasture-associated laminitis in ponies. J Am Vet Med Assoc 228, 1538-1545.

Tseng, G., Oh, M., Rohlin, L., Liao, J., Wong, W., 2001, Issues in cDNA microarray analysis: quality filtering, channel normalization, models of variations and assessment of gene effects. Nucleic Acids Res 29, 2549 - 2557.

Ueland, T., Bollerslev, J., Godang, K., Muller, F., Froland, S., Aukrust, P., 2001, Increased serum osteoprotegerin in disorders characterized by persistent immune activation or glucocorticoid excess--possible role in bone homeostasis. Eur J Endocrinol 145, 685-690.

van Eps, A.W., Pollitt, C.C., 2006, Equine laminitis induced with oligofructose. Equine Vet J 38, 203-208.

Vandenplas, L.M., Moore, N., James, H., David, J., Last, L., Grafton, M., Seamans, S., Sun, F., Liang, C., Cordonnier-Pratt, M.-M., Pratt, L.H., 2005, Equine cDNA microarrays for examining gene expression profiles in pro-inflammatory conditions and other diseases, Plant & Animal Genomes XIII Conference. San Diego. www.intl-pag.org:W091.

Vandesompele, J., De Preter, K., Pattyn, F., Poppe, B., Van Roy, N., De Paepe, A., Speleman, F., 2002, Accurate normalization of real-time quantitative RT-PCR data by geometric averaging of multiple internal control genes. Genome Biol 3 (7).

Vick, M.M., Adams, A.A., Murphy, B.A., Sessions, D.R., Horohov, D.W., Cook, R.F., Shelton, B.J., Fitzgerald, B.P., 2007, Relationships among inflammatory cytokines, obesity, and insulin sensitivity in the horse. J Anim Sci 85, 1144-1155.

Vincenti, M.P., Brinckerhoff, C.E., 2001, The potential of signal transduction inhibitors for the treatment of arthritis: is it all just JNK? The Journal of Clinical Investigation 108, 181-183.

Visser, M., Pollitt, C., 2010, Characterization of extracellular matrix macromolecules in primary cultures of equine keratinocytes. BMC Veterinary Research 6, 16.

Wade, C.M., Giulotto, E., Sigurdsson, S., Zoli, M., Gnerre, S., Imsland, F., Lear, T.L., Adelson, D.L., Bailey, E., Bellone, R.R., Blocker, H., Distl, O., Edgar, R.C., Garber, M., Leeb, T., Mauceli, E., MacLeod, J.N., Penedo, M.C.T., Raison, J.M., Sharpe, T., Vogel, J., Andersson, L., Antczak, D.F., Biagi, T., Binns, M.M., Chowdhary, B.P., Coleman, S.J., Della Valle, G., Fryc, S., Guerin, G., Hasegawa, T., Hill, E.W., Jurka, J., Kiialainen, A., Lindgren, G., Liu, J., Magnani, E., Mickelson, J.R., Murray, J., Nergadze, S.G., Onofrio, R., Pedroni, S., Piras, M.F., Raudsepp, T., Rocchi, M., Roed, K.H., Ryder, O.A., Searle, S., Skow, L., Swinburne, J.E., Syvanen, A.C., Tozaki, T., Valberg, S.J., Vaudin, M., White, J.R., Zody, M.C., Broad Institute Genome Sequencing Platform, Broad Institute Whole Genome Assembly Team, Lander, E.S., Lindblad-Toh, K., 2009, Genome sequence, comparative analysis, and population genetics of the domestic horse. Science 326, 865-867.

Waguespack, R.W., Cochran, A., Belknap, J.K., 2004a, Expression of the cyclooxygenase isoforms in the prodromal stage of black walnut-induced laminitis in horses. Am J Vet Res 65, 1724-1729.

Waguespack, R.W., Kemppainen, R.J., Cochran, A., Lin, H.C., Belknap, J.K., 2004b, Increased expression of MAIL, a cytokine-associated nuclear protein, in the prodromal stage of black walnut-induced laminitis. Equine Vet J 36, 285-291.

Wattle, O., Pollitt, C.C., 2004, Lamellar metabolism. Clinical Techniques in Equine Practice 3, 22-33.

Weiss, D.J., Evanson, O.A., McClenahan, D., Fagliari, J.J., Jenkins, K., 1997, Evaluation of platelet activation and platelet-neutrophil aggregates in ponies with alimentary laminitis. Am J Vet Res 58, 1376-1380.

Weiss, S.J., 1989, Tissue destruction by neutrophils. New England Journal of Medicine 320, 365-376.

Wessling-Resnick, M., 2010, Iron homeostasis and the inflammatory response. Annual Review of Nutrition 30, 105-122.

White, C.A., Salamonsen, L.A., 2005, A guide to issues in microarray analysis: application to endometrial biology. Reproduction 130, 1-13.

Wilson, H.L., Aich, P., Roche, F.M., Jalal, S., Hodgson, P.D., Brinkman, F.S., Potter, A., Babiuk, L.A., Griebel, P.J., 2005, Molecular analyses of disease pathogenesis: application of bovine microarrays. Vet Immunol Immunopathol 105, 277-287.

Woo, Y., Affourtit, J., Daigle, S., Viale, A., Johnson, K., Naggert, J., Churchill, G., 2004, A comparison of cDNA, oligonucleotide, and Affymetrix GeneChip gene expression microarray platforms. J Biomol Tech 15, 276-284.

Wylie, C., Collins, S., Newton, R., Verheyen, K., Durham, A., Rendle, D., 2009, Study on equine laminitis. Vet Rec 164, 250.

Yang, D., Chen, Q., Hoover, D.M., Staley, P., Tucker, K.D., Lubkowski, J., Oppenheim, J.J., 2003, Many chemokines including CCL20/MIP-3{alpha} display antimicrobial activity. J Leukoc Biol 74, 448-455.

Yang, J.-M., Mi Sim, S., Kim, H.-Y., Park, G.T., 2010, Expression of the homeobox gene, HOPX, is modulated by cell differentiation in human keratinocytes and is involved in the expression of differentiation markers. European Journal of Cell Biology 89, 537-546.

Yang, J.Y., 2008, Microarrays--planning your experiment. Methods Mol Med 141, 71-85.

Yang, Y., Dudoit, S., Luu, P., Lin, D., Peng, V., Ngai, J., Speed, T., 2002, Normalization for cDNA microarray data: a robust composite method addressing single and multiple slide systematic variation. Nucleic Acids Res 30, e15.

Yang, Y., Speed, T., 2002, Design issues for cDNA microarray experiments. Nat Rev Genet 3, 579 - 588.

Yao, B., Rakhade, S., Li, Q., Ahmed, S., Krauss, R., Draghici, S., Loeb, J., 2004, Accuracy of cDNA microarray methods to detect small gene expression changes induced by neuregulin on breast epithelial cells. BMC Bioinformatics 5, 99.

Yin, C., Pettigrew, A., Loftus, J.P., Black, S.J., Belknap, J.K., 2009, Tissue concentrations of 4-HNE in the black walnut extract model of laminitis: indication of oxidant stress in affected laminae. Vet Immunol Immunopathol 129, 211-215.

Yu, S.P., Canzoniero, L.M.T., Choi, D.W., 2001, Ion homeostasis and apoptosis. Current Opinion in Cell Biology 13, 405-411.

Yuan, Z.Q., Nicolson, L., Marchetti, B., Gault, E.A., Campo, M.S., Nasir, L., 2008, Transcriptional changes induced by bovine papillomavirus type 1 in equine fibroblasts. J Virol 82, 6481-6491.

Zhang, N., Ahsan, M.H., Purchio, A.F., West, D.B., 2005, Serum Amyloid A-luciferase transgenic mice: response to sepsis, acute arthritis, and contact hypersensitivity and the effects of proteasome inhibition. J Immunol 174, 8125-8134.

Zhao, S.H., Kuhar, D., Lunney, J.K., Dawson, H., Guidry, C., Uthe, J.J., Bearson, S.M., Recknor, J., Nettleton, D., Tuggle, C.K., 2006, Gene expression profiling in Salmonella Choleraesuis-infected porcine lung using a long oligonucleotide microarray. Mamm Genome 17, 777-789.

Zheng, H., Heiderscheidt, C.A., Joo, M., Gao, X., Knezevic, N., Mehta, D., Sadikot, R.T., 2010, MYD88-dependent and -independent activation of TREM-1 via specific TLR ligands. European Journal of Immunology 40, 162-171.

Zhernakova, A., van Diemen, C.C., Wijmenga, C., 2009, Detecting shared pathogenesis from the shared genetics of immune-related diseases. Nat Rev Genet 10, 43-55.

Zreiqat, H., Belluoccio, D., Smith, M., Wilson, R., Rowley, L., Jones, K., Ramaswamy, Y., Vogl, T., Roth, J., Bateman, J., Little, C., 2010, S100A8 and S100A9 in experimental osteoarthritis. Arthritis Research & Therapy 12, R16.

APPENDIX

Table A.1 List of all differentially expressed genes (P<0.01 and fold change>2) for the DEV/CON comparison. Fold change indicates expression level larger than 2 is up-regulation and expression level less than 0.5 is down-regulation.

Gene Name	Public Accession	Human Protein	P Value	Fold Change
PIGR	XM_001492298	NP_002635.2	5.947E-05	0.3348796
SNF8	XM_001502240	NP_009172.2	0.0012115	0.3395826
NULL	XM_001498378	NULL	0.0028365	0.3504448
NULL	NULL	NULL	0.0004497	0.359265
FLRT3	XM_001491950	NP_037413.1	0.0071702	0.372587
NULL	CX604746	NULL	0.0001236	0.3730017
SEPP1	XR_036255	NP_001087195.1	0.001416	0.3907
ZDHHC6	XM_001498439	NP_071939.1	0.0050028	0.3948714
NULL	NULL	NULL	0.0053603	0.3958571
PTPN6	XM_001497706	NP_002822.2	0.0078528	0.3958807
TIGD1	XM_001503915	NP_663748.1	0.0032456	0.4011188
C11orf59	XM_001499308	NP_060377.1	0.0080243	0.4040881
CA5B	XM_001490349	NP_009151.1	0.0070788	0.404286
CILP2	XR_036360	NP_694953.2	0.0006521	0.4063774
NULL	NULL	NULL	0.0040508	0.4197584
CDK5RAP2	XM_001501690	NP_060719.4	0.0022011	0.4202178
NULL	NULL	NULL	0.0084249	0.4269597
C8orf70	XM_001491870	NP_057094.1	0.0078665	0.4277105
PRR15	XM_001500279	NP_787083.1	0.0050108	0.4321916
NULL	NULL	NULL	0.0025279	0.4323748
NCAPG	XR_036336	NP_071741.2	0.0041005	0.4331997
NULL	CD535422	NULL	0.0005955	0.4369529
CRABP1	NULL	NP_004369.1	0.0011655	0.437203
ANKRD35	XM_001499402	NP_653299.3	0.0093994	0.4375781
BFAR	XM_001490098	NP_057645.1	0.0098486	0.4386322
ATP6V1B1	XM_001489315	NP_001683.2	0.0063162	0.439582
NULL	NULL	NULL	0.0024622	0.4434318
HERPUD2	XM_001501128	NP_071768.2	0.0089616	0.4436919
ARL6IP4	XM_001497593	NP_057722.2	0.0085555	0.4502788
NULL	DN507028	NULL	0.0024213	0.4529776
IGLL1	XM_001492772	NP_064455.1	0.0026492	0.4540942
ZNF709	XM_001496191	NP_689814.1	0.0087303	0.4553173

OR7A5	XM_001499777	NP_059976.1	0.00625	0.4557727
RNF138	XM_001496619	NP_057355.2	0.0052927	0.4587432
OR52B4	XM_001496850	NP_001005161.2	0.0095427	0.4590887
DNAL4	XM_001501707	NP_005731.1	0.0055489	0.4611828
NULL	NULL	NULL	0.0093934	0.461473
NULL	NULL	NULL	0.0078178	0.4633147
NULL	CD468881	NULL	0.003374	0.465527
CD1A	XM_001489596	NP_001754.2	0.0056835	0.4690903
CPXM1	XM_001497131	NP_062555.1	0.0044105	0.4693193
ERCC2	XM_001500474	NP_000391.1	0.0065647	0.4697824
ITGAX	XM_001495577	NP_000878.2	0.0044879	0.4709893
APOC4	XM_001502367	NP_001637.1	0.0025516	0.473609
NULL	NULL	NULL	0.0022607	0.4790313
FASN	XM_001491292	NP_004095.4	0.0099156	0.4825165
SCHIP1	CX601415	NP_055390.1	0.0062503	0.4870996
KIAA1430	XM_001491109	NP_065878.1	0.0077734	0.4875496
MAF	NULL	NP_001026974.1	0.0042664	0.4927487
LMO4	XM_001495584	NP_006760.1	0.0081393	0.4928831
ADAM20	NULL	NP_003805.3	0.0026238	0.4941237
RPUSD3	XM_001491328	NP_775930.1	0.0039738	0.4960581
LIPE	XM_001499337	NP_005348.2	0.0085767	0.4982896
NULL	DN505910	NULL	0.0052354	2.0308402
NULL	NULL	NULL	0.0005355	2.0335743
USP44	XM_001495993	NP_001035862.1	0.0095144	2.0710755
NULL	NULL	NULL	0.0060986	2.1888989
NULL	NULL	NULL	0.0027135	2.2296383
CLEC2L	XM_001496572	XP_499478.3	0.0098924	2.2764744
NULL	CX602928	NULL	0.0067592	2.3067414
CRYAB	XM_001501779	NP_001876.1	0.0030662	2.3516061
RSPH3	XM_001491976	NP_114130.3	0.0042391	2.3534586
NULL	NULL	NULL	0.0013585	2.3849153
HOPX	XM_001491312	NP_631957.1	0.009606	2.4503332
MFAP5	NULL	NP_003471.1	0.0071275	2.6792705
NULL	BI961659	NULL	1.498E-05	2.7866203
CCL2	AJ251189	NP_002973.1	0.0056063	3.0044443
NULL	BM734930	NULL	0.0026373	3.3508285

Table A.2 List of all differentially expressed genes (P<0.01 and fold change>2) for the OG1/CON comparison. Fold change indicates expression level larger than 2 is up-regulation and expression level less than 0.5 is down-regulation.

Gene Name	Public Accession	Human Protein	P Value	Fold Change
NULL	NULL	NULL	1.28E-06	0.2243435
SELENBP1	NULL	NP_003935.2	0.0004266	0.230477
OR7A10	NULL	NP_001005190.1	0.0002225	0.2455636
CD69	XM_001499388	NP_001772.1	0.0007847	0.2475105
CXCL14	XM_001502713	NP_004878.2	0.0021719	0.2476481
NULL	CD465749	NULL	3.38E-07	0.2489918
NULL	NULL	NULL	0.0015373	0.2517936
TPPP3	CX596053	NP_057048.2	0.0004892	0.2601816
NULL	CX604746	NULL	5.79E-05	0.3204686
NULL	CX603968	NULL	0.0026067	0.3230924
NULL	NULL	NULL	0.0017855	0.3352171
CD28	NM_001100179	NP_006130.1	0.0067911	0.3363899
MATN2	XM_001490965	NP_002371.3	0.0005736	0.3430338
FIBIN	AB302195	NP_976249.1	0.0049942	0.3565335
MNAT1	XM_001497949	NP_002422.1	0.0003989	0.3616633
ACBD7	XM_001498628	NP_001034933.1	0.0029252	0.3654203
NULL	NULL	NULL	0.001703	0.3706927
NULL	NULL	NULL	0.0005058	0.3741379
NULL	NULL	NULL	0.0094844	0.3771931
FLRT3	XM_001491950	NP_037413.1	0.0087306	0.3831077
NULL	NULL	NULL	0.0004609	0.3832289
NULL	NULL	NULL	0.000323	0.4031742
NULL	NULL	NULL	0.0023111	0.4090921
NULL	NULL	NULL	0.0030918	0.4141212
SNRPN	XM_001492702	NP_073718.1	0.0099055	0.416691
NULL	CX599404	NULL	0.0004803	0.4307558
NULL	NULL	NULL	0.0011537	0.4317607
NULL	NULL	NULL	0.0052625	0.4339479
BEX2	XM_001503044	NP_116010.1	0.0002856	0.4339661
NULL	XM_001489844	NULL	0.0084422	0.4405005
HMGB2	XM_001498819	NP_002120.1	0.0031908	0.4420842
NULL	BM734727	NULL	0.0017935	0.4429278
NULL	NULL	NULL	0.001481	0.4458845

IGFBP6	NULL	NP_002169.1	0.0002723	0.4479038
FOXN2	XM_001498254	NP_002149.2	0.005868	0.448417
HADHB	XR_036425	NP_000174.1	0.006971	0.4501272
SFRS5	XM_001500464	NP_001034554.1	0.0026026	0.4504911
P4HA3	XM_001495901	NP_878907.1	0.0007058	0.4510091
FLJ32810	XM_001498479	XP_001127623.1	0.0078741	0.4512612
PARP15	BI960814	NP_689828.1	0.0073446	0.4572764
NULL	CX601687	NULL	0.0069093	0.4577299
CLCN6	XM_001491741	NP_001277.1	0.0043323	0.4613162
NULL	NULL	NULL	0.009559	0.4646382
AMACR	XM_001500251	NP_055139.4	0.008385	0.4704083
NULL	NULL	NULL	0.0057003	0.471815
NULL	NULL	NULL	0.0052032	0.4731391
NULL	CX601418	NULL	0.0067509	0.4879627
NULL	NULL	NULL	0.0020198	0.4921633
HDAC3	XM_001503978	NP_003874.2	0.0098546	0.4945629
NULL	CX604949	NULL	0.0054996	0.4947603
DARC	XM_001490641	NP_002027.2	0.0032638	1.99601
CYCS	XM_001498822	NP_061820.1	0.0029425	2.0557252
FOLR2	XM_001499257	NP_000794.2	0.0063268	2.0609106
ODC1	XM_001502323	NP_002530.1	0.0041776	2.0729218
SEC11C	XM_001489285	NP_150596.1	0.0019041	2.105893
LOC390110	XM_001489817	NP_001027025.2	0.0058495	2.1211488
EREG	XM_001490281	NP_001423.1	0.007791	2.1255396
NULL	DN505910	NULL	0.0070953	2.1287296
TSPAN10	XM_001489838	NP_114151.3	0.0075185	2.1297393
NULL	NULL	NULL	0.0022141	2.1489989
NULL	NULL	NULL	8.419E-05	2.1599908
LCTL	XM_001497027	NP_997221.2	0.0075704	2.1607625
YTHDF2	XM_001500333	NP_057342.2	0.0085737	2.2031424
KRT33A	XM_001497042	NP_004129.2	0.0050126	2.2216277
ARRDC3	XM_001504616	NP_065852.1	0.0059223	2.2223945
NULL	NULL	NULL	0.0035004	2.2302144
NULL	XR_036017	NULL	0.0047643	2.2576145
C3orf43	XM_001501186	NP_001071125.1	0.0079749	2.2646277
NULL	CX602004	NULL	0.0095785	2.2898602
NULL	NULL	NULL	0.0001092	2.2916307
DUSP1	XM_001499555	NP_004408.1	0.0046203	2.3105742
SPI1	XM_001491380	NP_003111.2	0.0073011	2.3109014
USP48	XM_001504296	NP_115612.4	0.0073837	2.3224186

FGR	XM_001504019	NP_001036212.1	0.0005024	2.3310042
TOP1	XM_001500194	NP_003277.1	0.0069103	2.3448075
ALKBH6	XM_001492599	NP_116267.3	0.0010388	2.3519466
CD14	AF200416	NP_000582.1	0.00062	2.3583871
NULL	NULL	NULL	0.0061586	2.3739544
NULL	NULL	NULL	0.0033003	2.4071213
BACE2	DN509102	NP_036237.2	0.0046631	2.4221088
NULL	DN509649	NULL	0.0010582	2.4457472
NULL	NULL	NULL	0.0007546	2.4623677
BCL6	XM_001499813	NP_001697.2	0.002523	2.4815853
NULL	NULL	NULL	0.0009478	2.4840235
BIRC3	XM_001499875	NP_001156.1	0.0032213	2.5252948
IL10RB	XM_001498211	NP_000619.3	0.0006236	2.5356816
MCHR1	XM_001502221	NP_005288.3	0.0023582	2.5547138
TMEM49	XM_001503742	NP_112200.2	0.0014963	2.5553442
VASP	NULL	NP_003361.1	0.0094729	2.577176
NULL	CX605555	NULL	0.0014384	2.5904008
UTS2R	XM_001490444	NP_061822.1	0.0072268	2.5994938
NULL	NULL	NULL	0.0070955	2.6028953
RNF144B	XM_001494349	NP_877434.2	0.0003606	2.633142
SLC30A1	XM_001489279	NP_067017.2	0.0047388	2.6424103
ATP5B	NULL	NP_001677.2	0.001352	2.6531306
IFIT1L	XM_001498801	NP_001010987.1	0.0018264	2.6566017
LYZL6	XM_001494897	NP_065159.1	0.0008346	2.7076256
NULL	NULL	NULL	0.0004822	2.7748101
TIMP1	CX602739	NP_003245.1	0.0035118	2.8742931
OR7G2	XM_001500467	NP_001005193.1	0.0024333	3.0249114
RSPH3	XM_001491976	NP_114130.3	0.0019278	3.0788139
C13orf33	XM_001495031	NP_116238.2	0.0050774	3.1231197
SLC1A1	XM_001492215	NP_004161.4	0.0008968	3.1266973
NULL	CD470175	NULL	3.208E-05	3.2130747
NULL	CD472171	NULL	3.451E-05	3.2354271
SRGN	XM_001503648	NP_002718.2	0.0009494	3.2437712
LOC554251	XM_001491993	NP_001019851.1	0.0005633	3.2822625
ACAT2	XM_001491705	NP_005882.2	0.0001489	3.3253795
NULL	NULL	NULL	0.0039998	3.3416776
HTRA4	XM_001491574	NP_710159.1	0.0029486	3.3526877
RTEL1	XM_001492913	NP_057518.1	3.315E-05	3.4729818
CFB	XM_001492552	NP_001701.2	0.0003293	3.5048192
NULL	CX602140	NULL	0.0015575	3.6025274

EGR1	XM_001502553	NP_001955.1	0.0003762	3.6345378
HSPA5	CX604607	NP_005338.1	0.0016049	3.6835669
ADAMTS1	AF541975	NP_008919.3	6.16E-06	3.6920106
NULL	NULL	NULL	0.0002092	3.7164806
CEBPB	CX605423	NP_005185.2	3.39E-06	3.8388041
NULL	XM_001498707	NULL	0.0004245	3.8916559
NULL	NULL	NULL	0.0012631	3.9363377
ZNF452	XM_001504878	NP_443155.1	0.0001085	3.9371162
NULL	NULL	NULL	0.0012994	4.0195753
LYZ	XM_001494130	NP_000230.1	8.123E-05	4.0478677
PPA1	XM_001502747	NP_066952.1	1.628E-05	4.2789416
SEMA3C	XM_001489227	NP_006370.1	1.628E-05	4.3360604
S100P	BM734933	NP_005971.1	9.64E-06	4.4704722
CCL7	XM_001501551	NP_006264.2	7.51E-06	4.5401825
CITED1	XM_001488044	NP_004134.1	1.02E-05	4.7508868
TK1	XM_001491081	NP_003249.2	6.653E-05	5.3486915
NP	XM_001505137	NP_000261.2	0.0014357	5.4863287
ING5	NULL	XP_946119.1	7.90E-06	5.969279
NULL	NULL	NULL	1.64E-07	6.5516629
NULL	BI961659	NULL	7.63E-10	7.3082392
NULL	CX605648	NULL	1.286E-05	8.11198
SERPINB3	XM_001491507	NP_008850.1	7.806E-05	8.7247251
NULL	NULL	NULL	9.63E-07	9.2995608
CCL2	AJ251189	NP_002973.1	8.76E-06	9.7152828
S100A9	XM_001493530	NP_002956.1	0.0003288	10.4183
SAA1	NM_001081853	NP_000322.2	0.0002056	12.032089
NULL	NULL	NULL	1.88E-05	12.166194
PI3	BM734843	NP_002629.1	5.141E-05	15.338701
NULL	CD467650	NULL	2.66E-06	16.265843
S100A8	XM_001494358	NP_002955.2	7.27E-06	16.895748
SOD2	AB001693	NP_000627.2	3.45E-09	20.087348
NULL	BM734930	NULL	4.40E-09	22.847298
DEFB4	AY170305	NP_004933.1	3.16E-07	31.678786
S100A12	CD535886	NP_005612.1	2.97E-07	36.467473
S100A8	XM_001493589	NP_002955.2	1.92E-06	38.355221
NULL	NULL	NULL	4.17E-07	44.814777

Table A.3 List of all differentially expressed genes (P<0.01 and fold change>2) for the DEV/OG1 comparison. Fold change indicates expression level larger than 2 is up-regulation and expression level less than 0.5 is down-regulation.

Gene Name	Public Accession	Human Protein	P Value	Fold Change
S100A8	XM_001493589	NP_002955.2	9.57E-07	0.0288268
S100A12	CD535886	NP_005612.1	4.38E-06	0.0478126
NULL	NULL	NULL	2.756E-05	0.056055
S100A8	XM_001494358	NP_002955.2	7.54E-06	0.0737037
S100A9	XM_001493530	NP_002956.1	7.066E-05	0.0826332
SOD2	AB001693	NP_000627.2	2.39E-07	0.0921965
DEFB4	AY170305	NP_004933.1	0.0001131	0.0998139
NULL	CD467650	NULL	3.451E-05	0.1157475
NULL	CX605648	NULL	1.465E-05	0.1454532
NULL	BM734930	NULL	1.613E-05	0.1466619
SERPINB3	XM_001491507	NP_008850.1	0.0003378	0.1482778
ING5	NULL	XP_946119.1	3.43E-06	0.1510994
NULL	NULL	NULL	0.00032	0.1578443
SAA1	NM_001081853	NP_000322.2	0.002144	0.1603395
CITED1	XM_001488044	NP_004134.1	1.87E-06	0.1745981
PI3	BM734843	NP_002629.1	0.0037051	0.1888568
NULL	NULL	NULL	2.825E-05	0.1957813
TK1	XM_001491081	NP_003249.2	2.478E-05	0.2119661
NULL	NULL	NULL	7.23E-06	0.2137199
NP	XM_001505137	NP_000261.2	0.0017391	0.2150607
ZNF452	XM_001504878	NP_443155.1	1.99E-05	0.2328493
S100P	BM734933	NP_005971.1	1.038E-05	0.2550218
CCL7	XM_001501551	NP_006264.2	3.205E-05	0.2559178
SLC30A1	XM_001489279	NP_067017.2	0.0001117	0.2637864
MCHR1	XM_001502221	NP_005288.3	2.319E-05	0.2646922
LYZ	XM_001494130	NP_000230.1	0.0003195	0.2887071
CFB	XM_001492552	NP_001701.2	0.0001614	0.2915984
SEMA3C	XM_001489227	NP_006370.1	0.0001526	0.2919968
CEBPB	CX605423	NP_005185.2	4.64E-06	0.2952954
EGR1	XM_001502553	NP_001955.1	0.0003338	0.2977721
NULL	CX602140	NULL	0.0017299	0.3069089
CCL2	AJ251189	NP_002973.1	0.0034131	0.3092493
NULL	CX605555	NULL	0.0001424	0.3360394

SLC1A1	XM_001492215	NP_004161.4	0.0014339	0.3381174
USP48	XM_001504296	NP_115612.4	0.0003982	0.3387717
LYZL6	XM_001494897	NP_065159.1	0.0002152	0.3492745
SERPINB11	XM_001491598	NP_536723.2	0.009936	0.3503465
C13orf33	XM_001495031	NP_116238.2	0.0059983	0.3562235
NULL	NULL	NULL	1.48E-06	0.3584886
MYO1B	XM_001502243	NP_036355.2	0.0015173	0.3610238
OSMR	XM_001496993	NP_003990.1	0.0031108	0.3620245
TMEM49	XM_001503742	NP_112200.2	0.0003079	0.3639768
NULL	NULL	NULL	0.0003028	0.3640168
KLHDC1	XM_001496298	NP_751943.1	0.0016552	0.3667146
OR7G2	XM_001500467	NP_001005193.1	0.0055619	0.3690666
ADAMTS1	AF541975	NP_008919.3	0.0002115	0.3695796
NULL	NULL	NULL	0.000398	0.3710287
CLIC5	XM_001502577	NP_058625.2	0.0048234	0.3729854
RPUSD3	XM_001491328	NP_775930.1	0.0001867	0.3809596
LILRB4	CD467691	NP_001074907.1	2.143E-05	0.3812759
NULL	BI961659	NULL	3.397E-05	0.3812984
FCN1	XM_001498857	NP_001994.2	0.0027354	0.384454
NULL	NULL	NULL	0.0002537	0.3884835
FOLR2	XM_001499257	NP_000794.2	0.0003366	0.3961459
WDR46	XR_036191	NP_005443.2	0.0003122	0.39841
DC2	XM_001502983	NP_067050.1	0.0065113	0.4026614
EREG	XM_001490281	NP_001423.1	0.0009776	0.4027592
NULL	NULL	NULL	0.0076446	0.4061879
SCN3A	XM_001493704	NP_008853.3	0.0064515	0.4068865
NULL	CX605497	NULL	0.0036885	0.4070287
TUBGCP2	NULL	NP_006650.1	0.0026574	0.407333
ACAT2	XM_001491705	NP_005882.2	0.0029132	0.4106937
CD14	AF200416	NP_000582.1	0.0005103	0.4170751
TIMP1	CX602739	NP_003245.1	0.008357	0.4188957
ZFAND5	XM_001488383	NP_001095891.1	0.0016253	0.4212034
PDE4B	XM_001500306	NP_001032417.1	0.0074854	0.4212567
TOP1	XM_001500194	NP_003277.1	0.0063576	0.4222173
PDGFRB	XM_001501493	NP_002600.1	0.0080532	0.4222192
CHRNA1	XM_001499557	NP_000070.1	0.0026541	0.4262115
NULL	CX604543	NULL	0.0039756	0.4268117
SLC36A4	XM_001491833	NP_689526.2	0.0082755	0.427013
YTHDF2	XM_001500333	NP_057342.2	0.0029081	0.4284453
ARHGEF6	XM_001489854	NP_004831.1	0.0026054	0.4299731

CDK5RAP2	XM_001501690	NP_060719.4	0.0028398	0.4313085
LAMP3	XM_001496283	NP_055213.2	0.0025171	0.4329997
OR2AG1	XM_001499969	NP_001004489.1	0.0061342	0.4389212
NULL	DN504949	NULL	0.0077082	0.4400972
BCL6	XM_001499813	NP_001697.2	0.005757	0.4412427
SLC30A9	XM_001494445	NP_006336.3	0.0001669	0.4425522
BIRC3	XM_001499875	NP_001156.1	0.005193	0.4438224
C3orf43	XM_001501186	NP_001071125.1	0.008508	0.444991
SPI1	XM_001491380	NP_003111.2	0.0055936	0.4483773
RTEL1	XM_001492913	NP_057518.1	0.0015744	0.4495376
BCS1L	XM_001492073	NP_001073335.1	0.0030146	0.4546236
ATP5B	NULL	NP_001677.2	0.0042165	0.4570922
DNAJA1	XM_001499089	NP_001530.1	0.0014345	0.457459
TRA16	XM_001503457	NP_795361.1	0.0021945	0.4578523
NULL	DN506948	NULL	0.0043932	0.4586279
NULL	NULL	NULL	0.002963	0.4602054
RRS1	XM_001494813	NP_055984.1	0.0099761	0.4647966
LOX	NULL	NP_002308.2	0.003095	0.4657464
NULL	CX602993	NULL	0.0011721	0.4670793
NAGK	XM_001489139	NP_060037.2	0.0081676	0.4697813
AP3M2	XM_001489349	NP_006794.1	0.0047091	0.4733129
ARL4D	XM_001491841	NP_001652.2	0.0021579	0.4733809
PPFIA1	NULL	NP_003617.1	0.004967	0.4767974
NULL	NULL	NULL	0.0035033	0.4773099
TTK	XM_001499324	NP_003309.2	0.0056815	0.4791926
SLC36A3	XM_001501339	NP_861439.2	0.009041	0.4793468
NULL	NULL	NULL	0.007711	0.4796046
AP3S1	XR_036452	NP_001275.1	0.0088783	0.4810254
HIGD1A	CX601442	NP_001093138.1	0.000829	0.4814442
NULL	DN506142	NULL	0.0004433	0.4824114
NULL	NULL	NULL	0.0011598	0.4825585
TAS2R39	XM_001495492	NP_795362.2	0.0093784	0.4830005
SELS	XM_001490893	NP_060915.2	0.0051201	0.4831007
CKAP4	CX602638	NP_006816.2	0.0036315	0.484203
SERPINB8	XM_001492201	NP_002631.3	0.0022524	0.4859701
CCDC67	XM_001491708	NP_857596.2	0.0059073	0.4885446
PTMA	NULL	NP_002814.3	0.0045857	0.4941418
FLJ35773	XM_001503222	NP_689812.2	0.0053729	0.4944675
ODZ2	XM_001503295	XP_950879.2	0.0010627	0.4958106
EIF3J	NULL	NP_003749.2	0.0082104	0.4963824

CCDC50	XM_001498671	NP_848018.1	0.0082523	0.4977543
IL1B	XM_001495729	NP_000567.1	0.001322	0.4984435
NULL	CD470175	NULL	0.0027558	0.5009265
TM6SF1	XM_001497976	NP_075379.1	0.000401	0.5011357
SERPINH1	XM_001494685	NP_001226.2	0.0012734	0.5015004
JMJD1C	XR_036457	NP_116165.1	0.0025169	2.0141667
NULL	NULL	NULL	0.0077744	2.0860558
OR8B12	XM_001502045	NP_001005195.1	0.0007377	2.1098599
NULL	CX599404	NULL	0.0015285	2.1116958
NULL	CX605637	NULL	0.0097283	2.1189819
NULL	NULL	NULL	0.0042387	2.1365711
NULL	NULL	NULL	0.0005084	2.1655942
NULL	NULL	NULL	0.0052575	2.1707062
NULL	NULL	NULL	0.0068335	2.1760527
NULL	CX603435	NULL	0.0018159	2.2078648
NULL	NULL	NULL	0.008459	2.210933
HSPB8	XM_001490413	NP_055180.1	0.0002012	2.4258193
NULL	NULL	NULL	0.0097527	2.4467649
NULL	CX605682	NULL	0.0077231	2.4548339
39693	XM_001503016	NP_004395.1	0.0021521	2.4734803
IGFBP6	NULL	NP_002169.1	2.508E-05	2.4836402
MNAT1	XM_001497949	NP_002422.1	0.0003253	2.5929511
GSN	U31699	NP_000168.1	0.0002085	2.6573509
NULL	NULL	NULL	0.0030061	2.6591971
NULL	NULL	NULL	0.0003494	2.6708748
ENPP3	XM_001503291	NP_005012.2	0.0076128	2.7223846
39539	XM_001493843	NP_002961.1	0.0039058	2.7354169
NDEL1	XM_001504824	NP_001020750.1	0.0015702	2.7608585
NULL	NULL	NULL	0.0090299	2.7908398
CAT	CX593238	NP_001743.1	0.0023817	2.9414448
CRYAB	XM_001501779	NP_001876.1	0.000237	3.0568817
NULL	CD465749	NULL	2.93E-06	3.0858067
PPP2R3B	XM_001488015	NP_037371.2	0.0003873	3.0916075
OR7A10	NULL	NP_001005190.1	0.0015833	3.1780203
SLC22A12	XM_001489840	NP_653186.2	0.0031423	3.1816108
IGFBP7	XM_001491171	NP_001544.1	0.0004492	3.1864308
MFAP5	NULL	NP_003471.1	0.001718	3.2520741
FLJ36070	XM_001489063	NP_872380.1	0.0019684	3.2882248
NULL	NULL	NULL	2.509E-05	3.4534275
CALCB	AF257470	NP_000719.1	0.0008718	3.5857351

FAM82C	XM_001501075	NP_060615.1	0.0047303	3.6421132
HOPX	XM_001491312	NP_631957.1	0.000353	3.7320819
CXCL14	XM_001502713	NP_004878.2	0.0015326	3.7552859
NDUFA4L2	XM_001488582	NP_064527.1	0.0036162	3.7680783
CD69	XM_001499388	NP_001772.1	3.61E-05	4.8445118
NULL	CX601554	NULL	0.0073619	4.9493333
TPPP3	CX596053	NP_057048.2	1.407E-05	5.3052718

Table A.4 Overrepresented gene ontology terms identified among differentially expressed genes (P<0.05 and fold change>2) of the DEV/CON comparison. BP: biological process; CC: cellular component; MF: molecular function

	Term	Count	%	P
Upregulated Genes				
BP	GO:0009408~response to heat	4	14.81481	5.48E-05
	GO:0009266~response to temperature stimulus	4	14.81481	1.77E-04
	GO:0009725~response to hormone stimulus	5	18.51852	0.001278
	GO:0009628~response to abiotic stimulus	5	18.51852	0.001291
	GO:0009719~response to endogenous stimulus	5	18.51852	0.001838
	GO:0048545~response to steroid hormone stimulus	4	14.81481	0.002044
	GO:0040011~locomotion	5	18.51852	0.002307
	GO:0033273~response to vitamin	3	11.11111	0.003498
	GO:0051384~response to glucocorticoid stimulus	3	11.11111	0.00485
	GO:0042221~response to chemical stimulus	7	25.92593	0.005319
	GO:0031960~response to corticosteroid stimulus	3	11.11111	0.005733
	GO:0040008~regulation of growth	4	14.81481	0.01016
	GO:0051704~multi-organism process	5	18.51852	0.011657
	GO:0032870~cellular response to hormone stimulus	3	11.11111	0.013567
	GO:0010033~response to organic substance	5	18.51852	0.014157
	GO:0007584~response to nutrient	3	11.11111	0.014954
	GO:0006935~chemotaxis	3	11.11111	0.01924
	GO:0042330~taxis	3	11.11111	0.01924
	GO:0006950~response to stress	7	25.92593	0.019661
	GO:0051716~cellular response to stimulus	5	18.51852	0.021767
	GO:0007610~behavior	4	14.81481	0.023768
	GO:0009617~response to bacterium	3	11.11111	0.027299
	GO:0050896~response to stimulus	10	37.03704	0.027319

	GO:0001558~regulation of cell growth	3	11.11111	0.027561
	GO:0031667~response to nutrient levels	3	11.11111	0.028355
	GO:0032387~negative regulation of intracellular transport	2	7.407407	0.029218
	GO:0006916~anti-apoptosis	3	11.11111	0.03079
	GO:0009605~response to external stimulus	5	18.51852	0.031001
	GO:0009991~response to extracellular stimulus	3	11.11111	0.03474
	GO:0032526~response to retinoic acid	2	7.407407	0.043523
	GO:0007017~microtubule-based process	3	11.11111	0.044783
CC	GO:0005576~extracellular region	8	29.62963	0.015489
	GO:0044421~extracellular region part	5	18.51852	0.040395
MF	GO:0005212~structural constituent of eye lens	2	7.407407	0.020027
	GO:0005520~insulin-like growth factor binding	2	7.407407	0.02932
Downregulated Genes				
BP	none			
CC	GO:0005737~cytoplasm	60	50	0.013882
MF	GO:0042808~neuronal Cdc2-like kinase binding	2	1.666667	0.0189
	GO:0016836~hydro-lyase activity	3	2.5	0.031665
	GO:0016835~carbon-oxygen lyase activity	3	2.5	0.047539

Table A.5 Overrepresented gene ontology terms identified among differentially expressed genes (P<0.01 and fold change>2) of the OG1/CON comparison. BP: biological process; CC: cellular component; MF: molecular function

	Term	Count	%	P
Upregulated Genes				
BP	GO:0006954~inflammatory response	13	19.11765	4.08E-09
	GO:0009605~response to external stimulus	19	27.94118	6.89E-09
	GO:0006952~defense response	16	23.52941	1.01E-08
	GO:0009611~response to wounding	15	22.05882	1.27E-08
	GO:0002376~immune system process	18	26.47059	1.69E-07
	GO:0006950~response to stress	22	32.35294	7.70E-07
	GO:0050896~response to stimulus	32	47.05882	9.67E-07
	GO:0007610~behavior	12	17.64706	1.87E-06
	GO:0042221~response to chemical stimulus	18	26.47059	5.51E-06
	GO:0055080~cation homeostasis	9	13.23529	1.57E-05
	GO:0006935~chemotaxis	7	10.29412	3.92E-05
	GO:0042330~taxis	7	10.29412	3.92E-05
	GO:0055066~di-, tri-valent inorganic cation homeostasis	8	11.76471	4.18E-05
	GO:0040011~locomotion	10	14.70588	4.50E-05
	GO:0030003~cellular cation homeostasis	8	11.76471	6.15E-05
	GO:0001817~regulation of cytokine production	7	10.29412	7.80E-05
	GO:0007626~locomotory behavior	8	11.76471	9.89E-05
	GO:0006873~cellular ion homeostasis	9	13.23529	1.05E-04
	GO:0009617~response to bacterium	7	10.29412	1.11E-04
	GO:0055082~cellular chemical homeostasis	9	13.23529	1.18E-04
	GO:0009607~response to biotic stimulus	9	13.23529	1.26E-04
	GO:0048519~negative regulation of biological process	19	27.94118	1.39E-04

GO:0042592~homeostatic process	12	17.64706	1.48E-04
GO:0050801~ion homeostasis	9	13.23529	1.95E-04
GO:0051239~regulation of multicellular organismal process	13	19.11765	2.51E-04
GO:0030005~cellular di-, tri-valent inorganic cation homeostasis	7	10.29412	2.69E-04
GO:0048247~lymphocyte chemotaxis	3	4.411765	3.21E-04
GO:0006955~immune response	11	16.17647	3.37E-04
GO:0030595~leukocyte chemotaxis	4	5.882353	4.18E-04
GO:0065008~regulation of biological quality	16	23.52941	4.45E-04
GO:0019725~cellular homeostasis	9	13.23529	4.69E-04
GO:0060326~cell chemotaxis	4	5.882353	4.88E-04
GO:0048246~macrophage chemotaxis	3	4.411765	5.47E-04
GO:0016477~cell migration	7	10.29412	7.57E-04
GO:0006874~cellular calcium ion homeostasis	6	8.823529	7.75E-04
GO:0048878~chemical homeostasis	9	13.23529	8.70E-04
GO:0055074~calcium ion homeostasis	6	8.823529	8.75E-04
GO:0051707~response to other organism	7	10.29412	9.79E-04
GO:0042742~defense response to bacterium	5	7.352941	0.001004
GO:0006875~cellular metal ion homeostasis	6	8.823529	0.001055
GO:0055065~metal ion homeostasis	6	8.823529	0.001288
GO:0048870~cell motility	7	10.29412	0.001312
GO:0051674~localization of cell	7	10.29412	0.001312
GO:0006916~anti-apoptosis	6	8.823529	0.001316
GO:0050900~leukocyte migration	4	5.882353	0.001487
GO:0048523~negative regulation of cellular process	16	23.52941	0.001594
GO:0042493~response to drug	6	8.823529	0.001623
GO:0048518~positive regulation of biological process	18	26.47059	0.001693

GO:0030593~neutrophil chemotaxis	3	4.411765	0.002271
GO:0006928~cell motion	8	11.76471	0.002604
GO:0043066~negative regulation of apoptosis	7	10.29412	0.002692
GO:0051240~positive regulation of multicellular organismal process	6	8.823529	0.00276
GO:0043069~negative regulation of programmed cell death	7	10.29412	0.002886
GO:0060548~negative regulation of cell death	7	10.29412	0.002926
GO:0051716~cellular response to stimulus	10	14.70588	0.00466
GO:0051605~protein maturation by peptide bond cleavage	4	5.882353	0.004796
GO:0051704~multi-organism process	9	13.23529	0.005149
GO:0001819~positive regulation of cytokine production	4	5.882353	0.005444
GO:0008284~positive regulation of cell proliferation	7	10.29412	0.005778
GO:0050707~regulation of cytokine secretion	3	4.411765	0.006262
GO:0002526~acute inflammatory response	4	5.882353	0.006893
GO:0008219~cell death	9	13.23529	0.007093
GO:0016265~death	9	13.23529	0.007385
GO:0031667~response to nutrient levels	5	7.352941	0.007676
GO:0048145~regulation of fibroblast proliferation	3	4.411765	0.008457
GO:0007204~elevation of cytosolic calcium ion concentration	4	5.882353	0.00946
GO:0016485~protein processing	4	5.882353	0.009935
GO:0048583~regulation of response to stimulus	7	10.29412	0.009983
GO:0012501~programmed cell death	8	11.76471	0.010124
GO:0006953~acute-phase response	3	4.411765	0.010948
GO:0009991~response to extracellular stimulus	5	7.352941	0.011203
GO:0048522~positive regulation of cellular process	15	22.05882	0.011402
GO:0051480~cytosolic calcium ion homeostasis	4	5.882353	0.011442

	GO:0042127~regulation of cell proliferation	9	13.23529	0.011908
	GO:0051604~protein maturation	4	5.882353	0.012517
	GO:0042981~regulation of apoptosis	9	13.23529	0.013422
	GO:0043067~regulation of programmed cell death	9	13.23529	0.014182
	GO:0010941~regulation of cell death	9	13.23529	0.014475
	GO:0048513~organ development	14	20.58824	0.016602
	GO:0030155~regulation of cell adhesion	4	5.882353	0.01705
	GO:0031347~regulation of defense response	4	5.882353	0.019088
	GO:0050708~regulation of protein secretion	3	4.411765	0.022171
	GO:0080134~regulation of response to stress	5	7.352941	0.023179
	GO:0006915~apoptosis	7	10.29412	0.03133
	GO:0050727~regulation of inflammatory response	3	4.411765	0.036538
	GO:0006959~humoral immune response	3	4.411765	0.039204
	GO:0048468~cell development	7	10.29412	0.041457
	GO:0051046~regulation of secretion	4	5.882353	0.046027
	GO:0014823~response to activity	2	2.941176	0.046598
	GO:0048821~erythrocyte development	2	2.941176	0.046598
	GO:0006259~DNA metabolic process	6	8.823529	0.049662
	GO:0050793~regulation of developmental process	7	10.29412	0.049843
CC	GO:0005576~extracellular region	19	27.94118	1.88E-04
	GO:0044421~extracellular region part	11	16.17647	0.002261
	GO:0005615~extracellular space	8	11.76471	0.011893
MF	GO:0001664~G-protein-coupled receptor binding	4	5.882353	0.008416
	GO:0005515~protein binding	41	60.29412	0.008732
	GO:0005539~glycosaminoglycan binding	4	5.882353	0.015733

	GO:0004866~endopeptidase inhibitor activity	4	5.882353	0.017264
	GO:0030414~peptidase inhibitor activity	4	5.882353	0.019883
	GO:0030247~polysaccharide binding	4	5.882353	0.020225
	GO:0001871~pattern binding	4	5.882353	0.020225
	GO:0003796~lysozyme activity	2	2.941176	0.037021
	GO:0004553~hydrolase activity, hydrolyzing O-glycosyl compounds	3	4.411765	0.048811
Downregulated Genes				
BP	GO:0051726~regulation of cell cycle	4	17.3913	0.006806
CC	GO:0043231~intracellular membrane-bounded organelle	16	69.56522	0.021424
	GO:0043227~membrane-bounded organelle	16	69.56522	0.021626
MF	GO:0031406~carboxylic acid binding	3	13.04348	0.015252
	GO:0000062~acyl-CoA binding	2	8.695652	0.020934
	GO:0005504~fatty acid binding	2	8.695652	0.04904

Table A.6 Overrepresented gene ontology terms identified among differentially expressed genes (P<0.01 and fold change>2) of the DEV/OG1 comparison. BP: biological process; CC: cellular component; MF: molecular function

	Term	Count	%	P
Upregulated Genes				
BP	GO:0009408~response to heat	3	12	0.003093
	GO:0010035~response to inorganic substance	4	16	0.00331
	GO:0009266~response to temperature stimulus	3	12	0.006671
	GO:0048523~negative regulation of cellular process	8	32	0.008024
	GO:0042221~response to chemical stimulus	7	28	0.009092
	GO:0048519~negative regulation of biological process	8	32	0.012852
	GO:0040008~regulation of growth	4	16	0.013459
	GO:0009628~response to abiotic stimulus	4	16	0.016496
	GO:0050896~response to stimulus	11	44	0.019487
	GO:0000226~microtubule cytoskeleton organization	3	12	0.01987
	GO:0007010~cytoskeleton organization	4	16	0.025747
	GO:0065007~biological regulation	17	68	0.025906
	GO:0001558~regulation of cell growth	3	12	0.033248
	GO:0006461~protein complex assembly	4	16	0.037502
	GO:0070271~protein complex biogenesis	4	16	0.037502
	GO:0050789~regulation of biological process	16	64	0.041775
	GO:0006996~organelle organization	6	24	0.042058
CC	GO:0005819~spindle	3	12	0.017358
	GO:0015630~microtubule cytoskeleton	4	16	0.038667
	GO:0044421~extracellular region part	5	20	0.040395

MF	GO:0015631~tubulin binding	3	12	0.00998
	GO:0005520~insulin-like growth factor binding	2	8	0.037316
	GO:0008092~cytoskeletal protein binding	4	16	0.039597
	GO:0005515~protein binding	18	72	0.040335
Downregulated Genes				
BP	GO:0042221~response to chemical stimulus	24	26.37363	7.83E-08
	GO:0009611~response to wounding	16	17.58242	8.04E-08
	GO:0006954~inflammatory response	13	14.28571	1.11E-07
	GO:0050896~response to stimulus	40	43.95604	2.30E-07
	GO:0040011~locomotion	14	15.38462	3.22E-07
	GO:0002376~immune system process	20	21.97802	5.97E-07
	GO:0009605~response to external stimulus	19	20.87912	7.77E-07
	GO:0060326~cell chemotaxis	6	6.593407	1.73E-06
	GO:0006935~chemotaxis	9	9.89011	1.83E-06
	GO:0042330~taxis	9	9.89011	1.83E-06
	GO:0006952~defense response	15	16.48352	3.10E-06
	GO:0051674~localization of cell	11	12.08791	4.29E-06
	GO:0048870~cell motility	11	12.08791	4.29E-06
	GO:0007610~behavior	13	14.28571	5.31E-06
	GO:0006950~response to stress	24	26.37363	9.65E-06
	GO:0007626~locomotory behavior	10	10.98901	1.26E-05
	GO:0016477~cell migration	10	10.98901	1.33E-05
	GO:0042592~homeostatic process	15	16.48352	2.99E-05
	GO:0009607~response to biotic stimulus	11	12.08791	3.01E-05
	GO:0030595~leukocyte chemotaxis	5	5.494505	4.03E-05
	GO:0001817~regulation of cytokine production	8	8.791209	4.43E-05

GO:0030593~neutrophil chemotaxis	4	4.395604	1.07E-04
GO:0055080~cation homeostasis	9	9.89011	1.22E-04
GO:0006873~cellular ion homeostasis	10	10.98901	1.41E-04
GO:0019725~cellular homeostasis	11	12.08791	1.51E-04
GO:0055082~cellular chemical homeostasis	10	10.98901	1.59E-04
GO:0006928~cell motion	11	12.08791	1.76E-04
GO:0050900~leukocyte migration	5	5.494505	2.23E-04
GO:0006955~immune response	13	14.28571	2.28E-04
GO:0055066~di-, tri-valent inorganic cation homeostasis	8	8.791209	2.51E-04
GO:0050801~ion homeostasis	10	10.98901	2.75E-04
GO:0030003~cellular cation homeostasis	8	8.791209	3.62E-04
GO:0009617~response to bacterium	7	7.692308	5.18E-04
GO:0048247~lymphocyte chemotaxis	3	3.296703	5.60E-04
GO:0006916~anti-apoptosis	7	7.692308	7.29E-04
GO:0032675~regulation of interleukin-6 production	4	4.395604	8.72E-04
GO:0042493~response to drug	7	7.692308	9.33E-04
GO:0048246~macrophage chemotaxis	3	3.296703	9.53E-04
GO:0051239~regulation of multicellular organismal process	14	15.38462	0.001062
GO:0051716~cellular response to stimulus	13	14.28571	0.00107
GO:0006953~acute-phase response	4	4.395604	0.001189
GO:0030005~cellular di-, tri-valent inorganic cation homeostasis	7	7.692308	0.001206
GO:0010033~response to organic substance	12	13.18681	0.001261
GO:0001819~positive regulation of cytokine production	5	5.494505	0.001265
GO:0048878~chemical homeostasis	10	10.98901	0.001375
GO:0008284~positive regulation of cell proliferation	9	9.89011	0.00142
GO:0002526~acute inflammatory response	5	5.494505	0.001733
GO:0001944~vasculature development	7	7.692308	0.00201

GO:0045408~regulation of interleukin-6 biosynthetic process	3	3.296703	0.002369
GO:0051789~response to protein stimulus	5	5.494505	0.00239
GO:0043066~negative regulation of apoptosis	8	8.791209	0.002504
GO:0043069~negative regulation of programmed cell death	8	8.791209	0.002708
GO:0006874~cellular calcium ion homeostasis	6	6.593407	0.002712
GO:0060548~negative regulation of cell death	8	8.791209	0.00275
GO:0055074~calcium ion homeostasis	6	6.593407	0.003046
GO:0080134~regulation of response to stress	7	7.692308	0.003111
GO:0065008~regulation of biological quality	17	18.68132	0.003418
GO:0006875~cellular metal ion homeostasis	6	6.593407	0.00364
GO:0051179~localization	27	29.67033	0.003937
GO:0051707~response to other organism	7	7.692308	0.004108
GO:0055065~metal ion homeostasis	6	6.593407	0.004404
GO:0030155~regulation of cell adhesion	5	5.494505	0.005782
GO:0006986~response to unfolded protein	4	4.395604	0.006124
GO:0031347~regulation of defense response	5	5.494505	0.006716
GO:0050727~regulation of inflammatory response	4	4.395604	0.007393
GO:0048518~positive regulation of biological process	20	21.97802	0.00743
GO:0048513~organ development	18	19.78022	0.007506
GO:0042127~regulation of cell proliferation	11	12.08791	0.007736
GO:0051704~multi-organism process	10	10.98901	0.008999
GO:0051240~positive regulation of multicellular organismal process	6	6.593407	0.009066
GO:0001568~blood vessel development	6	6.593407	0.009218
GO:0048583~regulation of response to stimulus	8	8.791209	0.010833
GO:0048519~negative regulation of biological process	18	19.78022	0.011237
GO:0001701~in utero embryonic development	5	5.494505	0.013659
GO:0048585~negative regulation of response to stimulus	4	4.395604	0.015555

	GO:0042060~wound healing	5	5.494505	0.01792
	GO:0007204~elevation of cytosolic calcium ion concentration	4	4.395604	0.020007
	GO:0042742~defense response to bacterium	4	4.395604	0.020973
	GO:0010564~regulation of cell cycle process	4	4.395604	0.021965
	GO:0048523~negative regulation of cellular process	16	17.58242	0.023803
	GO:0051480~cytosolic calcium ion homeostasis	4	4.395604	0.024024
	GO:0048514~blood vessel morphogenesis	5	5.494505	0.024772
	GO:0048522~positive regulation of cellular process	17	18.68132	0.027909
	GO:0007169~transmembrane receptor protein tyrosine kinase signaling pathway	5	5.494505	0.029972
	GO:0045410~positive regulation of interleukin-6 biosynthetic process	2	2.197802	0.03105
	GO:0007167~enzyme linked receptor protein signaling pathway	6	6.593407	0.033556
	GO:0050671~positive regulation of lymphocyte proliferation	3	3.296703	0.033671
	GO:0032946~positive regulation of mononuclear cell proliferation	3	3.296703	0.034801
	GO:0007088~regulation of mitosis	3	3.296703	0.034801
	GO:0070665~positive regulation of leukocyte proliferation	3	3.296703	0.034801
	GO:0051783~regulation of nuclear division	3	3.296703	0.034801
	GO:0002684~positive regulation of immune system process	5	5.494505	0.036246
	GO:0045785~positive regulation of cell adhesion	3	3.296703	0.039469
	GO:0022414~reproductive process	9	9.89011	0.045467
	GO:0007346~regulation of mitotic cell cycle	4	4.395604	0.045581
	GO:0048745~smooth muscle tissue development	2	2.197802	0.046216
	GO:0000003~reproduction	9	9.89011	0.046941
	GO:0051222~positive regulation of protein transport	3	3.296703	0.048168
CC	GO:0044421~extracellular region part	14	15.38462	0.001339
	GO:0005615~extracellular space	11	12.08791	0.002927
	GO:0005576~extracellular region	21	23.07692	0.002965

	GO:0034358~plasma lipoprotein particle	3	3.296703	0.014314
	GO:0032994~protein-lipid complex	3	3.296703	0.014314
MF	GO:0004866~endopeptidase inhibitor activity	6	6.593407	6.69E-04
	GO:0030414~peptidase inhibitor activity	6	6.593407	8.52E-04
	GO:0004867~serine-type endopeptidase inhibitor activity	5	5.494505	0.001008
	GO:0005515~protein binding	51	56.04396	0.007611
	GO:0004857~enzyme inhibitor activity	6	6.593407	0.009736
	GO:0005102~receptor binding	11	12.08791	0.009742
	GO:0001664~G-protein-coupled receptor binding	4	4.395604	0.016446
	GO:0005539~glycosaminoglycan binding	4	4.395604	0.030077
	GO:0001871~pattern binding	4	4.395604	0.03826
	GO:0030247~polysaccharide binding	4	4.395604	0.03826
	GO:0003796~lysozyme activity	2	2.197802	0.047188

Table A.7 List of all differentially expressed genes (P<0.01 and fold change>2) for the HI/CON comparison. Fold change indicates expression level larger than 2 is up-regulation and expression level less than 0.5 is down-regulation.

Gene Name	Public Accession	Human Protein	P Value	Fold Change
MYBPC2	XM_001494408	NP_004524.3	0.0017275	0.0699979
NULL	NULL	NULL	0.0003498	0.1054814
SLC24A2	XM_001495010	NP_065077.1	0.004872	0.1442599
NULL	NULL	NULL	0.0013554	0.1473677
TIMM9	XM_001497047	NP_036592.1	0.0016536	0.1505449
NULL	NULL	NULL	0.0011128	0.1511689
NULL	NULL	NULL	0.0054514	0.1542023
SDF2L1	XM_001493091	NP_071327.2	0.0056883	0.1580587
RER1	NULL	NP_008964.3	0.0064773	0.1701455
RNF32	XM_001504692	NP_112198.1	0.0095354	0.1785734
NULL	CX603169	NULL	0.0078371	0.1887082
FANCF	NULL	NP_073562.1	0.0079414	0.1900315
C17orf64	XM_001501083	NP_859058.1	0.0025644	0.1916201
PSMD1	XM_001498019	NP_002798.2	0.0026899	0.1937769
C16orf77	XM_001500794	NP_689669.1	0.0026411	0.2000197
C16orf46	XM_001501937	NP_689550.2	0.0081165	0.2059071
NULL	CX593149	NULL	0.0093932	0.207234
PACSIN3	XM_001490695	NP_057307.2	0.0016852	0.2102296
CYP2S1	XM_001498467	NP_085125.1	0.0036436	0.2138021
NULL	NULL	NULL	0.0045124	0.2146746
NULL	NULL	NULL	0.0018411	0.2161441
ATXN7L1	XM_001491802	NP_065776.1	0.0071196	0.2180239
PIGS	XM_001504143	NP_149975.1	0.0054443	0.2185866
EGLN2	XM_001499481	NP_444274.1	0.0094036	0.2222128
MRPL18	XM_001500639	NP_054880.2	0.005535	0.2298689
PDE4B	XM_001500306	NP_001032417.1	0.0066108	0.2408653
PRKRA	XM_001497357	NP_003681.1	0.0039884	0.2409602
WDR34	XM_001499860	NP_443076.2	0.0074615	0.2486677
NULL	NULL	NULL	0.0017686	0.2571222
NULL	NULL	NULL	0.0005789	0.2643645
REEP3	XM_001502396	NP_001001330.1	0.0031271	0.2655691
EID1	DN506034	NP_055150.1	0.0014789	0.2659805
NULL	XR_036460	NULL	0.0099968	0.266661
LASP1	XM_001498270	NP_006139.1	0.0071777	0.26801

NULL	NULL	NULL	0.0044389	0.2787338
NULL	NULL	NULL	0.0013782	0.2822127
NULL	CX595121	NULL	0.0063358	0.2849044
NULL	NULL	NULL	0.0040474	0.2903837
WDR16	XM_001504842	NP_659491.4	0.0042109	0.2920273
CIB1	XM_001502860	NP_006375.2	0.0039233	0.2922247
CXCL14	XM_001502713	NP_004878.2	0.0049898	0.2933628
NULL	NULL	NULL	0.0015356	0.2975359
TCF12	XM_001500594	NP_996919.1	0.0054357	0.2999355
MGMT	XM_001488425	NP_002403.1	0.0022102	0.3012046
CKMT2	NULL	NP_001093206.1	0.0087914	0.3032878
NULL	CX603184	NULL	0.0065575	0.3035236
C16orf5	XM_001502354	NP_037531.2	0.002641	0.3041797
NULL	NULL	NULL	0.0007023	0.3046916
DDB2	XM_001490725	NP_000098.1	0.0014547	0.308985
DENND4A	XM_001497645	NP_005839.2	0.0061562	0.3125341
DAPP1	DN504745	NP_055210.2	0.0011481	0.318897
KLHL13	XM_001488075	NP_277030.2	0.0056754	0.3198587
SH3BP1	XM_001499540	NP_061830.3	0.0056837	0.3205051
CAST	XM_001503694	NP_001035907.1	0.0033652	0.3205195
DLX3	XM_001499545	NP_005211.1	0.0057972	0.3214089
RAD23B	XM_001492372	NP_002865.1	0.0011974	0.3216039
GFRA2	XM_001489919	NP_001486.4	0.0026619	0.3234562
SH3BGRL	XM_001490406	NP_003013.1	0.0062632	0.3265332
SCHIP1	CX601415	NP_055390.1	0.0062951	0.3288063
NULL	NULL	NULL	0.0065943	0.3306403
39701	XM_001492722	NP_653311.1	0.0068402	0.3344442
ATP13A4	XM_001498805	NP_115655.2	0.0079657	0.3356457
AVPI1	XM_001501347	NP_068378.1	0.009536	0.3357656
NULL	NULL	NULL	0.0081486	0.3363076
NULL	NULL	NULL	0.0058221	0.3368466
C10orf141	XM_001503213	NP_001034851.1	0.0086793	0.3395423
FAH	XM_001487834	NP_000128.1	0.0023979	0.3403649
NULL	NULL	NULL	0.0076579	0.3405396
NULL	NULL	NULL	0.0063836	0.347444
NXN	XM_001502168	NP_071908.2	0.0085644	0.3478976
CD1C	XM_001490135	NP_001756.2	0.0016166	0.3487102
HEPH	XM_001504864	NP_620074.1	0.0098591	0.3490278
NULL	XM_001492880	NULL	0.0044021	0.3505891
NULL	NULL	NULL	0.0022677	0.3528399

NULL	NULL	NULL	0.0085905	0.3577692
COL4A3BP	XM_001504676	NP_005704.1	0.0045915	0.3623331
NDRG2	XM_001505150	NP_963833.1	0.0059321	0.3638133
NULL	NULL	NULL	0.0014601	0.3651931
TFPI	XM_001498692	NP_006278.1	0.0091937	0.3657985
ANAPC11	DN504808	NP_001002249.1	0.0092178	0.3672803
ADAMDEC1	XM_001491607	NP_055294.1	0.0086452	0.3685127
ANKRD34B	XM_001504644	NP_001004441.1	0.0029363	0.369124
NULL	NULL	NULL	0.0035139	0.379051
SETDB2	XM_001489997	NP_114121.1	0.0032434	0.3810122
NULL	NULL	NULL	0.0017887	0.3849447
NULL	NULL	NULL	0.0035138	0.3854789
NULL	NULL	NULL	0.0064604	0.3866686
ABHD12	XM_001490613	NP_001035937.1	0.0093963	0.3904888
COL11A1	CX601563	NP_542196.2	0.0073889	0.3923163
NULL	CX600577	NULL	0.0090658	0.394568
PROM2	NULL	NP_653308.1	0.0023866	0.3973588
MBIP	XM_001491919	NP_057670.1	0.0058828	0.3993639
NULL	CX603925	NULL	0.0043601	0.4018999
FXYD5	XM_001491379	NP_054883.3	0.0098531	0.4019916
CPA6	XM_001494527	NP_065094.2	0.0066739	0.4020393
LPCAT2	XM_001490683	NP_060309.2	0.0073665	0.4074338
CFP	XM_001492656	NP_002612.1	0.0076536	0.4130272
NULL	XM_001504970	NULL	0.0061778	0.4167525
GRB7	XM_001501037	NP_001025173.1	0.0027385	0.4175093
NR2E1	XM_001502023	NP_003260.1	0.0091141	0.4221142
HES2	XM_001496558	NP_061962.2	0.0097561	0.4225404
LPIN1	XM_001502170	NP_663731.1	0.0082695	0.4303699
ALS2CR8	XM_001497530	NP_001098056.1	0.0045846	0.4304722
CRLS1	XM_001496092	NP_061968.1	0.003587	0.432384
RPE	XM_001488217	NP_954699.1	0.0096834	0.4347594
RPL17	XM_001493896	NP_000976.1	0.0080591	0.4399097
MIER2	XM_001497040	NP_060020.1	0.0080167	0.4414595
SEC11C	NULL	NP_150596.1	0.0070691	0.4417672
GLUL	NULL	NP_001028228.1	0.0053041	0.4426383
C13orf30	XM_001492527	NP_872314.1	0.0079363	0.4460854
KLHL20	XM_001493014	NP_055273.2	0.005155	0.4567624
EIF3F	CD468288	NP_003745.1	0.0057162	0.4573036
ASB17	XM_001497338	NP_543144.1	0.0098928	0.4708352
NULL	NULL	NULL	0.0084293	0.4715522

S100A1	XM_001494870	NP_006262.1	0.0082842	0.4727981
RCBTB2	XM_001489540	NP_001259.1	0.0058783	0.4741265
SC65	CX601224	NP_006446.1	0.0096569	0.4756731
PLCE1	XM_001502375	NP_057425.3	0.0059059	0.4761308
FABP2	AY536518	NP_000125.1	0.006261	0.476338
POU2AF1	XM_001501588	NP_006226.1	0.009337	0.477636
SELENBP1	NULL	NP_003935.2	0.0065238	0.4835818
LILRA5	AB120409	NP_067073.1	0.0065398	0.4844157
39517	XM_001495682	NP_001094345.1	0.008643	0.4858746
NULL	BM781161	NULL	0.0073275	0.4878836
LOC92345	XM_001498445	NP_612395.1	0.007841	0.4957594
NULL	DN508773	NULL	0.0085115	0.4965929
NULL	CX604543	NULL	0.0072708	2.0317136
GALM	XM_001500603	NP_620156.1	0.0071312	2.0410974
ZNF283	XM_001500016	NP_862828.1	0.0081688	2.0537128
RPS3A	XM_001490864	NP_000997.1	0.0093609	2.0562014
NULL	NULL	NULL	0.0067949	2.0970089
NULL	NULL	NULL	0.0088036	2.1053077
RLBP1L1	XM_001496222	NP_775790.1	0.0068557	2.1151309
SYF2	XM_001501117	NP_056299.1	0.0069305	2.1293155
NULL	NULL	NULL	0.0054865	2.1419173
RGS18	XR_035866	NP_570138.1	0.0082082	2.1520262
NULL	NULL	NULL	0.0058114	2.1797717
H3F3A	XM_001489242	NP_002098.1	0.0046879	2.1893185
SFXN3	XM_001500003	NP_112233.2	0.0096333	2.2047023
CYCS	XM_001498822	NP_061820.1	0.0063539	2.209556
NULL	NULL	NULL	0.0058887	2.2145204
RNF135	XM_001501660	NP_115698.3	0.0079646	2.2329259
CACYBP	XM_001493405	NP_055227.1	0.0043275	2.2517425
OR1L6	XM_001500963	NP_001004453.1	0.0065601	2.2640971
SULT1C4	XM_001504131	NP_006579.2	0.0071682	2.3009472
SIGLEC10	XM_001496570	NP_149121.2	0.0039808	2.3181673
NULL	NULL	NULL	0.006242	2.3424452
AOF1	XM_001496578	NP_694587.3	0.007793	2.3720352
NPHP4	XM_001497162	NP_055917.1	0.0062397	2.4110565
TRPM3	XM_001488577	NP_001007472.2	0.0033413	2.41156
NULL	NULL	NULL	0.0026967	2.4204938
GAPDH	XM_001488655	NP_002037.2	0.0094886	2.4477494
SF3B14	XM_001499114	NP_057131.1	0.0029253	2.4581919
NULL	NULL	NULL	0.0029608	2.4804581

NULL	NULL	NULL	0.0044353	2.5240682
NULL	BI961659	NULL	0.0053127	2.5607697
NULL	NULL	NULL	0.0046999	2.5902993
NULL	NULL	NULL	0.001759	2.6107841
OR5AK2	XM_001496889	NP_001005323.1	0.0030854	2.6149144
HSPA8	AF411802	NP_006588.1	0.0029975	2.6182568
SFN	XM_001504058	NP_006133.1	0.0035723	2.623244
C21orf56	XM_001488132	NP_115637.3	0.0092659	2.662824
SILV	XM_001504795	NP_008859.1	0.0093626	2.7194637
NULL	NULL	NULL	0.0014602	2.7591903
STC1	XM_001493195	NP_003146.1	0.0029398	2.782161
OR7G2	XM_001500467	NP_001005193.1	0.0022386	2.8307113
NULL	XM_001489334	NULL	0.0014855	2.8696375
NULL	NULL	NULL	0.0093799	2.885379
DNAJC8	XM_001503994	NP_055095.2	0.007485	2.890405
GAPDH	XR_036506	NP_002037.2	0.004779	2.9062039
PGAM1	XM_001500395	NP_002620.1	0.0039137	2.9154883
RAD17	XM_001504700	NP_579917.1	0.0073087	2.9186752
NPAS1	XM_001500899	NP_002508.2	0.0084239	2.9451486
BMF	XM_001503570	NP_001003940.1	0.0084744	2.9649022
OR5M3	XM_001496132	NP_001004742.1	0.0038709	2.9693139
APOA1	XM_001502469	NP_000030.1	0.0070588	2.9704195
HLA-DQA1	XM_001492558	NP_002113.2	0.0089639	2.9733437
GPR97	XM_001494146	NP_740746.3	0.0037309	2.9777741
NULL	CX602448	NULL	0.006728	2.9791469
NULL	CX601472	NULL	0.0018201	2.9905411
LRRC37B	XM_001494937	NP_443120.2	0.0089115	3.0183093
NULL	NULL	NULL	0.0032496	3.0774836
ACPL2	XM_001494614	NP_001032249.1	0.0034547	3.1550837
VSIG4	XM_001496244	NP_009199.1	0.0074554	3.1763793
GAPDH	XM_001502360	NP_002037.2	0.0096203	3.1938999
NULL	CD465724	NULL	0.0070584	3.3209467
TTN	NULL	NP_596869.3	0.0086814	3.339381
NULL	DN504249	NULL	0.007513	3.3861793
EPHA7	XM_001503790	NP_004431.1	0.0061345	3.3869069
NULL	CX603926	NULL	0.0065164	3.3872744
ZBTB11	XR_036400	NP_055230.1	0.0059493	3.4305652
SNRPB	XM_001497470	NP_003082.1	0.0042357	3.4408721
C1orf54	XM_001491679	NP_078855.1	0.0046856	3.449926
KLHL3	XM_001504326	NP_059111.1	0.0034031	3.4500373

OR2L2	XM_001496326	NP_001004686.1	0.0053988	3.4634571
RANGAP1	XM_001500278	NP_002874.1	0.0050138	3.4810165
VN1R4	XM_001495521	NP_776256.2	0.0042569	3.4827935
BNIP3	NULL	NP_004043.2	0.0072418	3.4921979
NULL	NULL	NULL	0.008618	3.5450256
NULL	NULL	NULL	0.0038346	3.6094531
SDC3	XM_001500186	XP_945760.2	0.0084942	3.6372938
KRT15	XM_001491980	NP_002266.2	0.0016547	3.6386009
CD33	XM_001496657	NP_001763.3	0.0033165	3.6905345
HSPA8	NULL	NP_006588.1	0.0066182	3.7094358
NPM1	XM_001503118	NP_002511.1	0.005857	3.7129388
POLM	XM_001495659	NP_037416.1	0.007816	3.7419811
SARDH	XM_001498978	NP_009032.2	0.0054667	3.8531574
NULL	NULL	NULL	0.0033287	3.9062824
RNF138	XM_001496619	NP_057355.2	0.0020209	3.9528493
ADAMTS1	AF541975	NP_008919.3	0.002452	4.024977
NULL	NULL	NULL	0.0038395	4.1332205
PHLDB1	XM_001500987	NP_055972.1	0.0025142	4.1600044
PEO1	XM_001499940	NP_068602.2	0.0032827	4.2657155
SPRR1B	XM_001494012	NP_003116.2	0.0040974	4.357908
RANBP6	XM_001493360	NP_036548.1	0.0049244	4.3649003
NULL	NULL	NULL	0.00289	4.4563701
HDC	XM_001499648	NP_002103.2	0.0025542	4.4688984
NRIP2	XM_001490793	NP_113662.1	0.0025741	4.5564965
LRRTM3	XM_001503559	NP_821079.3	0.0045826	4.6536439
TLE6	XM_001492284	NP_079036.1	0.0017777	4.7758165
ZNF264	XM_001492087	NP_003408.1	0.0095766	4.7787081
DNAJB1	NULL	NP_006136.1	0.0093279	4.8424844
SNW1	XM_001492123	NP_036377.1	0.0030075	4.8844098
FOSL1	XM_001494797	NP_005429.1	0.0090406	4.9200385
MAPK14	XM_001494719	NP_620581.1	0.0002011	4.95007
ZNF75A	XM_001499142	NP_694573.1	0.0019125	4.9926437
TULP3	XM_001490880	NP_003315.2	0.0017377	5.0402268
NULL	NULL	NULL	0.0032701	5.0787827
NULL	NULL	NULL	0.0083796	5.1162394
LMOD2	XM_001502348	NP_997046.1	0.0081939	5.1764298
NULL	NULL	NULL	0.0079539	5.2579312
S100A2	CX598422	NP_005969.1	0.0064023	5.3878673
C17orf79	CX605748	NP_060875.1	0.0073615	5.4793567
C16orf44	XM_001502352	NP_079007.2	0.0020625	5.5934822

HEMGN	XM_001504109	NP_060907.2	0.0008385	5.9338524
EIF1AX	XM_001492752	NP_001403.1	0.0065925	6.5976465
PTPRQ	XM_001492869	XP_945428.2	5.77E-05	6.6616652
MORN3	XM_001496205	NP_776254.2	0.0007549	6.8635457
RILPL2	DN504908	NP_659495.1	0.0047256	7.061033
SUGT1	XM_001492933	NP_006695.1	0.0042123	7.5801031
CRTAC1	XM_001501238	NP_060528.3	0.0008	7.6519913
NULL	NULL	NULL	7.77E-05	38.105349

Table A.8 Overrepresented gene ontology terms identified among differentially expressed genes (P<0.01 and fold change>2) of the HI/CON comparison. BP: biological process; CC: cellular component; MF: molecular function

	Term	Count	%	P
Upregulated Genes				
BP	GO:0002504~antigen processing and presentation of peptide or polysaccharide antigen via MHC class II	6	7.0588235	6.37E-07
	GO:0019882~antigen processing and presentation	6	7.0588235	6.39E-05
	GO:0006955~immune response	9	10.588235	0.023821
	GO:0051726~regulation of cell cycle	6	7.0588235	0.0268143
	GO:0008285~negative regulation of cell proliferation	6	7.0588235	0.0369433
	GO:0050896~response to stimulus	26	30.588235	0.0380858
	GO:0000377~RNA splicing, via transesterification reactions with bulged adenosine as nucleophile	4	4.7058824	0.0432814
	GO:0000375~RNA splicing, via transesterification reactions	4	4.7058824	0.0432814
	GO:0000398~nuclear mRNA splicing, via spliceosome	4	4.7058824	0.0432814
	GO:0051085~chaperone mediated protein folding requiring cofactor	2	2.3529412	0.0498665
CC	GO:0042613~MHC class II protein complex	6	7.0588235	2.36E-07
	GO:0042611~MHC protein complex	6	7.0588235	7.51E-06
	GO:0005829~cytosol	13	15.294118	0.0232556
	GO:0044428~nuclear part	15	17.647059	0.0483506
MF	GO:0032395~MHC class II receptor activity	6	7.0588235	3.98E-08
	GO:0060089~molecular transducer activity	21	24.705882	0.0128493
	GO:0004871~signal transducer activity	21	24.705882	0.0128493
	GO:0004872~receptor activity	18	21.176471	0.0143354
	GO:0004888~transmembrane receptor activity	14	16.470588	0.0187251

Downregulated Genes

BP	GO:0006508~proteolysis	12	13.483146	0.0172403
	GO:0051716~cellular response to stimulus	10	11.235955	0.0230598
	GO:0033554~cellular response to stress	8	8.988764	0.024984
	GO:0043632~modification-dependent macromolecule catabolic process	8	8.988764	0.0267112
	GO:0019941~modification-dependent protein catabolic process	8	8.988764	0.0267112
	GO:0042176~regulation of protein catabolic process	3	3.3707865	0.0288718
	GO:0051603~proteolysis involved in cellular protein catabolic process	8	8.988764	0.0328885
	GO:0044257~cellular protein catabolic process	8	8.988764	0.0336583
	GO:0051247~positive regulation of protein metabolic process	5	5.6179775	0.0354814
	GO:0030163~protein catabolic process	8	8.988764	0.0388161
	GO:0006974~response to DNA damage stimulus	6	6.741573	0.0415765
CC	GO:0044424~intracellular part	61	68.539326	0.0083676
	GO:0005622~intracellular	61	68.539326	0.0242054
	GO:0005829~cytosol	12	13.483146	0.0465824
MF	GO:0030674~protein binding, bridging	4	4.494382	0.009764
	GO:0005070~SH3/SH2 adaptor activity	3	3.3707865	0.0221178
	GO:0060090~molecular adaptor activity	3	3.3707865	0.0394082
	GO:0030234~enzyme regulator activity	9	10.11236	0.04201

Table A.9 List of all differentially expressed genes (P<0.01 and fold change>2) for the 12 h/CON comparison. Fold change indicates expression level larger than 2 is up-regulation and expression level less than 0.5 is down-regulation.

Gene Name	Public Accession	Human Protein	P Value	Fold Change
NULL	DN510842	NULL	0.0010388	0.2285384
NULL	NULL	NULL	0.0067226	0.2302249
NULL	NULL	NULL	0.007491	0.2430798
CKM	XM_001502522	NP_001815.2	0.0011477	0.2496086
LOC284890	XM_001489526	XP_208261.5	0.0080739	0.2521315
PTGFR	DQ385610	NP_000950.1	0.0082772	0.2551626
COMMD2	DN509689	NP_057178.2	0.0086175	0.2600997
OR7A10	XM_001492035	NP_001005190.1	0.0028144	0.2636787
NULL	NULL	NULL	0.0091277	0.2672035
ZNF451	XM_001499700	NP_001026794.1	0.0093143	0.2697189
DHRS2	XM_001489482	NP_005785.1	0.0016674	0.2697426
LOC26010	XM_001502795	NP_001093893.1	0.0032249	0.2907372
NULL	NULL	NULL	0.0059763	0.2977389
NULL	CX604266	NULL	0.0005164	0.2977975
TAOK3	XM_001490545	NP_057365.3	0.0021094	0.2981413
LGALS4	XM_001497350	NP_006140.1	0.0061987	0.3355403
RPS6KB2	XM_001497573	NP_003943.2	0.0028872	0.3372703
NULL	NULL	NULL	0.0082611	0.3478251
MAGED2	XM_001496158	NP_803182.1	0.0036666	0.3606807
BAX	NULL	NP_620119.1	0.0010662	0.3648417
AP1S1	XM_001492538	NP_001274.1	0.004469	0.373292
OR5M3	XM_001496132	NP_001004742.1	0.0070959	0.3799617
NULL	CD464177	NULL	0.0077033	0.3919731
RGS1	CD471812	NP_002913.3	0.0085076	0.4033988
39509	XM_001487921	NP_001005415.1	0.0087391	0.4061091
EBI2	XM_001491948	NP_004942.1	0.0069198	0.4141028
39701	XM_001492722	NP_653311.1	0.0053352	0.4143381
NULL	NULL	NULL	0.0069208	0.4160444
PPP1R16B	XM_001502590	NP_056383.1	0.0069937	0.4193189
ARPC5L	XM_001502042	NP_112240.1	0.0010492	0.4216098
SPHKAP	XM_001494233	NP_085126.1	0.002936	0.4224087
TTC25	XM_001496697	NP_113609.1	0.0083073	0.4581841
BTBD11	NULL	NP_001017523.1	0.0098254	0.4589088

MYO1E	CD470665	NP_004989.2	0.0012028	0.469526
ZNF75A	XM_001499142	NP_694573.1	0.0074739	0.4821721
NULL	NULL	NULL	0.0026163	0.4840725
FAM83B	XM_001503204	NP_001010872.1	0.0033558	0.4920167
LY96	AY398685	NP_056179.1	0.0095719	0.4975637
SLC25A36	XM_001494830	NP_001098117.1	0.0077008	2.00178
IGLL1	XM_001492822	NP_064455.1	0.0064467	2.0102886
SLC27A2	XM_001502007	NP_003636.1	0.0054066	2.1125642
PHF21B	XM_001488104	NP_612424.1	0.0027205	2.158315
SMS	XM_001493443	NP_004586.2	0.0073773	2.1605126
SFRS17A	XM_001499533	NP_005079.2	0.0095884	2.1943928
CD19	CX592103	NP_001761.3	0.0090144	2.2204638
ZBP1	XM_001489797	NP_110403.1	0.005605	2.2305589
NULL	NULL	NULL	0.0029069	2.2419775
UGT2B4	XM_001501836	NP_066962.2	0.0003995	2.2691945
IARS	XM_001491121	NP_002152.2	0.0090226	2.4354471
MED7	DN510032	NP_001094286.1	0.0089484	2.4395096
OGFR	CX594651	NP_031372.2	0.0071332	2.4645238
HDHD2	XM_001498811	NP_115500.1	0.0084142	2.4785925
RC3H2	XM_001502327	NP_001094058.1	0.0043159	2.6217118
ZNF30	XM_001493964	NP_919306.2	0.0042361	2.6287018
EZH2	XM_001504629	NP_004447.2	0.0081039	2.6480484
NULL	NULL	NULL	0.0058402	2.653315
NULL	CX593986	NULL	0.0073218	2.8820654
CCDC67	XM_001491708	NP_857596.2	0.0030146	2.8918394
CBARA1	XM_001503797	NP_006068.2	0.0024634	3.1009249
PARP6	XM_001494491	NP_064599.2	0.004096	3.1867118
CXCL2	AF053497	NP_002080.1	0.0023269	3.2086441
NULL	CX596707	NULL	0.0022732	3.316525
NULL	CX601068	NULL	0.0006656	3.3824369
NULL	XR_035808	NULL	0.0023138	3.4532776
BAIAP3	XM_001497570	NP_003924.2	0.0041313	3.6134225
MITD1	XM_001490447	NP_620153.1	0.0013292	3.7270823
NULL	NULL	NULL	0.0021472	3.9077373
PSIP1	DQ873682	NP_150091.2	0.0081126	3.9570482
GLMN	XM_001492771	NP_444504.1	0.0034141	4.3715151
IFI30	XM_001500556	NP_006323.2	0.0058657	4.6637277
NULL	NULL	NULL	0.0048743	5.1623082

Table A.10 List of all differentially expressed genes (P<0.01 and fold change>2) for the 24 h/CON comparison. Fold change indicates expression level larger than 2 is up-regulation and expression level less than 0.5 is down-regulation.

Gene Name	Public Accession	Human Protein	P Value	Fold Change
NDUFB3	XM_001503625	NP_002482.1	0.0008969	0.0955369
NULL	CX592434	NULL	0.0038225	0.1903698
PSMA4	XM_001489071	NP_001096137.1	0.0062061	0.1979544
NKX3-1	XM_001491242	NP_006158.2	0.0065995	0.2380197
NULL	NULL	NULL	0.0017236	0.2401955
SLC5A6	XM_001502487	NP_066918.1	0.0020126	0.254905
LOC650780	CD466835	XP_944952.1	0.0080678	0.2568331
NEB	NULL	NP_004534.2	0.0017782	0.2730702
ANKRD26	CX601264	NP_055730.2	0.0015177	0.3134063
NULL	NULL	NULL	0.0006725	0.3156989
EIF2AK4	XM_001501267	NP_001013725.2	0.0042304	0.3168934
TNNT1	NULL	NP_003274.2	0.0047804	0.3203982
NRBF2	XM_001502366	NP_110386.2	0.0040922	0.3216879
NPHP4	XM_001497162	NP_055917.1	0.0008924	0.3311557
ISCU	NULL	NP_998760.1	0.005719	0.3365259
NULL	CX601609	NULL	0.0069302	0.3551368
GMPS	XM_001488228	NP_003866.1	0.0070444	0.3603534
C9orf32	CD464166	NP_054783.2	0.0062808	0.3615934
CADPS	XM_001490163	NP_003707.2	0.0072232	0.3617686
NULL	NULL	NULL	0.0062248	0.3669122
NULL	NULL	NULL	0.005749	0.3713646
NULL	NULL	NULL	0.0040174	0.3810504
SAC3D1	NULL	NP_037431.3	0.0091259	0.3927282
PLA2G12A	XM_001502916	NP_110448.2	0.0049632	0.4025784
NSUN3	XM_001502968	NP_071355.1	0.0091709	0.4054896
NULL	NULL	NULL	0.0081703	0.4073516
C14orf140	XM_001491724	NP_078919.2	0.0099415	0.4102526
NULL	NULL	NULL	0.0087261	0.4302952
NULL	DN509452	NULL	0.0058838	0.4332689
STX8	XM_001503237	NP_004844.1	0.0042372	0.4365832
FAM71F1	XM_001501602	NP_115988.1	0.0053475	0.4379389
SLC25A15	XM_001499022	NP_055067.1	0.0054855	0.4407576
HFE	XM_001505039	NP_000401.1	0.0096566	0.4470755

LOC90113	XM_001497176	XP_291077.4	0.0033299	0.456717
NULL	NULL	NULL	0.0091437	0.4589917
LTBP1	XM_001500182	NP_996826.1	0.0038256	0.4673029
MBNL3	XM_001488749	NP_060858.2	0.0012634	0.4701863
NULL	NULL	NULL	0.008789	0.4712081
HOXB6	XM_001502088	NP_061825.2	0.0083336	0.4737989
RG9MTD2	XM_001498449	NP_689505.1	0.0085612	0.4802059
FABP9	XM_001489404	NP_001073995.1	0.0015799	0.4866081
CFP	XM_001492656	NP_002612.1	0.004921	0.4869356
FAM22G	XM_001492443	NP_001038942.1	0.0066396	0.4896364
ANKRD6	XM_001500748	NP_055757.2	0.0046097	0.4958728
C20orf19	XM_001492895	NP_060944.3	0.0057122	0.4961214
NULL	NULL	NULL	0.0039953	0.4962043
R3HCC1	XM_001491126	XP_114618.5	0.006939	2.0134575
NULL	NULL	NULL	0.0032318	2.0135209
C17orf85	XM_001504729	NP_061023.1	0.006464	2.0137738
LOC124512	XM_001491460	NP_001073979.2	0.0086618	2.0508085
DUSP1	XM_001499555	NP_004408.1	0.0016309	2.0559998
NULL	NULL	NULL	0.0061312	2.0680121
OR5M9	XM_001489238	NP_001004743.1	0.008824	2.0812068
POLR2B	XR_035933	NP_000929.1	0.0030154	2.1001999
CRISPLD2	XM_001499908	NP_113664.1	0.0092155	2.1038223
NULL	NULL	NULL	0.0074283	2.1076708
LOC283999	XM_001491026	XP_211287.4	0.0040496	2.1131741
NULL	NULL	NULL	0.0012577	2.1298418
SERPINB11	XM_001491598	NP_536723.2	0.004239	2.1331906
OR51G2	XM_001498239	NP_001005238.1	0.0047411	2.1755089
CHSY1	XM_001490809	NP_055733.2	0.0056188	2.1952397
ADAMTS1	AF541975	NP_008919.3	0.003679	2.2139889
NULL	NULL	NULL	0.0095705	2.2491883
GLRA2	XM_001489464	NP_002054.1	0.0024703	2.2839264
C1orf159	XM_001496587	NP_060361.2	0.0069137	2.2970038
LOC285588	XM_001499636	XP_209668.3	0.0013293	2.3281263
NULL	CX604081	NULL	0.0094071	2.3713775
SAA1	XM_001504959	NP_000322.2	0.0012686	2.3855719
TSSK4	XM_001489964	NP_777604.2	0.0007108	2.393651
NULL	NULL	NULL	0.0080698	2.3944199
TMEM49	XM_001503742	NP_112200.2	0.0048984	2.4131855
SAA1	BM780679	NP_000322.2	0.0019341	2.4186575
SAA1	XM_001504960	NP_000322.2	0.0025128	2.4286297

CD300LF	XM_001497307	NP_620587.2	0.0094142	2.4372623
CAPS	XM_001495900	NP_004049.1	0.0092483	2.4578076
QSOX1	XM_001488615	NP_002817.2	0.0024708	2.4984072
NULL	CX592382	NULL	0.0004705	2.4999978
ZFHX3	XM_001500141	NP_008816.3	0.0014035	2.5056612
SH3GL3	NULL	NP_003018.2	0.0088225	2.5246567
SEC11C	XM_001489285	NP_150596.1	0.0037914	2.5356077
PTMA	XM_001501542	NP_002814.3	0.0010587	2.543564
BMF	XM_001503570	NP_001003940.1	0.0081287	2.5437235
NULL	BM414570	NULL	0.0080186	2.5584218
NULL	NULL	NULL	0.006327	2.6014969
SLC2A9	NULL	NP_001001290.1	0.0032032	2.60651
NULL	CD466589	NULL	0.0071998	2.6128365
BIRC3	XM_001499875	NP_001156.1	0.0034269	2.6294381
SF3B14	XM_001503183	NP_057131.1	0.0056972	2.6374823
CEBPB	CX605423	NP_005185.2	0.0042483	2.6632929
NULL	CX604543	NULL	0.0016985	2.6685059
NULL	NULL	NULL	0.0035459	2.6711891
NULL	DN509256	NULL	0.0038003	2.6730442
NULL	NULL	NULL	0.0068815	2.6737607
C8orf53	XM_001496257	NP_115710.1	0.0065647	2.7108601
FAIM	XM_001495529	NP_001028203.1	0.0059779	2.7327459
ZNF182	XM_001501391	NP_001007089.1	0.0031242	2.751908
NULL	NULL	NULL	0.0076667	2.7568769
TIMM23	XM_001500113	NP_006318.1	0.0063184	2.7615193
GLUL	NULL	NP_001028228.1	0.0044547	2.7686658
TTC14	XM_001495771	NP_597719.1	0.0052194	2.7950877
NSMCE1	XM_001497008	NP_659547.2	0.0090951	2.8033414
RPL26	XR_036170	NP_000978.1	0.0018374	2.8379658
CYCS	XM_001500631	NP_061820.1	0.0073342	2.8626494
NULL	NULL	NULL	0.0045502	2.895858
TSC22D2	XM_001490871	NP_055594.1	0.0063014	2.9273247
POU5F1	XM_001490108	NP_002692.2	0.0088791	2.9318778
NULL	CX605490	NULL	0.0073967	2.9436673
MYO1E	CD470665	NP_004989.2	0.0086722	2.9699868
PI15	XM_001491205	NP_056970.1	0.0018505	3.0655083
TPH1	XM_001504954	NP_004170.1	0.002155	3.1246394
NULL	NULL	NULL	0.0034389	3.1249823
CTRC	XM_001489099	NP_009203.2	0.006641	3.1568459
FAM132A	XM_001496492	NP_001014980.1	0.0051963	3.1839855

NULL	NULL	NULL	0.0032521	3.1943672
NULL	BI961214	NULL	0.0008256	3.2503006
CD163	XM_001492693	NP_004235.3	0.0014443	3.2662141
MRPS23	XM_001500440	NP_057154.2	0.0029156	3.2826537
NULL	NULL	NULL	0.002071	3.2952712
DYNC1I2	XM_001498670	NP_001369.1	0.0007614	3.3686275
NULL	NULL	NULL	0.0084661	3.4226228
NULL	NULL	NULL	0.0025578	3.4708038
MED29	XM_001497555	NP_060062.1	0.0018667	3.5051673
NULL	NULL	NULL	0.0003051	3.5255789
NULL	NULL	NULL	0.0021702	3.5453521
ZNF567	XM_001492950	NP_689816.2	0.0027419	3.5917722
ARHGAP20	XM_001487839	NP_065860.2	0.0014472	3.7015039
NULL	NULL	NULL	0.0007026	3.7349927
CYBA	XM_001488006	NP_000092.2	3.94E-05	3.7631849
FKBP5	XM_001499198	NP_004108.1	0.0069106	3.8287248
LOC728937	DN510217	NP_001087200.2	0.0084396	3.8293137
PDK1	XM_001495093	NP_002601.1	0.0017783	3.8780423
HIST2H2AA4	CX603409	NP_001035807.1	0.0027317	3.879084
ATP6V1G3	XM_001494440	NP_573569.1	0.0080896	3.8896743
PI3	BM734843	NP_002629.1	0.0002748	3.8978023
KIAA1524	XM_001503233	NP_065941.1	0.0037366	3.9916696
GLUL	XM_001489235	NP_001028228.1	0.0005385	4.0227095
HINT2	NULL	NP_115982.1	0.0073188	4.0383714
NULL	BI961659	NULL	0.0001246	4.307964
NULL	CD535521	NULL	0.0011927	4.3849263
IL12A	Y11130	NP_000873.2	0.0032432	4.4546355
S100A9	XM_001493530	NP_002956.1	0.0047402	4.4561501
NULL	XM_001498707	NULL	0.0001833	4.4721561
FTH1	XM_001489262	NP_002023.2	0.0047984	4.7716089
NULL	CD467650	NULL	0.0001854	4.7858347
SAA1	NM_001081853	NP_000322.2	0.0018345	6.7685543
NULL	NULL	NULL	4.69E-06	6.8999429
EREG	XM_001490281	NP_001423.1	0.0001479	6.9077909
DEFB4	AY170305	NP_004933.1	1.57E-05	10.571007
SOD2	AB001693	NP_000627.2	1.07E-06	11.283848
S100A8	XM_001494358	NP_002955.2	0.0001049	13.808318
S100A8	XM_001493589	NP_002955.2	1.25E-05	24.756712

Table A.11 List of all differentially expressed genes (P<0.01 and fold change>2) for the 12 h/24 h comparison. Fold change indicates expression level larger than 2 is up-regulation and expression level less than 0.5 is down-regulation.

Gene Name	Public Accession	Human Protein	P Value	Fold Change
S100A12	CD535886	NP_005612.1	0.0002941	0.0312015
S100A8	XM_001494358	NP_002955.2	4.22E-07	0.0416582
S100A8	XM_001493589	NP_002955.2	5.81E-05	0.0576884
NULL	CD467650	NULL	1.99E-05	0.0583316
SOD2	AB001693	NP_000627.2	4.74E-06	0.0694325
S100A9	XM_001493530	NP_002956.1	0.0045247	0.1154095
PI3	BM734843	NP_002629.1	0.0006503	0.121293
DEFB4	AY170305	NP_004933.1	9.27E-05	0.1222276
SAA1	NM_001081853	NP_000322.2	0.0003899	0.1614716
NULL	NULL	NULL	0.0047673	0.1681315
NULL	NULL	NULL	0.0047756	0.1682847
NULL	NULL	NULL	0.0004048	0.1776457
OR5M9	XM_001488291	NP_001004743.1	0.0009264	0.188936
THBS1	XM_001503599	NP_003237.2	0.0007574	0.1940095
NULL	NULL	NULL	1.87E-05	0.1945179
SLA	XM_001498789	NP_001039022.1	0.0065622	0.1976541
ORMDL1	XM_001501956	NP_057551.1	0.0018282	0.2019237
HSPA8	NULL	NP_006588.1	0.0069204	0.2051958
NULL	NULL	NULL	0.0003183	0.2065697
MORC3	XM_001493319	NP_056173.1	0.007338	0.208536
LYZL6	XM_001494897	NP_065159.1	0.0014104	0.2086065
ARPC5	CX604507	NP_005708.1	0.0063349	0.2089287
ANKRD10	XM_001496718	NP_060134.2	0.006467	0.2186919
NULL	XM_001498707	NULL	0.0052303	0.2228975
LOC283999	XM_001491026	XP_211287.4	0.0086698	0.2252925
NULL	NULL	NULL	0.0008158	0.2266554
RLBP1L1	XM_001496222	NP_775790.1	0.0003398	0.2286446
NULL	BM735339	NULL	0.0022796	0.2324314
NULL	NULL	NULL	0.0026077	0.235477
CNPY2	NULL	NP_055070.1	0.0008219	0.2357222
RPUSD3	XM_001491328	NP_775930.1	0.00173	0.2366615
NULL	BI961659	NULL	0.0004196	0.2381768
ADAMTS1	AF541975	NP_008919.3	0.0013168	0.2406131
NULL	CX605648	NULL	0.0006864	0.2411547

PRDM11	XM_001490144	NP_064614.2	0.0088167	0.2417397
LOC730593	XM_001490568	XP_001126460.1	0.0081285	0.2430951
NULL	CX602359	NULL	0.0040223	0.2434114
COL9A1	CX605273	NP_001842.3	0.0082564	0.2468013
EREG	XM_001490281	NP_001423.1	0.0041863	0.2533209
PSENEN	XM_001492730	NP_758844.1	0.0031487	0.2537129
LINS1	XM_001490353	NP_001035706.1	0.0021945	0.2575248
THOP1	XM_001493535	NP_003240.1	0.0037074	0.2584734
GSTO2	XM_001499366	NP_899062.1	0.0040847	0.2584903
H2AFY2	XM_001503710	NP_061119.1	0.0058558	0.2597315
TAGLN	XM_001502596	NP_001001522.1	0.0014263	0.2604284
GCA	XM_001494347	NP_036330.1	0.0050796	0.2632455
HSPA5	CX604607	NP_005338.1	8.78E-05	0.2644439
PI15	XM_001491205	NP_056970.1	0.000651	0.2699115
FGFBP1	XM_001498741	NP_005121.1	0.0079345	0.2708487
SERPINB3	XM_001491507	NP_008850.1	0.0042591	0.2710106
HNRPAB	XM_001499029	NP_004490.2	0.0021627	0.2770756
ITPR2	XM_001502700	NP_002214.2	0.0026107	0.2823533
OR8B3	XM_001501898	NP_001005467.1	0.0052964	0.2841699
OGG1	XM_001494881	NP_002533.1	0.0031311	0.2844899
CALU	CX605787	NP_001210.1	0.0015659	0.2859299
GLUL	NULL	NP_001028228.1	0.0007799	0.2868079
RGS1	CD471812	NP_002913.3	0.0058246	0.2886835
EIF3I	XM_001503817	NP_003748.1	0.002652	0.2921869
DDX47	XM_001501444	NP_057439.2	0.0052828	0.2928334
NULL	CX601417	NULL	0.006105	0.2932302
NULL	NULL	NULL	0.0028286	0.2967394
GADD45B	XM_001493821	NP_056490.2	0.0082575	0.2968482
MYH3	XM_001504848	NP_002461.2	0.0038229	0.2983001
PTPN4	XM_001492520	NP_002821.1	0.0037175	0.2996852
NCBP2	XM_001501008	NP_031388.2	0.0043083	0.3009056
NULL	NULL	NULL	0.0043599	0.3020566
SAA1	XM_001504960	NP_000322.2	0.0001831	0.3021274
JAK2	XM_001492663	NP_004963.1	0.0058692	0.3024495
USP36	XM_001491130	NP_079366.3	0.0030133	0.3047215
PARP6	XM_001494491	NP_064599.2	0.00776	0.3050135
NULL	NULL	NULL	0.0078661	0.3055134
ADM	XM_001500996	NP_001115.1	0.0014336	0.3091763
NULL	NULL	NULL	0.0019154	0.3137025
NULL	XM_001503131	NULL	0.0050829	0.3147854

NULL	NULL	NULL	0.0030706	0.3152047
NULL	CD536247	NULL	0.0083626	0.315834
LRRC4C	XM_001488162	NP_065980.1	0.0067154	0.3159477
USP20	NULL	NP_001103773.1	0.0069376	0.3176783
MRPL48	XM_001498632	NP_057139.1	0.0031766	0.3182676
KRT222P	XM_001500146	NP_689562.1	0.005494	0.3208563
KIAA1949	XM_001491396	NP_597728.1	0.0049425	0.3209562
PPP3CC	XM_001490720	NP_005596.2	0.005101	0.3219688
HPSE	XM_001493282	NP_001092010.1	0.0051608	0.326519
IGLL1	DQ125416	NP_064455.1	0.0085744	0.3285533
HSP90B1	XM_001497922	NP_003290.1	0.0011107	0.3295273
BCL3	XM_001500256	NP_005169.1	0.0020051	0.3307912
TCF25	XM_001488412	NP_055787.1	0.0066937	0.3322528
SLC1A3	XM_001499617	NP_004163.2	0.0048886	0.3377181
NULL	NULL	NULL	0.0050383	0.3394779
PPP1R3B	XM_001494371	NP_078883.2	0.006617	0.3410787
PREP	DN505238	NP_002717.3	0.0077696	0.3421426
DHCR24	XM_001488247	NP_055577.1	0.0048868	0.3440417
NULL	NULL	NULL	0.0083784	0.3456873
RABL4	XM_001499264	NP_006851.1	0.0082317	0.3490061
NULL	NULL	NULL	0.0062878	0.3494084
EPN3	XM_001502825	NP_060427.2	0.0097246	0.3495553
THAP4	XM_001497749	NP_057047.3	0.0047282	0.3499826
HMGN4	XM_001505090	NP_006344.1	0.0077932	0.3518574
PGK1	XM_001502668	NP_000282.1	0.0076215	0.3525187
PDIA3	XM_001502988	NP_005304.3	0.0056393	0.3526035
GPSM2	XM_001493568	NP_037428.2	0.0090316	0.3541887
NULL	CX598740	NULL	0.0003692	0.3554258
CCL2	AJ251189	NP_002973.1	0.0022299	0.3596737
NULL	NULL	NULL	0.009343	0.3630632
MYO5B	XM_001499160	XP_944193.1	0.0054423	0.3688
NULL	NULL	NULL	0.000351	0.3703969
NULL	NULL	NULL	0.0026589	0.3736836
GLUL	XM_001489235	NP_001028228.1	0.0040854	0.3747821
ERO1L	CX601828	NP_055399.1	0.0090849	0.3760276
BIRC3	XM_001499875	NP_001156.1	0.0010892	0.3781491
CRISPLD2	XM_001499908	NP_113664.1	0.0030128	0.3807604
C11orf30	XM_001494053	NP_064578.2	0.003394	0.3838901
TOP1	XM_001500194	NP_003277.1	0.0033418	0.3843697
NULL	NULL	NULL	0.0029642	0.3853809

GNG8	XM_001503002	NP_150283.1	0.0022282	0.3941202
AARS	XM_001501012	NP_001596.2	0.0096603	0.3962516
MID1IP1	CX604299	NP_001092261.1	0.0014773	0.3967994
SAA1	XM_001504959	NP_000322.2	0.0018947	0.404232
OR7G2	XM_001500467	NP_001005193.1	0.0085642	0.406257
RNF144B	XM_001494349	NP_877434.2	0.0015145	0.406621
DCUN1D3	XM_001495107	NP_775746.1	0.0035036	0.4089635
DDX58	XM_001497845	NP_055129.2	0.0093733	0.4110164
MEF2A	CD464185	NP_005578.1	0.0022392	0.4128078
HSPA8	AF411802	NP_006588.1	0.0018211	0.4128337
HDAC4	XM_001497151	NP_006028.2	0.0068071	0.4145777
CCT6A	XM_001499414	NP_001753.1	0.0013151	0.4242592
PTMA	XM_001501542	NP_002814.3	0.0015005	0.4259638
GOLIM4	XM_001494089	NP_055313.1	0.0087559	0.4268391
GFAP	XM_001488816	NP_002046.1	0.0094357	0.4271732
LOC338809	XM_001495196	NP_001032760.1	0.0006908	0.4284314
TGIF2LX	XM_001501915	NP_620410.3	0.00406	0.4311837
ANKS4B	XM_001494691	NP_665872.2	0.0086163	0.4324151
YTHDF2	XM_001500333	NP_057342.2	0.0092936	0.4339689
SP140	XM_001494747	NP_009168.3	0.0088735	0.4372654
TLR4	AY005808	NP_612564.1	0.0066541	0.4388419
MUC16	XM_001494817	NP_078966.2	0.0050593	0.4389319
CCKBR	XM_001504583	NP_795344.1	0.0060558	0.4451907
ALMS1	XM_001491738	NP_055935.4	0.0064886	0.4452616
CCDC94	XM_001496436	NP_060544.2	0.0076663	0.4454342
C17orf56	XM_001489994	NP_653280.1	0.0046786	0.4496341
NULL	NULL	NULL	0.001173	0.4566383
CREBL1	XM_001493153	NP_004372.3	0.0076692	0.4657573
RPS14	NULL	NP_001020242.1	0.0098846	0.4664648
GAPDH	XR_036361	NP_002037.2	0.0032546	0.4668949
TPM1	NULL	NP_001018005.1	0.0013657	0.4679278
LOC285556	XM_001496866	XP_373030.3	0.0030353	0.4707343
TSSK4	XM_001489964	NP_777604.2	0.0030359	0.4719277
CAMK1G	XM_001490285	NP_065172.1	0.0060354	0.4732164
NULL	NULL	NULL	0.0098905	0.4732378
CLP1	XM_001497108	NP_006822.1	0.0059328	0.4759919
NULL	BI961150	NULL	0.0048967	0.476628
CYCS	XM_001498822	NP_061820.1	0.0062856	0.4811904
NULL	XR_036342	NULL	0.0088768	0.4822694
SEC61B	CX592223	NP_006799.1	0.0027511	0.4860176

SART1	NULL	NP_005137.1	0.00761	0.4907682
LHX6	XM_001501453	NP_055183.2	0.0042436	0.4943996
LDHA	XM_001504963	NP_005557.1	0.0035451	0.4974905
XPOT	NULL	NP_009166.2	0.0066458	0.4979606
LCN2	XM_001501148	NP_005555.2	0.0079727	0.499899
NULL	DN511229	NULL	0.008524	2.0078493
NULL	CX594466	NULL	0.0030845	2.017792
TRIM39	XM_001492176	NP_742013.1	0.0045124	2.0245279
COX10	XM_001503366	NP_001294.2	0.0046542	2.0440492
NULL	NULL	NULL	0.0038567	2.0543571
CD33	XM_001496603	NP_001763.3	0.0073252	2.07117
MCTS1	XR_036369	NP_054779.1	0.0078768	2.0724382
UNC5D	XM_001494091	NP_543148.1	0.0097519	2.0726267
OR5AR1	XM_001496569	NP_001004730.1	0.0046509	2.098321
MAGEB1	XM_001488253	NP_796379.1	0.0061232	2.1043499
ATP13A5	XM_001498779	NP_940907.2	0.002564	2.1065364
NULL	CX605497	NULL	0.0082547	2.1359314
NAPSA	XM_001490835	NP_004842.1	0.0091232	2.1466249
SUMO2	XM_001494020	NP_008868.3	0.0011291	2.1500866
MMP26	XM_001497732	NP_068573.2	0.0016409	2.1620324
NULL	NULL	NULL	0.0079301	2.1666932
LRRC49	XM_001495228	NP_060161.2	0.008344	2.1975564
C21orf58	XM_001489518	NP_478060.2	0.0066052	2.2163037
NULL	NULL	NULL	0.0071162	2.2233239
OR7A5	XM_001501205	NP_059976.1	0.0016227	2.2410455
NULL	NULL	NULL	0.0085577	2.262762
HDAC9	XM_001496688	NP_848512.1	0.0065964	2.2714248
GJB6	XM_001488823	NP_001103691.1	0.0040544	2.2841907
CEL	XM_001498274	NP_001798.2	0.0019936	2.2961466
TMPRSS11A	XM_001497444	NP_872412.2	0.0047899	2.3261182
GDF2	XM_001500654	NP_057288.1	0.0097597	2.333065
NULL	NULL	NULL	0.007887	2.3348297
BTN2A1	XM_001492502	NP_008980.1	0.0034012	2.3395265
SNAI2	XM_001488056	NP_003059.1	0.0009749	2.3772354
NULL	NULL	NULL	0.0024313	2.3961272
ANKRD6	XM_001500748	NP_055757.2	0.0057303	2.3985989
PCDHGA5	XM_001504024	NP_114443.1	0.0080952	2.409591
NULL	NULL	NULL	0.0020882	2.4255549
FKTN	XM_001493424	NP_001073270.1	0.0045699	2.4375705
MYOT	NULL	NP_006781.1	0.0015216	2.4438922

CXCL14	XM_001502713	NP_004878.2	0.0077398	2.4455754
NULL	NULL	NULL	0.0006983	2.4562982
NULL	NULL	NULL	0.0049686	2.4977797
NULL	NULL	NULL	0.002443	2.5023968
NULL	DN504122	NULL	0.0025977	2.5045382
RGS12	XM_001488851	NP_937872.1	0.0098584	2.5186997
OR56B1	XM_001504509	NP_001005180.1	0.0006266	2.5223909
SLC26A4	XM_001491415	NP_000432.1	0.0086054	2.5276036
NULL	NULL	NULL	0.0048109	2.5296504
NULL	NULL	NULL	0.0090193	2.6072912
OR2J3	XM_001492129	NP_001005216.1	0.0030346	2.6244782
OR52R1	XM_001497504	NP_001005177.2	0.007486	2.6292634
CCL11	AJ251188	NP_002977.1	0.0048805	2.6344786
SYNE2	XR_036037	NP_878918.2	0.0093788	2.6528621
SEC14L5	XM_001499664	NP_055507.1	0.0086505	2.6589973
NULL	XM_001494906	NULL	0.0053783	2.6917979
FAM149A	XM_001490364	NP_001006656.1	0.0025988	2.702849
NULL	DN510842	NULL	0.008927	2.7204253
AP2B1	XM_001503924	NP_001025177.1	0.0037447	2.7363777
SLC4A1	AB242565	NP_000333.1	0.0099905	2.7877988
KLHL31	XM_001499245	NP_001003760.2	0.0070629	2.8259552
NULL	NULL	NULL	0.0040293	2.8466627
UTP14A	XM_001491734	NP_006640.2	0.0067981	2.9413664
NULL	XR_035845	NULL	0.0017984	2.951134
TBC1D25	XM_001493681	NP_002527.1	0.0021183	2.9660242
NULL	NULL	NULL	0.0022093	2.972469
C7orf57	XM_001496533	NP_001093629.1	0.0029925	2.9983715
SLC12A6	NULL	NP_005126.1	0.0071002	3.0132056
CD1A	XM_001489552	NP_001754.2	0.0054223	3.0639925
TULP3	XM_001490880	NP_003315.2	0.005595	3.0661984
NULL	NULL	NULL	0.0047843	3.0882741
FXYD5	XM_001491379	NP_054883.3	0.0071221	3.1121611
NULL	NULL	NULL	0.0047815	3.1148616
NULL	XM_001495803	NULL	0.0058398	3.1148905
NULL	DN506907	NULL	0.0051779	3.1250039
P2RY13	XM_001489171	NP_076403.2	0.0041307	3.218154
NULL	NULL	NULL	0.004146	3.2214684
SPAG17	XM_001500885	NP_996879.1	0.0067862	3.230009
NULL	NULL	NULL	0.0090001	3.3905441
FREM1	XM_001493917	NP_659403.4	0.0050171	3.3969602

C17orf70	XM_001489884	NP_001103230.1	0.0027942	3.6009639
STAT4	XM_001502206	NP_003142.1	0.0019232	3.738519
NULL	CX603542	NULL	7.16E-05	3.7857016
NULL	NULL	NULL	0.0023883	3.8035913
RNF113A	XM_001491814	NP_008909.1	0.0031309	3.8284761
COCH	XM_001489788	NP_004077.1	0.0045814	3.9493985
NULL	NULL	NULL	0.0036349	4.0227201
BBS7	XM_001503097	NP_789794.1	0.0004973	4.0381013
HMGN3	XM_001499096	NP_004233.1	0.0020182	4.1234867
LGALS4	XM_001497350	NP_006140.1	0.0005165	4.1756397
ARHGAP11A	XM_001503656	NP_055598.1	0.0091897	4.3236811
NULL	NULL	NULL	0.0012487	4.3324721
NULL	NULL	NULL	0.005792	5.3811581
C3orf26	XM_001502207	NP_115735.1	0.0036829	5.7588642
NULL	NULL	NULL	0.0002427	9.5614929
NULL	NULL	NULL	0.0072642	11.197911
NULL	DN508706	NULL	0.0001121	14.586985

Table A.12 Overrepresented gene ontology terms identified among differentially expressed genes (P<0.01 and fold change>2) of the 12 h/CON comparison. BP: biological process; CC: cellular component; MF: molecular function

	Term	Count	%	P
Upregulated Genes				
BP	GO:0002376~immune system process	5	20	0.041001
CC	none			
MF	none			
Downregulated Genes				
BP	GO:0030097~hemopoiesis	4	14.28571	0.003668
	GO:0048534~hemopoietic or lymphoid organ development	4	14.28571	0.004811
	GO:0002520~immune system development	4	14.28571	0.005681
	GO:0002376~immune system process	6	21.42857	0.008822
	GO:0002521~leukocyte differentiation	3	10.71429	0.013181
	GO:0048569~post-embryonic organ development	2	7.142857	0.014712
	GO:0007165~signal transduction	9	32.14286	0.023998
	GO:0007166~cell surface receptor linked signal transduction	7	25	0.030381
	GO:0045321~leukocyte activation	3	10.71429	0.041325
CC	none			
MF	none			

Table A.13 Overrepresented gene ontology terms identified among differentially expressed genes (P<0.01 and fold change>2) of the 24 h/CON comparison. BP: biological process; CC: cellular component; MF: molecular function

	Term	Count	%	P
Upregulated Genes				
BP	GO:0006953~acute-phase response	4	5.970149	4.73E-04
	GO:0006952~defense response	10	14.92537	4.90E-04
	GO:0009605~response to external stimulus	12	17.91045	5.77E-04
	GO:0009611~response to wounding	9	13.43284	8.50E-04
	GO:0002376~immune system process	12	17.91045	0.001195
	GO:0006954~inflammatory response	7	10.44776	0.001449
	GO:0042330~taxis	5	7.462687	0.003237
	GO:0006935~chemotaxis	5	7.462687	0.003237
	GO:0007626~locomotory behavior	6	8.955224	0.003867
	GO:0001819~positive regulation of cytokine production	4	5.970149	0.004916
	GO:0001817~regulation of cytokine production	5	7.462687	0.005019
	GO:0002526~acute inflammatory response	4	5.970149	0.00623
	GO:0030595~leukocyte chemotaxis	3	4.477612	0.008781
	GO:0006950~response to stress	14	20.89552	0.009571
	GO:0060326~cell chemotaxis	3	4.477612	0.009722
	GO:0008285~negative regulation of cell proliferation	6	8.955224	0.012068
	GO:0031347~regulation of defense response	4	5.970149	0.017331
	GO:0050900~leukocyte migration	3	4.477612	0.020044
	GO:0045785~positive regulation of cell adhesion	3	4.477612	0.022068
	GO:0040011~locomotion	6	8.955224	0.024078
	GO:0048247~lymphocyte chemotaxis	2	2.985075	0.026478

	GO:0050665~hydrogen peroxide biosynthetic process	2	2.985075	0.026478
	GO:0042981~regulation of apoptosis	8	11.9403	0.032605
	GO:0007610~behavior	6	8.955224	0.033032
	GO:0048246~macrophage chemotaxis	2	2.985075	0.033916
	GO:0043067~regulation of programmed cell death	8	11.9403	0.034147
	GO:0010941~regulation of cell death	8	11.9403	0.034737
	GO:0006955~immune response	7	10.44776	0.047176
	GO:0042554~superoxide anion generation	2	2.985075	0.048625
CC	GO:0005758~mitochondrial intermembrane space	3	4.477612	0.007857
	GO:0031970~organelle envelope lumen	3	4.477612	0.010586
	GO:0005739~mitochondrion	10	14.92537	0.017982
	GO:0005576~extracellular region	14	20.89552	0.03039
	GO:0032991~macromolecular complex	19	28.35821	0.033603
	GO:0005744~mitochondrial inner membrane presequence translocase complex	2	2.985075	0.043624
MF	GO:0022884~macromolecule transmembrane transporter activity	2	2.985075	0.046219
	GO:0015450~P-P-bond-hydrolysis-driven protein transmembrane transporter activity	2	2.985075	0.046219
Downregulated Genes				
BP	GO:0006520~cellular amino acid metabolic process	3	9.677419	0.043891
	GO:0009267~cellular response to starvation	2	6.451613	0.046574
CC	GO:0044444~cytoplasmic part	17	54.83871	6.18E-05
	GO:0005737~cytoplasm	18	58.06452	0.002863
	GO:0043226~organelle	20	64.51613	0.002998
	GO:0043229~intracellular organelle	19	61.29032	0.011782

	GO:0005865~striated muscle thin filament	2	6.451613	0.020554
	GO:0044424~intracellular part	20	64.51613	0.035828
	GO:0005813~centrosome	3	9.677419	0.037901
	GO:0044430~cytoskeletal part	5	16.12903	0.039349
	GO:0005815~microtubule organizing center	3	9.677419	0.047229
MF	GO:0008168~methyltransferase activity	3	9.677419	0.027161
	GO:0016741~transferase activity, transferring one-carbon groups	3	9.677419	0.028054

Table A.14 Overrepresented gene ontology terms identified among differentially expressed genes (P<0.01 and fold change>2) of the 12 h/24 h comparison. BP: biological process; CC: cellular component; MF: molecular function

	Term	Count	%	P
Upregulated Genes				
BP	GO:0007600~sensory perception	9	16.07143	0.002744
	GO:0003008~system process	12	21.42857	0.004431
	GO:0050890~cognition	9	16.07143	0.005538
	GO:0050877~neurological system process	9	16.07143	0.027768
	GO:0007605~sensory perception of sound	3	5.357143	0.035163
	GO:0050954~sensory perception of mechanical stimulus	3	5.357143	0.039222
	GO:0007608~sensory perception of smell	5	8.928571	0.041482
CC	GO:0005886~plasma membrane	20	35.71429	0.006195
MF	GO:0004984~olfactory receptor activity	5	8.928571	0.044169

Downregulated Genes

BP	GO:0006950~response to stress	31	25.83333	6.47E-07
	GO:0051240~positive regulation of multicellular organismal process	12	10	9.79E-07
	GO:0009607~response to biotic stimulus	14	11.66667	2.42E-06
	GO:0001819~positive regulation of cytokine production	8	6.666667	2.92E-06
	GO:0042221~response to chemical stimulus	25	20.83333	5.01E-06
	GO:0050896~response to stimulus	45	37.5	1.10E-05
	GO:0009611~response to wounding	15	12.5	1.67E-05
	GO:0051716~cellular response to stimulus	18	15	4.44E-05
	GO:0009605~response to external stimulus	19	15.83333	5.04E-05
	GO:0042981~regulation of apoptosis	17	14.16667	1.24E-04
	GO:0043067~regulation of programmed cell death	17	14.16667	1.39E-04
	GO:0010941~regulation of cell death	17	14.16667	1.45E-04
	GO:0048519~negative regulation of biological process	27	22.5	1.95E-04
	GO:0001817~regulation of cytokine production	8	6.666667	2.63E-04
	GO:0006952~defense response	14	11.66667	3.20E-04
	GO:0048523~negative regulation of cellular process	24	20	8.24E-04
	GO:0008285~negative regulation of cell proliferation	10	8.333333	9.00E-04
	GO:0051707~response to other organism	9	7.5	9.16E-04
	GO:0048247~lymphocyte chemotaxis	3	2.5	9.79E-04
	GO:0012501~programmed cell death	13	10.83333	0.00105
	GO:0002376~immune system process	17	14.16667	0.001343
	GO:0055066~di-, tri-valent inorganic cation homeostasis	8	6.666667	0.001368
	GO:0048246~macrophage chemotaxis	3	2.5	0.001664
	GO:0006874~cellular calcium ion homeostasis	7	5.833333	0.001717
	GO:0006954~inflammatory response	9	7.5	0.001891
	GO:0055074~calcium ion homeostasis	7	5.833333	0.001968

GO:0030595~leukocyte chemotaxis	4	3.333333	0.002125
GO:0009617~ response to bacterium	7	5.833333	0.002246
GO:0001666~response to hypoxia	6	5	0.002399
GO:0006875~cellular metal ion homeostasis	7	5.833333	0.002426
GO:0060326~cell chemotaxis	4	3.333333	0.002474
GO:0065009~regulation of molecular function	16	13.33333	0.002699
GO:0070482~response to oxygen levels	6	5	0.00299
GO:0006915~apoptosis	12	10	0.003001
GO:0055065~metal ion homeostasis	7	5.833333	0.003032
GO:0006916~anti-apoptosis	7	5.833333	0.003106
GO:0031347~regulation of defense response	6	5	0.003177
GO:0043066~negative regulation of apoptosis	9	7.5	0.003204
GO:0043069~negative regulation of programmed cell death	9	7.5	0.003488
GO:0060548~negative regulation of cell death	9	7.5	0.003548
GO:0055080~cation homeostasis	8	6.666667	0.003749
GO:0008219~cell death	13	10.83333	0.004057
GO:0034504~protein localization in nucleus	5	4.166667	0.004134
GO:0016265~death	13	10.83333	0.004287
GO:0006913~nucleocytoplasmic transport	6	5	0.004602
GO:0051169~nuclear transport	6	5	0.004856
GO:0030005~cellular di-, tri-valent inorganic cation homeostasis	7	5.833333	0.004986
GO:0006935~chemotaxis	6	5	0.00512
GO:0042330~taxis	6	5	0.00512
GO:0051239~regulation of multicellular organismal process	15	12.5	0.005153
GO:0033554~cellular response to stress	11	9.166667	0.005861
GO:0032732~positive regulation of interleukin-1 production	3	2.5	0.006062
GO:0006091~generation of precursor metabolites and energy	8	6.666667	0.006103

GO: 0030593~neutrophil chemotaxis	3	2.5	0.00679
GO:0007204~elevation of cytosolic calcium ion concentration	5	4.166667	0.007195
GO:0050900~leukocyte migration	4	3.333333	0.00724
GO:0044093~positive regulation of molecular function	11	9.166667	0.007423
GO:0048513~organ development	22	18.33333	0.007446
GO:0051704~multi-organism process	12	10	0.007501
GO:0042742~defense response to bacterium	5	4.166667	0.00766
GO:0045785~positive regulation of cell adhesion	4	3.333333	0.008341
GO:0051091~positive regulation of transcription factor activity	4	3.333333	0.008341
GO:0030003~cellular cation homeostasis	7	5.833333	0.008495
GO:0051480~cytosolic calcium ion homeostasis	5	4.166667	0.009172
GO:0051235~maintenance of location	4	3.333333	0.009956
GO:0051101~regulation of DNA binding	5	4.166667	0.009996
GO:0032652~regulation of interleukin-1 production	3	2.5	0.010977
GO:0010332~response to gamma radiation	3	2.5	0.010977
GO:0010033~response to organic substance	12	10	0.011238
GO:0065008~regulation of biological quality	19	15.83333	0.011738
GO:0007626~locomotory behavior	7	5.833333	0.012046
GO:0080134~regulation of response to stress	7	5.833333	0.012046
GO:0043388~positive regulation of DNA binding	4	3.333333	0.012696
GO:0006986~response to unfolded protein	4	3.333333	0.013191
GO:0046677~response to antibiotic	3	2.5	0.013912
GO:0009628~response to abiotic stimulus	8	6.666667	0.014095
GO:0042592~homeostatic process	12	10	0.014877
GO:0030155~regulation of cell adhesion	5	4.166667	0.0152
GO:0006873~cellular ion homeostasis	8	6.666667	0.015281

GO:0019725~cellular homeostasis	9	7.5	0.015687
GO:0050727~regulation of inflammatory response	4	3.333333	0.015828
GO:0007610~behavior	9	7.5	0.016244
GO:0055082~cellular chemical homeostasis	8	6.666667	0.016537
GO:0051099~positive regulation of binding	4	3.333333	0.016959
GO:0006928~cell motion	9	7.5	0.017402
GO:0033365~protein localization in organelle	5	4.166667	0.018759
GO:0009266~response to temperature stimulus	4	3.333333	0.019983
GO:0042127~regulation of cell proliferation	12	10	0.020352
GO:0051098~regulation of binding	5	4.166667	0.021858
GO:0006606~protein import into nucleus	4	3.333333	0.02193
GO:0000060~protein import into nucleus, translocation	3	2.5	0.02317
GO:0034976~response to endoplasmic reticulum stress	3	2.5	0.02317
GO:0051170~nuclear import	4	3.333333	0.023284
GO:0050801~ion homeostasis	8	6.666667	0.023656
GO:0006984~ER-nuclear signaling pathway	3	2.5	0.024464
GO:0048145~regulation of fibroblast proliferation	3	2.5	0.024464
GO:0043523~regulation of neuron apoptosis	4	3.333333	0.024682
GO:0032101~regulation of response to external stimulus	5	4.166667	0.024749
GO:0048878~chemical homeostasis	9	7.5	0.02589
GO:0048731~system development	25	20.83333	0.026994
GO:0006979~response to oxidative stress	5	4.166667	0.027327
GO:0042327~positive regulation of phosphorylation	4	3.333333	0.029928
GO:0043065~positive regulation of apoptosis	8	6.666667	0.029978
GO:0040011~locomotion	8	6.666667	0.030305
GO:0043068~positive regulation of programmed cell death	8	6.666667	0.030966
GO:0007275~multicellular organismal development	29	24.16667	0.031193

	GO:0010942~positive regulation of cell death	8	6.666667	0.031637
	GO:0010562~positive regulation of phosphorus metabolic process	4	3.333333	0.032342
	GO:0045937~positive regulation of phosphate metabolic process	4	3.333333	0.032342
	GO:0050790~regulation of catalytic activity	12	10	0.032381
	GO:0032507~maintenance of protein location in cell	3	2.5	0.032825
	GO:0006457~protein folding	5	4.166667	0.034761
	GO:0051090~regulation of transcription factor activity	4	3.333333	0.034855
	GO:0048518~positive regulation of biological process	22	18.33333	0.037669
	GO:0051789~response to protein stimulus	4	3.333333	0.038359
	GO:0046907~intracellular transport	10	8.333333	0.038678
	GO:0010225~response to UV-C	2	1.666667	0.040946
	GO:0050867~positive regulation of cell activation	4	3.333333	0.042036
	GO:0006096~glycolysis	3	2.5	0.042135
	GO:0016477~cell migration	6	5	0.043113
	GO:0042108~positive regulation of cytokine biosynthetic process	3	2.5	0.043772
	GO:0051651~maintenance of location in cell	3	2.5	0.043772
	GO:0045185~maintenance of protein location	3	2.5	0.043772
	GO:0007243~protein kinase cascade	7	5.833333	0.043879
	GO:0051223~regulation of protein transport	4	3.333333	0.044906
	GO:0022900~electron transport chain	4	3.333333	0.044906
	GO:0048522~positive regulation of cellular process	20	16.66667	0.049407
CC	GO:0005737~cytoplasm	70	58.33333	2.19E-05
	GO:0044432~endoplasmic reticulum part	9	7.5	0.001979
	GO:0044424~intracellular part	84	70	0.002372
	GO:0042470~melanosome	5	4.166667	0.00275
	GO:0048770~pigment granule	5	4.166667	0.00275

	GO:0044444~cytoplasmic part	46	38.33333	0.004665
	GO:0043233~organelle lumen	22	18.33333	0.006581
	GO:0031974~membrane-enclosed lumen	22	18.33333	0.008192
	GO:0005789~endoplasmic reticulum membrane	7	5.833333	0.008442
	GO:0005622~intracellular	84	70	0.009877
	GO:0070013~intracellular organelle lumen	21	17.5	0.010619
	GO:0042175~nuclear envelope-endoplasmic reticulum network	7	5.833333	0.010847
	GO:0005788~endoplasmic reticulum lumen	4	3.333333	0.015503
	GO:0044446~intracellular organelle part	39	32.5	0.015922
	GO:0044422~organelle part	39	32.5	0.017551
	GO:0005576~extracellular region	22	18.33333	0.019132
	GO:0044421~extracellular region part	13	10.83333	0.022679
	GO:0031410~cytoplasmic vesicle	10	8.333333	0.02465
	GO:0005829~cytosol	16	13.33333	0.02597
	GO:0016023~cytoplasmic membrane-bounded vesicle	9	7.5	0.027658
	GO:0032991~macromolecular complex	30	25	0.029611
	GO:0031982~vesicle	10	8.333333	0.031262
	GO:0031988~membrane-bounded vesicle	9	7.5	0.032597
	GO:0048471~perinuclear region of cytoplasm	6	5	0.040617
	GO:0005783~endoplasmic reticulum	12	10	0.048897
MF	GO:0008201~heparin binding	5	4.166667	0.004804
	GO:0005515~protein binding	67	55.83333	0.008985
	GO:0005539~glycosaminoglycan binding	5	4.166667	0.013854
	GO:0030247~polysaccharide binding	5	4.166667	0.018999
	GO:0001871~pattern binding	5	4.166667	0.018999
	GO:0030554~adenyl nucleotide binding	18	15	0.02872

GO:0001883~purine nucleoside binding	18	15	0.032598
GO:0001882~nucleoside binding	18	15	0.034501
GO:0051082~unfolded protein binding	4	3.333333	0.040575

VITA

Jixin Wang
Department of Veterinary Integrative Biosciences
College of Veterinary Medicine & Biomedical Sciences
Texas A&M University, 4458 TAMU
College Station, Texas 77843-4458
(979)-458-0520
jixinwang@hotmail.com

EDUCATION

Ph.D., Biomedical Sciences, Texas A&M University 2010
College Station, Texas
M.S., Poultry Science, Texas A&M University 2006
College Station, Texas
M.S., Animal Physiology, South China Agricultural University 2002
Guangzhou, China
B.S., Animal Science, Tarim University of Agricultural Reclamation 1999
Alar, China

PROFESSIONAL CERTIFICATION

SAS Certified Professional: SAS Base Programmer for SAS 9.2 2008

HONORS AND AWARDS

1. Neal A. Jorgensen Genome Travel Award from National Animal Genome Research Program, Plant & Animal Genomes XVIII Conference, 2010.
2. Travel Award for Plant & Animal Genomes XVIII Conference, College of Veterinary Medicine & Biomedical Sciences, Texas A&M University, 2009.
3. Student Scholarship Award, SCSUG SAS Conference, San Antonio, TX, 2009.
4. Travel Scholarship Award, Bioconductor Conference, Fred Hutchinson Cancer Research Center, Seattle, WA, 2008.

PUBLICATIONS

1. **Wang, J.**, Adelson, D. L., Yilmaz, A., Sze, S. H., Jin, Y., Zhu, J. J. 2005. Genomic organization, annotation, and ligand-receptor inferences of chicken chemokines and chemokine receptor genes based on comparative genomics. BMC Genomics, 6(1):45.

2. **Wang, J.**, Jiang, Q. Y., and Fu, W. L. 2002. Establishment of in vitro culture for porcine skeletal muscle satellite cell. Journal of South China Agricultural University, 23(1), 89-91.